

WASHINGTON STATE HIGHWAY DEPARTMENT RESEARCH PROGRAM  
REPORT

1.0

# AEROTRIANGULATION ANALYSIS & CONTROL POINT ERROR DETECTION

MARCH 1972

PREPARED FOR  
WASHINGTON STATE HIGHWAY COMMISSION  
IN COOPERATION WITH  
U.S. DEPARTMENT OF TRANSPORTATION  
FEDERAL HIGHWAY ADMINISTRATION

CHENG-YEH HOU  
RESEARCH ENGINEER

PHOTOGRAMMETRY BRANCH  
DEPARTMENT OF HIGHWAYS

The opinions, findings, and conclusions expressed in this research report are those of the author and not necessarily those of the State of Washington, Department of Highways and U.S. Department of Transportation, Federal Highway Administration.

## FOREWORD

This research administered by the Washington State Highways Department under the supervision of Mr. W.M. Foster, Assistant Director for Highway Development; Mr. J.H. Cooper, Roadway Development Engineer; Mr. D. A. Yates, Photogrammetric Engineer; Mr. G.A. Egge, Photogrammetrist. The mathematical analysis and computer programs, and final report performed by Mr. C.Y. Hou, Photogrammetric Research Engineer.

Sincere appreciation is extended to Mr. H.R. Goff, Assistant Director of Planning, Research, and State Aid; Mrs. W.W. Mylroie, Research and Special Assignments Engineer; and Mr. O.R. Dinsmore, Research Coordinator, for the interest and enthusiasm in this research.

The assistance in this project of all colleagues of the Photogrammetric Branch, Roadway Development Division, Washington State Highways is thankfully acknowledged.

The author wishes to express his thanks to the Washington State Highway Commission and the Federal Highway Administration for their financial support of this research project.

## ABSTRACT

A major problem faced by personnel responsible for manipulating aerotriangulation data through transformation and adjustment programs in an electronic computer is that of isolating and detecting blunders and other erroneous data. This study created an automated data analysis and rejection program to reduce the turn around time from initial entry to certification of the final adjustment. Parameters for establishing the smallest detectable errors for rejection were determined by analyses of error sources in ground control surveys, aerial photography, and aerotriangulation theory and operations. Some seldom considered theoretical and practical error sources in ground control surveys are discussed and resolved. The data rejection program chart is listed in the appendix.

— TABLE OF CONTENTS

	Page
FOREWORD AND ABSTRACT. . . . .	(I)
TABLE OF CONTENTS . . . . .	(IV )
LIST OF TABLES . . . . .	(VIII)
LIST OF FIGURES. . . . .	( X )
CHAPTER	
I. INTRODUCTION . . . . .	(1)
1-1. Background . . . . .	(1)
1-2. The purpose and scope of the investigation. . . . .	(2)
1-3. Error analysis. . . . .	(4)
1-3-1. Definition of the errors. . . . .	(4)
1-3-2. Standard error. . . . .	(6)
II. GROUND CONTROL ERRORS . . . . .	(11)
2-1. Background. . . . .	(11)
2-2. Deflection of the vertical from geodetic and astronomic azimuth . . . . .	(11)
2-2-1. Introduction. . . . .	(11)
2-2-2. Deflection of the vertical. . . . .	(12)
2-2-3. Conclusion. . . . .	(18)
2-3. Earth curvature corrections of traverse computation. (18)	
2-3-1. Introduction. . . . .	(18)
2-3-2. Second term correction. . . . .	(18)
2-3-3. Conclusion. . . . .	(22)

2-4.	Refraction of the precise leveling . . . . .	(27)
2-4-1.	Introduction . . . . .	(27)
2-4-2.	Theory of systematic refraction in precise leveling . . . . .	(27)
2-4-3.	Conclusion . . . . .	(35)
III.	MAGNITUDE OF ERRORS IN PHOTOGRAPHS AND INSTRUMENTS . . . . .	(39)
3-1.	Introduction . . . . .	(39)
3-2.	Flight height of the photographs . . . . .	(40)
3-3.	Solar altitude . . . . .	(41)
3-4.	Image blur . . . . .	(44)
3-5.	Lens distortion and film shrinkage . . . . .	(48)
3-6.	Accuracy of the instruments. . . . .	(54)
3-7.	Conclusion . . . . .	(57)
IV.	ERRORS OF THE AEROTRIANGULATION. . . . .	(58)
4-1.	Introduction . . . . .	(58)
4-2.	Earth curvature. . . . .	(59)
4-3.	Refraction . . . . .	(63)
4-4.	Refraction of the targets. . . . .	(67)
4-5.	Scale and azimuth of a strip . . . . .	(68)
4-6.	Longitudinal bend of a strip . . . . .	(73)
4-7.	Transversal tilt of a strip. . . . .	(76)
4-8.	Conclusion . . . . .	(76)
V.	AEROTRIANGULATION PRECISION ATTAINABLE FOR HIGHWAYS PHOTOGRAMMETRY. . . . .	(79)
5-1.	Introduction . . . . .	(79)
5-2.	Three dimension linear transformation. . . . .	(80)
5-3.	Strip adjustment and testing . . . . .	(81)
5-4.	Testing of ten strips of the flight at 1500 feet . . . . .	(83)

5-5.	Testing of ten strips of the flight at 3000 feet. . .	(123)
5-6.	Testing of two strips of the flight at 6000 feet. . .	(163)
5-7.	Testing of three strips of the flight at 12,000 feet.	(171)
5-8.	Precision determination of the aerotriangulation requirements of Highway Engineering . . . . .	(183)
5-9.	Conclusion. . . . .	(188)
VI.	DATA REJECTION . . . . .	(189)
6-1.	Introduction. . . . .	(189)
6-2.	General working equations . . . . .	(189)
6-3.	Computer program. . . . .	(191)
6-4.	Testing . . . . .	(193)
6-5.	Conclusion. . . . .	(194)
VII.	CONCLUSIONS & RECOMMENDATIONS . . . . .	(195)
VIII.	FUTURE RESEARCH . . . . .	(200)

APPENDICES

A.	COMPUTER PROGRAM CHART . . . . .	(203)
B.	INSTRUCTION OF THE COMPUTER PROGRAM OF DATA REJECTION . . .	(204)
C.	SAMPLE DATA SHEETS. . . . .	(206)
D.	LIST OF REFERENCES. . . . .	(207)

LIST OF TABLES

	Page
1. The second term corrections for traverse computation. . . . .	(23)
2. Comparison of the coordinates computed with and without second term corrections. . . . .	(25)
3. The correction or refraction and earth curvature. . . . .	(38)
4. Results of different adjustment procedures of test strip 1. .	(86)
5. Results of different adjustment procedures of test strip 2. .	(90)
6. Results of different adjustment procedures of test strip 3. .	(94)
7. Results of different adjustment procedures of test strip 4. .	(98)
8. Results of different adjustment procedures of test strip 5. .	(102)
9. Results of different adjustment procedures of test strip 6. .	(106)
10. Results of different adjustment procedures of test strip 7. .	(110)
11. Results of different adjustment procedures of test strip 8. .	(114)
12. Results of different adjustment procedures of test strip 9. .	(118)
13. Results of different adjustment procedures of test strip 10 .	(122)
14. Results of different adjustment procedures of test strip 11 .	(126)
15. Results of different adjustment procedures of test strip 12 .	(130)
16. Results of different adjustment procedures of test strip 13 .	(134)
17. Results of different adjustment procedures of test strip 14 .	(138)
18. Results of different adjustment procedures of test strip 15 .	(142)
19. Results of different adjustment procedures of test strip 16 .	(146)
20. Results of different adjustment procedures of test strip 17..	(150)



21.	Results of different adjustment procedures of test strip 18 .	(154)
22.	Results of different adjustment procedures of test strip 19 .	(158)
23.	Results of different adjustment procedures of test strip 20..	(162)
24.	Results of different adjustment procedures of test strip 21 .	(166)
25.	Results of different adjustment procedures of test strip 22 .	(170)
26.	Results of different adjustment procedures of test strip 23 .	(174)
27.	Results of different adjustment procedures of test strip 24 .	(178)
28.	Results of different adjustment procedures of test strip 25 .	(182)
29.	The standard errors in various flight height. . . . .	(187)

## LIST OF FIGURES

	Page
1. Histogram . . . . .	(7)
2. Deflections of the vertical . . . . .	(14)
3. The components of the deflection of the vertical. . . . .	(15)
4. The relationship between geodetic-grid-measured-Azimuth . . .	(21)
5. Second correction of angle D.D.R. . . . .	(24)
6. Second correction of angle D.R.P. . . . .	(24)
7. Second correction of angle R.P.D. . . . .	(24)
8. Second correction of angle P.D.D. . . . .	(24)
9. Difference between the coordinates without and with the second term corrections of a testing traverse. . . . .	(26)
10. Refraction in leveling. . . . .	(32)
11. Example of the relationship between temperature and height. .	(33)
12. Total errors of earth curvature and refraction. . . . .	(36)
13. Errors of closure of testing and classified leveling. . . . .	(37)
14. Solar altitude. . . . .	(42)
15. Reflected image of sun on the photograph. . . . .	(43)
16. Graph to show camera shutter speed and aircraft speed require- ments for limiting forward image blur on photos flown at a given height. . . . .	(50)
17. Image motion of a testing flight at 1500 feet above the ground	(51)
18. Film shrinkage. . . . .	(52)
19. Relationship between the focal length and systematic film shrinkage . . . . .	(52)
20. Accuracies of the tested instruments. . . . .	(55)

21.	Accuracies of the tested instruments (continued) . . . . .	(56)
22.	Earth curvature in x direction. . . . .	(61)
23.	Earth curvature in z direction. . . . .	(62)
24.	Photogrammetric refraction. . . . .	(65)
25.	Snell's law of refraction . . . . .	(65)
26.	Refraction at a boundary between two layers . . . . .	(66)
27.	Standard target for Washington State Highways . . . . .	(69)
28.	Transference of scale in aerotriangulation. . . . .	(70)
29.	Swing errors in the strip . . . . .	(72)
30.	Longitudal bend of a strip. . . . .	(75)
31.	Transversal tilt of a strip . . . . .	(77)
32.	ASR-33 teletype terminal with cards reader. . . . .	(82)
33.	IBM 2780 remote teleprocessing terminal . . . . .	(82)
34.	Layout of ground control points of test strip 1 . . . . .	(84)
35.	Comparison of discrepancies resulting from different adjustment of test strip 1 . . . . .	(85)
36.	Layout of ground control points of test strip 2 . . . . .	(88)
37.	Comparison of discrepancies resulting from different adjustment of test strip 2 . . . . .	(89)
38.	Layout of ground control points of test strip 3 . . . . .	(92)
39.	Comparison of discrepancies resulting from different adjustment of test strip 3 . . . . .	(93)
40.	Layout of ground control points of test strip 4 . . . . .	(96)
41.	Comparison of discrepancies resulting from different adjustment of test strip 4 . . . . .	(97)
42.	Layout of ground control points of test strip 5 . . . . .	(100)
43.	Comparison of discrepancies resulting from different adjustment of test strip 5 . . . . .	(101)
44.	Layout of ground control points of test strip 6 . . . . .	(104)
45.	Comparison of discrepancies resulting from different adjustment of test strip 6 . . . . .	(105)

46.	Layout of ground control points of test strip 7 . . . . .	(108)
47.	Comparison of discrepancies resulting from different adjustment of test strip 7 . . . . .	(109)
48.	Layout of ground control points of test strip 8 . . . . .	(112)
49.	Comparison of discrepancies resulting from different adjustment of test strip 8 . . . . .	(113)
50.	Layout of ground control points of test strip 9 . . . . .	(116)
51.	Comparison of discrepancies resulting from different adjustment of test strip 9 . . . . .	(117)
52.	Layout of ground control points of test strip 10. . . . .	(120)
53.	Comparison of discrepancies resulting from different adjustment of test strip 10. . . . .	(121)
54.	Layout of ground control points of test strip 11. . . . .	(124)
55.	Comparison of discrepancies resulting from different adjustment of test strip 11. . . . .	(125)
56.	Layout of ground control points of test strip 12. . . . .	(128)
57.	Comparison of discrepancies resulting from different adjustment of test strip 12. . . . .	(129)
58.	Layout of ground control points of test strip 13. . . . .	(132)
59.	Comparison of discrepancies resulting from different adjustment of test strip 13. . . . .	(133)
60.	Layout of ground control points of test strip 14. . . . .	(136)
61.	Comparison of discrepancies resulting from different adjustment of test strip 14. . . . .	(137)
62.	Layout of ground control points of test strip 15. . . . .	(140)
63.	Comparison of discrepancies resulting from different adjustment of test strip 15. . . . .	(141)
64.	Layout of ground control points of test strip 16. . . . .	(144)
65.	Comparison of discrepancies resulting from different adjustment of test strip 16. . . . .	(145)
66.	Layout of ground control points of test strip 17. . . . .	(148)
67.	Comparison of discrepancies resulting from different adjustment of test strip 17. . . . .	(147)

68.	Layout of ground control points of test strip 18. . . . .	(152)
69.	Comparison of discrepancies resulting from different adjustment of test strip 18. . . . .	(153)
70.	Layout of ground control points of test strip 19. . . . .	(156)
71.	Comparison of discrepancies resulting from different adjustments of test strip 19. . . . .	(157)
72.	Layout of ground control points of test strip 20. . . . .	(160)
73.	Comparison of discrepancies resulting from different adjustment of test strip 20. . . . .	(161)
74.	Layout of ground control points of test strip 21. . . . .	(164)
75.	Comparison of discrepancies resulting from different adjustment of test strip 21. . . . .	(165)
76.	Layout of ground control points of test strip 22. . . . .	(168)
77.	Comparison of discrepancies resulting from different adjustment of test strip 22. . . . .	(169)
78.	Layout of ground control points of test strip 23. . . . .	(172)
79.	Comparison of discrepancies resulting from different adjustments of test strip 23. . . . .	(173)
80.	Layout of ground control points of test strip 24. . . . .	(174)
81.	Comparison of discrepancies resulting from different adjustment of test strip 24. . . . .	(177)
82.	Layout of ground control points of test strip 25. . . . .	(180)
83.	Comparison of discrepancies resulting from different adjustments of test strip 25. . . . .	(181)
84.	The relationship between standard errors, flight height . . . . .	(186)
85.	Generalized flow for data rejection and adjustment. . . . .	(192)
86.	Test strip for data rejection . . . . .	(193)

## CHAPTER I

### INTRODUCTION

#### I-1. Background

Highway Engineering Surveys are optimized through proper application of photogrammetry. The greatest optimization or cost savings are realized through establishing supplemental controls by aerotriangulation. Of course, it is necessary to attain the greatest accuracy possible under standard production techniques.

However, the accuracy of the aerotriangulation is dependent upon the ground control surveying, photographic quality, and photogrammetric process which may contain mistakes or systematic errors. The consideration and correction of those systematic errors or mistakes in terms of their sources could improve the final results.

For example, in the traverse computation the application of the second term correction effects the azimuth up to 5 seconds in a 22 mile course. On this course, the northing changed 3 feet, easting changed 1.0 feet. If these points appear in the aerotriangulation adjustment, the results of the transformed coordinates will contain relative errors.

On the other hand, the image displacement on the diapositives are nonuniform, and are large enough to create errors of three feet or more in the transformed points. (Flight height = 3000 feet)

Preparation of ground control data normally has a reasonable amount of checking of arithmetic work. For example: angle note reductions are rechecked by another person; computer traverse input data forms are checked the same way. Nevertheless, human errors are overlooked. Transcribing work is plagued by transpositions and control points are misinterpreted and misidentified.

Usually there are enough redundant control points so that a blunder in one can be detected by examining residual errors. The point with the largest residual error is removed from the control group and the strip is recomputed.

The above system usually produces reliable adjustments after three or more passes through the computer. However, as the number of erroneous points increase the difficulty of detection radically increases, resulting in excessive entries to the computer. Excessive man hours in analysis or remeasurements of ground control points cause disastrous delays to project scheduling. Therefore, the aerotriangulation operation must be based upon a complete knowledge of the fundamental problems in all phases of the geodetic computation, photographic and photogrammetric processings in order to detect the errors in the adjustment of aerotriangulation.

## I-2. The Purpose and Scope of the Investigation

This investigation's principal aim is to establish routines that will detect erroneous data that make strip adjustments too inaccurate for highway engineering surveys. This is to be accomplished by the study of the application

of the theoretical and empirical methods to aerotriangulation considering the different errors of ground control surveying, photographic processing, and aero-polygon, aero-leveling.

A major problem in refining and certifying aerotriangulation adjustments for mapping control is the detection and isolation of erroneous ground control points. One possible solution to this problem is the development of an automated editing routine to check the errors in the adjustment.

The theoretical studies and testing of sources of ground control survey errors should be keyed on the following problems:

1. Azimuth adjustment prior to traverse computation.
2. Effect of earth curvature on surveys in the plane coordinate system.
3. Atmospheric refraction effects in precise leveling.

The theoretical and testings of sources of errors in aerial photographs should cover the following problems:

1. The relationship between flight height and accepted errors.
2. Solar altitude.
3. Image motion.
4. Film shrinkage and distortion.

The magnitude of errors to be expected using the photogrammetric instruments such as Zeiss stereo-planigraph C8; Zeiss stereo comparator PSK; Wild Autograph A7, A8, B8; Santoni IIC; and Kelsh plotters will be determined.



The mathematic and numerical analysis of a testing strip and computer program for a strip adjustment using a computer system should be developed on the basis of data from a large number of models and strips of medium to low altitude photography to determine the accuracies that can be expected from flight strips of given height, lengths, and with various distributions and densities of control points. The results will be expressed in the polynomial equation to be used to determine if the standard errors of the aerotriangulation will meet the requirements of Highway Engineering.

Finally, an automated editing computer program will be written and using the above standard errors as parameters, will automatically detect and isolate erroneous or misidentified ground control points in strip or block adjustment in order to save man hours, computer time and maintain project schedules in spite of erroneous control.

### I-3 Error Analysis

#### I-3-1 Definition of the Errors:

The adjustment of aerotriangulation deals with those errors which were introduced during the measurement of the ground control surveying, photogrammetric processings, and the error propagation of the bridging process according to the three types of existing errors, namely blunders, systematic, and accidental.

Blunders are caused by faults and mistakes during the working procedure such as misrecordings; however, sometimes blunders include also the theoretical errors for example; most textbooks of surveying

have given a questionable theory of systematic refraction in precise levels as reverse of the correction of the earth curvature; however, the correction of systematic refraction may be as much as the correction of the earth curvature and may have the same sign.

Systematic errors are those errors whose influence on the measurement always follows a certain mathematical function. For example, the systematic film shrinkage should be corrected by changing the principal distance for analogue instruments. Results show that the principal distance of changing 0.1mm will affect the elevation of a control point up to 0.4 feet at the flight height of 1500 feet. The sign of systematic errors can be negative or positive depending upon the fixed mathematical law which they follow. Constant and systematic errors must always be detected and either the correction to the measurement must be established using the mathematical function or their source must be eliminated. Aerotriangulation adjustment does not deal with systematic errors of the ground surveying and photogrammetric processings, only accidental errors of those and sytematic errors of aero-polygon and aero-leveling can be adjusted.

Accidental errors are those small errors which are due to the imperfectness of the instrument, the film, the flight height, of the aircraft, and the observer. This type of error has a changing sign and quantity. In the case of an infinite number of measurements, the number of positive errors is equal to the number of negative errors. Since it is impossible to have an infinite number of measurements, the true value cannot be computed, but the most probable value which is computed from a definite number of measurements with the help of adjustment computation

must be as close to the true value as possible.

### I-3-2 Standard Error:

In the aerotriangulation adjustment, the standard error is always an indicator related to the accuracy of the project involved, and the adjustment normally assumes only the existence of accidental errors. It is, therefore, required to have a mathematical conception of the limit of the standard errors of various flight heights in order to detect the systematic errors or blunders.

Accordingly, the Gaussian theory of errors is based upon the following conception:

- A. Small errors are more frequent than large ones.
- B. The arithmetic mean is the best value of a quantity.
- C. Probability of negative and positive errors is equal.

This can be represented in graphical form. On the X axis, it indicates the class intervals, and the classes are represented in the form of columns. The number of deviations represented in each class or column can be plotted on the Y axis of the graph, and obtain a certain form of distribution of errors which is called a histogram. The histogram is represented in Figure 1.

Fig. 1 expresses the accidental errors of a Wild A-7 single model, photographs taken at 1500 feet.

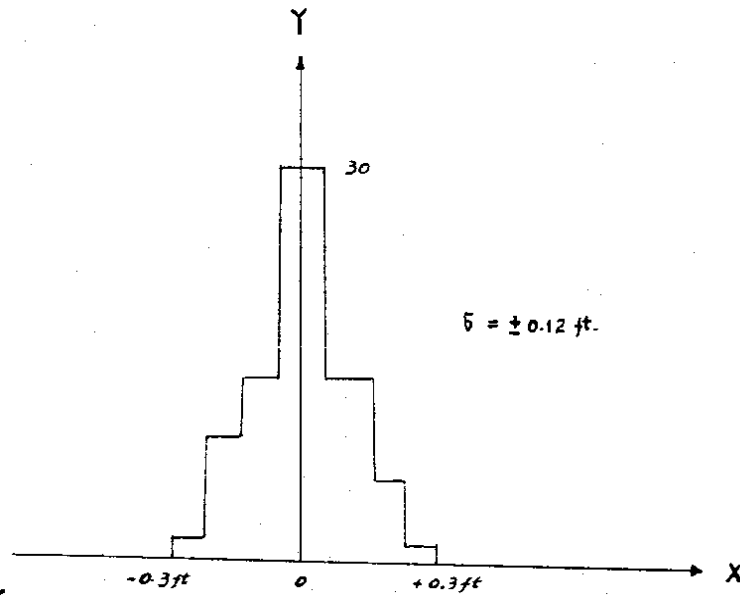


Fig. 1. Histogram

An exact value of a known measurement is defined as:

$$E_i = M_i - T_i \quad (1)$$

where

E = True error

M = Measured value

T = True value

i = 1 to n

If the measurements  $n'$  is equal to infinity, it is evident that the sum of the accidental errors would be equal to zero, but since  $n'$  will never be as great as infinity, it is desirable to express the errors as a sum of the squares of the individual errors, which is called a standard error mathematically.

$$\sigma^2 = \frac{E_1^2 + E_2^2 + \dots + E_n^2}{n}$$

$$= \frac{(EE)}{n}$$

or

$$\sigma = \sqrt{\frac{(EE)}{n}} \quad (2)$$

$\sigma$  means in this definition the square root of the arithmetic mean of the squares of all  $E_1, \dots, E_n$  and is the statistical expression for each of the errors.

This is the common equation of the standard error for the photogrammetric measurements. However, if the photographs are taken at 300 feet

above the ground, the accuracies between the ground control surveying and aerotriangulation will be equal. Therefore, the ground control surveying cannot assume an exact value, as shown in equation (2).

Thus, one must determine the corrections  $V$  for  $\bar{5}$ .

One assumes the true value of the average  $X$  to be  $T'$  and would obtain the true errors  $E$  as in equation (1):

$$\begin{aligned} E_1 &= M_1 - T' \\ E_2 &= M_2 - T' \\ &\dots\dots\dots \\ E_n &= M_n - T' \end{aligned} \tag{1}$$

The corrections with respect to the average  $X$  is

$$\begin{aligned} X &= \frac{M_1 + M_2 + M_n}{n} \\ V_1 &= X - M_1 \end{aligned} \tag{3}$$

$$[V] = nX - \sum[M] = 0$$

and consequently

$$\begin{aligned} E_1 &= -V_1 - (T'-X) \\ &\dots\dots\dots \\ E_n &= -V_n - (T'-X) \end{aligned} \tag{4}$$

---


$$[E] = [V] + n(T'-X)$$

Applying this expression to  $n'$  measurements, one finds

$$\begin{aligned}
 E_1^2 &= V_1^2 + (T-X)^2 + 2V_1 (T-X) \\
 &\dots\dots\dots \\
 E_{n'}^2 &= V_{n'}^2 + (T-X)^2 + 2V_{n'} (T-X) \qquad (5)
 \end{aligned}$$


---


$$[EE] = [VV] + n' (T-X)^2 + 2 (T-X) [V]$$

According to equation (3),  $[V] = 0$ ; thus

$$\begin{aligned}
 [E] &= n' (T-X) \\
 \text{and} \\
 [EE] &= [VV] + n' (T-X)^2 \\
 &= [VV] + \frac{[E]^2}{n'} = [VV] + \frac{1}{n'} (E_1 + E_2 + \dots + E_{n'})^2 \qquad (6)
 \end{aligned}$$

Substitution of the value  $[EE]$  from equation (2) into (6) and one obtains

$$\begin{aligned}
 n'^2 &= [VV] + \sigma^2 \\
 \text{or} \\
 \sigma^2 &= \frac{[VV]}{n'-1} \\
 \text{or} \\
 \sigma &= \sqrt{\frac{[VV]}{n'-1}} \qquad (7)
 \end{aligned}$$

In this equation one can determine the standard error of the individual measurements directly from the corrections  $V$ .

## CHAPTER II

### GROUND CONTROL ERRORS

#### 2-1. Background.

The horizontal and vertical ground control points for aerotriangulation adjustment usually take the form of a traverse and precise levels. These points should be connected to trigonometric stations and bench marks.

The measurements of the angles, distances, and elevations are unable to provide a true value because the results of any measurement always contain certain errors which were introduced during measuring. Such errors can be categorized as mistake, systematic, and accidental, which were presented in an earlier chapter.

However, many textbooks and published papers have also expressed the wrong theories in the traverse and leveling computations, and lead to errors. This chapter will serve to prove and correct those errors in ground control surveying.

#### 2-2. Deflection of the Vertical from Geodetic and Astronomic Azimuth

##### 2-2-1 Introduction:

According to reference [10] "The traverse is a method of surveying



in which the lengths and angles between the adjacent points of the network are measured in previous by azimuths determined in previous surveys or by astronomical means," and "Azimuth closure is the difference between an azimuth at a point that has been computed from a known azimuth using the field observed angles of the traverse and an azimuth at the point that has been previously determined. The known azimuths may have been determined astronomically."

The astronomic azimuths are not quite the same as those determined by a geodetic survey. In theory and practice, the geodetic azimuth is normal to the ellipsoid; (Fig. 2) and the measured astronomic azimuth is gravity acted upon the physical surface of the earth, which represents the equipotential surface (Geoid), the difference between astronomic and geodetic azimuth is the deflection of the vertical. Therefore, the previously determined azimuth is not identical with the observed astronomic azimuth. The investigation herein presented serves to show how the deflection of the vertical for azimuth in traverse should be made.

#### 2-2-2 Deflection of the Vertical of Azimuth

The standard method of obtaining the deflections of the vertical consists of determining geodetic coordinates  $(\phi_G, \lambda_G)$  of a trigonometric point, observing its astronomic position  $(\phi_A, \lambda_A)$  and obtaining the deflection components in the meridian  $\varphi$  and prime vertical  $\chi$  from the relationship on Fig. 3.

In the triangle  $PZ'F$ , is a very small angle, thus

$$PZ' = PF$$

and the deflection of the vertical in latitude can be obtained:

$$\begin{aligned} \zeta &= PZ - PF = PZ - PZ' = (90^\circ - \phi_G) - (90^\circ - \phi_R) \\ &= \phi_R - \phi_G \quad (8) \end{aligned}$$

where

$\zeta$  = deflection of the vertical in latitude

$\phi_G$  = geodetic latitude

$\phi_R$  = astronomic latitude

P = North pole

In order to construct the deflection of the vertical in longitude, equation (9) may be used:

$$\sin \alpha' = \frac{\sin \eta}{\sin (90^\circ - \phi_R)}$$

or

$$\alpha' = \eta \sec \phi_R \quad (9)$$

where

$\alpha'$  = deflection of the vertical in longitude =  $\lambda_R - \lambda_G$

$\eta$  = deflection component in prime vertical

The deflection of the vertical in azimuth may follow from Fig. 3 that:

$$A_A - A_G = (\varepsilon' - \varepsilon) + (\mu' - \mu) \quad (10)$$

where

$A_G = \varepsilon + \mu$  = ellipsoid azimuth

$A_A = \varepsilon' + \mu'$  = astronomic azimuth

T = point of terrestrial target

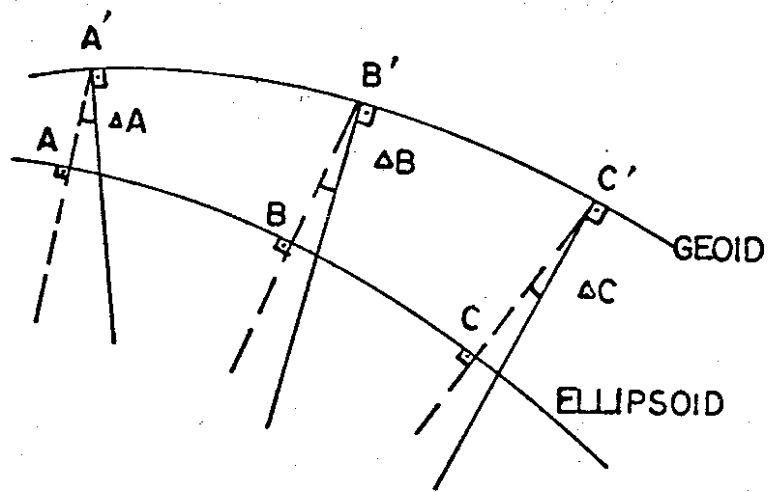


Fig. 2. Deflection of the vertical.



When the law of contangent in the triangle PZZ' is used, the component of  $(\varepsilon' - \varepsilon)$  of equation (10) has the form:

$$\cot(90^\circ - \phi_A) \sin D = \cos D \cos(180^\circ - \varepsilon') + \sin(180^\circ - \varepsilon') \cot \varepsilon$$

or

$$\begin{aligned} D \tan \phi_A &= -\cos \varepsilon' + \sin \varepsilon \cdot \frac{\cos \varepsilon}{\sin \varepsilon} \\ &= -\frac{\sin(\varepsilon' - \varepsilon)}{\sin \varepsilon} \end{aligned}$$

thus

$$\varepsilon' - \varepsilon = D \sin \varepsilon \tan \phi_A \quad (11)$$

Substitution of the value of  $\chi = D \sin \varepsilon$  into equation (11) we obtain:

$$\varepsilon' - \varepsilon = \chi \tan \phi_A \quad (11)$$

It follows also from Fig. 3 that:

$$\cot(90^\circ - h'') \sin D = \cos D \cdot \cos \mu + \sin \mu \cot(180^\circ - \mu')$$

or

$$\begin{aligned} D \cdot \tan h'' &= \cos \mu - \sin \mu \frac{\cos \mu'}{\sin \mu'} \\ &= \sin \mu' \cos \mu - \cos \mu' \sin \mu \\ &= \frac{\sin(\mu' - \mu)}{\sin \mu'} \end{aligned}$$

therefore:

$$\sin(\mu' - \mu) = D \cdot \tan h'', \sin \mu'$$

$$\text{or} \quad (12)$$

$$\mu' - \mu = D \cdot \tan h'' \cdot \sin \mu'$$

where

$h''$  = vertical angle of the terrestrial target

After substitution of the values from (11), (12) into (10), we will have:

$$A_R - A_G = \eta \tan \phi_A + D \cdot \sin \mu' \cdot \tan h'' \quad (13)$$

It is known, that the vertical angle of terrestrial target  $h''$  is always small, thus

$$A_A - A_G = \eta \tan \phi_A \quad (14)$$

Taking into account that  $\eta = \alpha' \cos \phi_A$ , the computed deflection of vertical in azimuth can be derived by equation (15).

$$\begin{aligned} A_A - A_G &= \alpha' \cdot \sin \phi_A \\ &= (\lambda_A - \lambda_G) \cdot \sin \phi_A \quad (15) \end{aligned}$$

or

$$A_G = A_A - \Delta$$

where

- $\Delta = (\lambda_A - \lambda_G) \cdot \sin \phi_A =$  deflection of the vertical
- $A_A =$  observed astronomic azimuth
- $A_G =$  geodetic azimuth
- $\lambda_A =$  astronomic longitude
- $\lambda_G =$  geodetic longitude
- $\phi_A =$  astronomic latitude

This is the well-known Laplace equation. The deflection of the vertical may be as much as five seconds and contain an error about ten times greater than the probable errors of astronomic azimuth observation for second order traverse, therefore, when astronomic azimuths are used to check the angles of a long traverse, it is necessary also to determine the geographic position, "latitude and longitude" for the computation of the deflection of the vertical.

### 2-2-3 Conclusion:

The astronomic azimuths are not quite the same as those determined by a geodetic survey. It should be pointed out, that reference [52] should be included, also the standard of accuracy for the determined geographic positions.

## 2-3 Earth Curvature Corrections of Traverse Computation

### 2-3-1. Introduction:

Computation of traverse data in a plane coordinate system must consider differences in geodetic angles from grid angles which are a result of spherical excess. Some questions have been raised regarding the instructions for application of second term corrections contained in literature published by the U.S. Const. and Geodetic Surveys. [46], [62]

A demonstration of proper application of second term corrections is contained in this chapter. It explains why, when, and how the azimuth correction of the second term should be made.

### 2-3-2. Second Term Correction

The geodetic azimuth is not identical with the grid azimuth; however, the computed grid azimuth is equal to the geodetic azimuth minus the angle of meridian, convergence of the grid, plus the corrections of the second term. The computed grid azimuth does not equal the measured azimuth. The relationship between the geodetic azimuth, computed grid azimuth, and measured

grid azimuth are shown graphically in Fig. 4.

N indicates grid North, N' is geodetic North, O' shows the angle of meridian convergence on the grid. AB represents the connecting line between the points A and B on the grid. If one would observe point B at point A, his sight becomes AB' (the tangent to the line observed, which is caused by the earth curvature). Therefore, the measured grid azimuth M ~~does not equal~~ the computed azimuth C.

The definitions of the Azimuths G, M, and C are as follows:

G = Geodetic Azimuth: This is the angle from geodetic North to the point observed.

M = Measured Grid Azimuth: This is the angle on the grid from grid North to the tangent to the line observed, at the station occupied.

C = Computed Grid Azimuth: This is the angle from the grid North to a straight line on the grid running from the point of observation to the point observed or defined as:

$$C = \text{arc tan } \frac{X_2 - X_1}{Y_2 - Y_1} \quad (16)$$

Where  $X_1, Y_1$  are the coordinates of the point of observation instrument station, and  $X_2$  and  $Y_2$  are those of the target point observed.

S = Second term = Correction of curvature = Azimuth Correction. This is the difference between the observed grid azimuth and the computed azimuth.



Now the following relationship can be used for Azimuth Computation:

$$G = M + O' \quad (17)$$

$$G = C + O' - S \quad (18)$$

$$M = G - O' \quad (19)$$

$$M = C - S \quad (20) \quad (18)$$

$$C = G - O' + S \quad (21)$$

$$C = M + S \quad (22)$$

$$S \text{ (seconds)} = \frac{(X_2 - X_1)}{2 \rho_e^2 \sin 1''} (Y_1 - Y_0 + \frac{Y_2 - Y_1}{3}) \quad (23)$$

where  $Y_0$  and  $\frac{1}{2 \rho_e^2 \sin 1''}$  can be taken from the tables. [46]

For traverse with courses shorter than three miles, the second term corrections are negligible.

For courses longer than three miles, the correction will be greater than 0.4 seconds, and should be applied in the computations.

Computation and application of the Second Term Corrections of a Traverse are as follows:

- A. Computation of the computed grid azimuth from given ground control points as in equation (16).
- B. Computation of preliminary coordinates (X,Y) of each point of a traverse in order to determine the second term correction in each course.

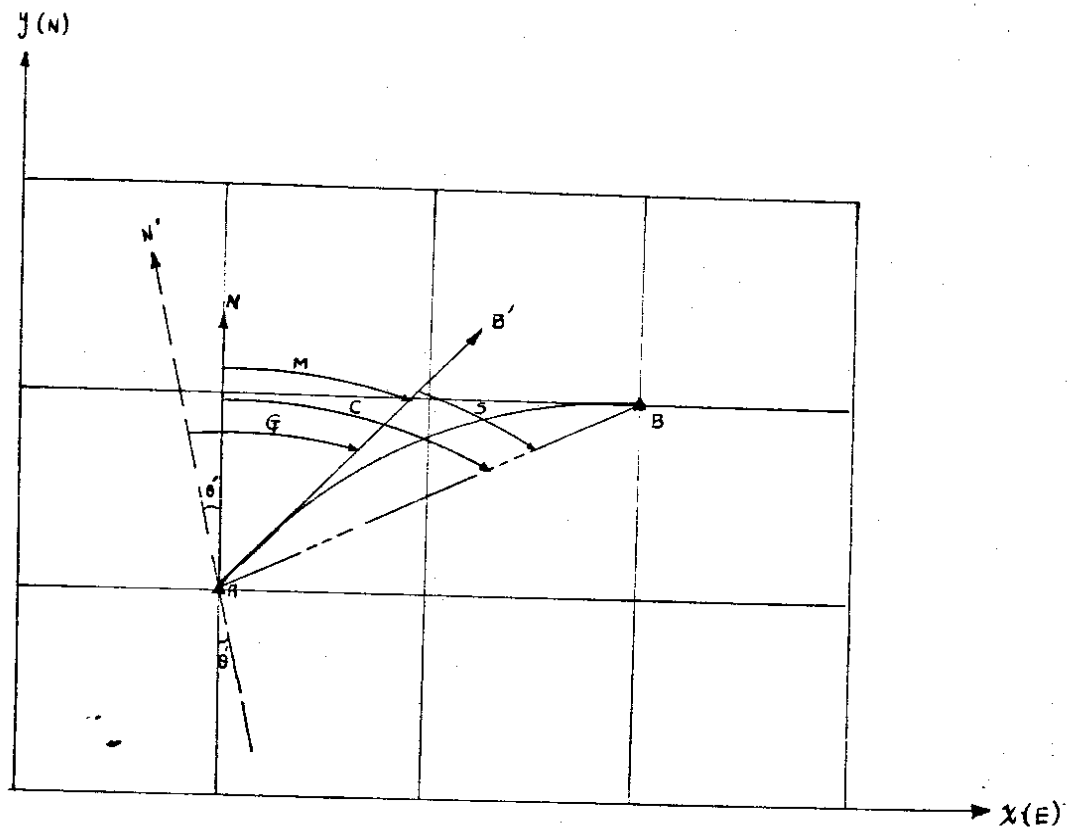


Fig. 4. THE RELATIONSHIP BETWEEN GEODETIC-, GRID-, MEASURED-AZIMUTH

C. Computation of the second term. (See Table 1 and Fig. 5, 6, 7, 8)

The angle correction of the second term is computed by the subtraction corrections to backsight from foresight with clockwise measurement.

D. Final computation and adjustment of the traverse by applying corrected azimuths.

2-3-3. Conclusion:

The demonstration traverse shows that application of the second term correction affects the azimuth up to five seconds in a 22-mile course. On this course, with azimuth of  $75^{\circ}$  (approximate), the northing changed +2.76 feet, and the eastings changed -0.65 feet (see Table 2 and Fig. 9).

This correction for azimuth determination of the ground surveying can now be incorporated into the Washington State Highway Department's surveys procedure.

Point To	From	Second Term	Measured Angle	For.-Back Sight	Cor. Angle
Delm	Delphi	0			
Rock	Delphi	+0.3"	32° 04' 09.7"	+0.3"	32° 04' 10.0"
Delphi	Rock	-0.3"			
P-40	Rock	+4.6"	227° 38' 02.9"	+4.9	227° 38' 07.8"
Rock	P-40	-4.8"			
Delm	P-40	-5.1"	357° 22' 07.3"	-0.3	357° 22' 07.0"
P-40	Delm	+4.8"			
Delphi	Delm	0	102° 55' 41.3"	-4.8	102° 55' 36.4"

Table 1. The second term corrections for azimuth computation.

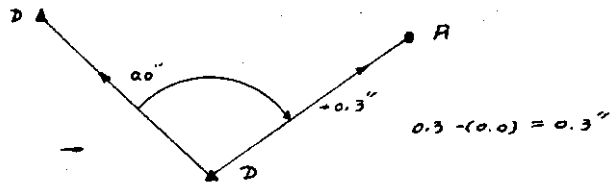


Fig. 5. Second correction of angle D.D.R.

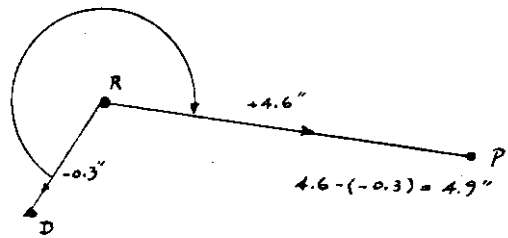


Fig. 6. Second correction of angle D.R.P.

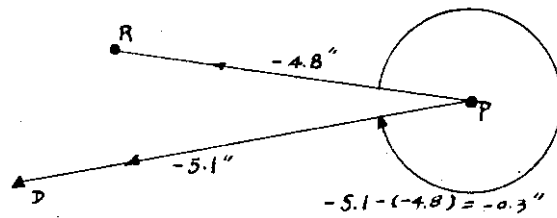


Fig. 7. Second correction of angle R.P.D.

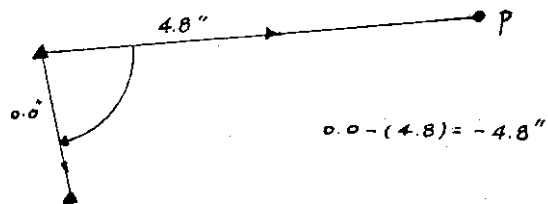


Fig. 8. Second correction of angle P.D.D.

Points	Y(N)			X(E)		
	with	without	diff.	with	without	diff.
Begin: Delphi	608908.88	608908.88	0.00	1341533.25	1341533.25	0.00
Rock	621748.93	621748.92	0.01	1349025.41	1349025.43	+0.02
P-40	646019.62	646022.38	+2.76	1462227.72	1462227.07	-0.65
End: Delm	614238.47	614238.47	0.00	1341365.22	1341365.22	0.00

Table 2. Comparison of the coordinates computed with and without second term corrections.

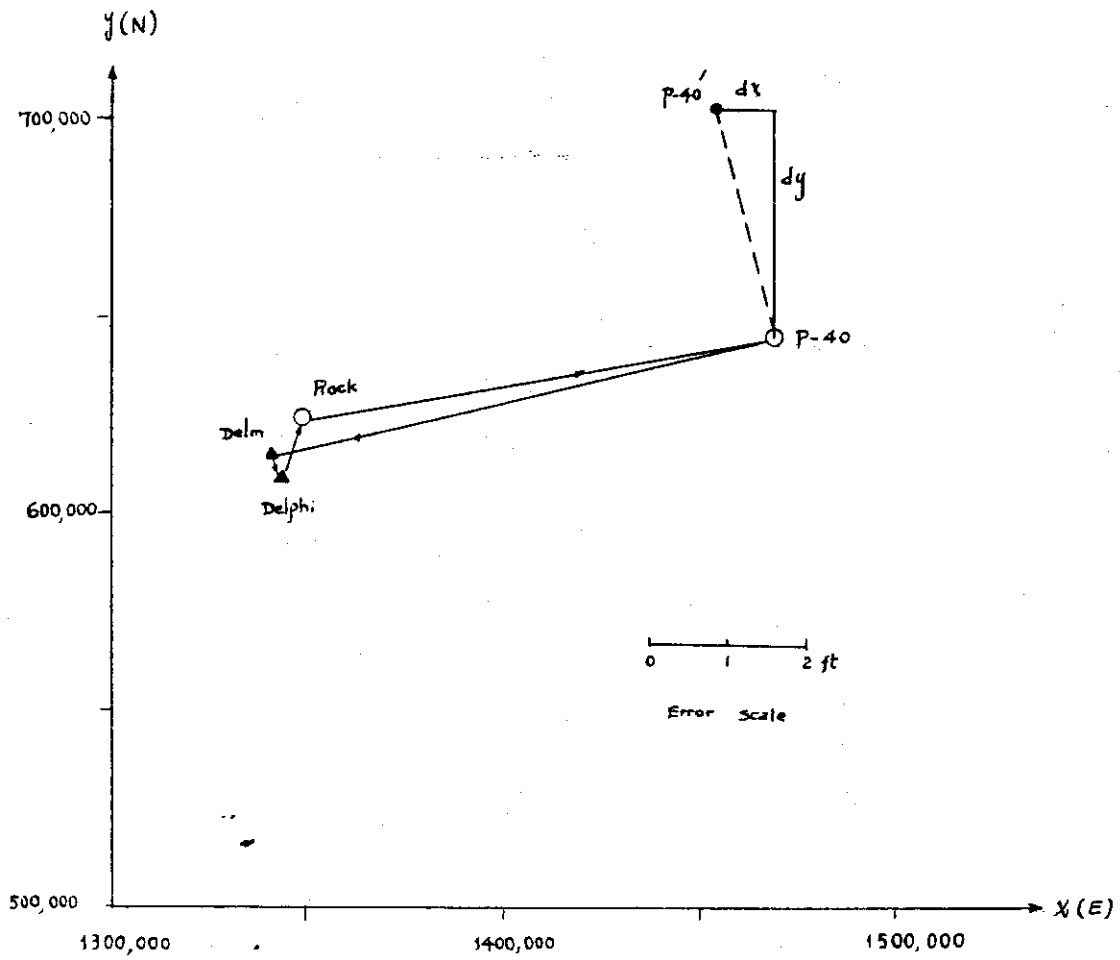


Fig. 9. DIFFERENCE BETWEEN THE COORDINATES WITHOUT AND WITH SECOND TERM CORRECTIONS OF A TESTING TRAVERSE

## 2-4 Refraction of the Precise Leveling

### 2-4-1 Introduction

In precise levels, systematic errors can be caused by such factors as: earth curvature, refraction, instrument error, settling (or subsiding of instrument and rods during the measurement), rods out of plumb, inaccuracy of rod intervals and personal reading errors. According to textbooks on surveying [34], [9], [43], the refraction of the curved atmosphere bends the line of sight downward. Kukkamaki [35] developed a new formula for terrestrial systematic refraction which states that the deflection of sight, due to refraction from the horizontal line in a distance of 200 feet is 0.001 feet upward when the temperature near the earth's surface is greater than at 10 meters above. This investigation herein presented serves to prove that the complete derivation of systematic refraction can be arrived at by general forms.

### 2-4-2 Theory of Systematic Refraction in Precise Leveling

Horizontal lines taken by an instrument as back sight and fore sight become curved lines by refraction. This phenomenon occurs when a light ray passes through atmosphere layers of different densities. Under real conditions, the air temperature decreases with increasing heights above the earth surface, and affects the refractive index of the atmosphere which in turn influences the sights observed with levels.

The systematic refraction index is related to the refractive index of standard air, which can be expressed by an approximate formula [57]:

$$(n_0 - 1) \cdot 10^6 = 6432.8 + \frac{2949810}{140 - 1/\lambda^2} + \frac{25540}{41 - 1/\lambda^2} \quad (24)$$



Where pressure  $P = 760$  mm Hg (hydrargyrum) at  $0^\circ\text{C}$  and  $g_0 = 980.665$  cm/sec<sup>2</sup>, temperature =  $+15^\circ\text{C}$  and carbon dioxide (Co<sub>2</sub>) content 0.03% by volume at  $0^\circ\text{C}$  and wavelength  $\lambda$  is measured in microns.

According to H. Burrell and J. E. Sears [3], or Jordan [27], or Hoepcke [14], the relationship between refractive index  $n$  and the refractive index  $n_0$  of the standard air is given by the following formula:

$$(n-1) = \frac{(n_0-1)P}{(1+2t)760} - \frac{5.5 \cdot 10^{-8}}{(1+at)} \lambda \quad [25]$$

where

$n$  = index of refraction

$n_0$  = refractive index of standard air

$a$  = coefficient of linear expansion = 0.00367

$P$  = pressure at mm Hg.

$\lambda$  = vapor pressure at mm Hg.

$t$  = temperature at  $^\circ\text{C}$

If the temperature is assumed as absolute centigrade degree ( $T = 273.16 + t$ ), equation (25) can be rewritten as (26).

$$(n-1) = (n_0-1)0.3594 \frac{P}{T} - 15.02 \cdot 10^{-6} \frac{\lambda}{T} \quad (26)$$

Differentiation of equation (26) and considering that only the change of the temperature affected the index of refraction of precise levels and the numerical value of  $dp, d\lambda$  can be omitted without noticeable error, then:

$$dn = \frac{1}{T^2} [(n_0-1)0.3594P - 15.02 \cdot 10^{-6}\lambda] dT \quad (27)$$

Taking the value of wavelength  $\lambda = 0.56$  micrometers and  $n_0 = 1.0003$  into account, after minor computation, one obtains:

$$dn = \frac{-1}{T^2} [100.63P - 15.02e] \cdot 10^{-6} dT \quad (28)$$

In this equation, if the temperature changes  $1^\circ\text{C}$  in the range from  $0^\circ\text{C}$  to  $30^\circ\text{C}$ , and pressure  $P = 750$  to  $680$  mm Hg. and  $e = 0$  to  $10$  mm Hg., the mean effect for the index of refractions is obtained:

$$dn = -1.10^{-6} dt \quad (29)$$

In equation (29)  $dt$  stands for temperature between two stations of different elevations, thus:

$$dt = t - t_0 \quad (30)$$

where

$t$  = temperature at point  $h$  on plumbline of instrument

$t_0$  = temperature at point  $h_0$  on plumbline on instrument (See Fig. 10)

Under real conditions, an increase of altitude is reflected by decrease of temperature, therefore, we find varied values of temperatures at different elevations. It is possible to express them in polynomial form as a function of height by using the method of least squares, thereby fitting the sum of squares of all errors to a curve expressing a minimum of error. Thus, the temperature  $t$  may be adequately represented by:

$$t = a + bh + ch^2 + dh^3 \quad (31)$$

and the polynomial expression for the temperature is plotted in Fig. (11)

where

$a, b, c, d$  = the coefficients

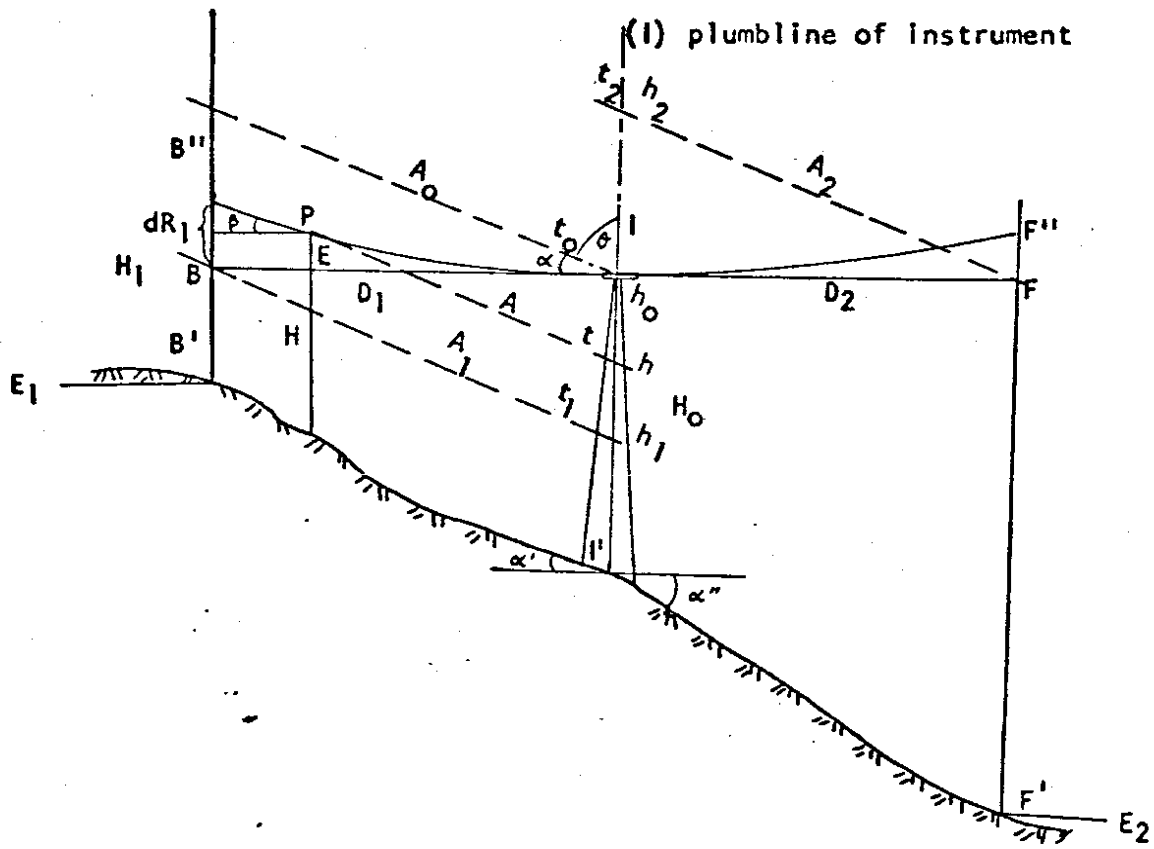


Fig. 10 Refraction in leveling

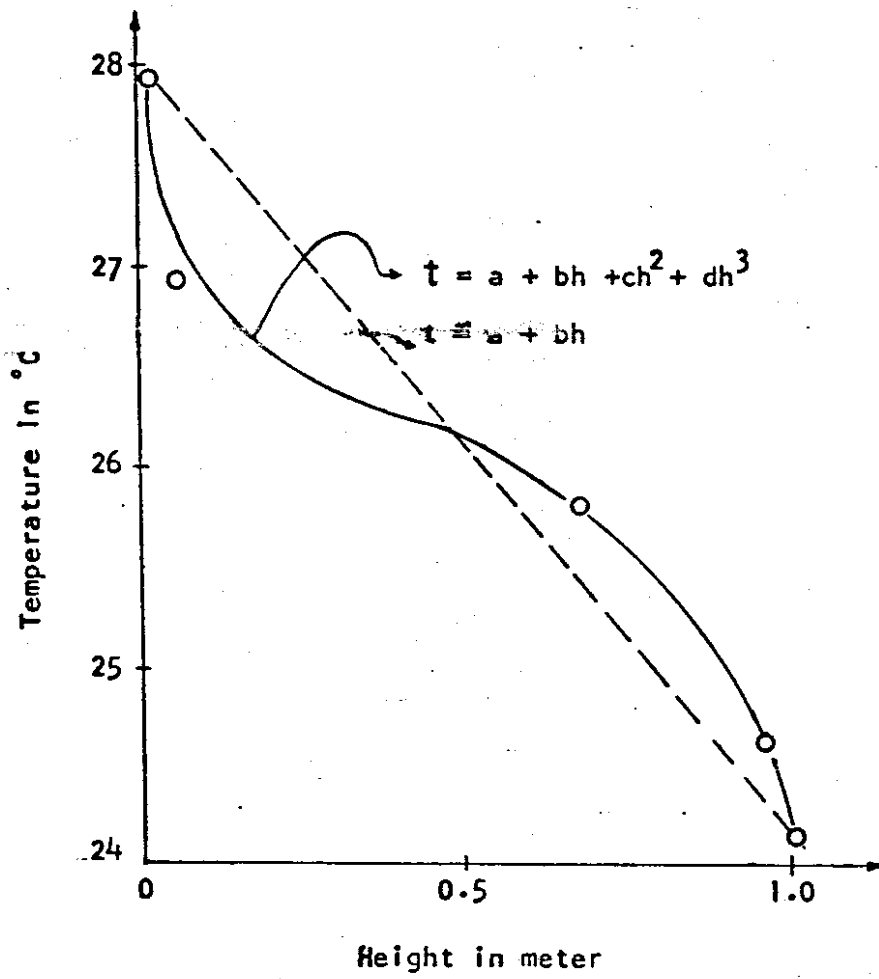


Fig. 11 Example of the relationship between temperature and height

A number of formulas have been used in the past to relate height to temperature. An extensive discussion of these is given by Jordan [28]. The best agreement found, however, is presented by equation (31) of this publication. It should be recognized that these various equations are essentially empirical. For the practice of precise leveling, equation (31) may be assumed as a linear equation, thus:

$$t = a + bh \quad (32)$$

The relationship between temperature and elevation in precise levels can be seen from Fig. 10. The straight BF indicates a horizontal line. B'B'' and F'F'' are the reading of back sight and fore sight. D<sub>1</sub>, D<sub>2</sub>, are the length between the instrument station I and two rods. E<sub>1</sub> and E<sub>2</sub> are the elevation of B.F points. dR<sub>1</sub> is the error of refraction in leveling of back sight. Lines A<sub>0</sub>, A, A<sub>1</sub>, A<sub>2</sub> are the same atmospheric condition of height at h<sub>0</sub>, h, h<sub>1</sub>, h<sub>2</sub> on plumbline of instrument I. Thus, equation (32) in different heights may be written by:

$$\begin{aligned} t_0 &= a + bh_0 \\ t &= a + bh \\ t_1 &= a + bh_1 \\ t_2 &= a + bh_2 \end{aligned} \quad (32)$$

The value of the temperature difference may be determined directly by equation (32) thus:

$$dt = t - t_0 = \frac{(t_2 - t_1)}{(h_2 - h_1)} \cdot (h - h_0) \quad (33)$$

Combining equation (29), (30), and (33) one obtains the deflection of

the index for refraction.

$$dn = 1.10^{-6} \frac{(t_2 - t_1)}{(h_2 - h_1)} \cdot (h - h_0) \quad (34)$$

According to Snell's law of refraction, when a light ray arrives at point I with an angle of  $\theta$  then (See Fig. 10)

$$n \cdot \sin \theta = \text{constant} \quad (33)$$

where  $\theta$  = angle between the light ray and the vertical axis of instrument

From Fig. 10 the angle  $\alpha = 90^\circ - \theta$  thus

$$n \cdot \cos \alpha = \text{constant} \quad (36)$$

The angle of refraction, that is the difference  $d\alpha$  between the values of  $\alpha$  can be expressed as a function of the difference  $dn$  between the indexes of refraction by differentiating equation (36) and gives the following relation between the absolute values of  $d\alpha$  and  $dn$  [57]

$$-n \cdot \sin \alpha \, d\alpha + \cos \alpha \, dn = 0 \quad (37)$$

and

$$d\alpha = \frac{\cot \alpha}{n} \, dn \quad (38)$$

Determining the angles of light rays,  $\beta$ , at any point, *f.e.* at "P" of Fig. 1. This may be accomplished by integrating equation (38), thus:

$$\beta = \int_{n_I}^{n_P} \frac{\cot \alpha}{n} \, dn \quad (39)$$

Where  $n_I, n_P$  are index of refraction at point I and p. If the index

of refraction stays constant = 1 and  $\alpha = \alpha' = \alpha''$ , then:

$$\beta = \cot \alpha' \cdot 10^{-6} \frac{(t_2 - t_1)}{(h_2 - h_1)} (h - h_0) \quad (40)$$

The correction of refraction in precise levels on IB is carried out by integrating in the following manner:

$$E = \int_0^D \beta \, dn = \cot \alpha' \cdot 10^{-6} \frac{(t_2 - t_1)}{(h_2 - h_1)} \int_0^D (h - h_0) \, dD \quad (41)$$

Take  $h = h_0 - \tan \alpha \cdot D$  and  $dD = -\cot \alpha'' \, dh$  into account. The total angle of correction over the interval between the height of instrument  $H_0$  and of backsight  $H_1$  may be found from

$$\begin{aligned} dR_1 &= \int_{H_0}^{H_1} E = \cot^2 \alpha' \cdot 10^{-6} \frac{(t_2 - t_1)}{(h_2 - h_1)} \int_{H_0}^{H_1} (h - h_0) \, dh \\ &= \cot^2 \alpha' \cdot 10^{-6} \frac{(t_2 - t_1)}{(h_2 - h_1)} \left[ \frac{H_1}{H_0} \frac{1}{2} H^2 - H_0 H \right] \\ &= \cot^2 \alpha' \cdot 10^{-6} \frac{(t_2 - t_1)}{(h_2 - h_1)} \left[ \frac{1}{2} (H_1^2 - H_0^2) - H_0 (H_1 - H_0) \right] \quad (42) \end{aligned}$$

Equation (41) shows the computation for the correction of systematic refraction to be applied in precise levels. The computations for the example are based on the instrument height of 4.5 feet, with a 1.5 foot height of backsight, 8.0 feet for fore sight. The temperature is assumed to change  $0.1^\circ\text{C}$  per foot [28]. The distance interval for rod-setting are from 30 ft. to 400 ft. (See Table 3 and Fig. 12)

The values of the refractive corrections in precise levels are identical with the one computed by Kukkamaki [25]. Thus the results can be regarded as sufficiently reliable.

The correction of refraction may be simply written:

$$dR_1 = -5 \cdot 10^{-8} \cdot D^2 \quad (42)$$

where

D = length of sight in feet and  $dR_1$  is also in feet.

#### 2-4-3. CONCLUSION:

Most textbooks of surveying have given the questionable theory of systematic refraction in precise levels. The correction of systematic refraction is as much as the correction of the earth curvature, (See Table 3) with same sign (-0.001 for 150 feet), meaning that the combined correction of the two causes for the length of 150 feet is 0.002 ft.

In interpreting the systematic errors in precise levels, the following facts should be taken into consideration:

Every value to be recorded in the field must be checked immediately in order to avoid mistakes, all systematic errors should be eliminated as far as possible, and the instrument should be tested before measurement.

The systematic errors of earth curvature, systematic refraction, and small instrument error must be eliminated by the balanced sights.

In order to avoid any error of the setting of instrument and rods, the tripod of instrument and footplates in their turning points must be securely set before measuring.



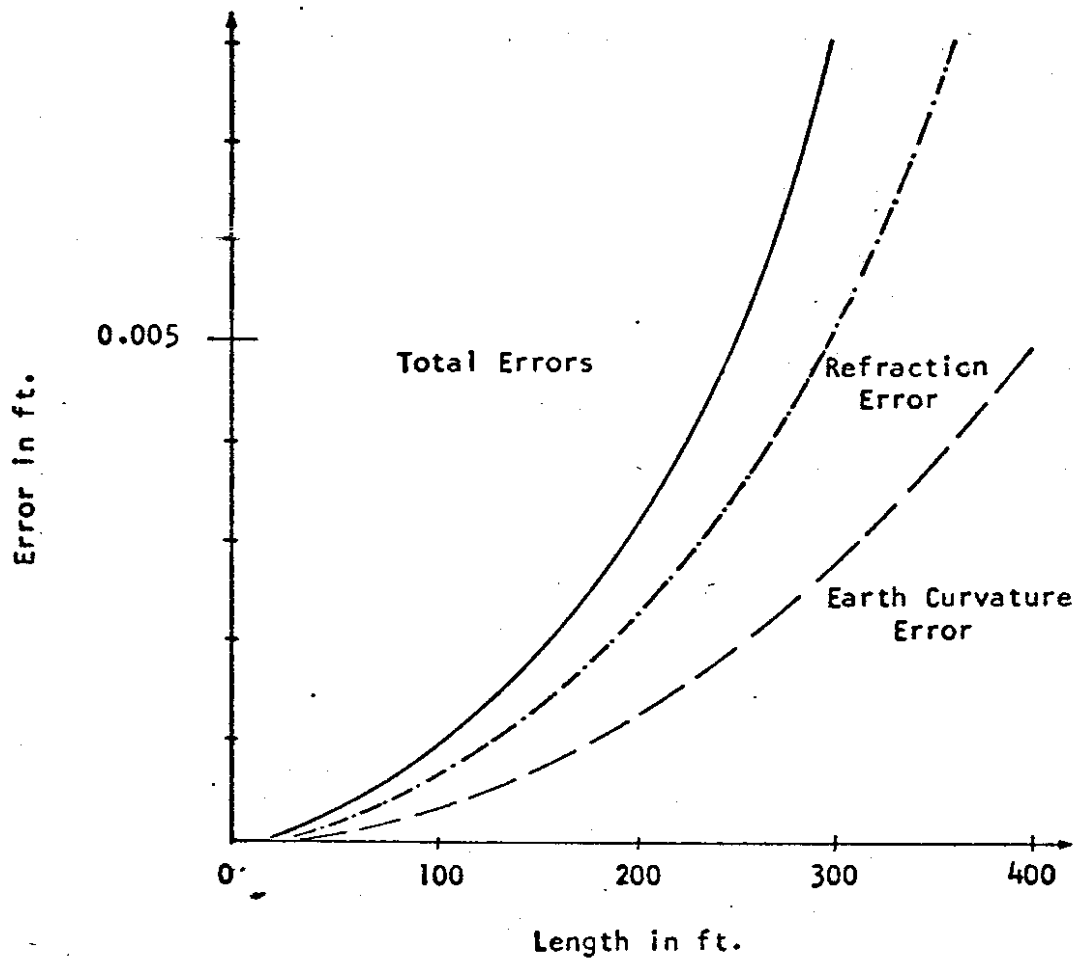


Fig. 12 Total errors of refraction and earth curvature

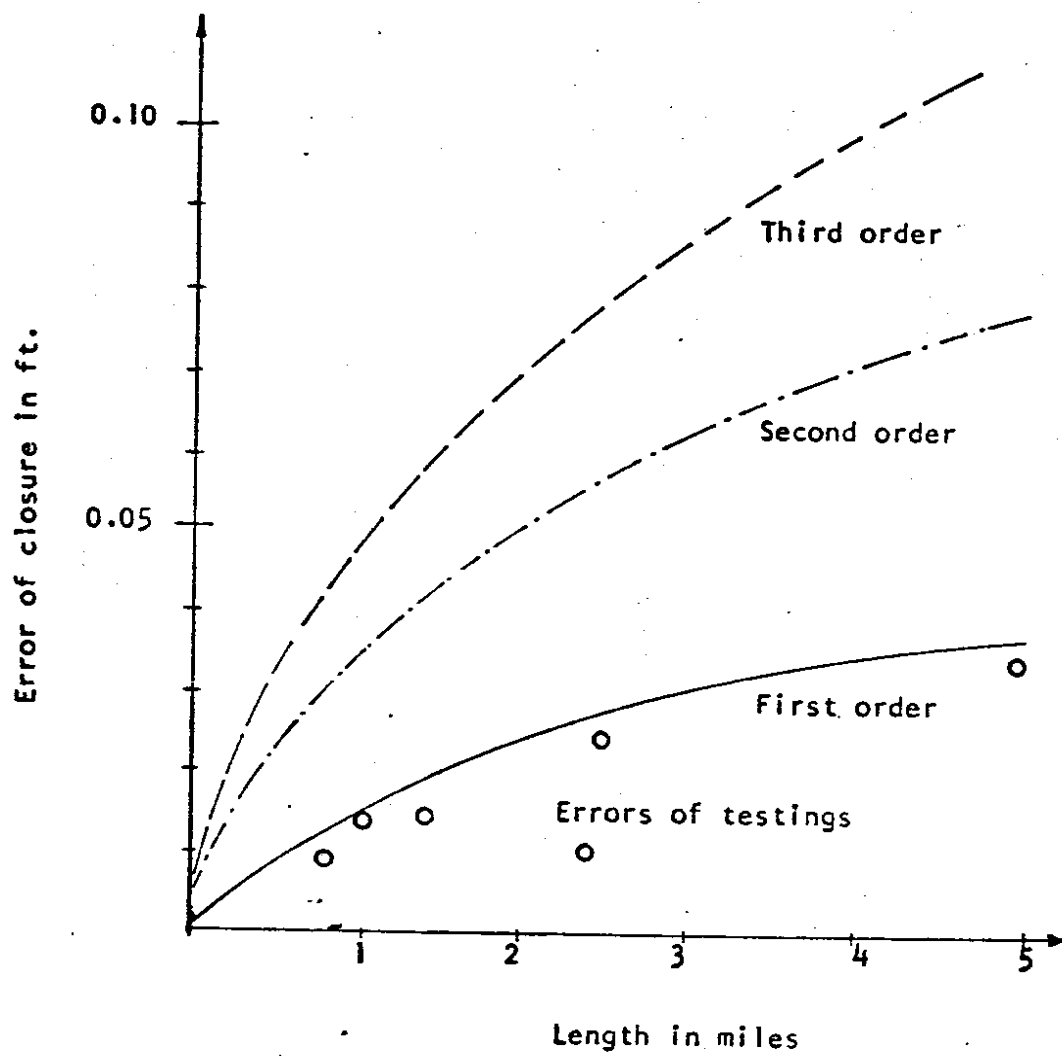


Fig. 13 Errors of closure for testing and classified leveling

Table 3. The corrections of refraction and earth curvature.

Distance ft.	Earth-Curvature ft.	Refraction ft.	Total Correction ft.
30	$-2.5 \cdot 10^{-5}$	$-5.7 \cdot 10^{-5}$	$-8.3 \cdot 10^{-5}$
60	$-1.0 \cdot 10^{-4}$	$-2.3 \cdot 10^{-4}$	$-3.3 \cdot 10^{-4}$
100	$-2.3 \cdot 10^{-4}$	$-5.2 \cdot 10^{-4}$	$-7.5 \cdot 10^{-4}$
150	$-6.4 \cdot 10^{-4}$	$-1.4 \cdot 10^{-3}$	$-2.0 \cdot 10^{-3}$
300	$-2.5 \cdot 10^{-4}$	$-5.7 \cdot 10^{-3}$	$-5.8 \cdot 10^{-3}$
900	$-4.5 \cdot 10^{-3}$	$-1.0 \cdot 10^{-2}$	$-1.4 \cdot 10^{-2}$

The error of unsystematic refraction in back and fore sights can be reduced by carefully choosing a location of the sight high enough above the ground, 1.5 ft.

According to test, the six testings of levels with Zeiss Ni-2 and yard rods, (hundredth of yard intervals), show all the closure errors within first order requirement. (See Fig. 13)

An extensive discussion of the theory of the density of the air change in the micro-climatic region when taking precise level is given by [25].

## CHAPTER III

### MAGNITUDE OF ERRORS IN PHOTOGRAPHS AND INSTRUMENT

#### 3-1. Introduction

In photogrammetric processes, the importance of high precision has been well recognized. Much work has been done over the years to improve camera design, to minimize lens distortion (max.  $5\mu$ ), and to provide better measuring instruments (1 to  $10\mu$ ). A very important component is the quality of the imagery, and this has been receiving increasing attention in recent years.

In considering the standard of accuracy required of a photograph, one should study the sources of errors in sequential steps of the photograph, which could be grouped in four parts.

1. Flight height of the photographs and solar altitude.
2. Image blur.
3. Lens distortion and film shrinkage.
4. Accuracies of instruments.

In this chapter, the mathematical and practical studies and testings of the image motion, film shrinkage, solar altitude, flight height, and instrument testings are explained. It gives the coupling of the theory and practical procedure of the image quality and provides a useful tool in the field of photogrammetry.

### 3-2. Flight Height of the Photographs

Governing requirements of aerial photography in mapping and its subsequent uses are dependent upon the extension of control points and parameters of project. Therefore, the flight height is of extreme importance. Usually the flight height is determined by the desired map scale, the contour interval to be used, and the characteristics of the plotting instrument. For example, the standard Kelsh type plotting map scale would be 1 inch to 50 feet scale for a given flight 1500 feet. It means that the Kelsh plotter with optimum projection distance compiles at 5 times magnification from negative to finished map. A universal plotting machine such as (Wild A-7) could draw the map from the negative exposed at 2700 feet directly at a scale of 1"/50' and meet all standards. However, in order to fulfill the requirements of accuracy for supplemental control as used for measuring profiles, cross sections, spot elevations, and the determination of points on property boundaries with a universal instrument; the flight height "H" may be expressed as a function of the acceptable error tolerance with an empirical constant as equation (43).

$$H = \frac{e}{k} \quad (43)$$

where

H = flight height

e = accepted error of horizontal or vertical points

K = 0.01% = empirical constant for using a 6-inch camera,  
such as Wild RC8

( see chapter v )

### 3-3. Solar Altitude

In order to shorten the objectionable shadows and eliminate hot spots (over-exposed areas owing to diffused reflection of sun), the solar altitude must be taken into consideration when taking photography. The value of the solar altitude is dependent upon the area, time of day, and the date. This can be computed from fig. 1 as follows:

$$\sin h = \sin \phi \cos \delta + \cos \phi \sin \delta \cos t \quad (44)$$

where

$h$  = altitude of the sun

$\phi$  = mean latitude of the area to be photographed

$\delta$  = declination of the sun

$t$  = hour angle of the sun

or

$$t^\circ = (\text{GMT}^h + 12^h + E) \cdot \frac{15^\circ}{1^h} - \lambda_w$$

$E$  = equation of the time

$\lambda_w$  = longitude

$\text{GMT}^h$  = Greenwich mean time

$$= (\text{LMT}^h + \text{Zone}^h)$$

$\text{LMT}^h$  = Local mean time

$\text{Zone}^h$  = hour angle between meridian of Greenwich

and the standard time zone

Since for most purposes a minimum solar altitude of  $20^\circ$  is considered necessary for satisfactory aerial photography, [40] photography should not



62

C-69-1-6

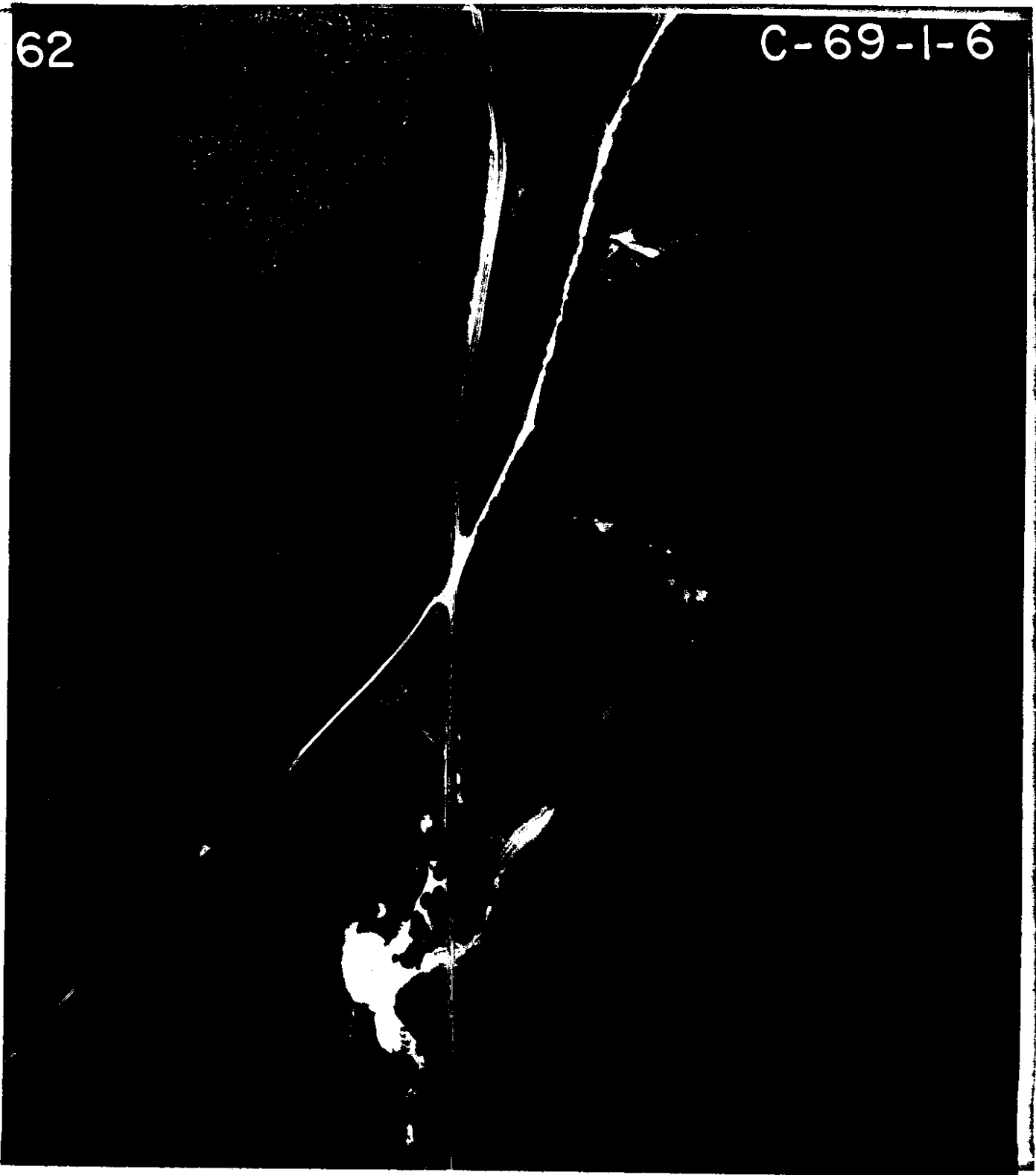


Figure 15. Reflected image of sun on the photograph.



be taken at a time when the computed solar altitude is less than this value in order to avoid the long shadows and darkness of the objects. During the time period when the solar altitude is over 45° (for Wild RC8, 6-inch camera) the reflected image of the sun is recorded on the photograph as shown in Fig. 15. It is then preferable to expose photography between certain time limits so that no hot spot will occur on the vertical negative from sun reflection.

### 3-4 Image Blur

The image motion is a function of the camera shutter speed and aircraft speed at a given flight height whose magnitude also depends upon the camera focal length, the location of the point on the image, and the camera orientation.

In the first consideration, if the camera is vertical, the image coordinates  $x, y, f$  may be obtained from ground coordinates system  $X, Y, H$  as equation (4):

$$x = f \frac{X}{H} \quad (45)$$

$$y = f \frac{Y}{H}$$

where

$x, y$  are the photo coordinates from principal points,  $f$  is the focal length,  $X, Y$  are the ground coordinates from nadir point (camera station) and  $H$  is the flight height.

If the ground points are in motion, there will be image motion in the focal plane, which is obtained by differentiation equation (45).

$$\begin{aligned}
 m_x &= \frac{dx}{dt} = \frac{H(dx/dt) - X(dH/dt)}{H^2} \\
 m_y &= \frac{dy}{dt} = \frac{H(dy/dt) - Y(dH/dt)}{H^2}
 \end{aligned}
 \tag{46}$$

In the second consideration, assume the motion of the perspective center of the camera station  $X, Y, H$  is rotated through the angles  $\omega, \varphi, K$  respectively to ground coordinate system  $X' Y' H'$ , ( $H = H'$ ), which can be written in the matrix form:

$$\begin{pmatrix} X \\ Y \\ H \end{pmatrix} = \begin{pmatrix} m_{11} & m_{12} & m_{13} \\ m_{21} & m_{22} & m_{23} \\ m_{31} & m_{32} & m_{33} \end{pmatrix} \cdot \begin{pmatrix} X' \\ Y' \\ H' \end{pmatrix}
 \tag{47}$$

or  $X = M \cdot X'$

where

$m$ 's are the elements of rotational  $M$  orthogonal matrix consisting of direction cosines or the exterior ( $\omega, \varphi, K$ ) orientation elements of the camera station.

$$m_{11} = \cos \varphi \cos \kappa ; m_{12} = \cos \varphi \sin \kappa ; m_{13} = -\sin \varphi$$

$$m_{21} = \sin \omega \sin \varphi \cos \kappa - \cos \omega \sin \kappa$$

$$m_{22} = \sin \omega \sin \varphi \sin \kappa + \cos \omega \cos \kappa$$

$$m_{23} = \cos \varphi \sin \omega$$

$$m_{31} = \cos \omega \sin \varphi \cos \kappa + \sin \omega \sin \kappa$$

$$m_{32} = \cos \omega \sin \varphi \sin \kappa - \sin \omega \cos \kappa$$

$$m_{33} = \cos \omega \cos \varphi$$

Differentiation of equation (47), one obtained:

$$\begin{pmatrix} dX/dt \\ dY/dt \\ dH/dt \end{pmatrix} = M \cdot \begin{pmatrix} dX'/dt \\ dY'/dt \\ dH'/dt \end{pmatrix} \quad (48)$$

Assume X' is defined as the direction of the image motion, thus

$$dX'/dt = V \quad dY'/dt = 0 \quad dH'/dt = 0$$

where

V = velocity

Taking these into consideration, equation (48) may be carried out by the following components:

$$\begin{aligned} dX/dt &= m_{11}V \\ dY/dt &= m_{21}V \\ dH/dt &= m_{31}V \end{aligned} \quad (49)$$

Substituting equations (49) and (45) into equation (46), and considering the motion within the exposure time t, the general image motion equation can be obtained:

$$\begin{aligned} m_x &= \frac{Vt \cdot (fm_{11} - xm_{31})}{H} \\ m_y &= \frac{Vt \cdot (fm_{21} - ym_{31})}{H} \end{aligned} \quad (50)$$

where

t = exposure time

In the vertical photography of medium to low altitude (H = 12000 to 1500 or to 300 ft.), the rotation angles are always within a few degrees. If  $w = \varphi = K = 0$ , equation (50) may be rewritten as following:

$$\begin{aligned} m_x &= \frac{fVt}{H} \\ m_y &= 0 \end{aligned} \quad (51)$$

assume

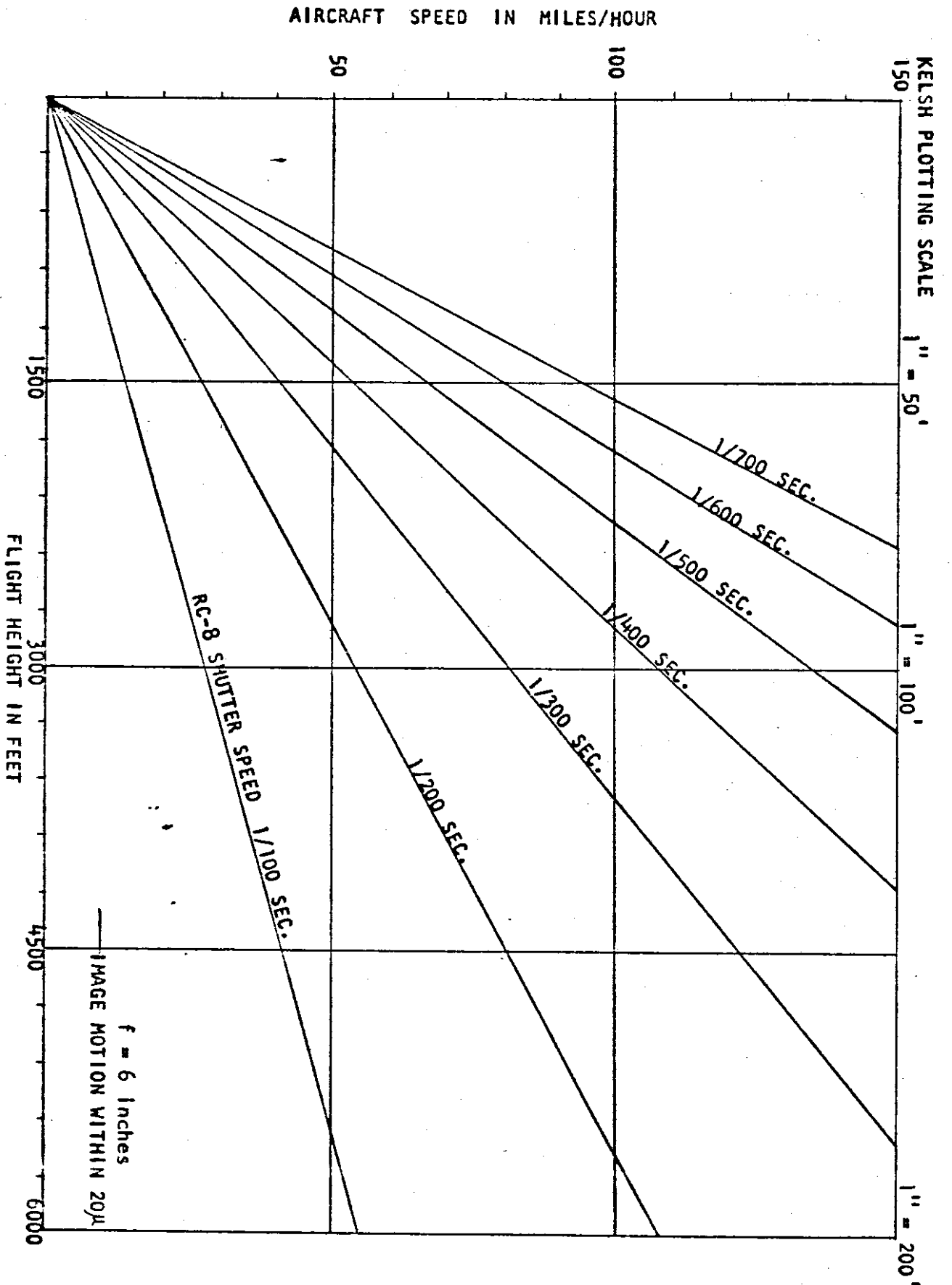
$w = \varphi = K = 2^\circ$ , the equation of image motion is:

$$\begin{aligned} m_x &= \frac{Vt}{H} (0.9998f - 0.002x) \\ m_y &= \frac{Vt}{H} (-0.144f - 0.002y) \end{aligned} \quad (52)$$

These show that the image blur depends on the aircraft velocity, rotation, and the image distance from the center of the format, the photo scale, and the camera shutter speed. It should be pointed out, the aircraft should have good stability in order to reduce the effects of blurred images caused by tilting at the time of exposure.

Fig. 16 shows the above relationships with an assumed tolerance of image blur of 20 microns. On the graph, using a flight height of 1500 feet and the speed of aircraft constant at 90 mile/hour, the shutter speed can be found to be 1/700 of a second. If the shutter speed chosen is 1/600, 1/500, and 1/400 of a second, the image motion will be blurred within 22, 27, and 34 microns respectively, which is shown in Fig. 17. It should be pointed out, that as the flight height increases the minimum limit of the shutter speed decreases if the aircraft speed remains constant.

FIG. 16 GRAPH TO SHOW CAMERA SHUTTER SPEED AND AIRCRAFT SPEED REQUIREMENTS FOR LIMITING FORWARD IMAGE BLUR ON PHOTOS FLOWN AT A GIVEN HEIGHT



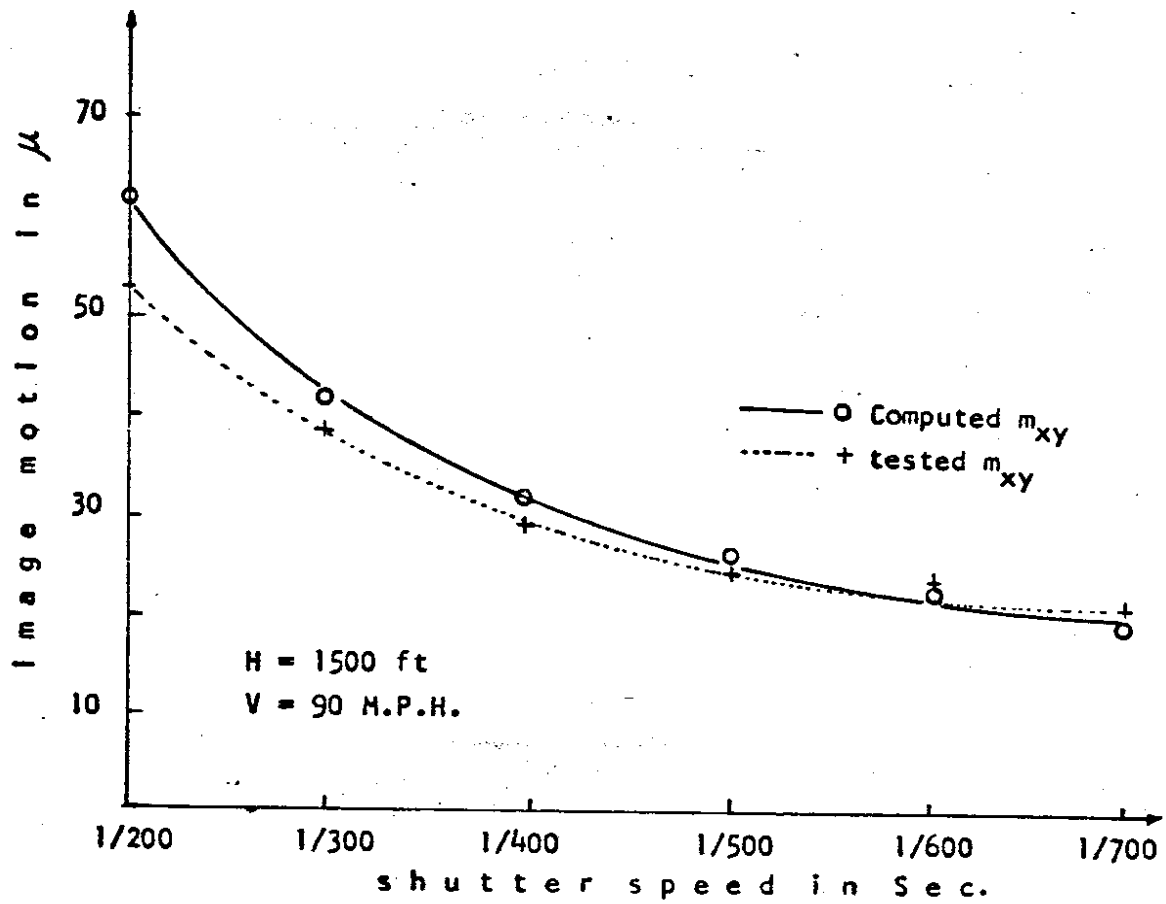


Fig. 17 Image motion of a testing flight at 1500 feet above ground.

For a very large scale map, such as requires the photographs be taken at 300 feet above the ground, helicopter may be used to reduce blurring due to motion. [66]

#### 3-4. Lens Distortion and Film Dimensional Change

The lens distortion results in a variation of the scale of an image. However, in ~~the photographic case~~ lens distortion keeps within limits of  $5 \mu$  to  $10 \mu$  (maximum), and the distortion values are given in a table or a curve which can be applied and corrected to the x, y image coordinates.

A very important factor is the distortion of film due to dimensional change, which may be uniform or nonuniform; the systematic distortions may be corrected for scale by principal distance changes, but the nonuniformity of dimensional change in different directions or areas of the film which will result in noncorrectable errors. Investigations of the nonuniform distortions in aerial film have been conducted by several research workers using a reseau exposed on the film, the displacement of the grid intersections up to 0.03mm (30 microns) was reported. [5]

The procedure used to study the maximum size changes of the film and diapositive by means of a flash plate has been used. The film (Dupont 114R) is exposed and after processing is contact printed onto the diapositive plate under controlled conditions, then the measurements of the four fiducial marks of the flash plate, film, and diapositive were made. The results of the measurements (Fig. 18) show that the

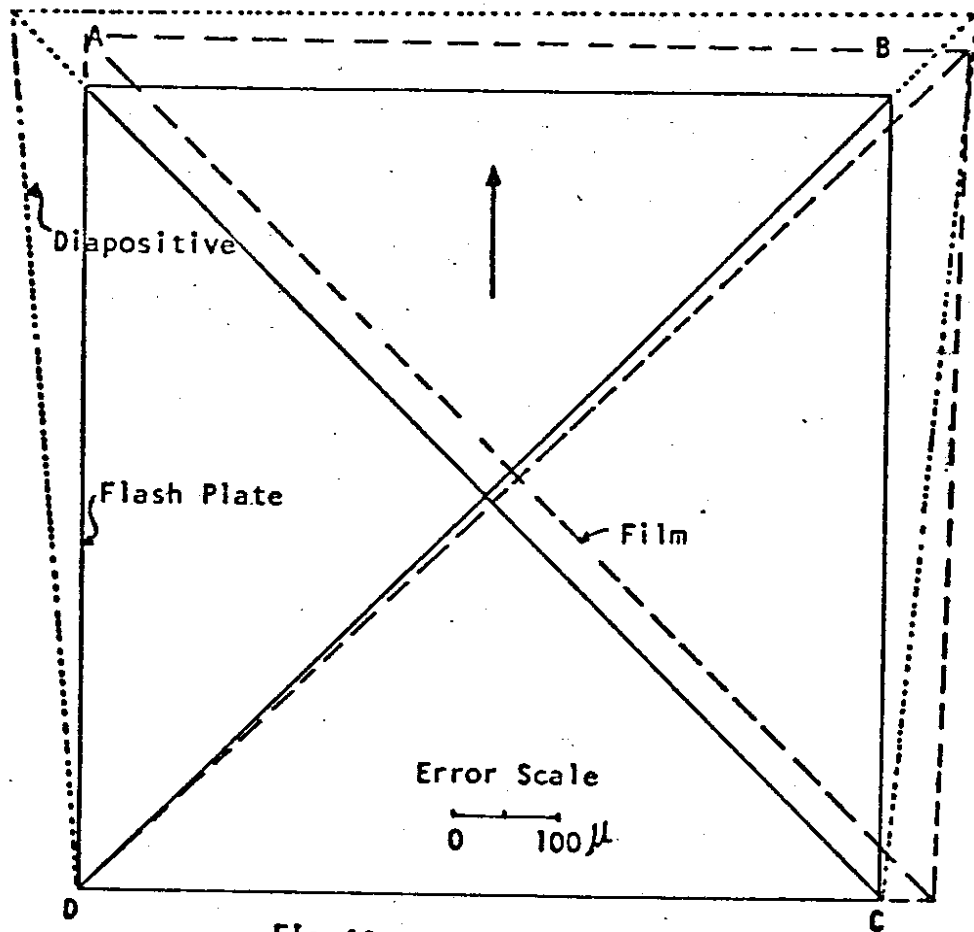


Fig. 18 Film Shrinkage

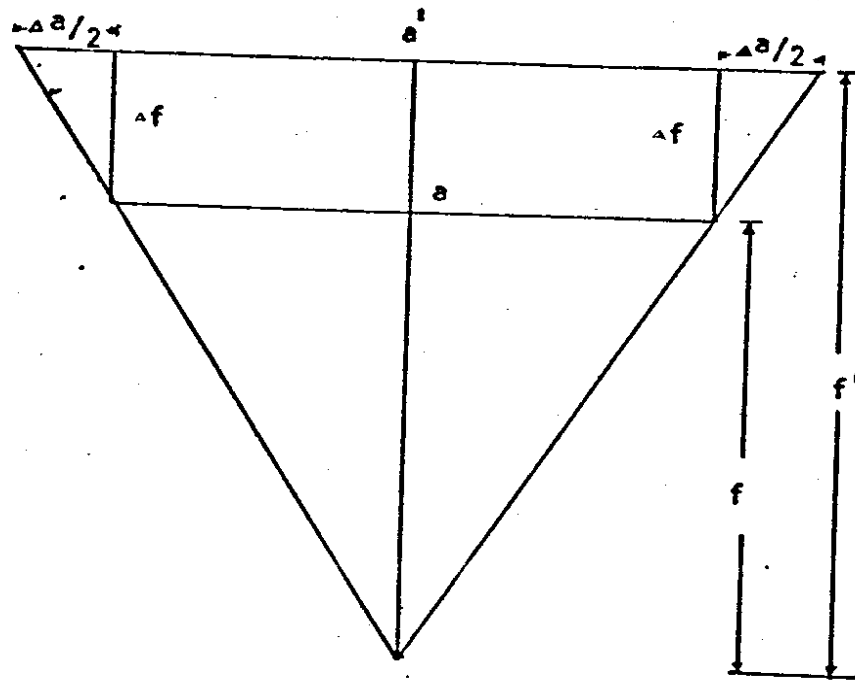


Fig. 19 Relationship between the focal length and systematic film shrinkage



film dimensional change is generally larger than is often assumed. The difference in the directions of DA, DB, DC in the film are overall systematically enlarged. (Maximum 0.07mm)

The systematical displacement of the film may be corrected by changing the focal length of the projectors for analogue plotters or by numerical refinements of the photo coordinates by using analytical photogrammetry.

According to Fig. 19, the relationship between the focal length and film shrinkage is as follows:

$$\Delta f = \frac{\Delta a}{a} f \quad (53)$$

where

$\Delta f$  = correction of the focal length of film dimensional change

$f$  = focal length of the camera

$\Delta a = a' - a$

$a$  = given distance between two fiducial marks

$a'$  = measured distance between two fiducial marks

A tested model (flight height = 1500 feet) shows that the focal length changed 0.1mm, effected in the elevation 0.4 feet on the ground.

If the principal distance is not changed for the film shrinkage, the affine restitution must be used in order to obtain the corrected elevation.

The affine factor can be computed from the given vertical control points and plotter or tracing table reading of the same points, thus:

$$A_f = \frac{\sum_{i=1}^n (G_i/M_i)}{n} \quad (54)$$

where

$A_f$  = mean affine factor

$M_i$  = given elevation of control points

$G_i$  = measured elevation of control points in plotter

$n$  = number of used control points

The relationship between the elevation measured on the model and given values can be calculated by:

$$\text{Elevation in ft.} = \frac{\text{measured value in plotter}}{A_f}$$

or

$$\text{Setting value in plotter} = A_f \times \text{elevation in ft. (given)}$$

However, the displacements of the diapositive are nonuniform, which shows a distortion greater than 100 microns and results in aerotriangulation transformed points of horizontal and vertical ground control points in error by three feet (nonuniform distortion caused the model deformation).

It should be pointed out, that this value refers to the nonuniformity in size change which cannot be corrected by simple magnification of the diapositive or by affine correction.

The displacement of film or diapositive image may be caused by the changes in temperature, relative humidity, tension of the film during the processing in the machine, water droplets left on the surface of the emulsion during drying, and the effect of the temperature and relative humidity changes during the processing from film to diapositive. Therefore, the temperature and the relative humidity of the film and diapositive processing must be carefully controlled according to the information given by the ~~film manufacturer~~.

### 3-5. Accuracy of the Instruments

The accuracy of photogrammetric results depend upon the photographic qualities of the image and also the precision of the measuring plotters. A test of a single model by using different instruments such as Zeiss Stereoplanigraph C-8; Stereo-Comparator PSK; Wild Autograph A-7, A-8, B-8; Santoni IIC; and Kelsh plotter has been made. The photographs were taken at an altitude of 1500 feet above the ground with Wild RC8 camera. There were 78 very accurately surveyed elevation points in the model, and the relative orientation (except PSK) was carried out in the usual manner. The measured instrument coordinates were then transformed to the ground coordinates system. The standard error of 78 check points was 0.24 feet for C-8, 0.18 feet for PSK, 0.14 for A7, 0.15 feet for A8, 0.16 feet for B8, 0.16 feet for Santoni IIC, and 0.23 feet for Kelsh, (Fig. 20, 21) which shows that the accuracies are approximately equal for the above instruments. (C-8 needs changing of the focal length for film shrinkage). However, the flight height has a direct bearing on the accuracy of photogrammetric measurements. The results of the testing

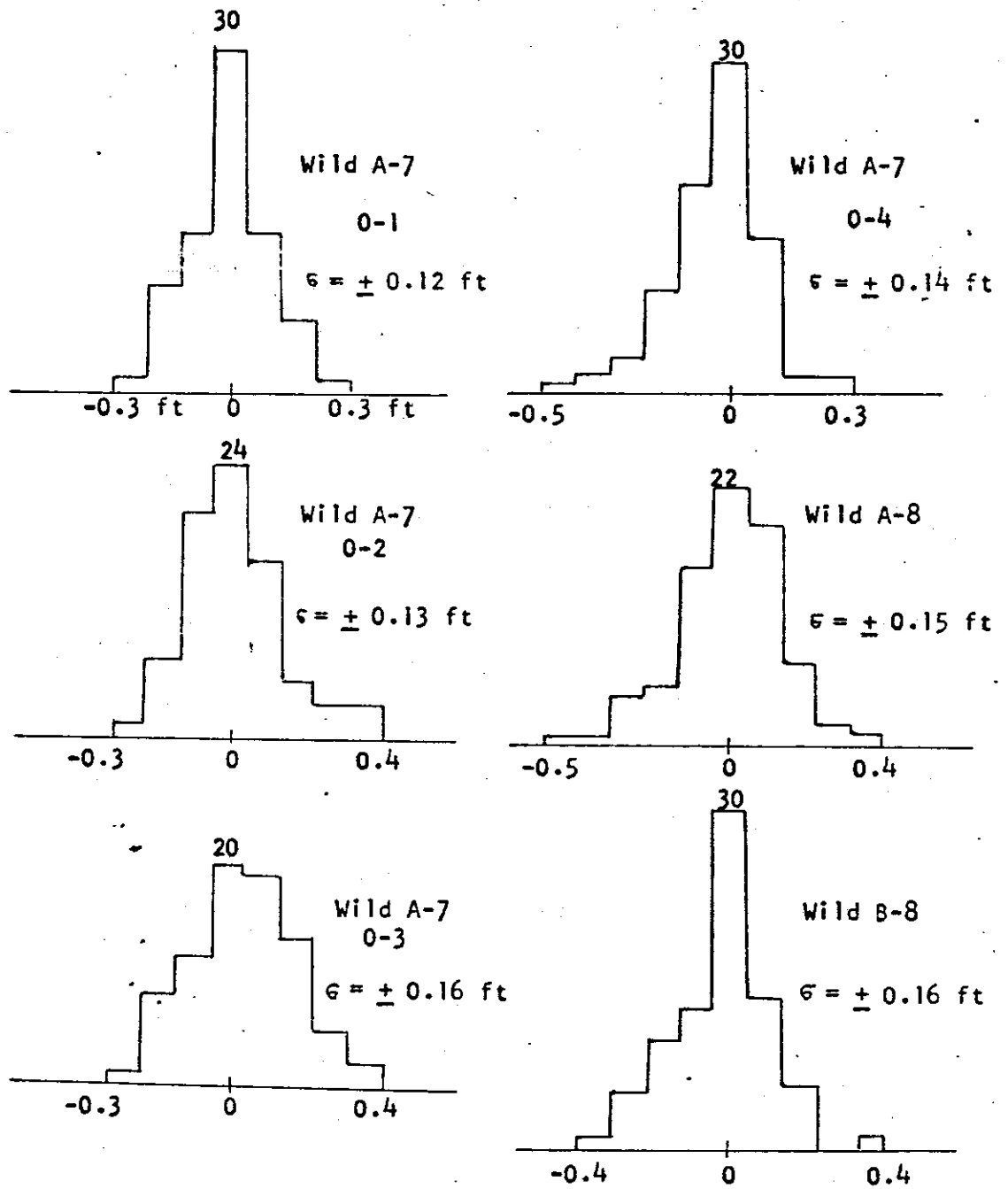
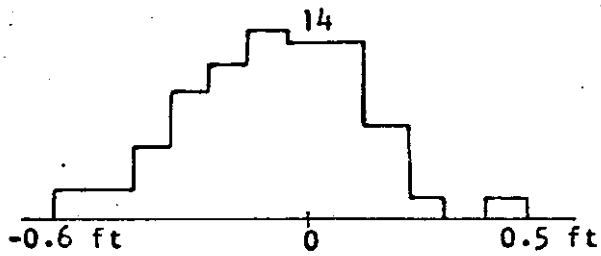


Fig.20 Accuracies of the tested instruments

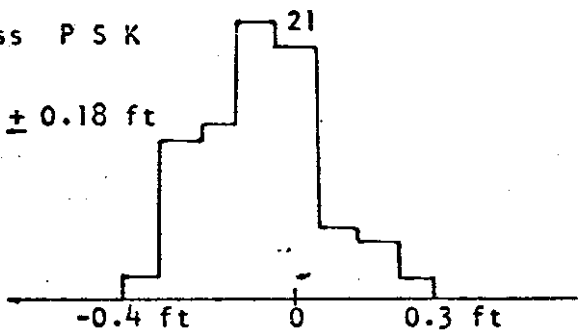
Zeiss C-8

(needs changing the focal length for film shrinkage)  
 $\sigma = \pm 0.24$  ft



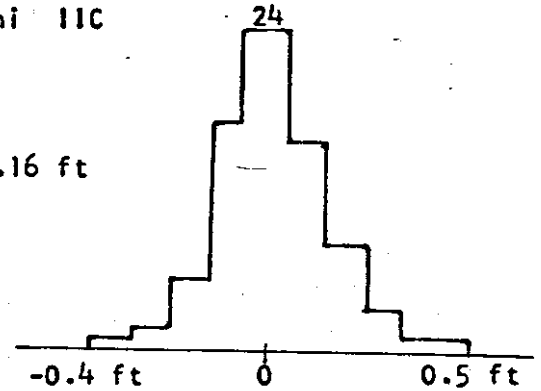
Zeiss P S K

$\sigma = \pm 0.18$  ft



Santoni IIC

$\sigma = \pm 0.16$  ft



Kelsh

0-1 —

$\sigma = \pm 0.17$  ft

0-2 ····

$\sigma = \pm 0.28$  ft

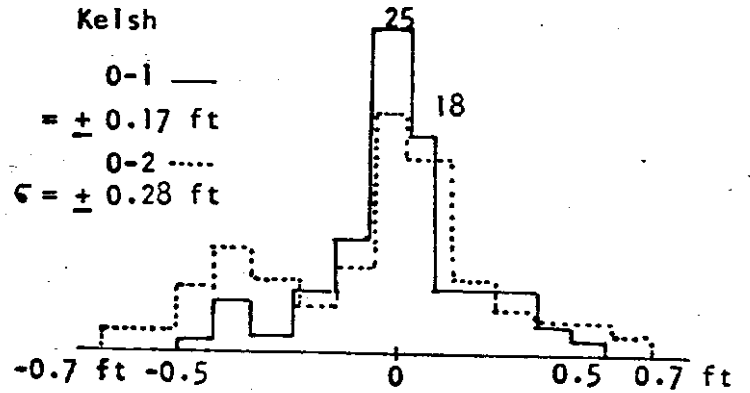


Fig. 21 Accuracies of the tested instruments (continued)

meet the requirements of the empirical equation (43) for the accepted error of a given flight height.

### 3-6 Conclusion

The results of this investigation show that the photogrammetric accuracies vary in accordance also with the three sources of errors:

1. Blunder: A blunder is a mistake in the photogrammetric process. Such as reflected image for solar altitude, image blurring, and improper processing of film and diapositives.

2. Systematic errors: A systematic error is an error that under the same conditions will always be of the same size and sign, such as lens distortion, systematic film shrinkage, instrument errors, and refractions.

3. Accidental errors: The accidental error is the difference between the measured value (free from blunders and systematic errors) and the known value.

All blunders must be avoided before photogrammetric processing, and all systematic errors should be eliminated or corrected as far as possible. The accidental errors are dependent upon the flight height, the model deformation, and the model point measurements. It could be concluded that all errors must be taken into consideration, no matter how well the other conditions are fulfilled.

## CHAPTER IV

### ERRORS OF THE AEROTRIANGULATION

#### 4-1. Introduction:

Aerotriangulation is a method for determining the ground positions of objects through Photogrammetric measurement of images in strips or blocks of overlapping aerial photographs using relatively few known ground control points. The photogrammetric strip coordinates are transformed to make a "best fit" with known ground surveyed coordinates by the application of polynomial curve fitting procedure.

The application and analysis of aerotriangulation requires a knowledge of the source of errors and error propagation laws throughout the strips.

The errors occurring in aerotriangulation, according to the procedures, are divided roughly into single model errors and strip errors. The single model errors of a stereotriangulation can be defined as a constant amount and sign, occurring in each model, such as lens distortion, earth curvature, refraction, film shrinkage, pointing errors, model deformation, etc. The strip may contain errors in scale, azimuth, longitudinal bend, and transversal tilt.

The single model errors were presented in an earlier chapter (III).

Strip errors will be explained in following procedures.

#### 4-2. Earth Curvature

The effect of the curvature of the earth along the length of the strip can be applied to x and z directions. The situations are shown in figures 22 and 23.

In these figures, a vertical photograph and a spherical reference surface for the earth are assumed.

The x coordinates recorded at the stereoplotting instrument correspond to the projection of the s distances onto the tangent plane through N. It is a well known fact that they are not identical with the correct geodetic s distances. From figure 22, the correction of x - direction is obtained.

$$dx = s - x$$

$$\text{since } s = \alpha \cdot R \text{ and } S = S'$$

$$dx = R \cdot \alpha - R \cdot \sin \alpha$$

$$= R \left( \alpha - \left( \frac{\alpha^3}{1!} - \frac{\alpha^3}{3!} + \frac{\alpha^5}{5!} - \dots \right) \right)$$

$$= R \left( \alpha - \alpha + \frac{\alpha^3}{6} - \dots \right) \quad (57)$$

$$\approx \frac{x^3}{6R^2}$$

The errors dx for the distance  $s_1, s_2, \dots, s_n$  between successive nadir points in x direction of a strip are:

$$dx_1 = 0$$

and



$$dx_3 = dx_1 + dx_2$$

.....

.....

.....

.....

$$dx_n = dx_1 + dx_2 + \dots + dx_{n-1}$$

assume  $dx_1 = dx_2 = dx_3 = \dots = dx_{n-1} = dx$

thus  $dx = (n-1)dx_1$  (59)

where  $n = \frac{x}{b}$

and  $n =$  number of the models  
 $b =$  airbase

From figure 23 it can be seen that

$$\alpha = \frac{A}{R} \quad (60)$$

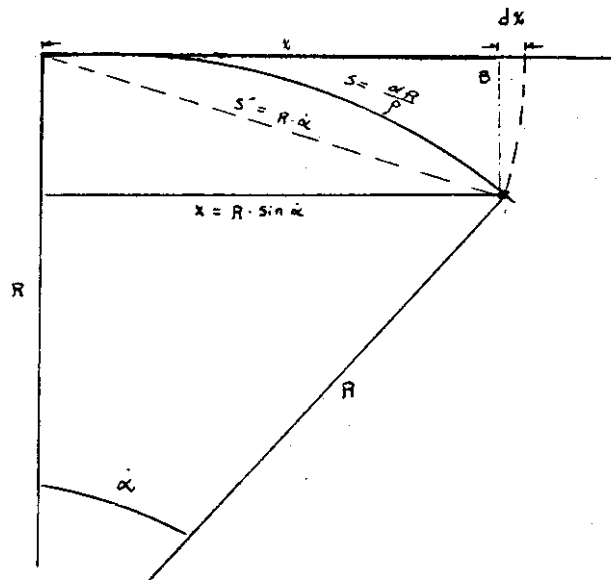


Fig. 22. Earth Curvature in x direction.

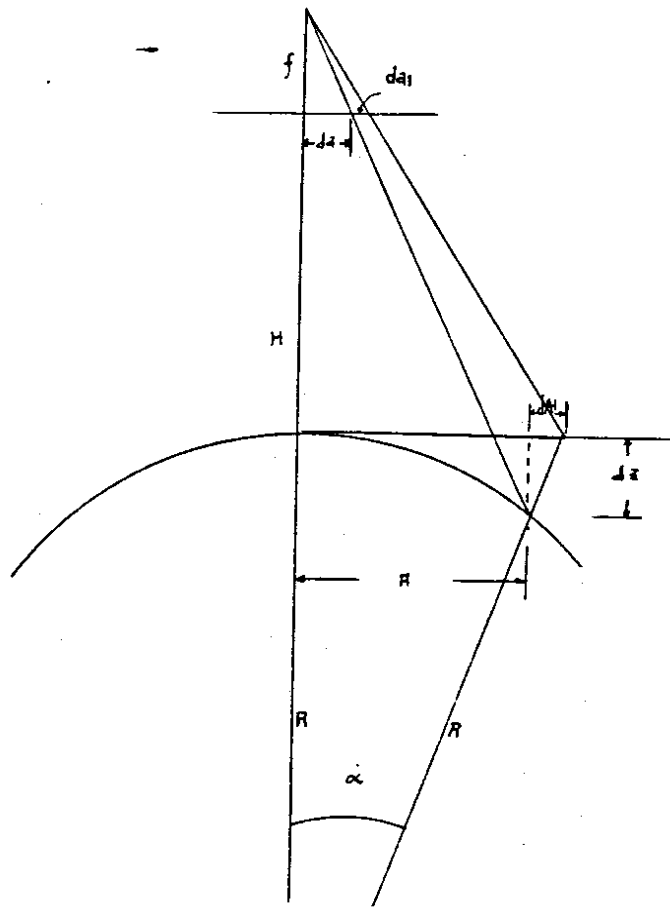


Fig. 23. Earth Curvature in z direction.

and

$$R-dz = R \cdot \cos \alpha \quad (61)$$

since

$$\begin{aligned} \cos \alpha &= 1 - \frac{\alpha^2}{2!} + \frac{\alpha^4}{4!} - \frac{\alpha^6}{6!} + \dots \\ &= 1 - \frac{\alpha^2}{2} + \frac{\alpha^4}{18} \end{aligned} \quad (62)$$

Substitution of equation (62) into (61), thus

$$\begin{aligned} R - dz &= R \left( 1 - \frac{\alpha^2}{2} + \frac{\alpha^4}{18} - \dots \right) \\ &= R \left( 1 - \left( \frac{A}{R} \right)^2 + \left( \frac{A}{R} \right)^4 - \dots \right) \\ &= R - \frac{A^2}{2R} + \dots \end{aligned}$$

or

$$dz = \frac{A^2}{2R} \quad (63)$$

#### 4-3. Atmospheric Refraction:

The atmospheric refraction causes a radial displacement of image points due to bending of the optical rays from between the terrain to the camera.

From Fig. 24. The photogrammetric refraction is a small angle at the camera between the ray from a ground point and the straight line from this point. It is a function of the refractive indices of the air in all the points along the ray. The refractive index is function of temperature,

pressure, and humidity, which are explained early in Chapter 2-4.

According to Snell's Law of Refraction, for a light ray which pierces a boundary and has the form as shown in Fig. 25.

$$\frac{n}{n+dn} = \frac{\sin B}{\sin (B+dB)} \quad (64)$$

Where  $n$ ,  $dn$  are the refractive indexes of the layers  $n$  and  $n + dn$ .

Expanding  $\sin (B + dB)$  into a series and limiting the term of the first order of magnitude, one has the differential equation with absolute values:

$$dB = \frac{dn}{n} \tan B \quad (65)$$

According to Schutt [57] and Fig 26, each refraction  $dB$  contributes to the photogrammetric refraction, the amount:

$$d\gamma = \frac{z_i - z_g}{z_c - z_g} dB \quad (66)$$

Where  $z_i$ ,  $z_g$  and  $z_c$  are the height of the boundary, of the ground, and camera respectively.

Taking  $dB$  as a function of the change in density instead of refractive index, one obtained the simplest equation as (67): [57]

$$n^2 = 1 + 2 \rho g \quad (67)$$

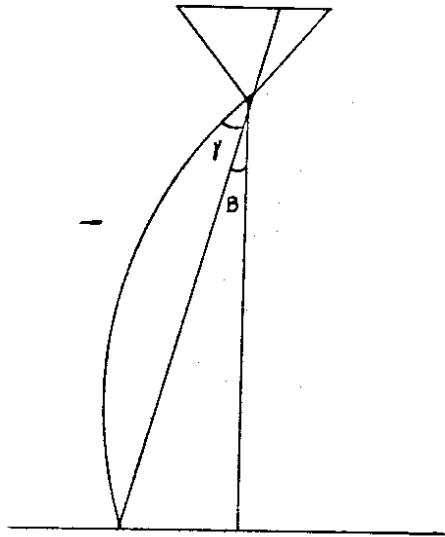


Fig. 24. Photogrammetric Refraction.

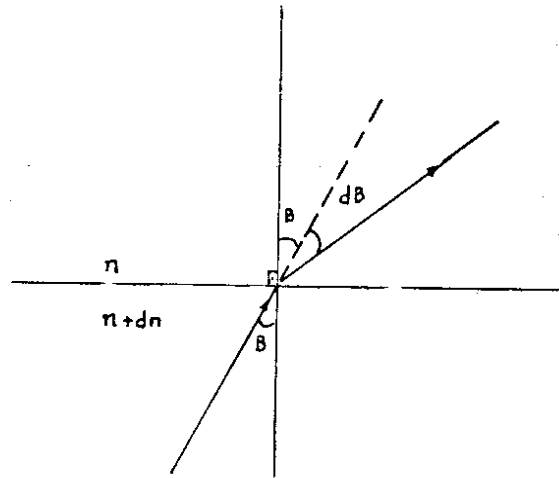


Fig. 25. Snell's Law of Refraction.

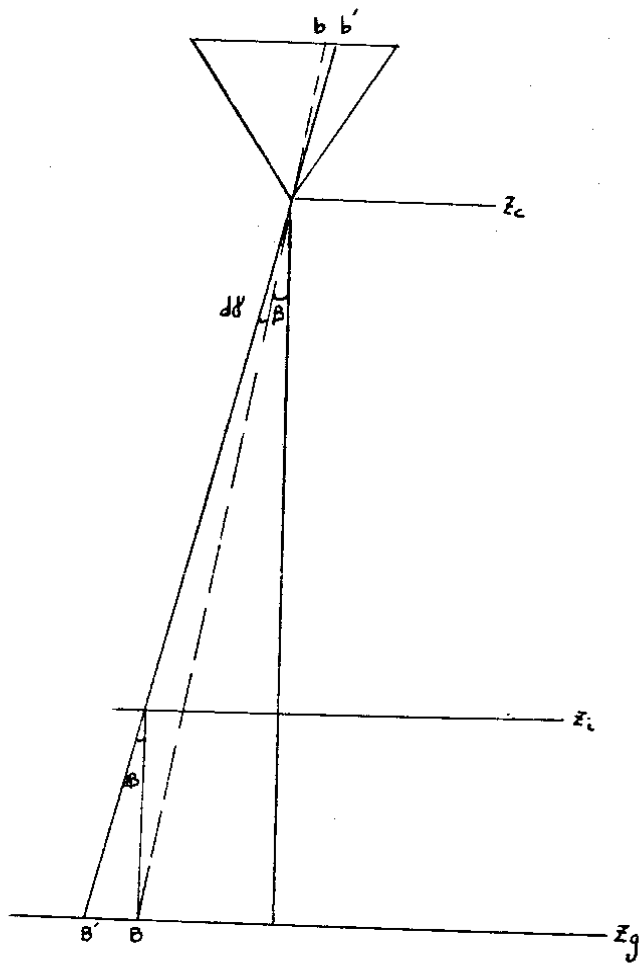


Fig. 26. Refraction at a Boundary Between Two Layers.

Where  $g$  is the density  $C = 0.00022667$  with  $a = 0.56 \mu$  from equation (24).

Differentiation of equation (67) obtains

$$\frac{dn}{n} = \frac{c}{n^2} dg \quad (68)$$

$n$  varies about 1.00022 to 1 from ground level to space, thus

$$\frac{dn}{n} = 0.0002266 dg \quad (69)$$

Combining equations (65) (66) and (69) and forming the sum over all boundaries between ground level and camera height, one obtains for the photogrammetric refraction as equation (70).

$$\bar{\alpha} = 0.000226 \frac{\tan B}{Z_2 - Z_g} ( (Z_i - Z_g) dg ) \quad (70)$$

The resulting corrections to the photogrammetric refraction for an angle  $36^\circ$  of wide angle camera for a flight height at 20,000 feet is  $10 \mu$  [57] therefore the corrections of the photogrammetric refractions in large scale photographs (flight height 300 feet - 12,000 feet) can be neglected.

#### 4-4. Refraction of the Targets.

The accuracy of the aerotriangulation is also dependent upon the resolution of the targets in the photographs. According to testings of the different targets, it is found that the standard target utilized by the Washington State Highways Department after extensive experimentation gives the best results. This target contains four bright lines and a



square in the center on a background as shown in Fig. 27. It should be noted that the amount of light reflected from the target is a function of the reflectance of the white bars and a dark background as well as the quantity of incidental light falling upon it. The maximum brightness value of the targets with white bars is about ten times that reflected from the minimum brightness value of the overall dark background of the target.

#### 4-5. Scale and Azimuth of a Strip.

Transference of scale in aerotriangulation by using a universal instrument is accomplished by means of height measurements at points close to the nadir points. One can derive the errors in scale by considering the errors in height measurement. Errors in scale will affect the x-coordinates of the points mainly as shown in Fig. 28.

$$\Delta x_1 = 0 \quad \text{first model}$$

$$\Delta x_2 = dbx_1 \quad \text{second model}$$

$$\Delta x_3 = 2dbx_1 + dbx_2 \quad \text{third model}$$

$$\Delta x_4 = 3dbx_1 + 2dbx_2 + dbx_3 \quad \text{fourth model}$$

$$\Delta x_5 = 4dbx_1 + 3dbx_2 + 2dbx_3 + dbx_4 \quad \text{fifth model}$$

Since

$$dbx_1 = dbx_2 = dbx_3 = dbx_4 = \dots = dbx$$

thus

$$xn' = (1+2+3+\dots+n'-1) dbx$$




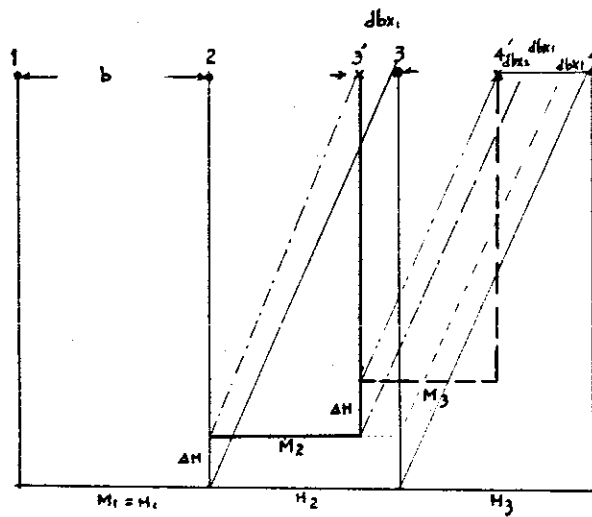
Scale   
0 1ft.

Fig. 27. Standard Target for Washington State Highways.



$H_i$  = True Scale  
 $M_i$  = Actual Scale

Fig. 28. Transference of Scale in Aerotriangulation.

and

$$1+2+3+\dots+n'-1 = \frac{n'(n'-1)}{2}$$
$$\Delta x_{n'} = \frac{n'(n'-1)}{2} dbx \quad (72)$$

Let

$$n' = \frac{x}{b}$$

then

$$\Delta x_n = \frac{1}{2} \left[ \frac{x}{b} \left( \frac{x}{b} - 1 \right) \right] dbx$$

or

(73)

$$\Delta x_s = \frac{dbx}{2b} x + \frac{dbx}{2b^2} x^2$$

where

$\Delta x_s$  = scale errors in x

b = base

According to equation (73), one finds that the scale change of each model in the strip manifests itself as the double summation errors. Therefore, the bx must be set as accurately as possible.

The azimuth errors are mainly relative orientation errors, primarily swing errors (dk), which result in faulty connections between models as shown in Fig. 29.

$$\Delta x_1 = xdk_1^2$$

$$\Delta x_2 = x \left( dk_1 + \frac{1}{2} dk_2 \right)^2$$

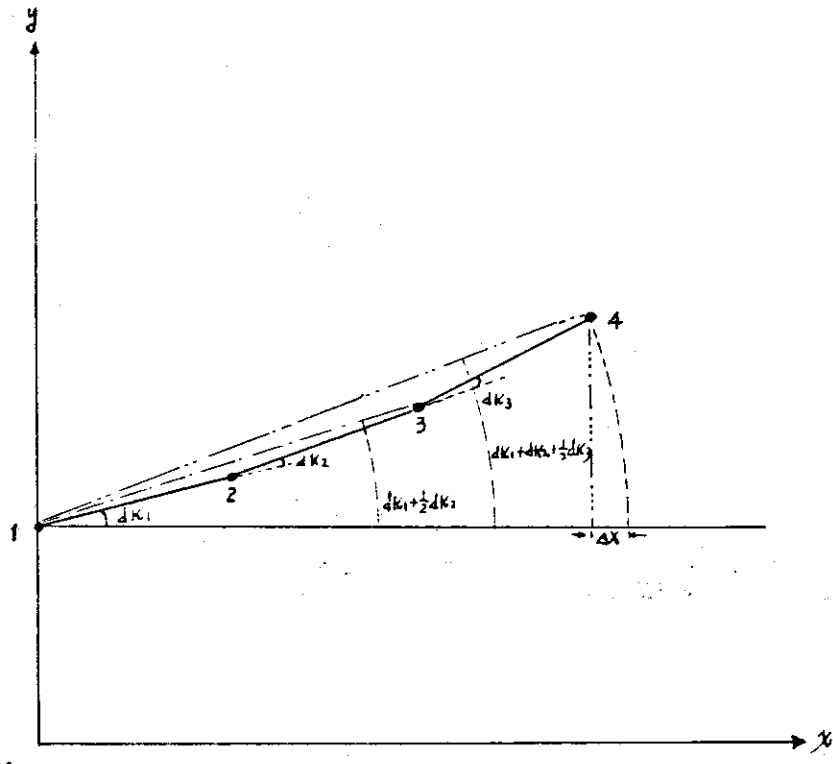


Fig. 29. Swing Errors in the Strip.

$$\Delta x_3 = x \left( dk_1 + dk_2 + \frac{1}{2} dk_3 \right)^2$$

⋮  
⋮  
⋮

since

$$dk_1 = dk_2 = dk_3 \dots = dk$$

thus

$$\Delta x_1 = x dk^2$$

$$\Delta x_2 = x \left( \frac{3}{2} dk \right)^2$$

$$\Delta x_3 = x \left( \frac{5}{2} dk \right)^2$$

⋮  
⋮

$$\Delta x_n = x \left[ \frac{(2n-1)^2}{4} dk^2 \right]$$

(74)

$$\Delta x_k = x^3 \frac{dk^2}{b^2} + x^2 \left[ \frac{dk^2}{4b} - \frac{dk^2}{b} \right]$$

This error affects mainly the y - coordinates of the points in the strip.

#### 4-6. Longitudinal Bend of a Strip.

Errors in longitudinal bend of a strip occur because of faulty connections between models of  $\varphi$  tilt and due to earth's curvature as shown in Fig. 30.

$$\Delta x = \frac{b}{2} \Delta \alpha^2$$

$$\Delta x_1 = \frac{b}{2} (\Delta \phi + d\varphi)^2$$

$$\Delta x_2 = \frac{b}{2} (\Delta \phi + d\varphi + d\gamma)^2$$

$$\Delta x_3 = \frac{b}{2} (\Delta\phi + d\psi + 2d\gamma)^2$$

⋮  
⋮  
⋮  
⋮  
⋮  
⋮  
⋮  
⋮  
⋮  
⋮

$$x_n = \frac{b}{2} (\Delta\phi + d\psi + n'-1d\gamma)^2$$

---


$$\sum_1^{n'} \Delta x_n = n' \frac{b(\Delta\phi + d\psi)^2}{2} + n' (n'-1) \frac{b(\Delta\phi + d\psi) d\gamma}{2} +$$

$$[n' (n'-1) (2n'-1)] \frac{bd\gamma^2}{12}$$

since

$$n' = \frac{x}{b}$$

$$x_{L.B.} = \Delta x_n = x \left[ \frac{(\Delta\phi + d\psi)^2}{2} \right] + x^2 \frac{[d\gamma (\Delta\phi + d\psi)]}{2db} -$$

$$x \frac{[d\gamma (\Delta\phi + d\psi)]}{2} + x^3 \frac{d\gamma^2}{6b^2} - x^2 \frac{d\gamma^2}{4b} + x \cdot \frac{d\gamma^2}{12}$$

$$= x \left[ \frac{(\Delta\phi + d\psi)}{2} - \frac{d\gamma (\Delta\phi + d\psi)}{2} + \frac{d\gamma^2}{12} \right] +$$

$$x^2 \left[ \frac{d\gamma (\Delta\phi + d\psi)}{2b} - \frac{d\gamma^2}{4b} \right] + x^3 \frac{[d\gamma^2]}{6b^2} \quad (76)$$

This systematic error ( $d\phi$ ) for an aeropolygon strip has the same effect as the earth's curvature and causes a systematic error in x- and z-coordinates, and the influence of longitudinal bend of each consecutive

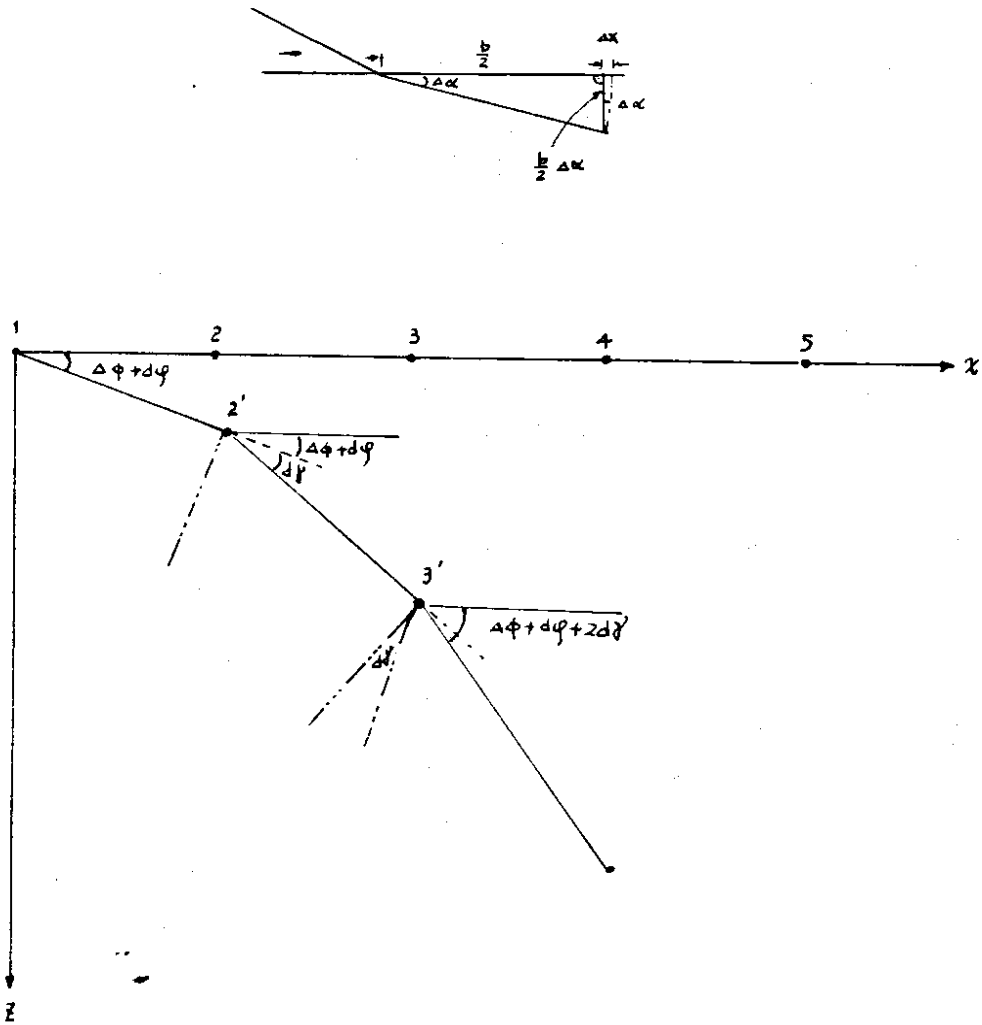


Fig. 30. Longitudinal Bend of a Strip.



model in the strip is also a double summation of errors.

#### 4-7. Transversal Tilt of a Strip.

The error propagation caused by a transversal tilt is shown in Fig. 31.

$$w = ndw = \frac{x}{b} dw$$

and

$$\Delta x = 0$$

$$\Delta y = z w = xz \frac{dw}{b} \quad (77)$$

$$\Delta z = -y w = -xy \frac{dw}{b}$$

This gives y and z - coordinate errors. They are not cumulative but are transferable from model to model.

#### 4-8. Conclusion.

The total effects of all these errors are revealed in the closing discrepancies in the coordinates of individual points as observed during the procedure of aerotriangulation. If all systematic errors, including earth's curvature, are combined, the following systematic error propagation formulas are obtained:

$$\Delta x = dx + \Delta x_s + \Delta x_{T.T.} + x_{L.B.} + x_k + \dots$$

or

$$= a_0 + a_1 x + a_2 y + a_3 xy + a_4 y^2 + \dots \quad (78)$$

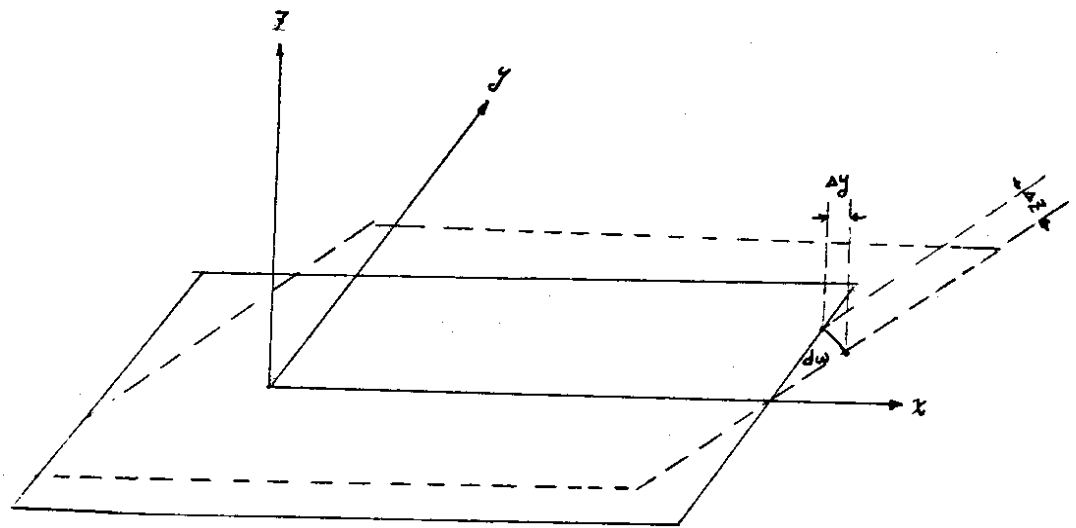


Fig. 31. Transversal Tilt of a Strip.

where

$x$  is the total error in  $x$  coordinate of a point.

$a_0, a_1 \dots a_4$  are certain constant

$x, y$  are the coordinates of the particular point in the strip

similar expressions are derived for  $y$  and  $z$ .

These polynomials are nonlinear because of the systematic accumulation of errors ~~throughout the strip~~.

The adjustment of these polynomials of aerotriangulation strips has been the subject of numerous articles and publications [7], [12], [15], [17], [33], [40], [42], [54]. The articles agree in general that the equation for transforming photogrammetric coordinates into ground coordinates can be expressed by polynomials in second or third degree. (Schut [55], Mikhail [42], Keller & Tewinkel [33] show that a conformal transformation in three dimension is not possible if the polynomial degree is greater than one.) The strip adjustment computation is first performed by linear transformation; this consists of scaling, rotating, and translating the strip with the help of the ground control points, then elevation and horizontal adjustments are performed. Finally, the strip coordinates of all points will be transformed to the ground coordinates systems.

## CHAPTER V

### AEROTRIANGULATION PRECISION ATTAINABLE FOR HIGHWAYS PHOTOGRAMMETRY

#### 5-1. Introduction.

Since it is ~~erare~~ ~~usually~~ advantageous to use photogrammetric methods to obtain topographic maps, cross sections, and other data for highway engineering applications such as reconnaissance, location, right of way requirements, bridge sites, earthwork quantities etc., it is imperative to know what accuracy to expect from aerotriangulation to control the mapping plotters performing such work.

A series of tests of medium to low altitude photographs by analog aerotriangulation through a Wild Autograph A-7 was recently conducted to determine the practical accuracies that can be expected from flight strips of given heights, lengths, and various distributions and densities of control points.

The photographs were taken by a 6-inch Wild RC-8 camera with 60 percent overlap from heights of 1,500 feet; 3,000 feet; 6,000 feet; and 12,000 feet in different areas. The number of models treated in this series is over 150 in 25 flight strips.

Relative orientation was carried out in the usual manner. The measured instrument coordinates were then transformed and adjusted

to the ground coordinates. The residuals of all test points with various distributions, densities of control points are plotted and the standard error of each strip is then computed.

Given the standard errors, of different flights, it is possible to express them in polynomial form as a function of flight height, which can be used for determination of the aerotriangulation precision.

## 5-2. Linear Transformation.

After each strip of aerotriangulation, the measured instrument coordinates must be transformed to a ground coordinates system.

The linear transformation may be employed, which consists of scale change and rotation as shown in equation (79).

$$\begin{aligned} E &= a_{11}x + a_{12}y \\ N &= a_{21}x + a_{22}y \\ H &= a_{31}x + a_{32}y + a_{33}z \end{aligned} \quad (79)$$

In which E-N are ground coordinates H is elevation.  $x, y, z$  are strip coordinates.  $a_{11}, \dots, a_{33}$  are coefficients of the transformation.

Since the transformation formulas are linear in the coefficients  $a_{11}, \dots, a_{33}$ , the computation of the coefficients from the coordinates of ground control points known in both systems is a simple matter. Each control point gives three equations. As a minimum, two horizontal and three vertical ground control points are required for a linear transformation. Using more control points, the least squares method

of adjustment may be applied.

### 5-3. Strip Adjustment and Tests

Since the instrument coordinates are transformed to ground coordinates, the entire strip will become systematically deformed horizontally and vertically.

Theoretical investigations have indicated that the error propagation under uniform conditions can be expressed by at least second-degree functions of  $x$ ,  $y$ ,  $z$  coordinates of the strip as shown in Chapter IV.

The most frequently used method for aerotriangulation adjustment is based upon the equation (78) in  $x$ ,  $y$ ,  $z$  related to  $E$ ,  $N$ ,  $H$  corrections. The transformation adjustments used by the Washington State Highway Department of Photogrammetry for strip and block adjustments have been programmed to utilize I.B.M. (Model 360/50) computer (Schut[54]) and G.E. Timeshare Computer Services (Hou, [21]).

The 25 flight strips were independently adjusted by three different procedures. (1) Linear transformation with minimum ground control points. (2) The second order polynomial equations with ground control points in beginning, middle, and end of the strip. (3) The traverse method. All test points were targeted and surveyed by ground methods. The photogrammetric errors of the test points were obtained by comparison with the ground surveyed values of north, east, and elevation. Standard

errors of adjustment points and check points were computed with equation (7). The maximum errors for each case were also given.

The different adjustment procedures and results of 25 strips are shown in the following pages.

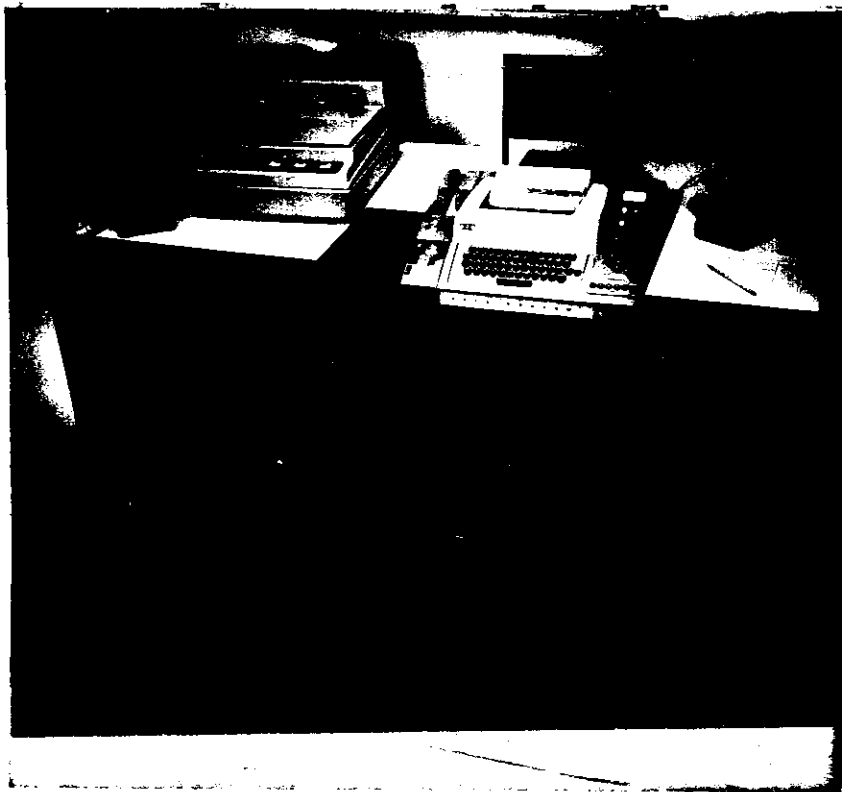


Fig. 32 ASR-35 Teletype terminal with card reader

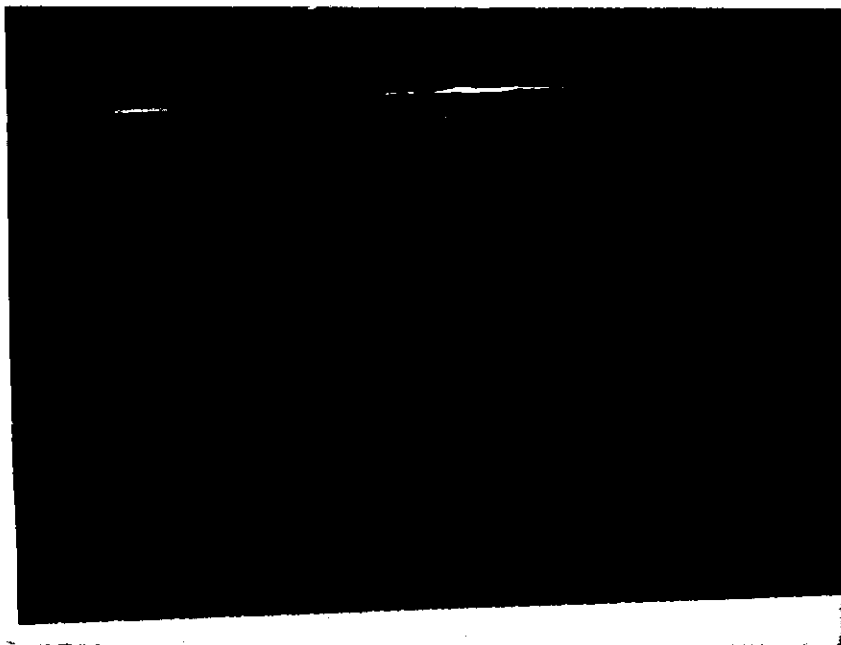


Fig. 34 IBM 2780 Remote teleprocessing terminal

5-4. Testing of ten strips of the flight at 1500 feet.

5-4-1. TEST STRIP NO. 1

Test area: "R" St. in Anacortes, 71-7-15

Flight height  $\cong$  1500 feet; Mean elevation  $\cong$  100 feet.

Models: 4

Horizontal control points: 8

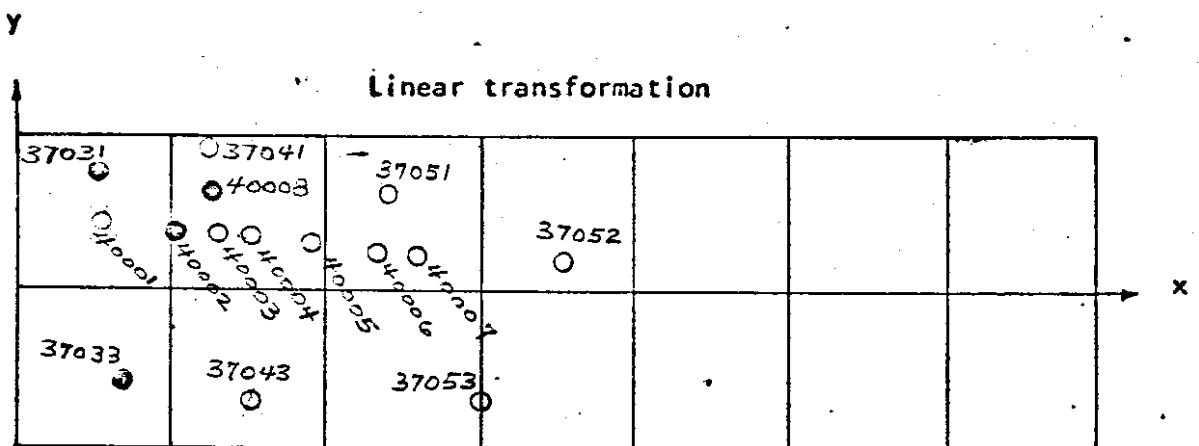
Vertical control points: 14

Location of all ground control points shown in Figure: 34

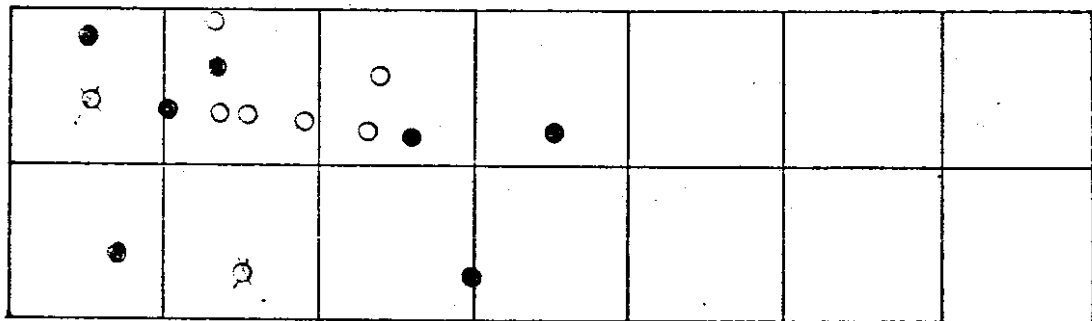
Residuals of all check points shown in Figure: 35

Stand errors of three different adjustment procedures, of this strip  
shown in Table: 4

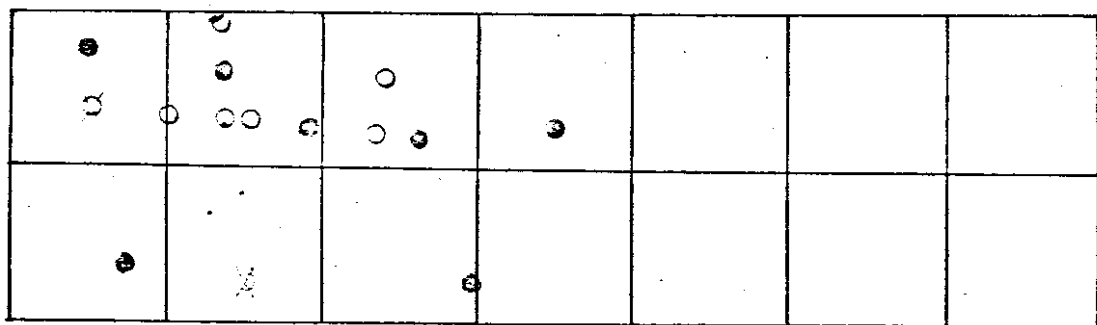




**Beginning, middle and end (2nd)**



**Traverse method (2nd)**



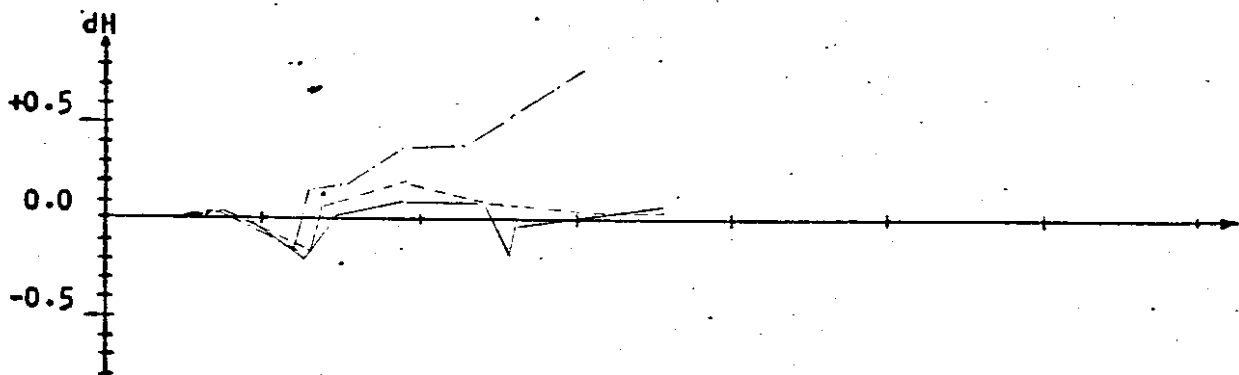
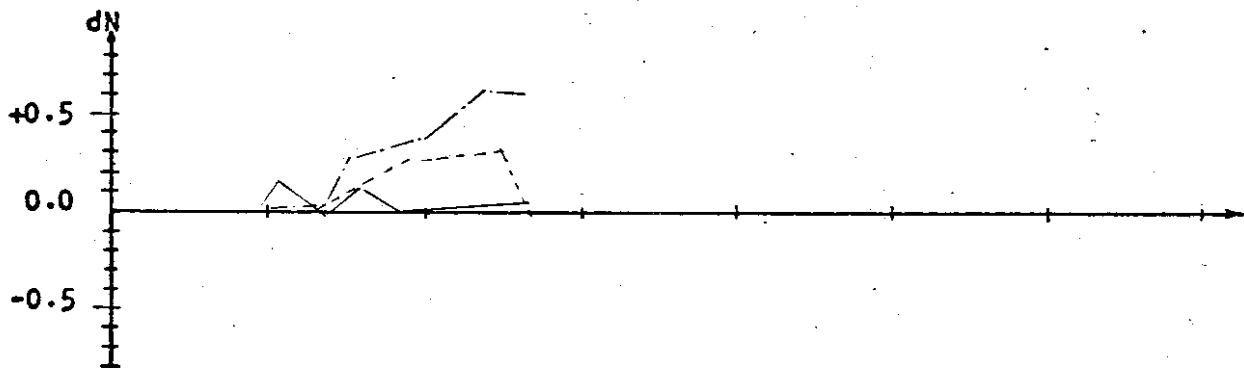
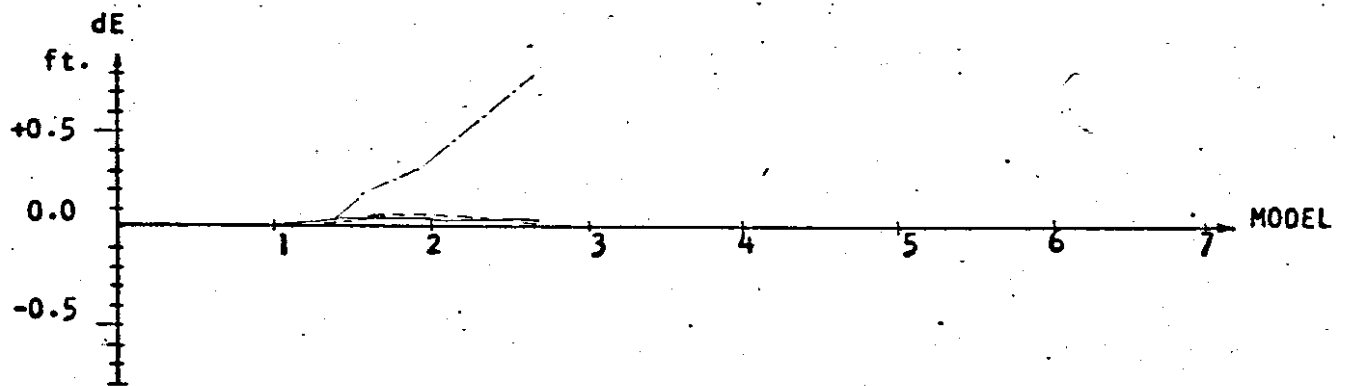
⊗ Detected ground control point in error

● Control points

○ Check points

"2" Horizontal point; "3" Vertical point; "4" Horizontal & vertical point

**Fig. 34 Layout of ground control points of test strip 1**



- Linear transformation
- Beginning, middle and end (2nd)
- Traverse method (2nd)

Fig. 35. Comparison of Discrepancies Resulting from Different Adjustment Procedures of Test Strip 1 at Flight Height of 1500 Feet

TABLE 4 RESULTS OF DIFFERENT ADJUSTMENT  
 PROCEDURES OF TEST STRIP 1 AT FLIGHT  
 HEIGHT OF 1500 FEET

Method	Linear Transformation	Beginning, Middle and End (2nd)	Traverse Method(2nd)
<b>Control points only</b>			
RMSE of dE in ft.	0.00	0.00	0.00
RMSE of dN	0.00	0.00	0.00
RMSE of dP	0.00	0.00	0.00
RMSE of dH	0.04	0.02	0.05
MAX, dE	0.00	0.00	0.00
MAX, dN	0.00	0.00	0.00
MAX, dH	-0.07	0.05	0.11
<b>Check points</b>			
RMSE of dE in ft.	0.43	0.07	0.13
RMSE of dN	0.41	0.21	0.12
RMSE of dP	0.42	0.16	0.13
RMSE of dH	0.57	0.14	0.15
MAX, dE	0.72	0.09	0.21
MAX, dN	0.59	0.24	0.19
MAX, dH	1.28	0.20	-0.27

5-4-2

TEST STRIP NO. 2

Test area: Tanner to Lower x-ing, 71-4-29

Flight height  $\approx$  1500 feet; Mean elevation  $\approx$  700 feet

Models: 7

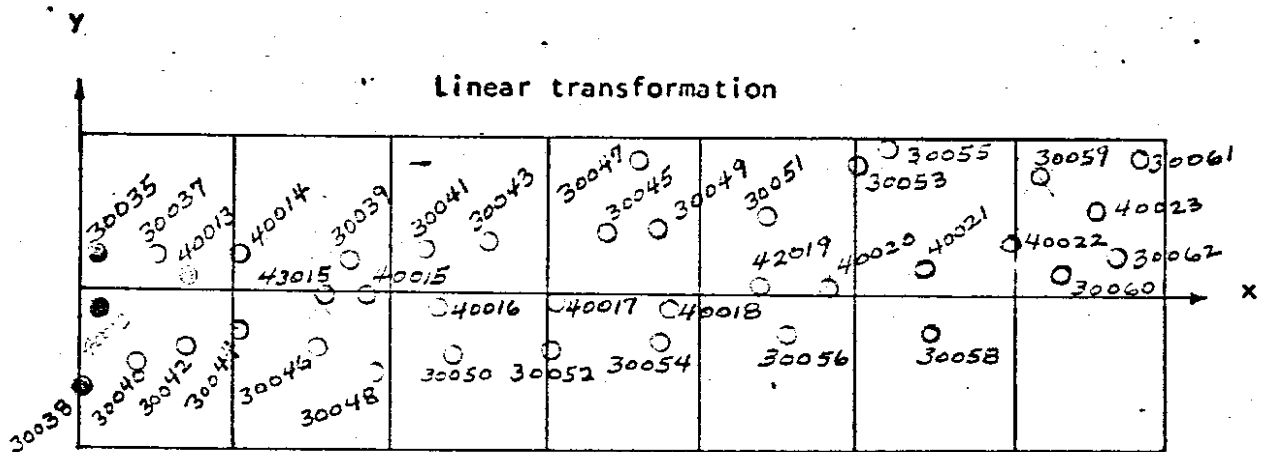
Horizontal control points: 12

Vertical control points: 38

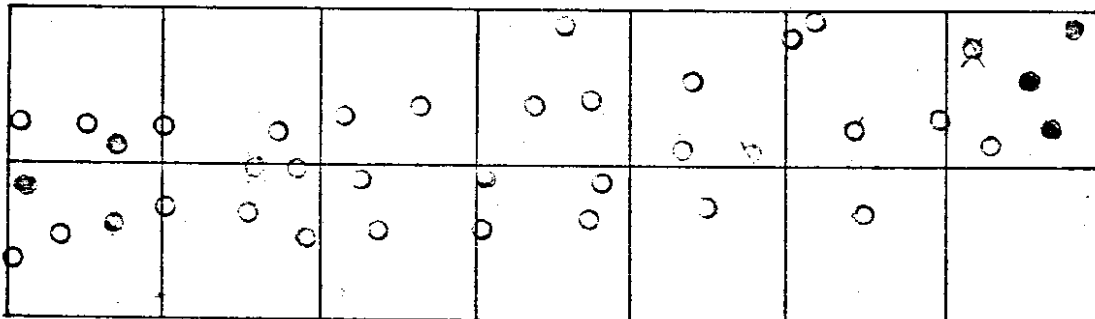
Location of all ground control points shown in Figure: 36

Residuals of all check points shown in Figure: 37

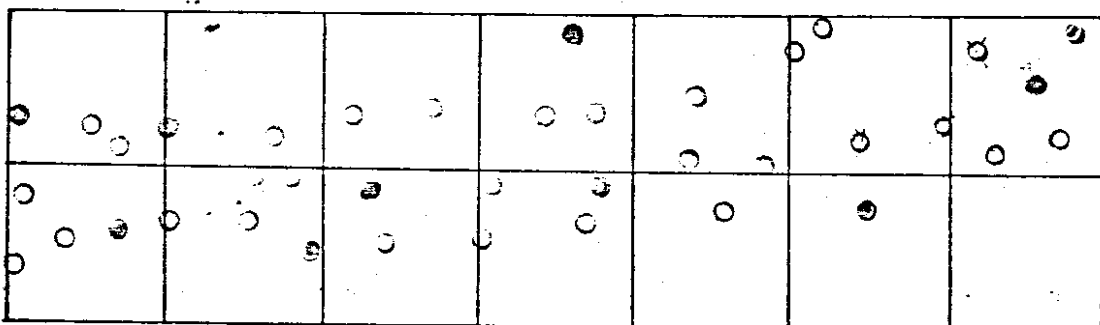
Stand errors of three different adjustment procedures of this strip  
shown in Table: 5



**Beginning, middle and end (2nd)**



**Traverse method (2nd)**



⊗ Detected ground control point in error

● Control points

○ Check points

"2" Horizontal point; "3" Vertical point; "4" Horizontal & vertical point

**Fig.36** Layout of ground control points of test strip 2

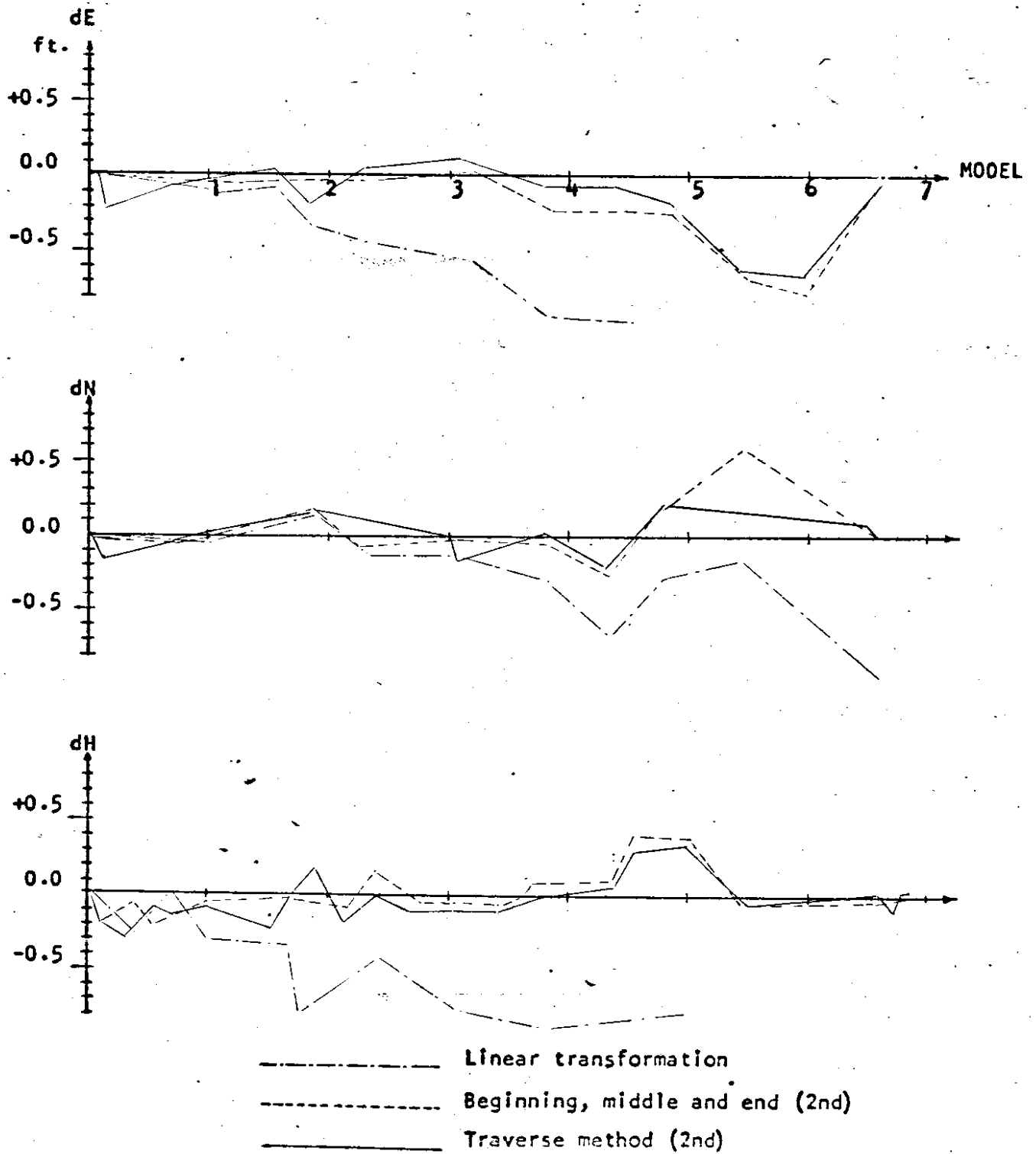


Fig. 37 Comparison of Discrepancies Resulting from Different Adjustment Procedures of Test Strip 2 at Flight Height of 1500 Feet

TABLE 5 RESULTS OF DIFFERENT ADJUSTMENT  
 PROCEDURES OF TEST STRIP 2 AT FLIGHT  
 HEIGHT OF 1500 FEET

Method	Linear Transformation	Beginning, Middle and End (2nd)	Traverse Method(2nd)
<b>Control points only</b>			
RMSE of dE in ft.	0.04	0.03	0.04
RMSE of dN	0.01	0.01	0.01
RMSE of dP	0.02	0.02	0.02
RMSE of dH	0.09	0.06	0.09
MAX, dE	0.07	0.04	0.07
MAX, dN	0.02	0.01	0.02
MAX, dH	0.19	0.07	0.13
<b>Check points</b>			
RMSE of dE in ft.	1.04	0.13	0.11
RMSE of dN	0.86	0.14	0.14
RMSE of dP	0.95	0.14	0.13
RMSE of dH	0.95	0.18	0.20
MAX, dE	0.20	0.21	0.20
MAX, dN	0.20	0.26	0.20
MAX, dH	0.52	0.43	0.52

5-4-3.

TEST STRIP NO. 3

Test area: ~~Waltby~~ W. Vine St. 212th & Vine Chann. 71-6-16

Flight height  $\approx$  1500 feet; Mean elevation  $\approx$  250 feet.

Models: 4

Horizontal control points: 7

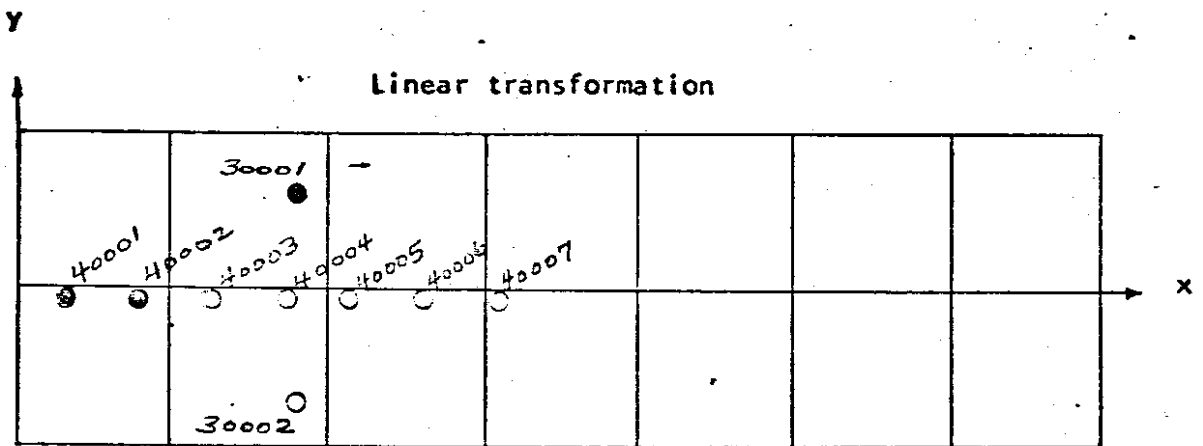
Vertical control points: 9

Location of all ground control points shown in Figure: 38

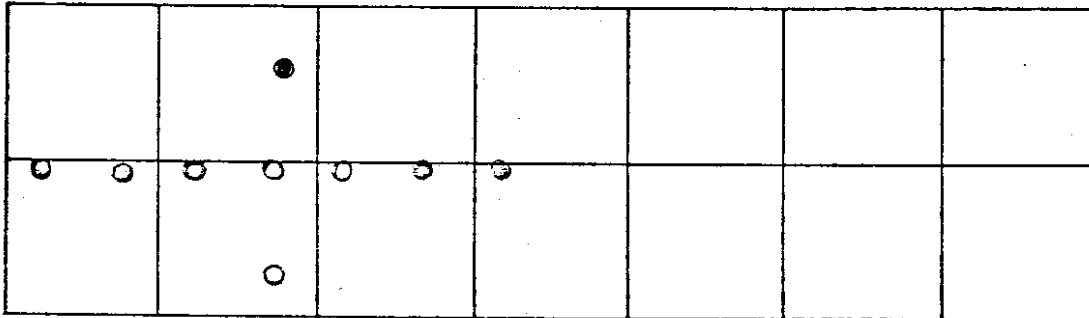
Residuals of all check points shown in Figure: 39

Stand errors of three different adjustment procedures of this strip  
shown in Table: 6

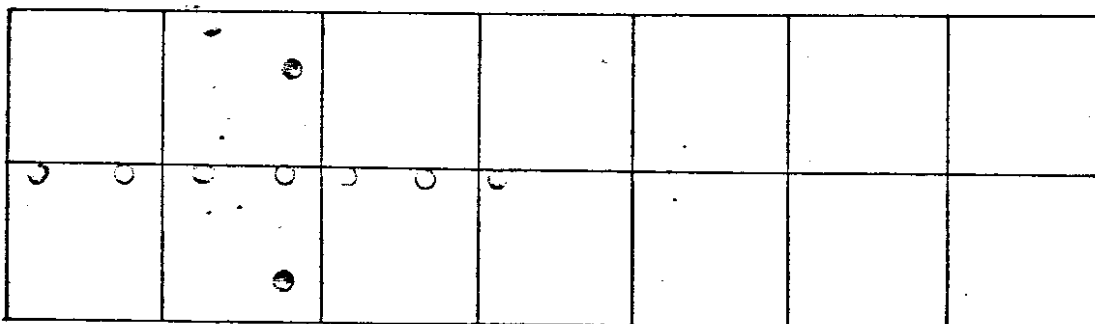




**Beginning, middle and end (2nd)**



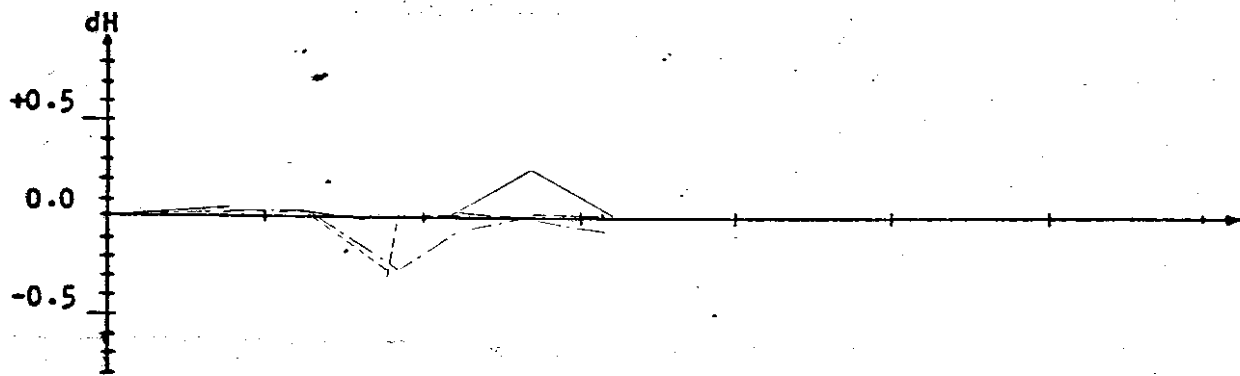
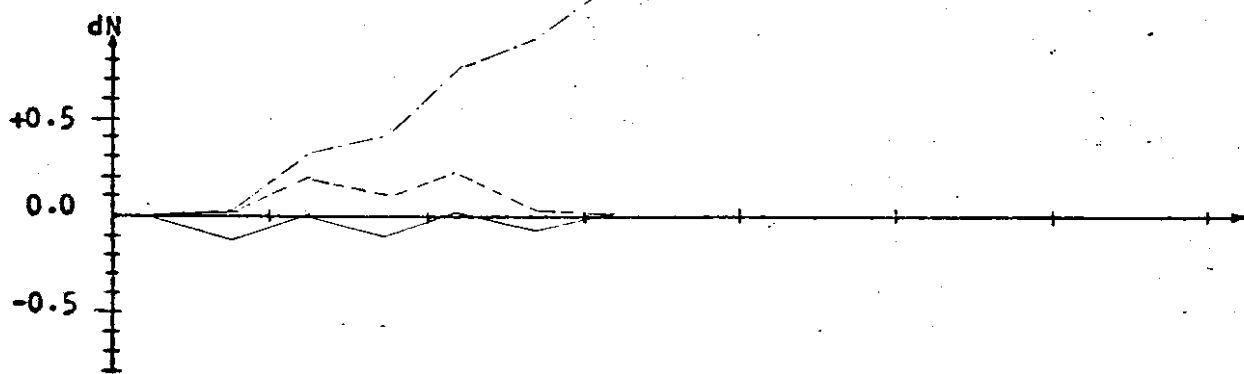
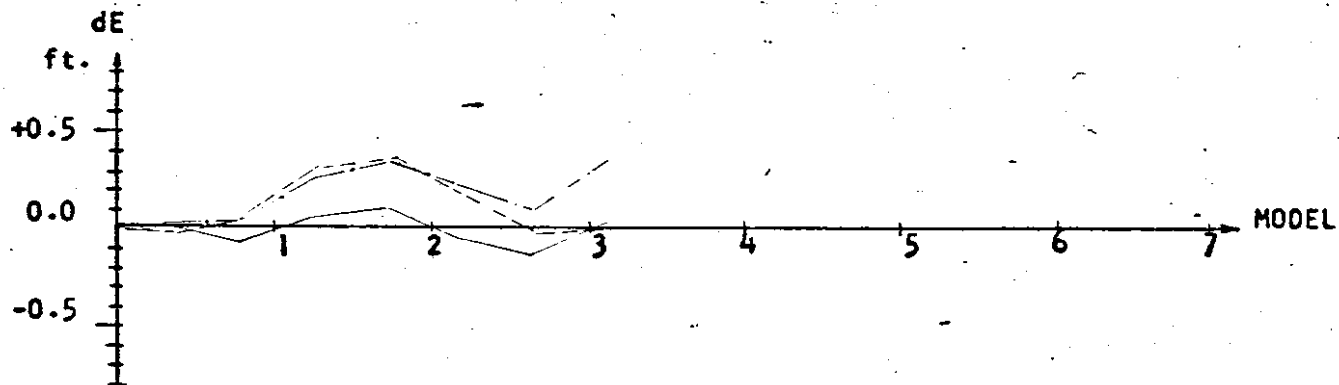
**Traverse method (2nd)**



- Control points
- Check points

"2" Horizontal point; "3" Vertical point; "4" Horizontal & vertical point

**Fig-38** Layout of ground control points of test strip 3



- Linear transformation
- - - - - Beginning, middle and end (2nd)
- · - · - Traverse method (2nd)

Fig. 39 Comparison of Discrepancies Resulting from Different Adjustment Procedures of Test Strip 3 at Flight Height of 1500 Feet

TABLE 6 RESULTS OF DIFFERENT ADJUSTMENT  
 PROCEDURES OF TEST STRIP 3 AT FLIGHT  
 HEIGHT OF 1500 FEET

Method	Linear Transformation	Beginning, Middle and End (2nd)	Traverse Method(2nd)
<b>Control points only</b>			
RMSE of dE in ft.	0.00	0.02	0.04
RMSE of dN	0.00	0.01	0.01
RMSE of dP	0.00	0.01	0.02
RMSE of dH	0.00	0.00	0.01
MAX. dE	0.00	0.03	0.06
MAX. dN	0.00	0.02	0.01
MAX. dH	0.00	0.00	0.02
<b>Check points</b>			
RMSE of dE in ft.	0.24	0.28	0.13
RMSE of dN	0.65	0.17	0.11
RMSE of dP	0.40	0.23	0.12
RMSE of dH	0.13	0.17	0.13
MAX. dE	0.35	0.34	0.16
MAX. dN	0.93	0.20	0.13
MAX. dH	0.27	0.34	0.22

5-4-4.

TEST STRIP NO. 4

Test area: SR 405 - 40th St., 71-158, Rebridge 71-4-15

Flight height  $\cong$  1500 feet, Mean elevation  $\cong$  200 feet

Models: 5

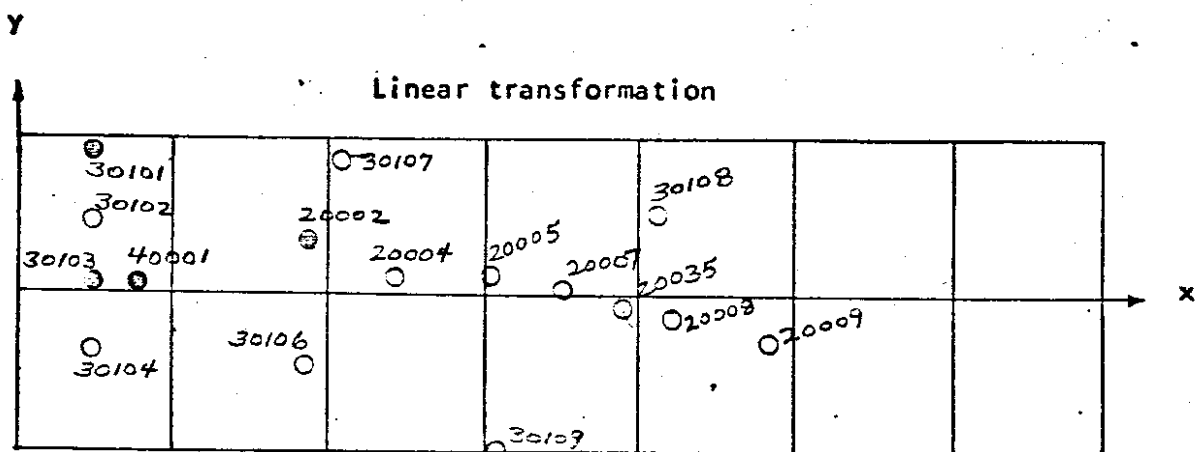
Horizontal control points: 8

Vertical control points: 9

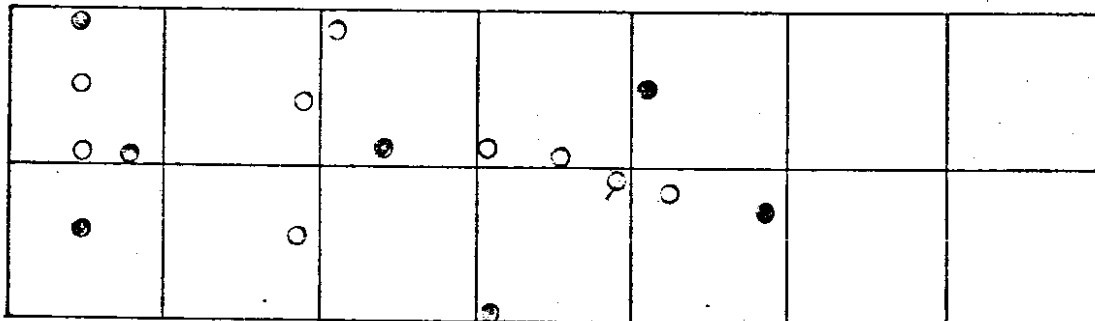
Location of all ground control points shown in Figure: 40

Residuals of all check points shown in Figure: 41

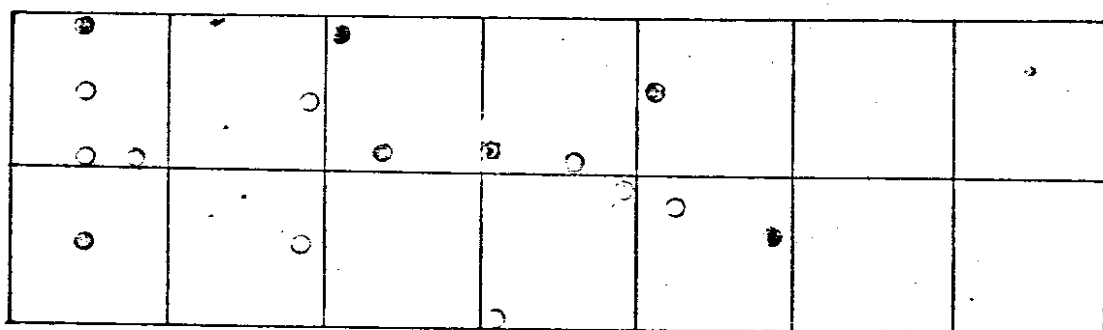
Stand errors of three different adjustment procedures of this strip  
shown in Table: 7



**Beginning, middle and end (2nd)**



**Traverse method (2nd)**



⊗ Detected ground control point in error

● Control points

○ Check points

"2" Horizontal point; "3" Vertical point; "4" Horizontal & vertical point

**Fig-40** Layout of ground control points of test strip 4

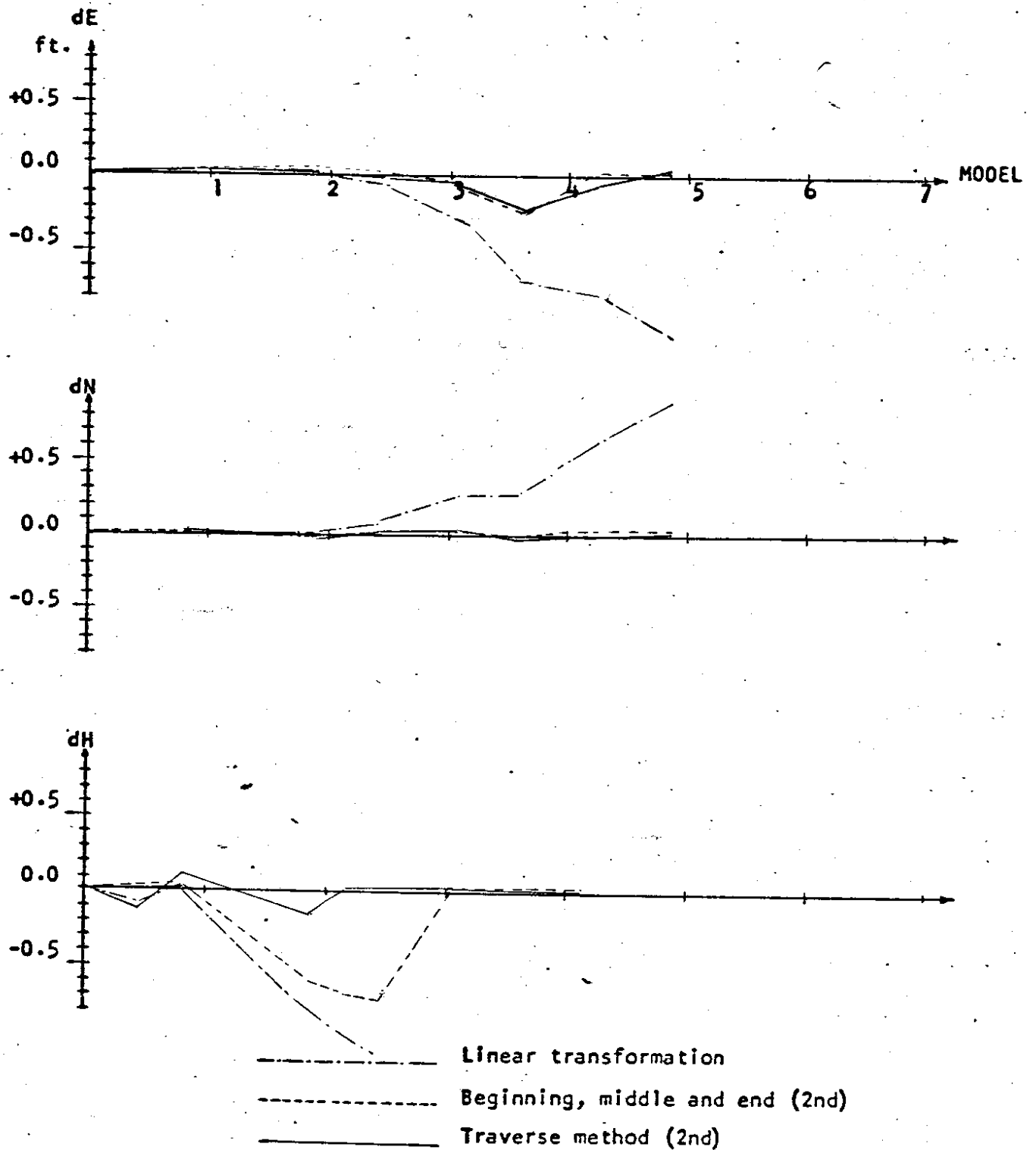


Fig. 41 Comparison of Discrepancies Resulting from Different Adjustment Procedures of Test Strip 4 at Flight Height of 1500 Feet

TABLE 7 RESULTS OF DIFFERENT ADJUSTMENT  
 PROCEDURES OF TEST STRIP 4 AT FLIGHT  
 HEIGHT OF 1500 FEET

Method	Linear Transformation	Beginning, Middle and End (2nd)	Traverse Method(2nd)
<b>Control points only</b>			
RMSE of dE in ft.	0.00	0.00	0.00
RMSE of dN	0.00	0.00	0.00
RMSE of dP	0.00	0.00	0.00
RMSE of dH	0.00	0.00	0.05
MAX, dE	0.00	0.00	0.00
MAX, dN	0.00	0.00	0.00
MAX, dH	0.00	0.00	0.11
<b>Check points</b>			
RMSE of dE in ft.	0.72	0.16	0.15
RMSE of dN	0.50	0.28	0.03
RMSE of dP	0.62	0.23	0.11
RMSE of dH	1.42	0.46	0.14
MAX, dE	-1.17	0.04	0.29
MAX, dN	0.88	-0.04	0.05
MAX, dH	-2.28	0.70	0.18

5-4-5.

TEST STRIP NO. 5

Test area: Connecticut St. Viaduct 4, 71-4-25

Flight height  $\approx$  1200 feet, Mean elevation  $\approx$  50 feet

Models: 7

Horizontal control points: 9

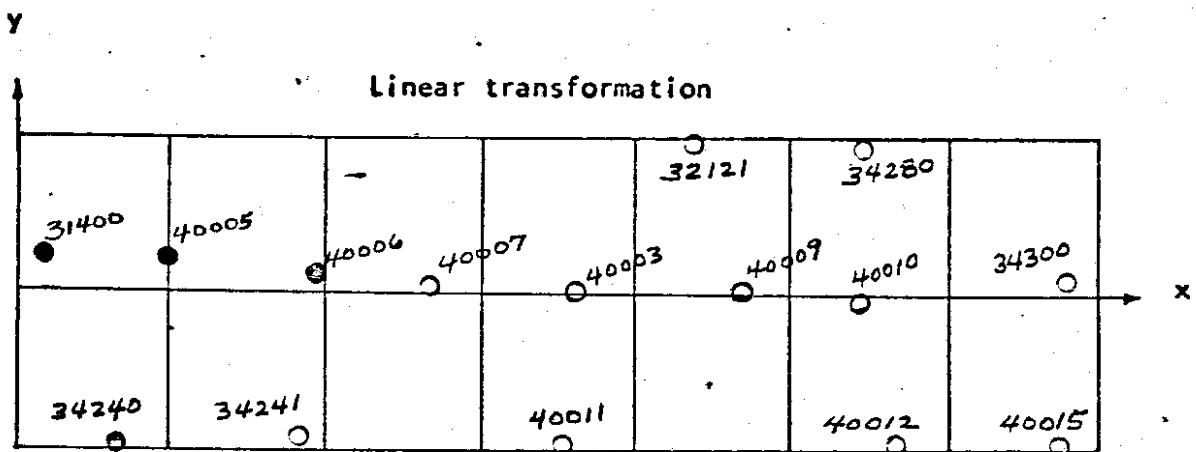
Vertical control points: 15

Location of all ground control points shown in Figure: 42

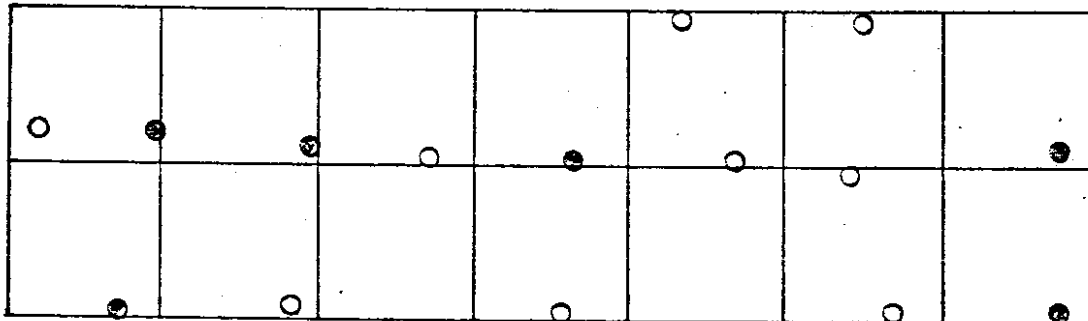
Residuals of all check points shown in Figure: 43

Stand errors of three different adjustment procedures of this strip  
shown in Table: 8

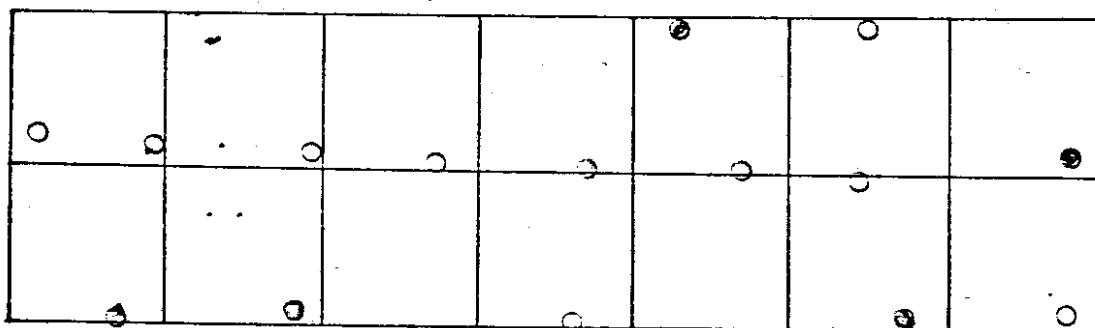




**Beginning, middle and end (2nd)**



**Traverse method (2nd)**

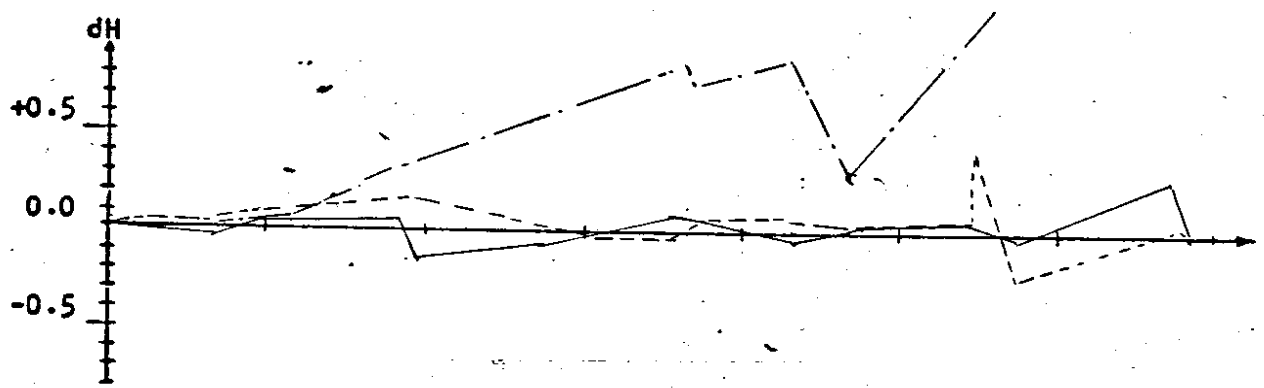
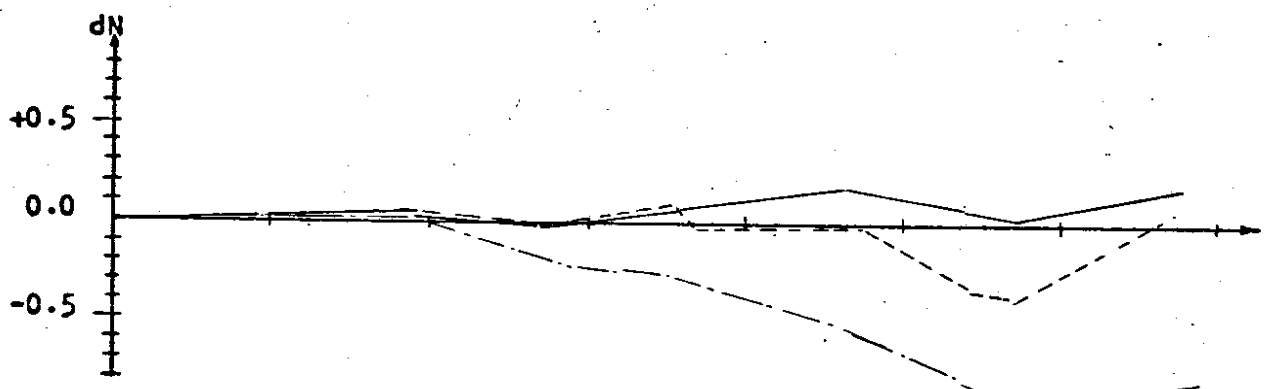
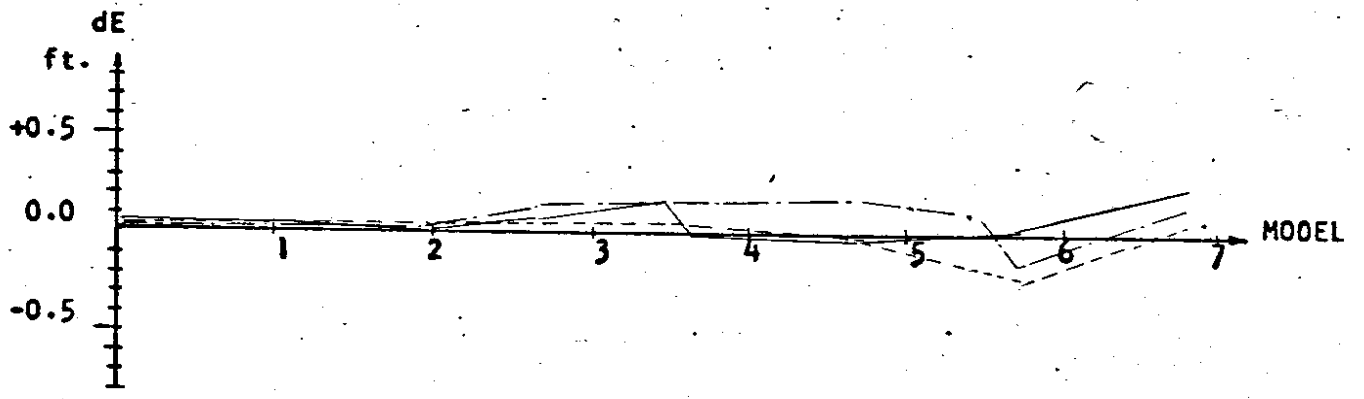


● Control points

○ Check points

"2" Horizontal point; "3" Vertical point; "4" Horizontal & vertical point

**Fig.42** Layout of ground control points of test strip 5



- Linear transformation
- .-.-.-.- Beginning, middle and end (2nd)
- \_\_\_\_\_ Traverse method (2nd)

Fig. 43 Comparison of Discrepancies Resulting from Different Adjustment Procedures of Test Strip 5 at Flight Height of 1500 Feet

TABLE 8 RESULTS OF DIFFERENT ADJUSTMENT  
 PROCEDURES OF TEST STRIP 5 AT FLIGHT  
 HEIGHT OF 1500 FEET

Method	Linear Transformation	Beginning, Middle and End (2nd)	Traverse Method(2nd)
<b>Control points only</b>			
RMSE of dE in ft.	0.00	0.01	0.00
RMSE of dN	0.00	0.04	0.00
RMSE of dP	0.00	0.02	0.00
RMSE of dH	0.04	0.07	0.08
MAX, dE	0.00	0.02	0.00
MAX, dN	0.00	0.06	0.00
MAX, dH	0.06	0.14	0.08
<b>Check points</b>			
RMSE of dE in ft.	0.13	0.15	0.13
RMSE of dN	0.67	0.24	0.10
RMSE of dP	0.48	0.20	0.12
RMSE of dH	1.64	0.16	0.17
MAX, dE	0.17	0.26	0.23
MAX, dN	-1.11	-0.40	0.17
MAX, dH	2.75	0.40	0.32

5-4-6.

TEST STRIP NO. 6

Test area: Connecticut Street viaduct. 2. 71-4-25

Flight height  $\approx$  1500 feet, Mean elevation = 50 feet.

Models: 4

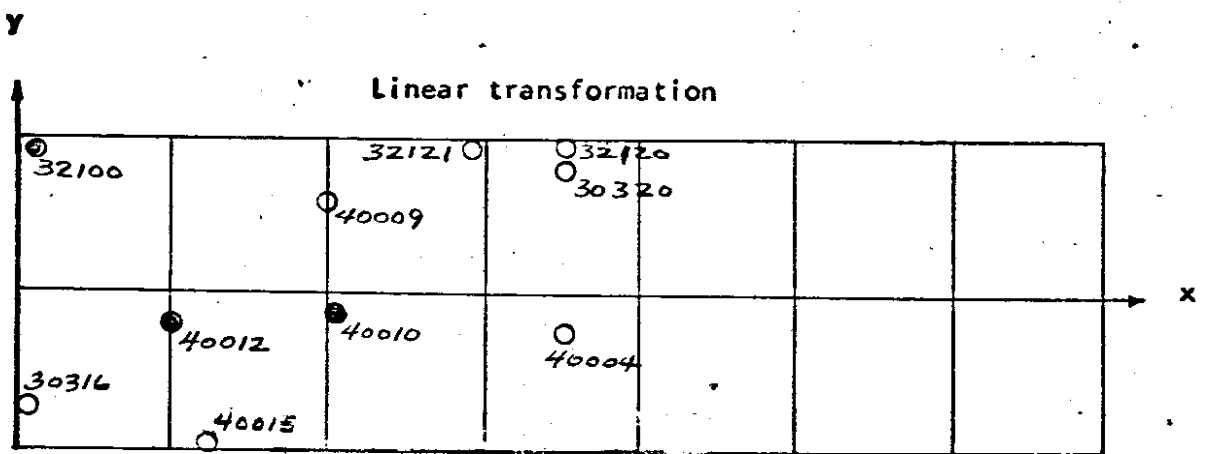
Horizontal control points: 5

Vertical control points: 10

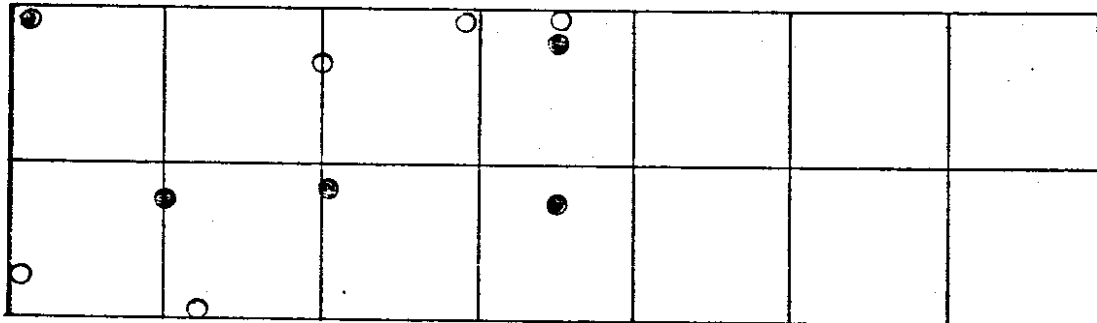
Location of all ground control points shown in Figure: 44

Residuals of all check points shown in Figure: 45

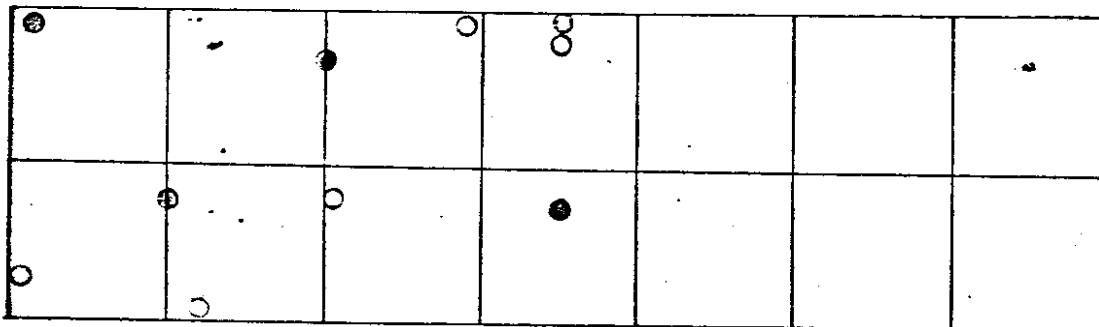
Stand errors of three different adjustment procedures of this strip  
shown in Table: 9



**Beginning, middle and end (2nd)**



**Traverse method (2nd)**



✘ Detected ground control point in error

● Control points

○ Check points

"2" Horizontal point; "3" Vertical point; "4" Horizontal & vertical point

Fig. 44 Layout of ground control points of test strip 6

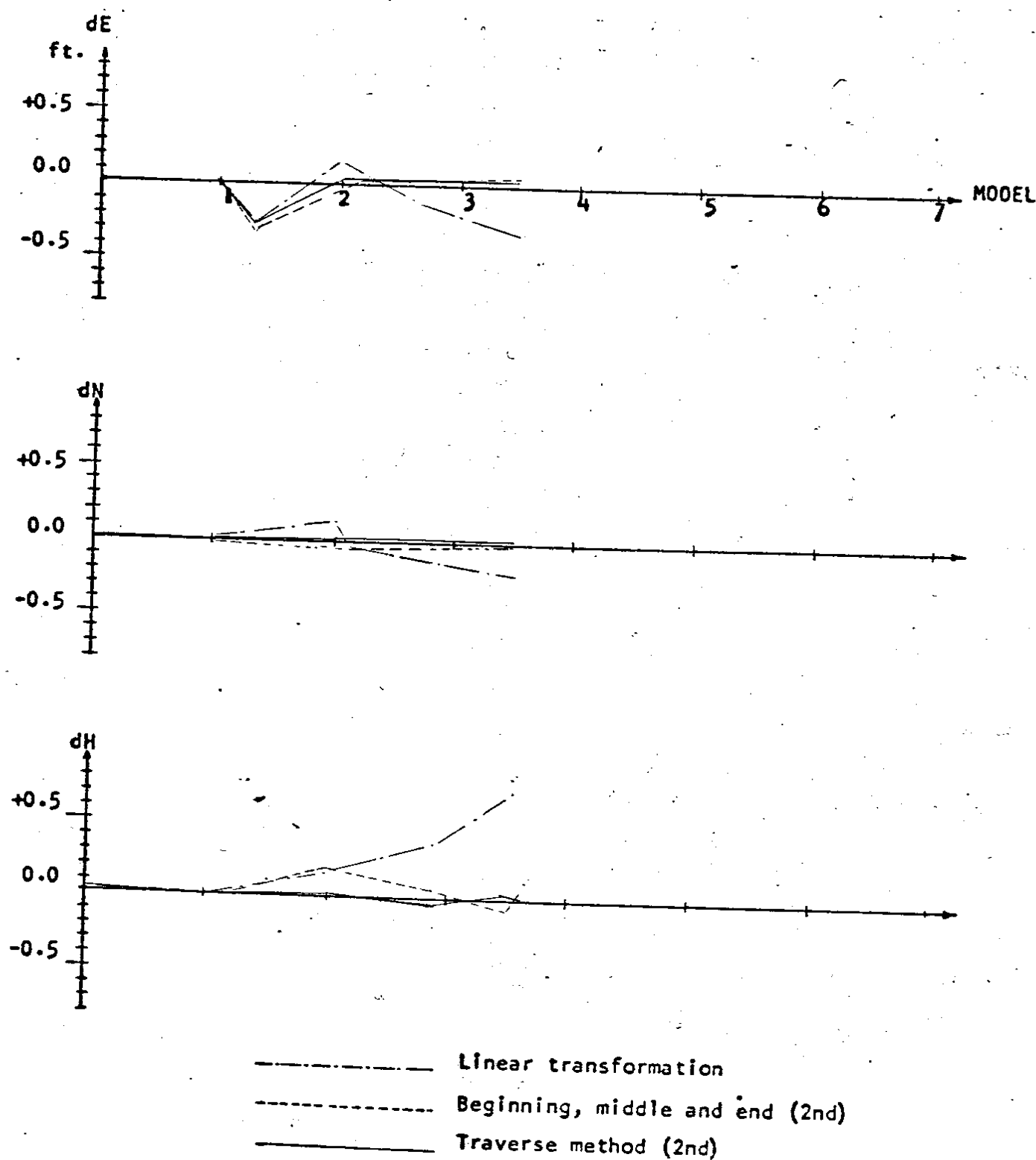


Fig. 45 Comparison of Discrepancies Resulting from Different Adjustment Procedures of Test Strip 6 at Flight Height of 1500 Feet

TABLE 9 RESULTS OF DIFFERENT ADJUSTMENT  
PROCEDURES OF TEST STRIP 6 AT FLIGHT  
HEIGHT OF 1500 FEET

Method	Linear Transformation	Beginning, Middle and End (2nd)	Traverse Method(2nd)
<b>Control points only</b>			
RMSE of dE in ft.	0.00	0.00	0.00
RMSE of dN	0.00	0.00	0.00
RMSE of dP	0.00	0.00	0.00
RMSE of dH	0.00	0.00	0.00
MAX, dE	0.00	0.00	0.00
MAX, dN	0.00	0.00	0.00
MAX, dH	0.00	0.00	0.00
<b>Check points</b>			
RMSE of dE in ft.	0.21	0.05	0.05
RMSE of dN	0.19	0.17	0.09
RMSE of dP	0.20	0.13	0.07
RMSE of dH	0.62	0.14	0.09
MAX, dE	-0.28	0.05	0.05
MAX, dN	-0.20	0.17	-0.09
MAX, dH	0.82	0.20	-0.14

5-4-7.

TEST STRIP NO. 7

Test area: Connecticut Street viaduct, 3. 71-4-25

Flight height  $\approx$  1500 feet; Mean elevation  $\approx$  50 feet

Models: 7

Horizontal control points: 7

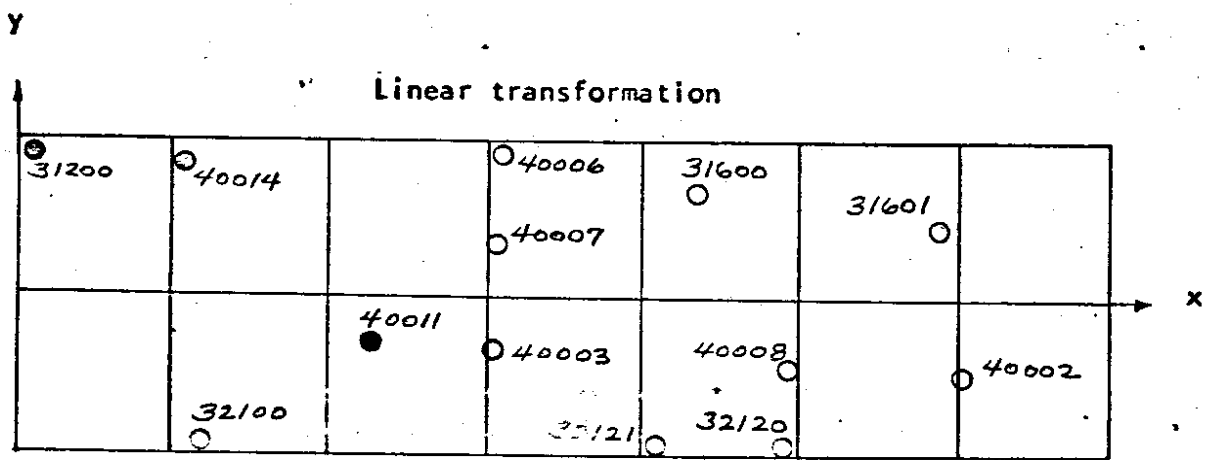
Vertical control points: 13

Location of all ground control points shown in Figure: 46

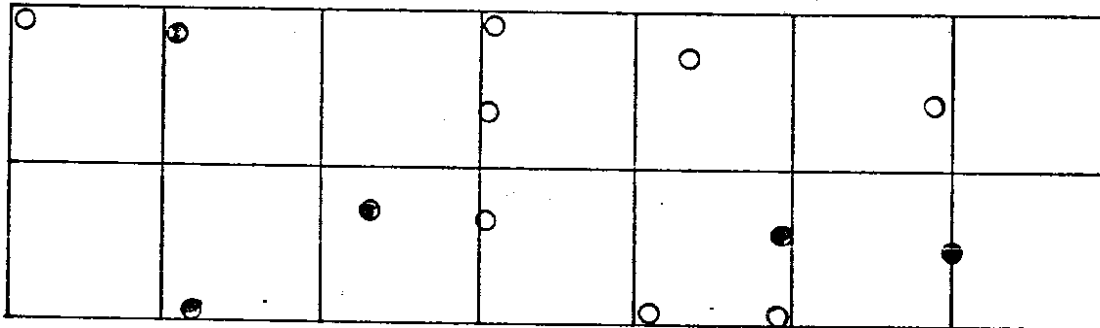
Residuals of all check points shown in Figure: 47

Stand errors of three different adjustment procedures of this strip  
shown in Table: 10

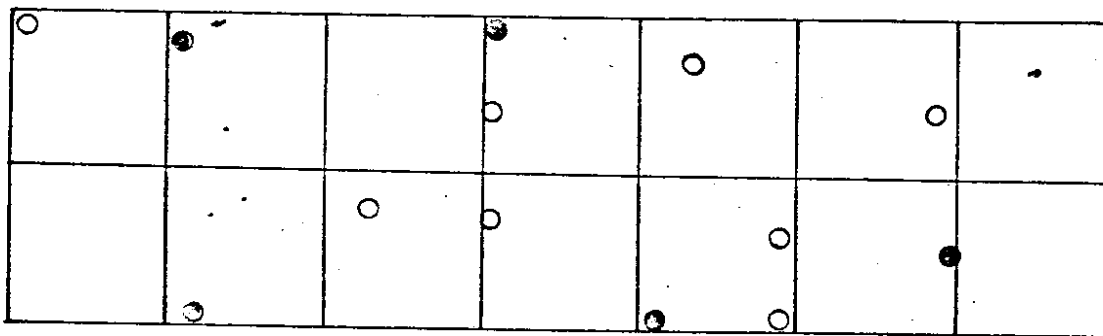




**Beginning, middle and end (2nd)**



**Traverse method (2nd)**

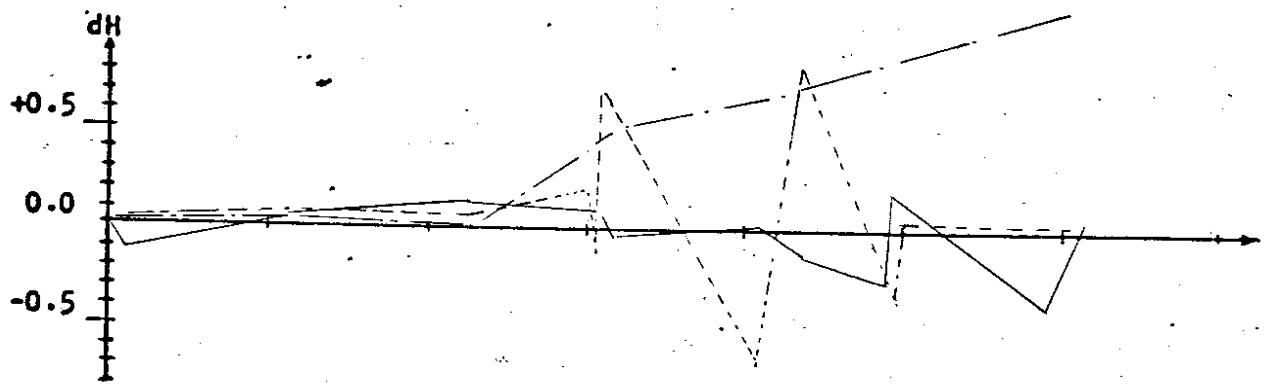
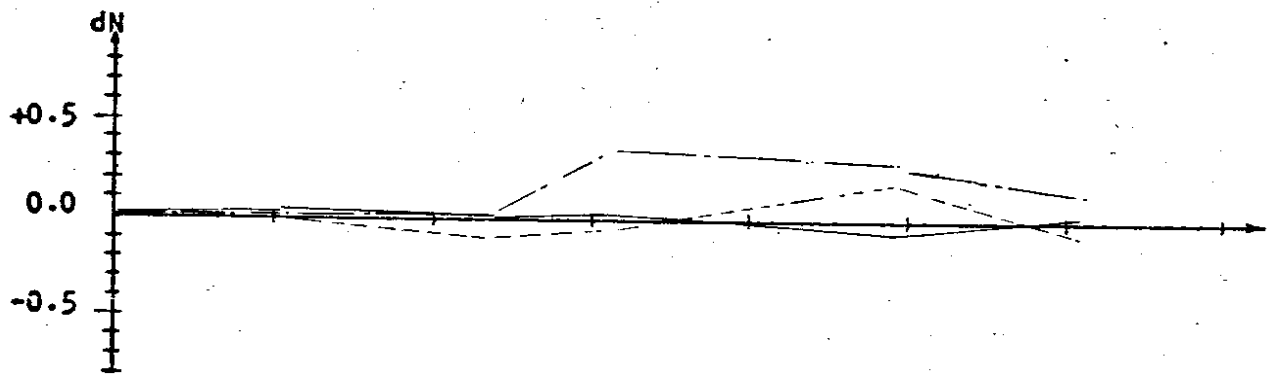
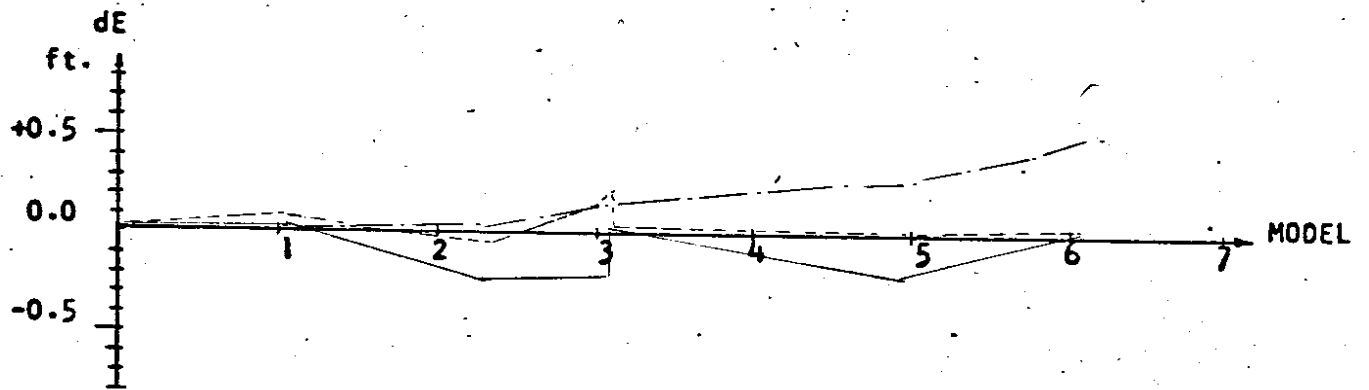


● Control points

○ Check points

"2" Horizontal point; "3" Vertical point; "4" Horizontal & vertical point

**Fig.46** Layout of ground control points of test strip 7



- Linear transformation
- Beginning, middle and end (2nd)
- Traverse method (2nd)

Fig. 47 Comparison of Discrepancies Resulting from Different Adjustment Procedures of Test Strip 7 at Flight Height of 1500 Feet

TABLE 10 RESULTS OF DIFFERENT ADJUSTMENT  
PROCEDURES OF TEST STRIP . 7 AT FLIGHT  
HEIGHT OF 1500 FEET

Method	Linear Transformation	Beginning, Middle and End (2nd)	Traverse Method(2nd)
<b>Control points only</b>			
RMSE of dE in ft.	0.00	0.06	0.00
RMSE of dN	0.00	0.09	0.00
RMSE of dP	0.00	0.08	0.00
RMSE of dH	0.02	0.00	0.00
MAX, dE	0.00	0.07	0.00
MAX, dN	0.00	0.14	0.00
MAX, dH	0.03	0.00	0.00
<b>Check points</b>			
RMSE of dE in ft.	0.31	0.18	0.22
RMSE of dN	0.22	0.06	0.08
RMSE of dP	0.27	0.13	0.17
RMSE of dH	1.30	0.65	0.23
MAX, dE	0.53	0.25	0.32
MAX, dN	0.34	0.09	0.10
MAX, dH	2.41	1.09	0.35

\*More control points needed.

5-4-8.

TEST STRIP NO. 8

Test area: Riverton Hts 1/C 71-8-24

Flight height  $\approx$  1500 feet; Mean elevation  $\approx$  350 feet.

Models: 5

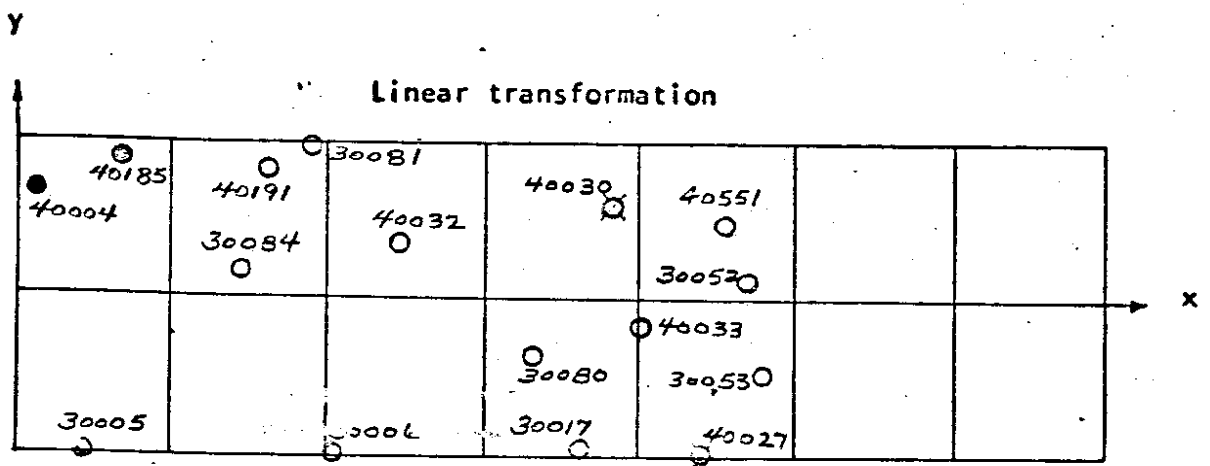
Horizontal control points: 8

Vertical control points: 16

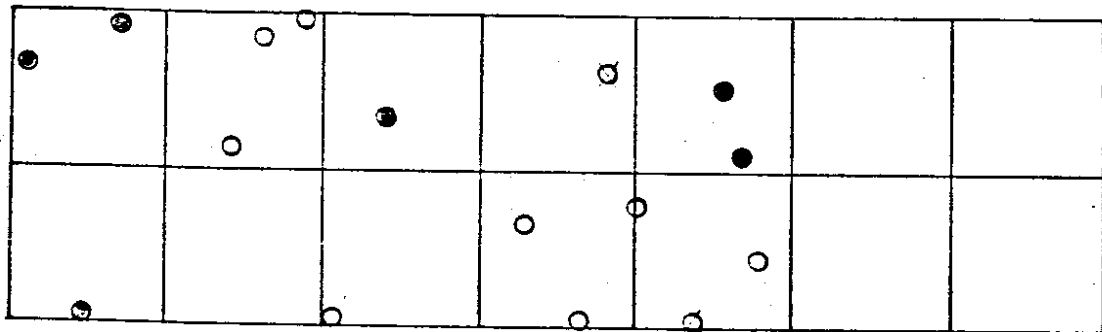
Location of all ground control points shown in Figure: 48

Residuals of all check points shown in Figure: 49

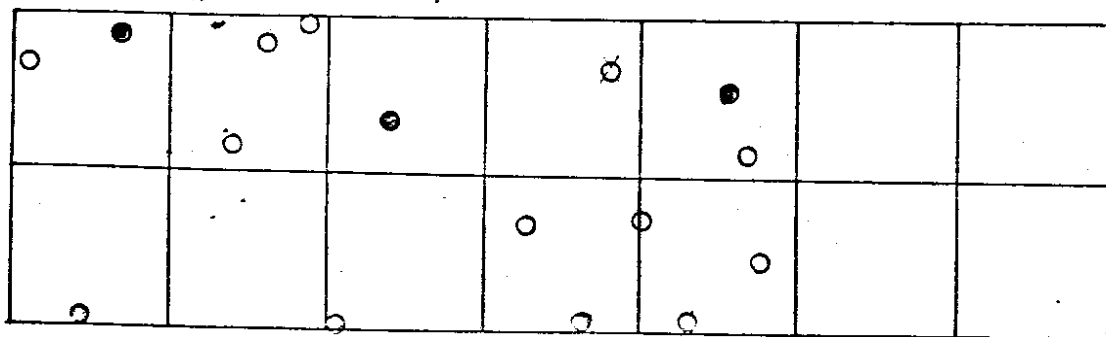
Stand errors of three different adjustment procedures of this strip  
shown in Table: 11



**Beginning, middle and end (2nd)**



**Traverse method (2nd)**



○ Detected ground control point in error

● Control points

○ Check points

"2" Horizontal point; "3" Vertical point; "4" Horizontal & vertical point

**Fig.48** Layout of ground control points of test strip 8

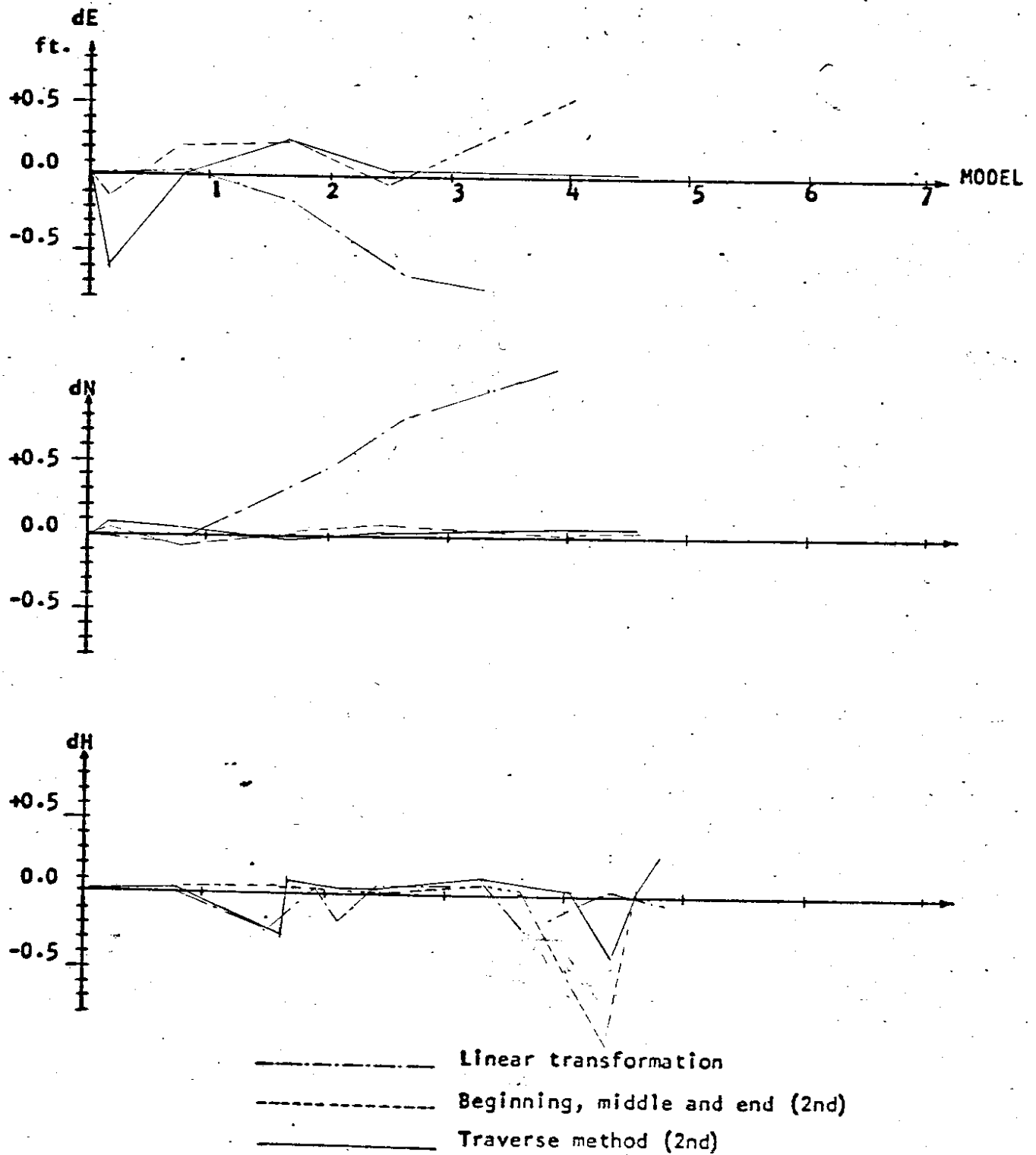


Fig. 49 Comparison of Discrepancies Resulting from Different Adjustment Procedures of Test Strip 8 at Flight Height of 1500 Feet

TABLE 11 RESULTS OF DIFFERENT ADJUSTMENT  
PROCEDURES OF TEST STRIP 8 AT FLIGHT  
HEIGHT OF 1500 FEET

Method	Linear Transformation	Beginning, Middle and End (2nd)	Traverse Method(2nd)
<b>Control points only</b>			
RMSE of dE in ft.	0.00	0.13	0.00
RMSE of dN	0.00	0.05	0.00
RMSE of dP	0.00	0.10	0.00
RMSE of dH	0.00	0.00	0.02
MAX. dE	0.00	0.21	0.00
MAX. dN	0.00	0.08	0.00
MAX. dH	0.00	0.00	0.03
<b>Check points</b>			
RMSE of dE in ft.	0.52	0.42	0.56
RMSE of dN	1.00	0.01	0.06
RMSE of dP	0.80	0.30	0.40
RMSE of dH	0.13	0.86	0.15
MAX. dE	0.75	0.56	0.74
MAX. dN	1.29	0.01	0.06
MAX. dH	0.30	1.71	0.21

\*More control points needed.

5-4-9.

TEST STRIP NO. 9

Test area: So. 160th To 136th 71-8-24

Flight height  $\cong$  1500 feet; Mean elevation  $\cong$  250 feet.

Models: 6

Horizontal control points: 5

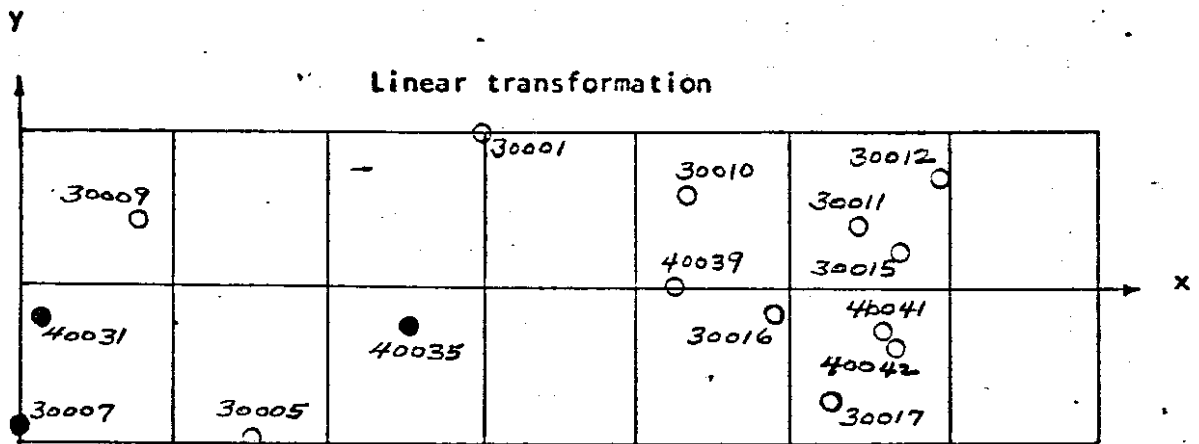
Vertical control points: 15

Location of all ground control points shown in Figure: 50

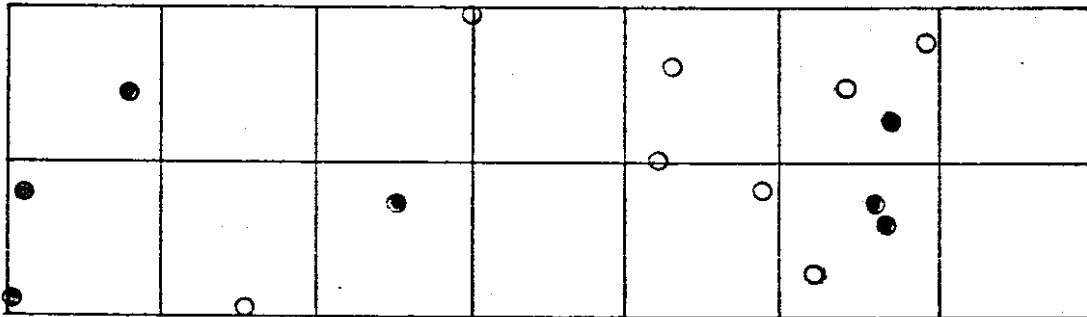
Residuals of all check points shown in Figure: 51

Stand errors of three different adjustment procedures of this strip  
shown in Table: 12

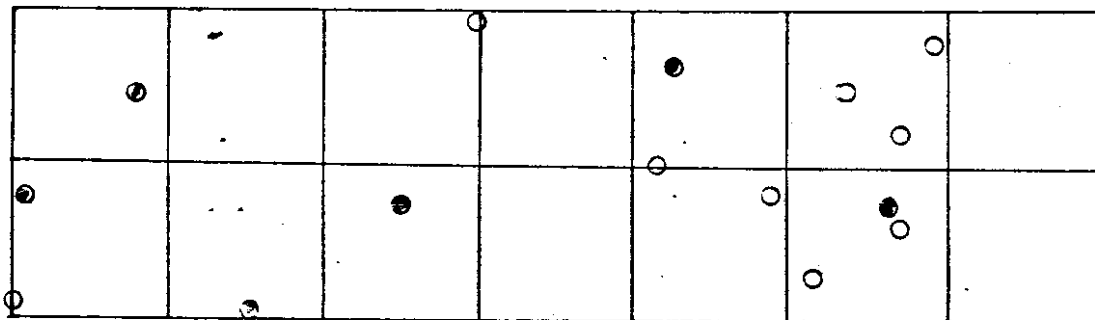




**Beginning, middle and end (2nd)**



**Traverse method (2nd)**

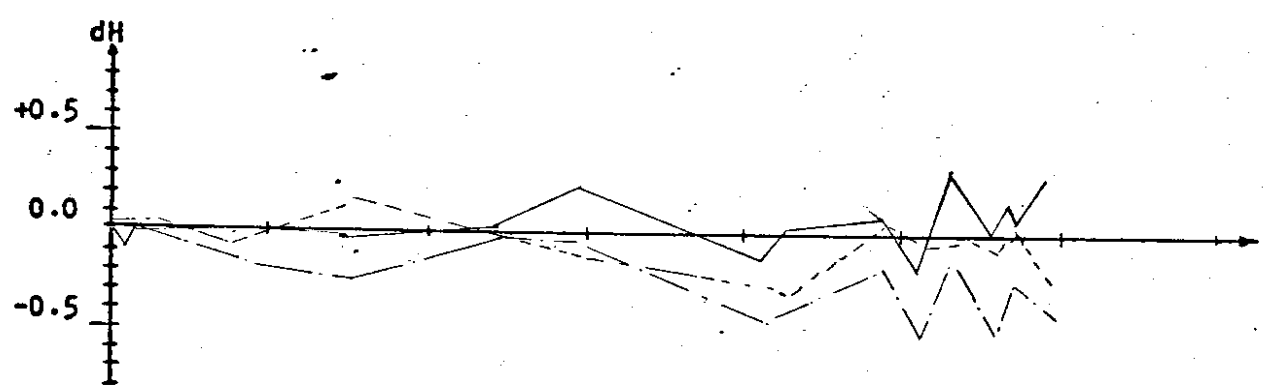
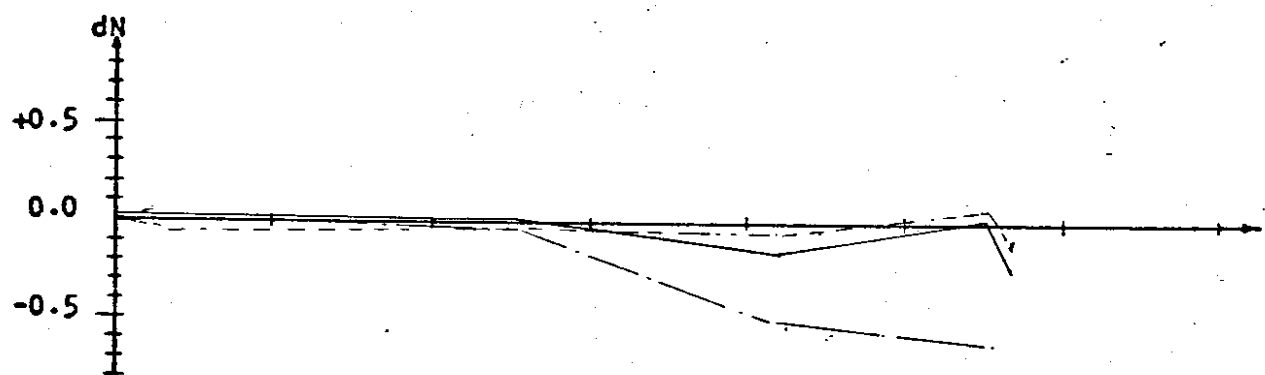
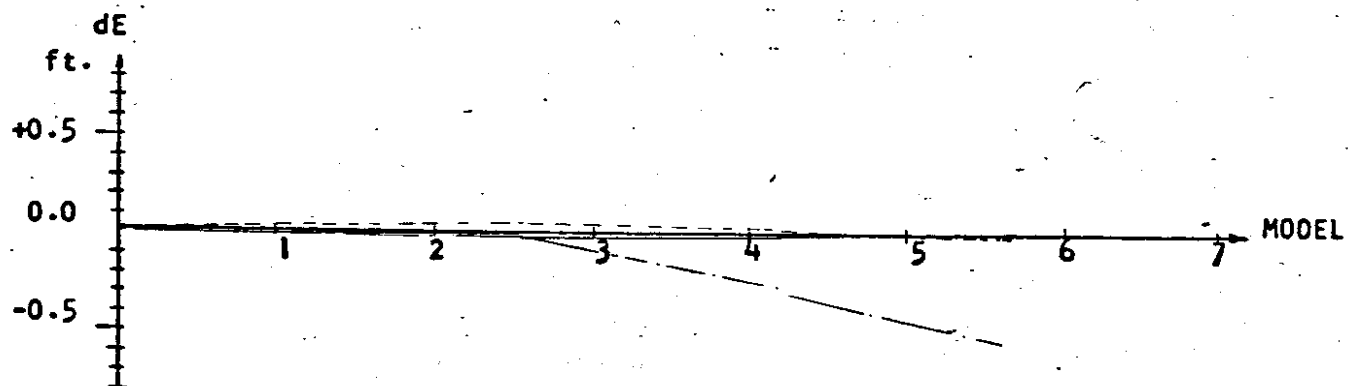


● Control points

○ Check points

"2" Horizontal point; "3" Vertical point; "4" Horizontal & vertical point

**Fig. 50 Layout of ground control points of test strip 9**



- Linear transformation
- Beginning, middle and end (2nd)
- Traverse method (2nd)

Fig. 51 Comparison of Discrepancies Resulting from Different Adjustment Procedures of Test Strip 9 at Flight Height of 1500 Feet

TABLE 12 RESULTS OF DIFFERENT ADJUSTMENT  
 PROCEDURES OF TEST STRIP 9 AT FLIGHT  
 HEIGHT OF 1500 FEET

Method	Linear Transformation	Beginning, Middle and End (2nd)	Traverse Method(2nd)
<b>Control points only</b>			
RMSE of dE in ft.	0.00	0.00	0.00
RMSE of dN	0.00	0.08	0.00
RMSE of dP	0.00	0.05	0.00
RMSE of dH	0.00	0.04	0.01
MAX. dE	0.00	0.00	0.00
MAX. dN	0.00	0.11	0.00
MAX. dH	0.00	0.07	0.02
<b>Check points</b>			
RMSE of dE in ft.	0.53	0.02	0.02
RMSE of dN	0.56	0.09	0.19
RMSE of dP	0.54	0.07	0.14
RMSE of dH	0.31	0.17	0.21
MAX. dE	0.62	0.02	0.02
MAX. dN	0.72	0.09	0.23
MAX. dH	0.42	0.29	0.33

5-4-10.

TEST STRIP NO. 10

Test area: Pidchach Lake I/C 71-10-15

Flight height  $\approx$  1500 feet; Mean elevation  $\approx$  100 feet.

Models: 4

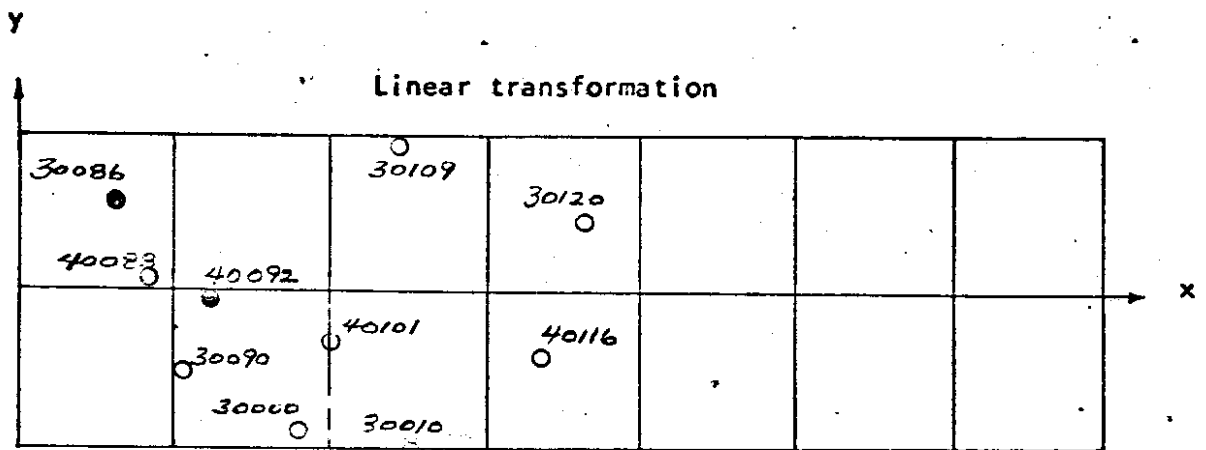
Horizontal control points: 4

Vertical control points: 10

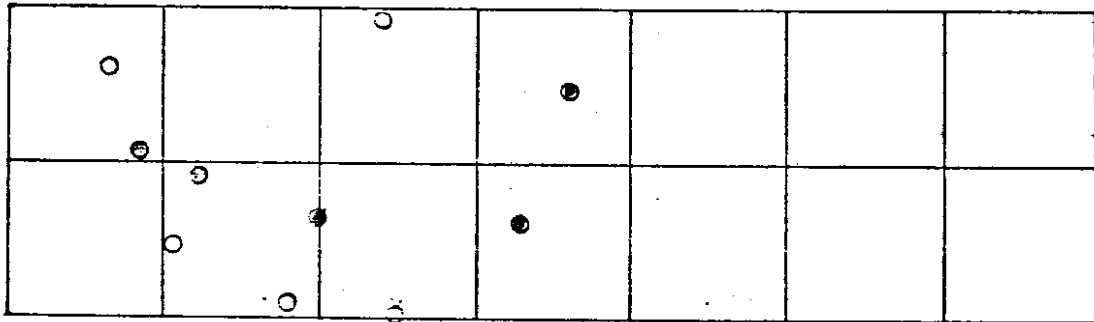
Location of all ground control points shown in Figure: 52

Residuals of all check points shown in Figure: 53

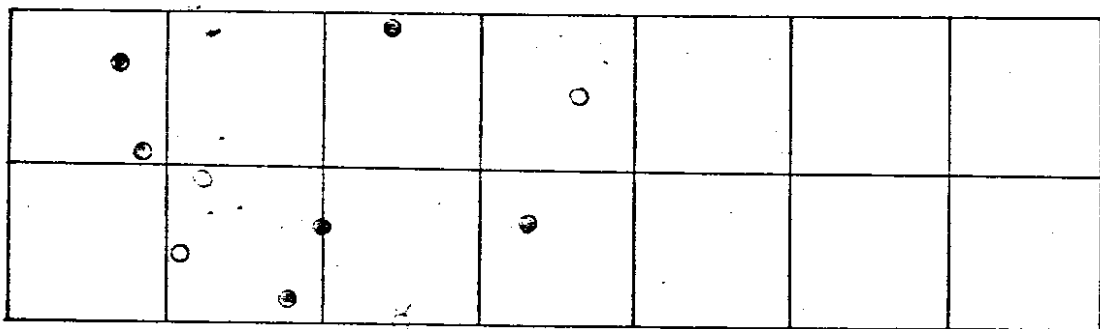
Stand errors of three different adjustment procedures of this strip  
shown in Table: 13



**Beginning, middle and end (2nd)**



**Traverse method (2nd)**



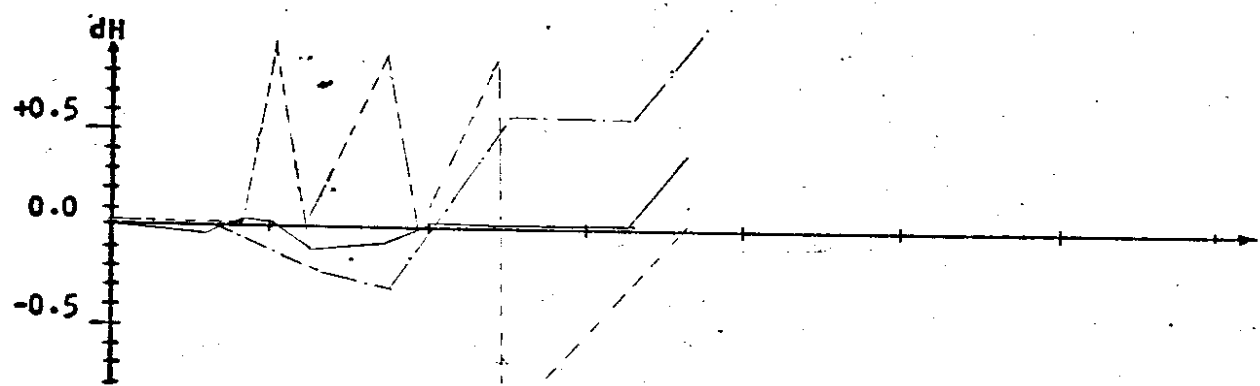
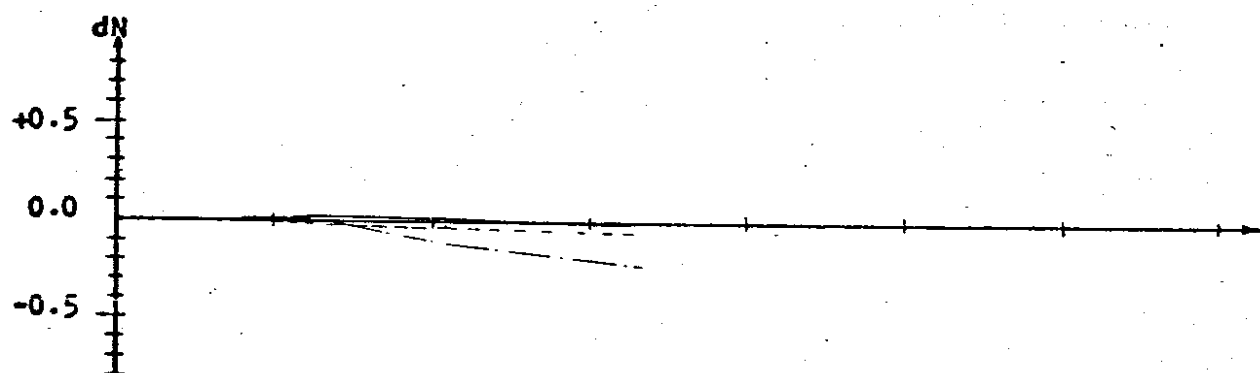
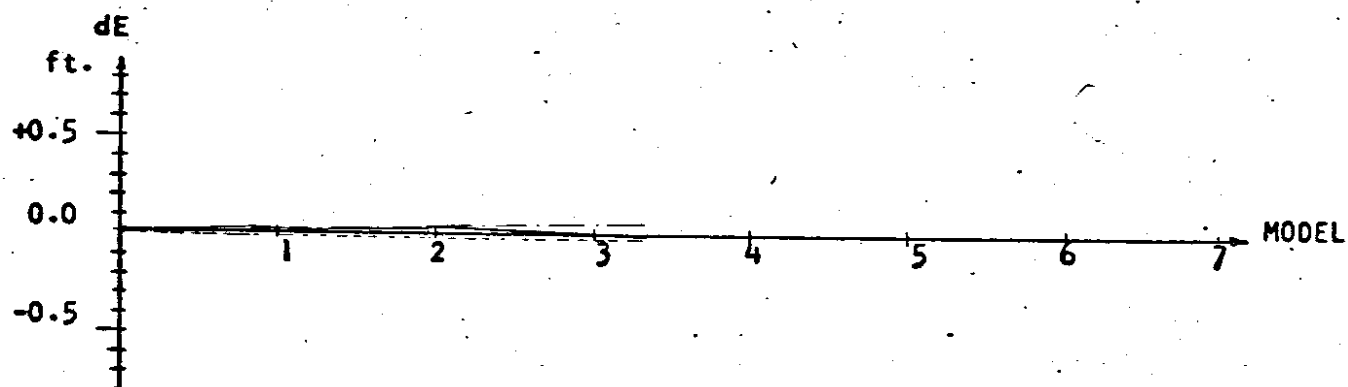
⊗ Detected ground control point in error

● Control points

○ Check points

"2" Horizontal point; "3" Vertical point; "4" Horizontal & vertical point

**Fig-52** Layout of ground control points of test strip 10



- Linear transformation
- Beginning, middle and end (2nd)
- Traverse method (2nd)

Fig. 53 Comparison of Discrepancies Resulting from Different Adjustment Procedures of Test Strip 10 at Flight Height of 1500 Feet

TABLE 13 RESULTS OF DIFFERENT ADJUSTMENT  
 PROCEDURES OF TEST STRIP 10 AT FLIGHT  
 HEIGHT OF 1500 FEET

Method	Linear Transformation	Beginning, Middle and End (2nd)	Traverse Method(2nd)
<b>Control points only</b>			
RMSE of dE in ft.	0.00	0.00	0.00
RMSE of dN	0.00	0.01	0.00
RMSE of dP	0.00	0.01	0.00
RMSE of dH	0.00	0.00	0.04
MAX. dE	0.00	0.00	0.00
MAX. dN	0.00	0.02	0.00
MAX. dH	0.00	0.00	0.05
<b>Check points</b>			
RMSE of dE in ft.	0.06	—	0.01
RMSE of dN	0.16	—	0.03
RMSE of dP	0.12	—	0.02
RMSE of dH	0.73	3.11	0.23
MAX. dE	0.07	—	0.01
MAX. dN	-0.20	—	0.03
MAX. dH	1.55	4.26	0.39

\*More control points needed.

5-5. Testing of ten strips of the flight at 3000 feet.

5-5-1. TEST STRIP NO. 11

Test area: Trooper Rd. to Martin Way, 5, 70-10-27.

Flight height  $\cong$  3000 feet, mean elevation  $\cong$  140

Models: 8

Horizontal control points: 4

Vertical control points: 12

Location of all ground control points shown in Figure: 54

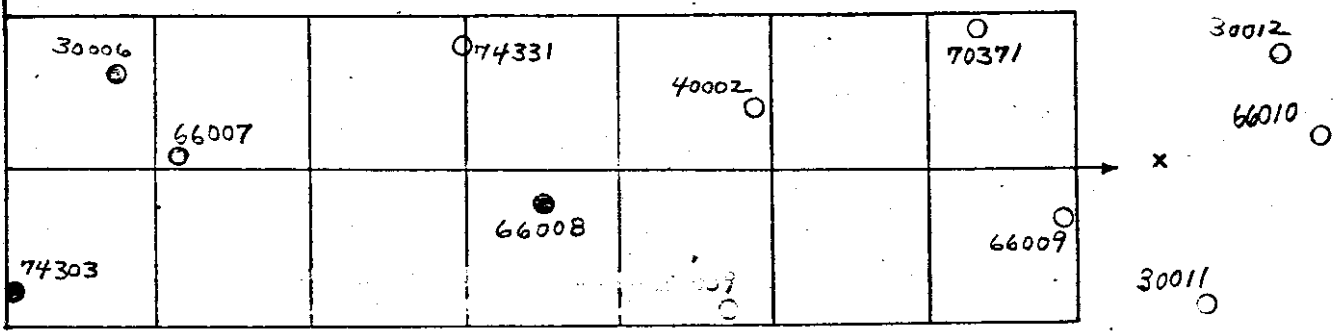
Residuals of all check points shown in Figure: 55

Stand errors of three different adjustment procedures of this strip  
shown in Table: 14

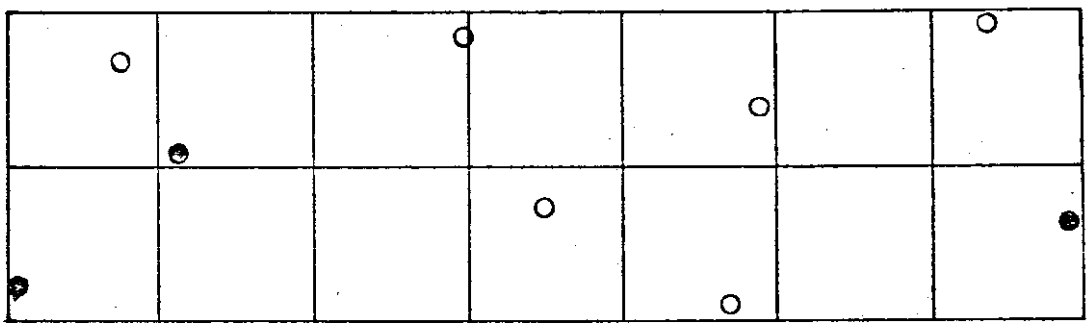


Y

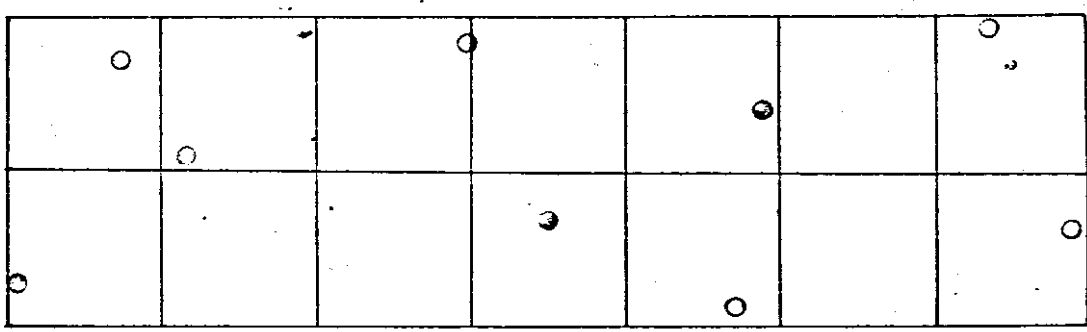
Linear transformation



Beginning, middle and end (2nd)



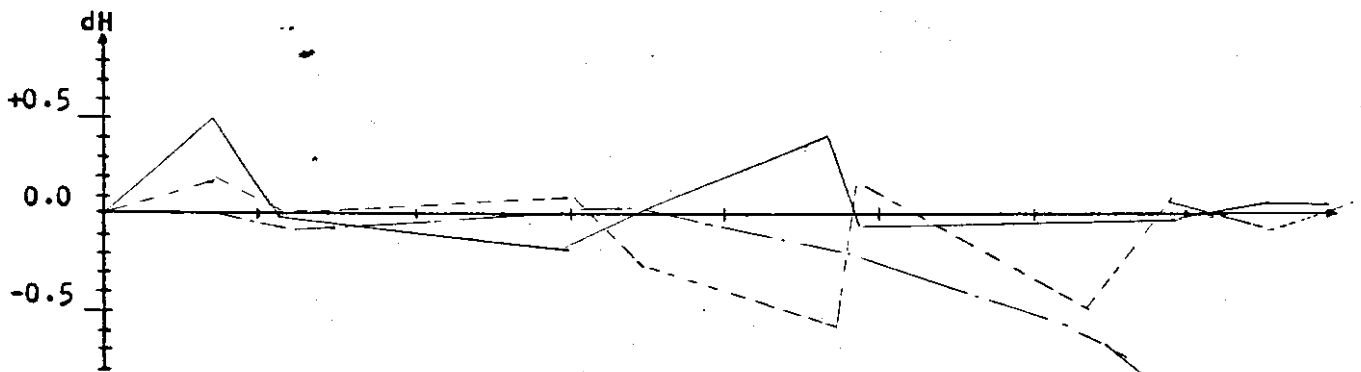
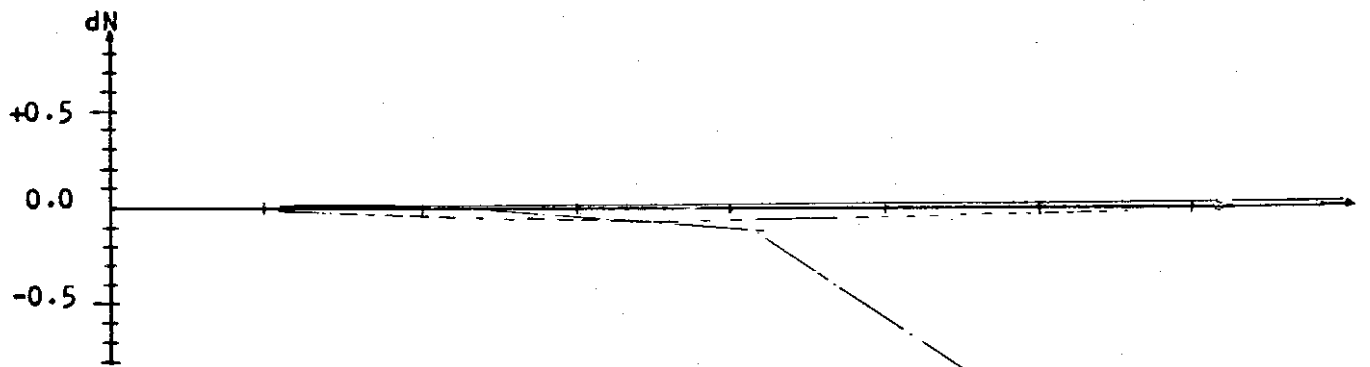
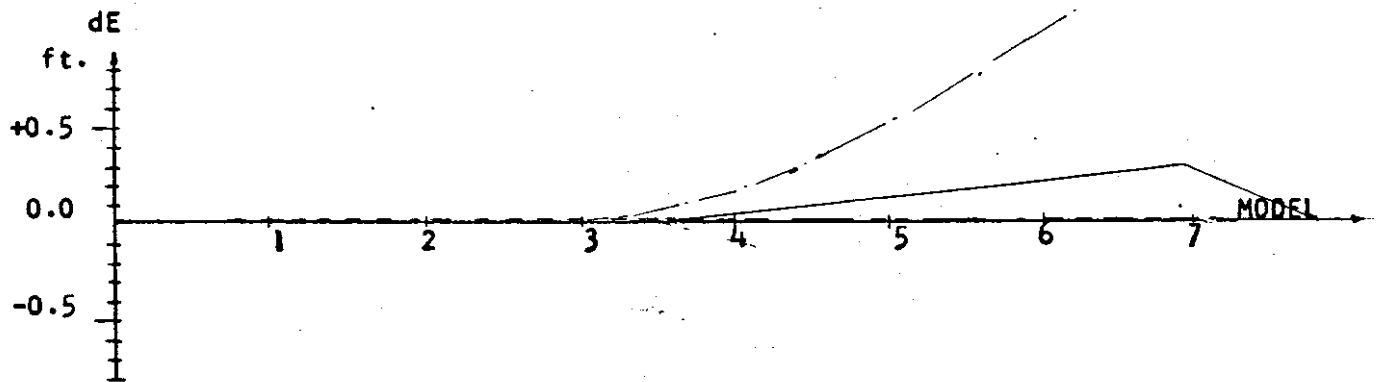
Traverse method (2nd)



- Control points
- Check points

"2" Horizontal point; "3" Vertical point; "4" Horizontal & vertical point

Fig.54 Layout of ground control points of test strip 11



- Linear transformation
- Beginning, middle and end (2nd)
- Traverse method (2nd)

Fig. 55 Comparison of Discrepancies Resulting from Different Adjustment Procedures of Test Strip 11 at Flight Height of 1500 Feet

TABLE 14 RESULTS OF DIFFERENT ADJUSTMENT  
PROCEDURES OF TEST STRIP 11 AT FLIGHT  
HEIGHT OF 3000 FEET

Method	Linear Transformation	Beginning, Middle and End (2nd)	Traverse Method(2nd)
<b>Control points only</b>			
RMSE of dE in ft.	0.00	0.00	0.00
RMSE of dN	0.00	0.00	0.00
RMSE of dP	0.00	0.00	0.00
RMSE of dH	0.04	0.07	0.04
MAX. dE	0.00	0.00	0.00
MAX. dN	0.00	0.00	0.00
MAX. dH	0.07	0.09	0.06
<b>Check points</b>			
RMSE of dE in ft.	0.58	0.27	0.18
RMSE of dN	2.52	0.39	0.43
RMSE of dP	1.83	0.33	0.33
RMSE of dH	1.21	0.36	0.34
MAX. dE	1.12	0.27	0.18
MAX. dN	4.76	0.39	0.43
MAX. dH	2.81	0.27	0.46

5-5-2.

TEST STRIP NO. 12

Test area: 80th NE to SR 405, 1, 71-3-5

Flight height  $\cong$  3000 feet, Mean elevation = 120 feet.

Models: 7

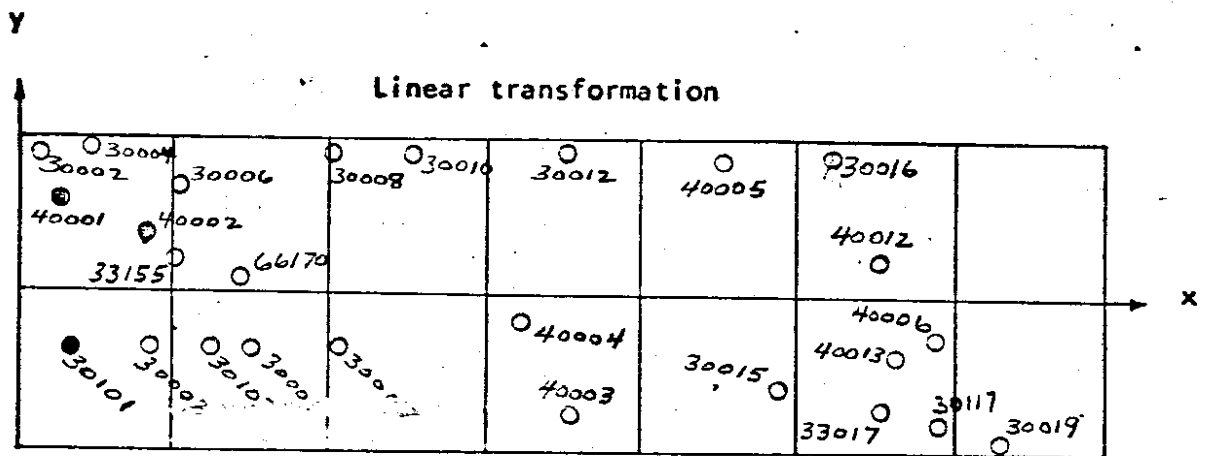
Horizontal control points: 9

Vertical control points: 26

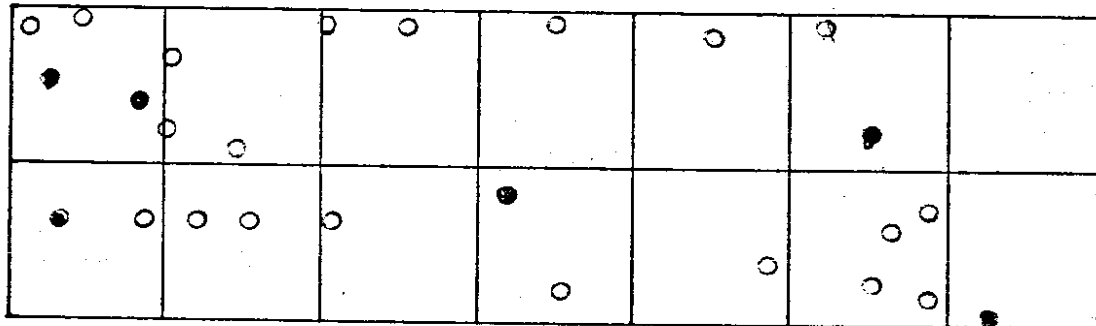
Location of all ground control points shown in Figure: 56

Residuals of all check points shown in Figure: 57

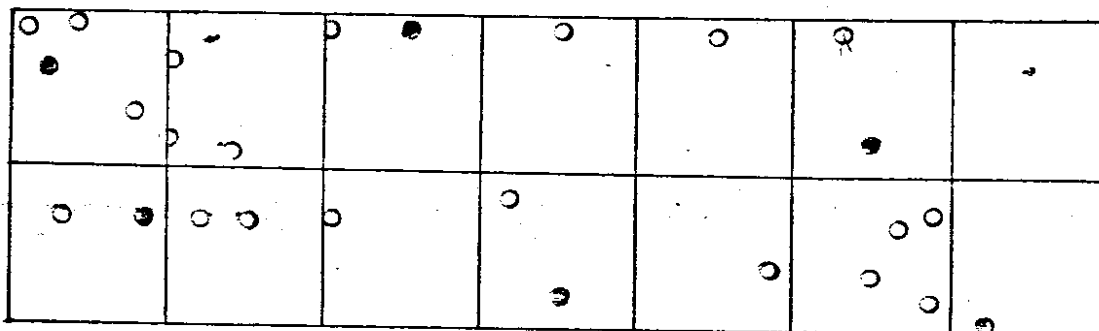
Stand errors of three different adjustment procedures of this strip  
shown in Table: 15



**Beginning, middle and end (2nd)**



**Traverse method (2nd)**

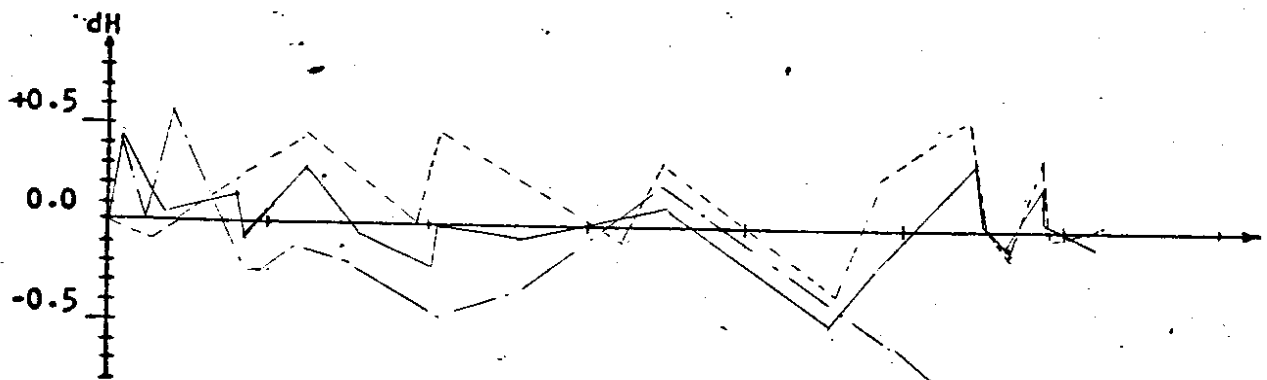
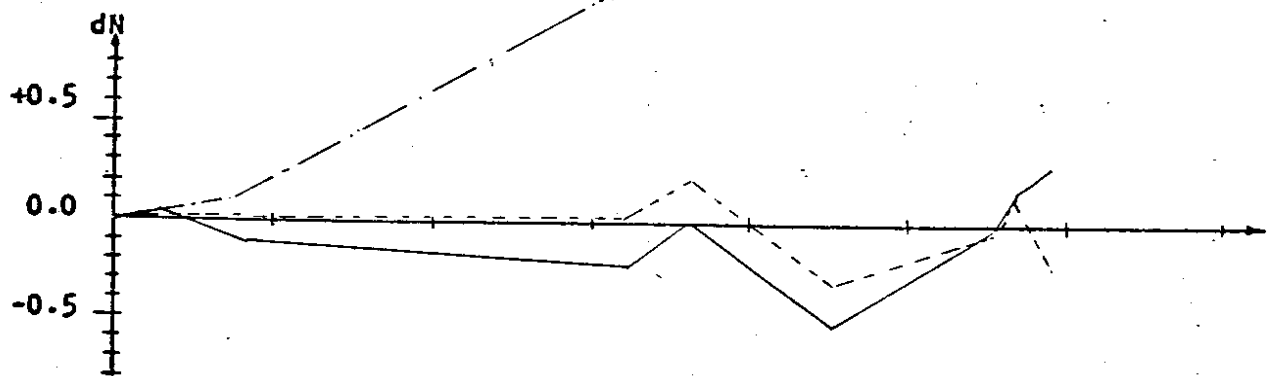
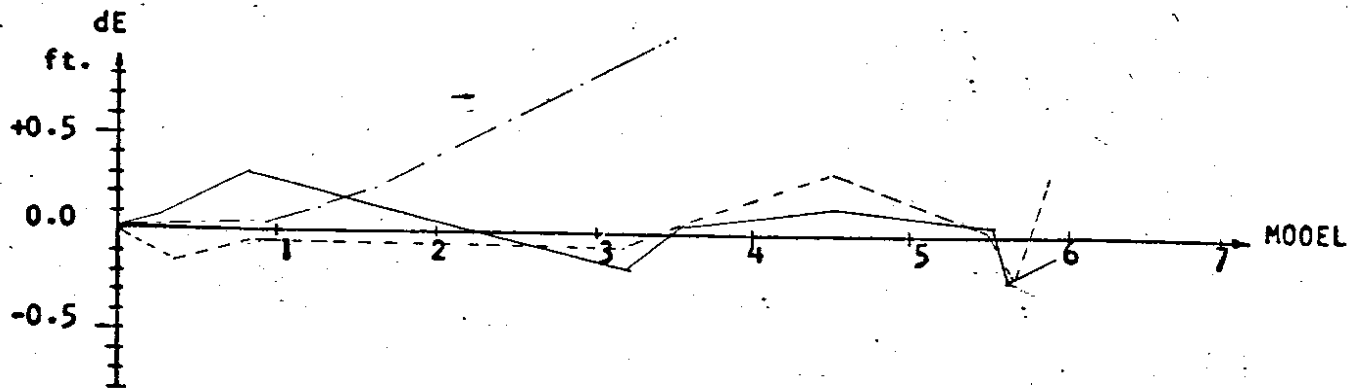


Detected ground control point in error

- Control points
- Check points

"2" Horizontal point; "3" Vertical point; "4" Horizontal & vertical point

Fig.56 Layout of ground control points of test strip 12



- ..... Linear transformation
- Beginning, middle and end (2nd)
- Traverse method (2nd)

Fig. 57 Comparison of Discrepancies Resulting from Different Adjustment Procedures of Test Strip 12 at Flight Height of 3000 Feet

TABLE 15. RESULTS OF DIFFERENT ADJUSTMENT  
 PROCEDURES OF TEST STRIP 12 AT FLIGHT  
 HEIGHT OF 3000 FEET

Method	Linear Transformation	Beginning, Middle and End (2nd)	Traverse Method(2nd)
<b>Control points only</b>			
RMSE of dE in ft.	0.00	0.15	0.00
RMSE of dN	0.00	0.03	0.00
RMSE of dP	0.00	0.11	0.00
RMSE of dH	0.00	0.12	0.09
MAX. dE	0.00	0.23	0.00
MAX. dN	0.00	0.04	0.00
MAX. dH	0.00	0.24	0.10
<b>Check points</b>			
RMSE of dE in ft.	0.65	0.23	0.19
RMSE of dN	2.31	0.25	0.30
RMSE of dP	1.70	0.24	0.25
RMSE of dH	0.77	0.38	0.32
MAX. dE	1.40	0.31	0.26
MAX. dN	3.74	0.33	0.48
MAX. dH	1.67	0.81	0.76

5-5-3.

TEST STRIP NO. 13

Test area: 80th To SR 405. 2, 71-8-5.

Flight height  $\approx$  3000 feet. Mean elevation  $\approx$  250 feet.

Models: 5

Horizontal control points: 4

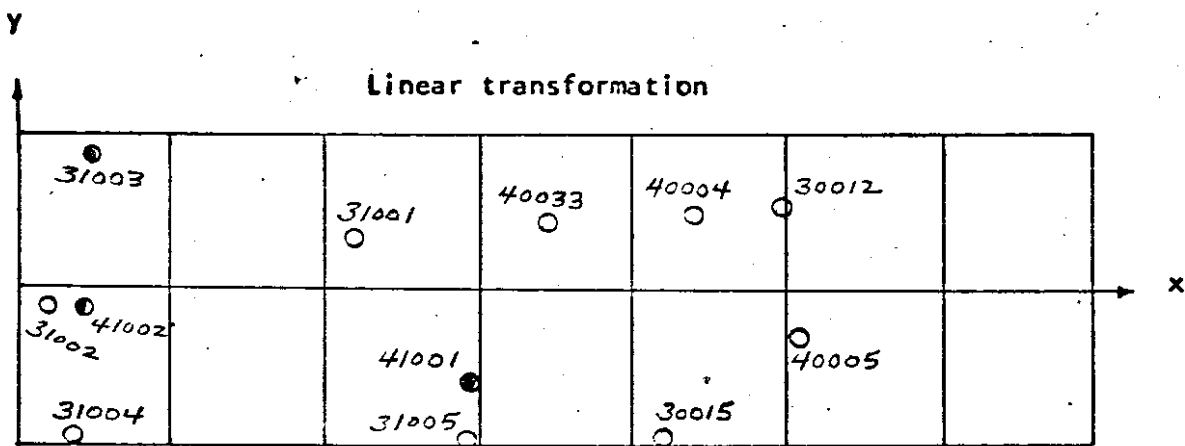
Vertical control points: 12

Location of all ground control points shown in Figure: 58

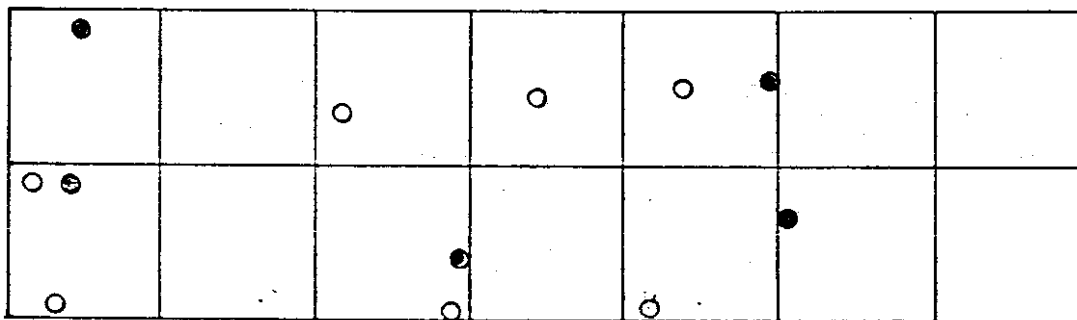
Residuals of all check points shown in Figure: 59

Stand errors of three different adjustment procedures of this strip  
shown in Table: 16

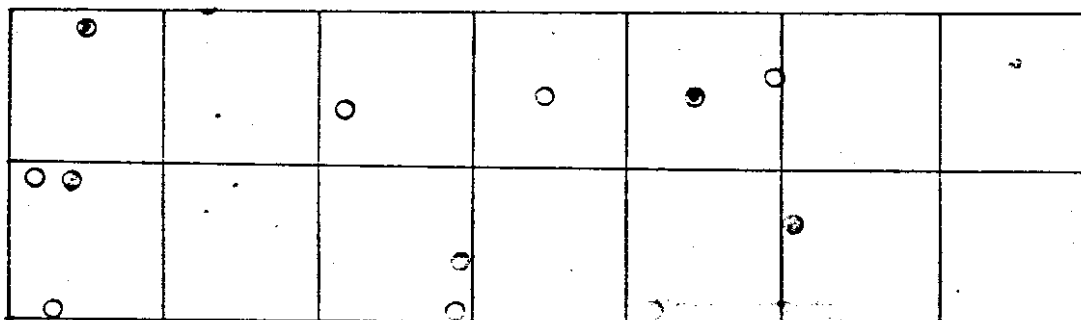




**Beginning, middle and end (2nd)**



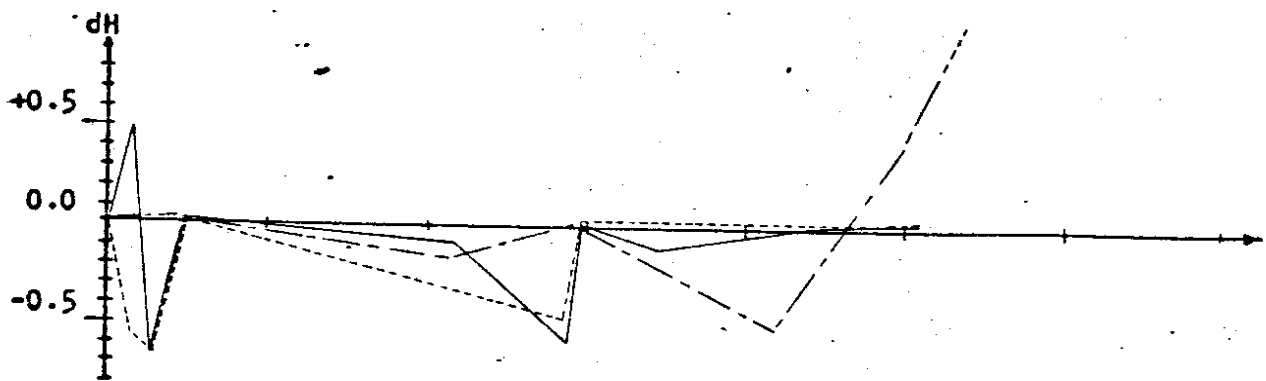
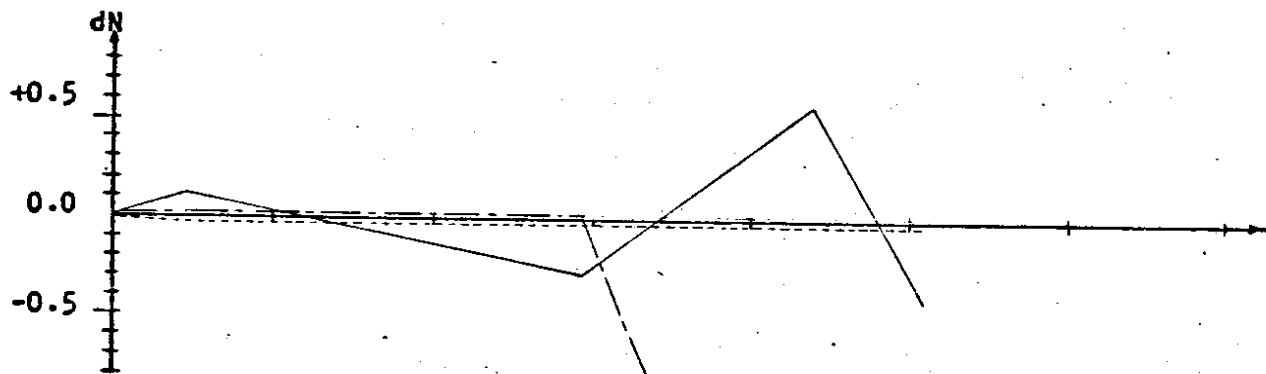
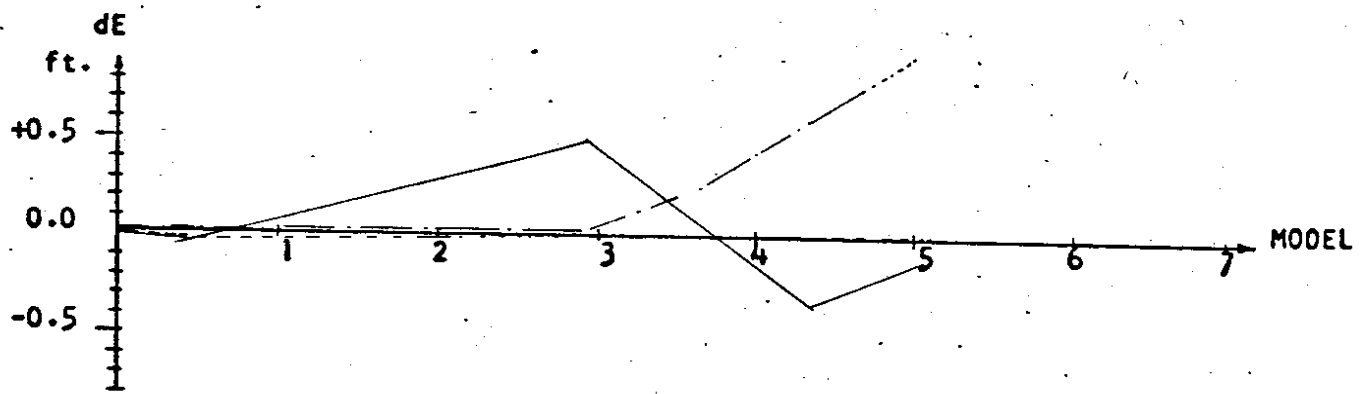
**Traverse method (2nd)**



- Detected ground control point in error
- Control points
- Check points

"2" Horizontal point; "3" Vertical point; "4" Horizontal & vertical point

Fig-58 Layout of ground control points of test strip 13



- Linear transformation
- Beginning, middle and end (2nd)
- Traverse method (2nd)

Fig. 59 Comparison of Discrepancies Resulting from Different Adjustment Procedures of Test Strip 13 at Flight Height of 3000 Feet

TABLE 16 RESULTS OF DIFFERENT ADJUSTMENT  
 PROCEDURES OF TEST STRIP 13 AT FLIGHT  
 HEIGHT OF 3000 FEET

Method	Linear Transformation	Beginning, Middle and End (2nd)	Traverse Method(2nd)
Control points only			
RMSE of dE in ft.	0.00	0.00	0.30
RMSE of dN	0.00	0.00	0.40
RMSE of dP	0.00	0.00	0.00
RMSE of dH	0.00	0.00	0.00
MAX. dE	0.00	0.00	0.49
MAX. dN	0.00	0.00	0.59
MAX. dH	0.00	0.00	0.00
Check points			
RMSE of dE in ft.	1.41	0.64	—
RMSE of dN	0.93	1.19	—
RMSE of dP	1.19	0.94	—
RMSE of dH	1.28	0.77	0.58
MAX. dE	2.56	0.64	—
MAX. dN	1.69	1.19	—
MAX. dH	2.60	1.06	0.94

\*More control points needed.

5-5-4.

TEST STRIP NO. 14

Test area: Boundary to International Border, 71-10-8.

Flight height  $\cong$  3000 feet, mean elevation  $\cong$  1600 feet

Models: 4

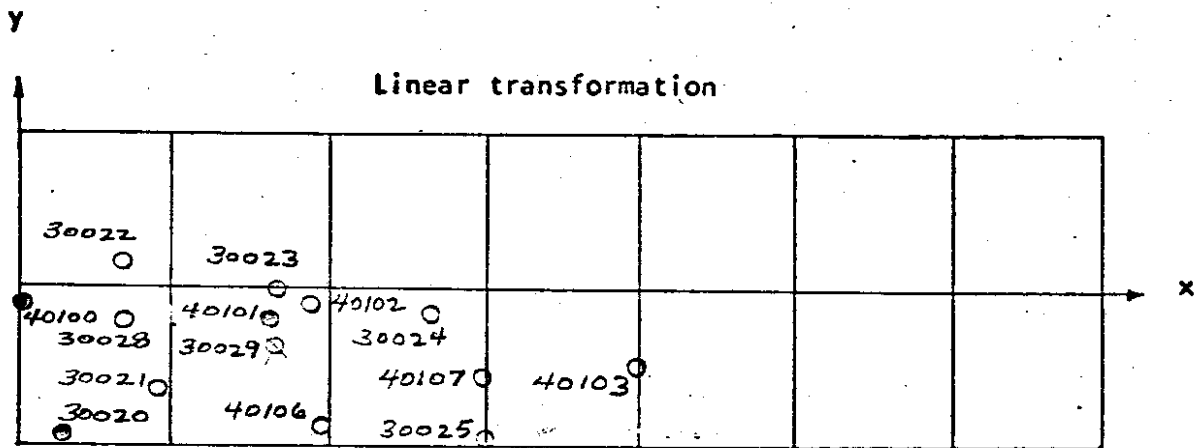
Horizontal control points: 6

Vertical control points: 14

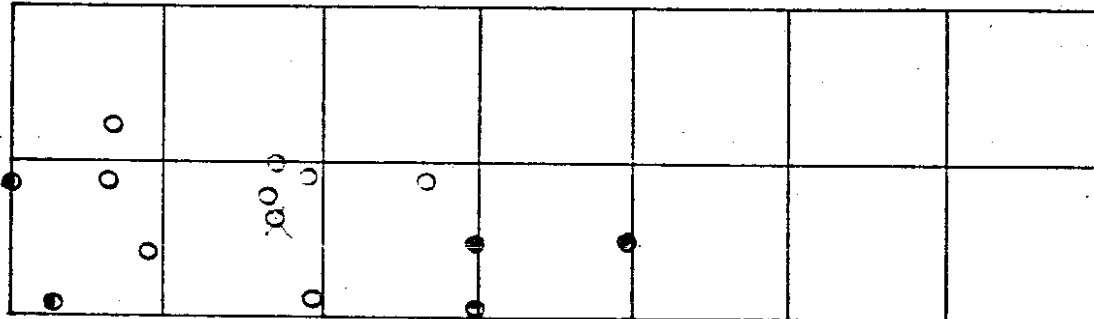
Location of all ground control points shown in Figure: 60

Residuals of all check points shown in Figure: 61

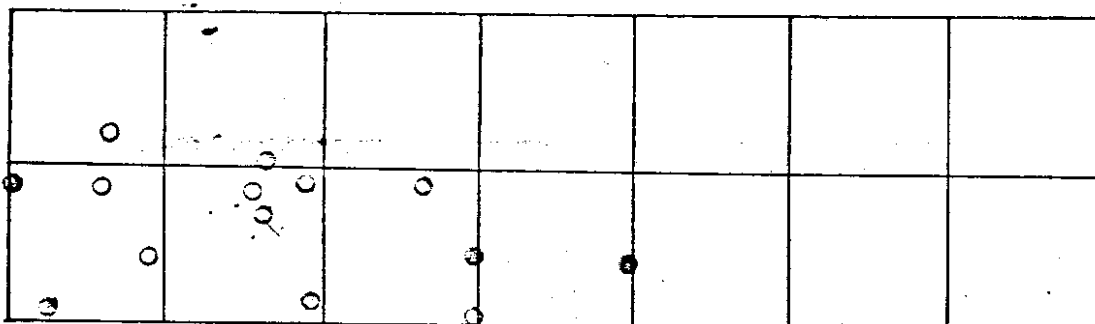
Stand errors of three different adjustment procedures of this strip  
shown in Table: 17



**Beginning, middle and end (2nd)**



**Traverse method (2nd)**



○ Detected ground control point in error

● Control points

○ Check points

"2" Horizontal point; "3" Vertical point; "4" Horizontal & vertical point

**Fig-60** Layout of ground control points of test strip 14

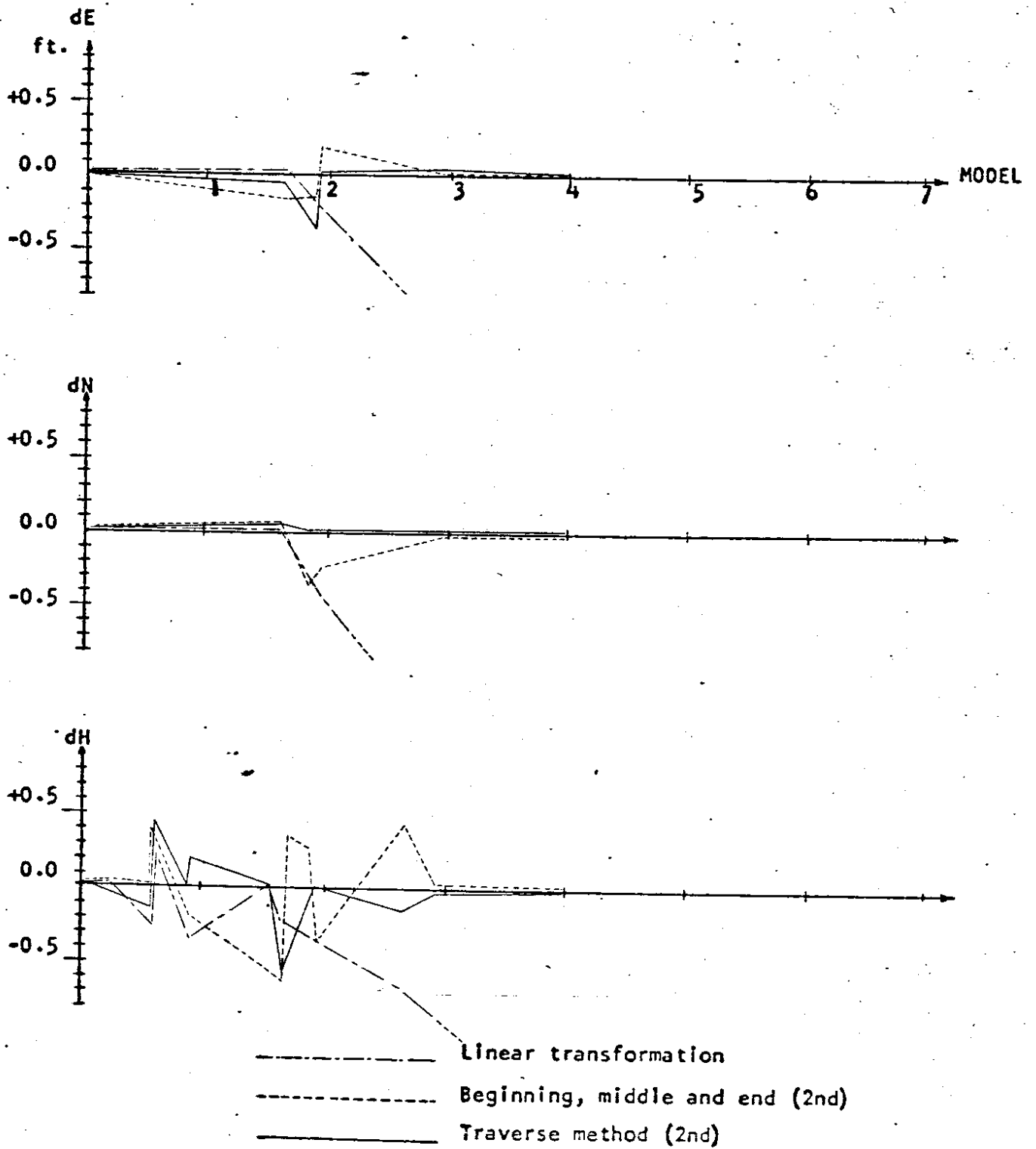


Fig. 61 Comparison of Discrepancies Resulting from Different Adjustment Procedures of Test Strip 14 at Flight Height of 3000 Feet

TABLE 17 RESULTS OF DIFFERENT ADJUSTMENT  
PROCEDURES OF TEST STRIP 14 AT FLIGHT  
HEIGHT OF 3000 FEET

Method	Linear Transformation	Beginning, Middle and End (2nd)	Traverse Method(2nd)
<b>Control points only</b>			
RMSE of dE in ft.	0.00	0.00	0.004
RMSE of dN	0.00	0.00	0.02
RMSE of dP	0.00	0.00	0.03
RMSE of dH	0.00	0.00	0.03
MAX. dE	0.00	0.00	0.05
MAX. dN	0.00	0.00	0.04
MAX. dH	0.00	0.00	0.07
<b>Check points</b>			
RMSE of dE in ft.	1.13	0.19	0.02
RMSE of dN	1.54	0.23	0.38
RMSE of dP	1.35	0.21	0.27
RMSE of dH	0.81	0.38	0.79
MAX. dE	2.53	0.21	0.02
MAX. dN	3.33	0.31	0.38
MAX. dH	1.85	0.63	1.79

\*More control points needed.

5-5-5.

TEST STRIP NO. 15

Test area: Sumner to King Co. Line, 0, 67-5-11.

Flight height  $\cong$  3000 feet Mean elevation  $\cong$  60 feet.

Models: 8

Horizontal control points: 7

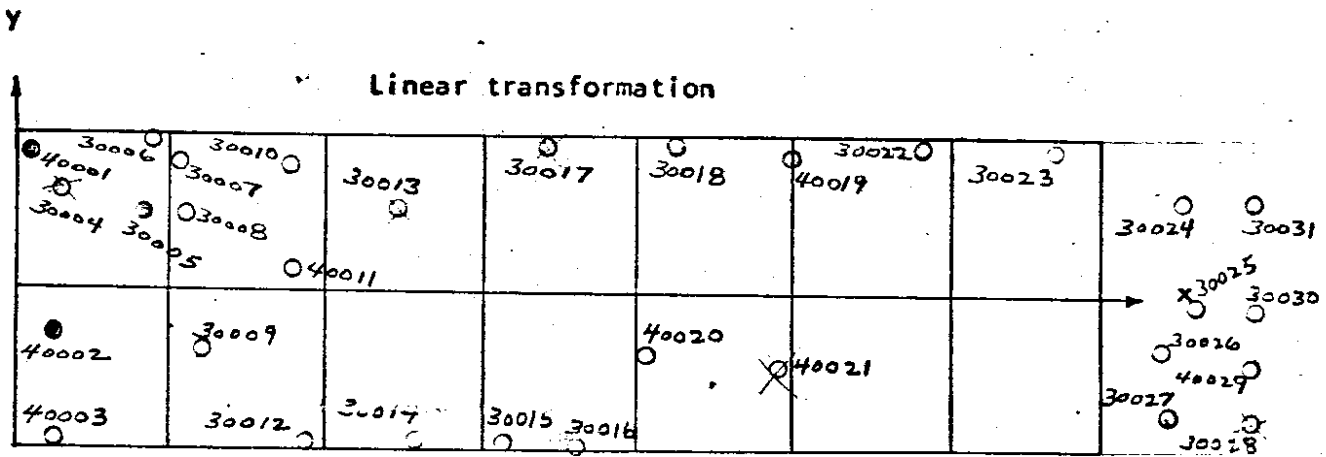
Vertical control points: 31

Location of all ground control points shown in Figure: 62

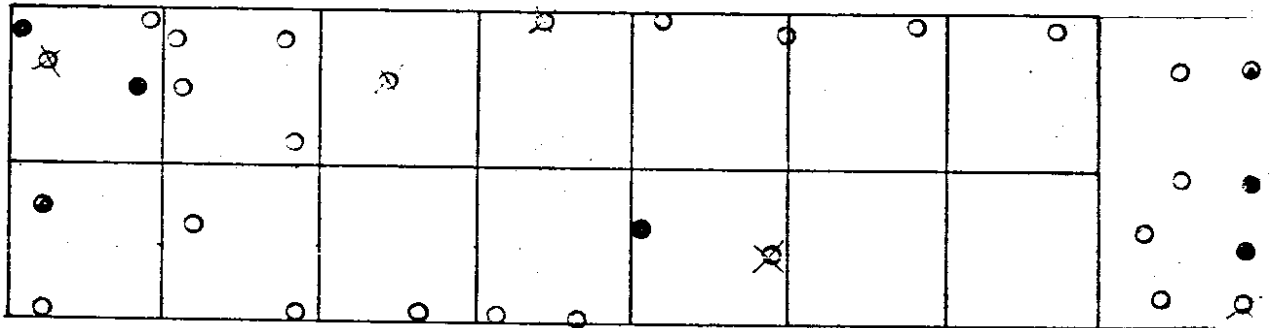
Residuals of all check points shown in Figure: 63

Stand errors of three different adjustment procedures of this strip  
shown in Table: 18

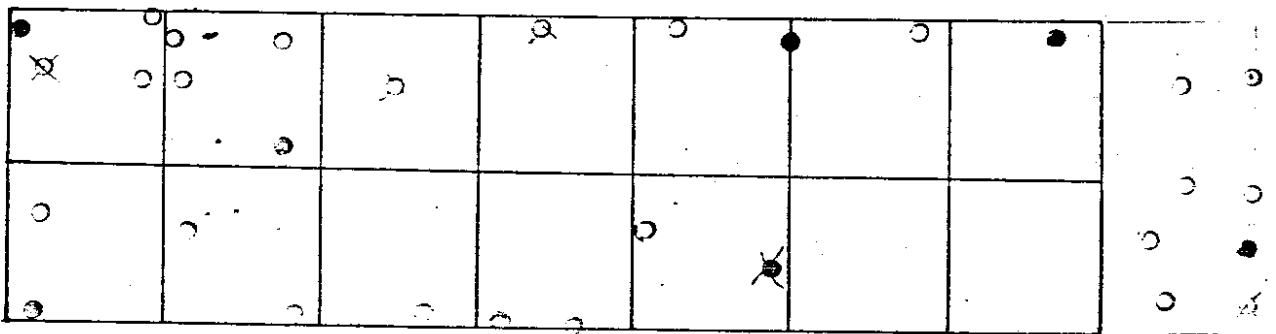




**Beginning, middle and end (2nd)**



**Traverse method (2nd)**



⊗ Detected ground control point in error

● Control points

○ Check points

"2" Horizontal point; "3" Vertical point; "4" Horizontal & vertical point

Fig-62 Layout of ground control points of test strip 15

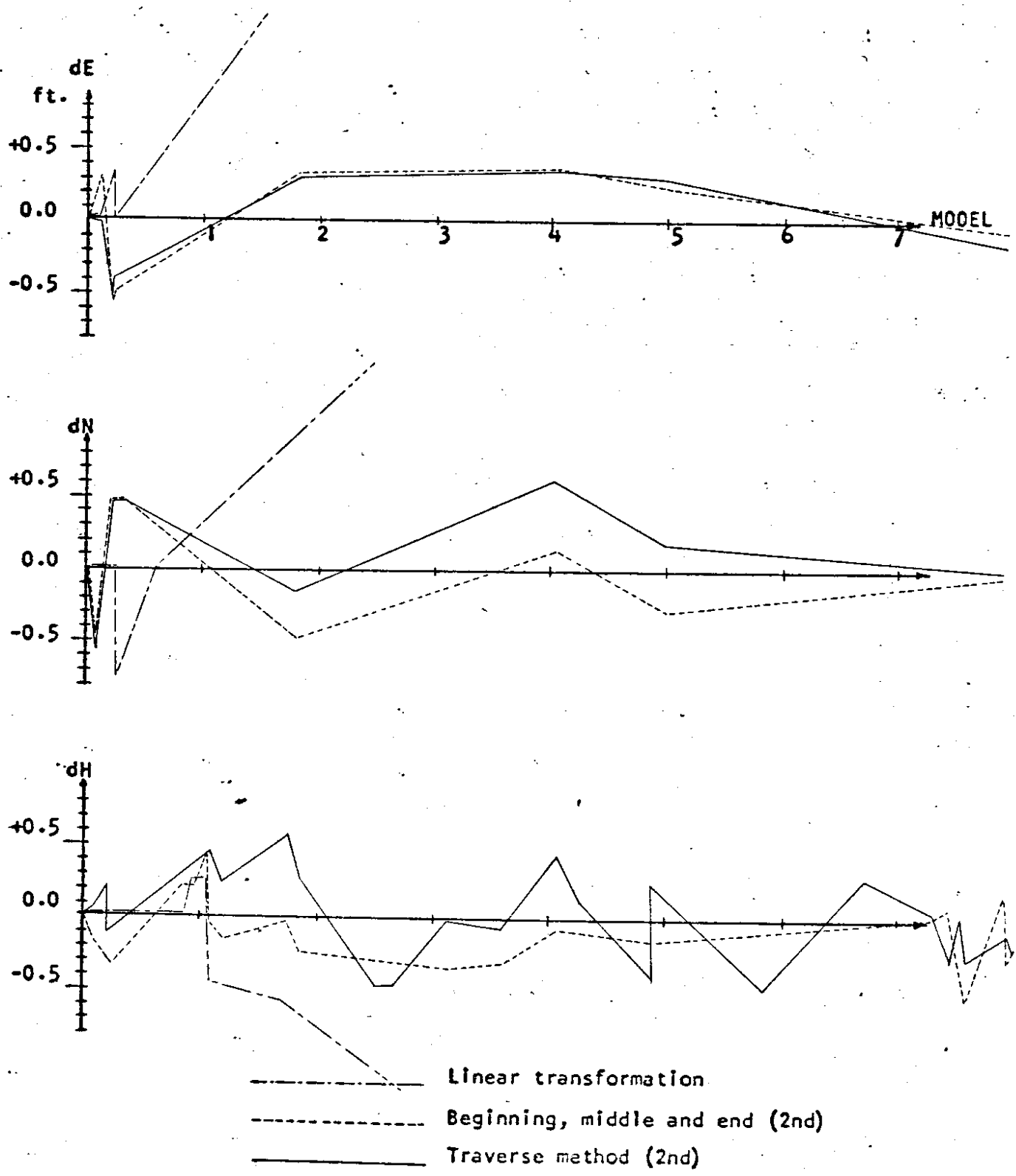


Fig. 63. Comparison of Discrepancies Resulting from Different Adjustment Procedures of Test Strip 15 at Flight Height of 3000 Feet

TABLE 18 RESULTS OF DIFFERENT ADJUSTMENT  
PROCEDURES OF TEST STRIP 15 AT FLIGHT  
HEIGHT OF 3000 FEET

Method	Linear Transformation	Beginning, Middle and End (2nd)	Traverse Method(2nd)
<b>Control points only</b>			
RMSE of dE in ft.	0.00	0.34	0.28
RMSE of dN	0.00	0.36	0.34
RMSE of dP	0.00	0.35	0.31
RMSE of dH	0.00	0.15	0.22
MAX, dE	0.00	0.52	0.43
MAX, dN	0.00	0.54	0.48
MAX, dH	0.00	0.22	0.39
<b>Check points</b>			
RMSE of dE in ft.	1.51	0.38	0.38
RMSE of dN	2.63	0.54	0.58
RMSE of dP	2.44	0.47	0.49
RMSE of dH	10.08	0.54	0.46
MAX, dE	3.03	0.58	0.52
MAX, dN	6.26	0.65	0.63
MAX, dH	20.48	1.03	0.93

\*

\*

\* More control points needed.

5-5-6.

TEST STRIP NO. 16

Test area: Sumner to King Co. Line, 1, 67-5-11.

Flight height  $\cong$  3000 feet, mean elevation  $\cong$  60 feet

Models: 8

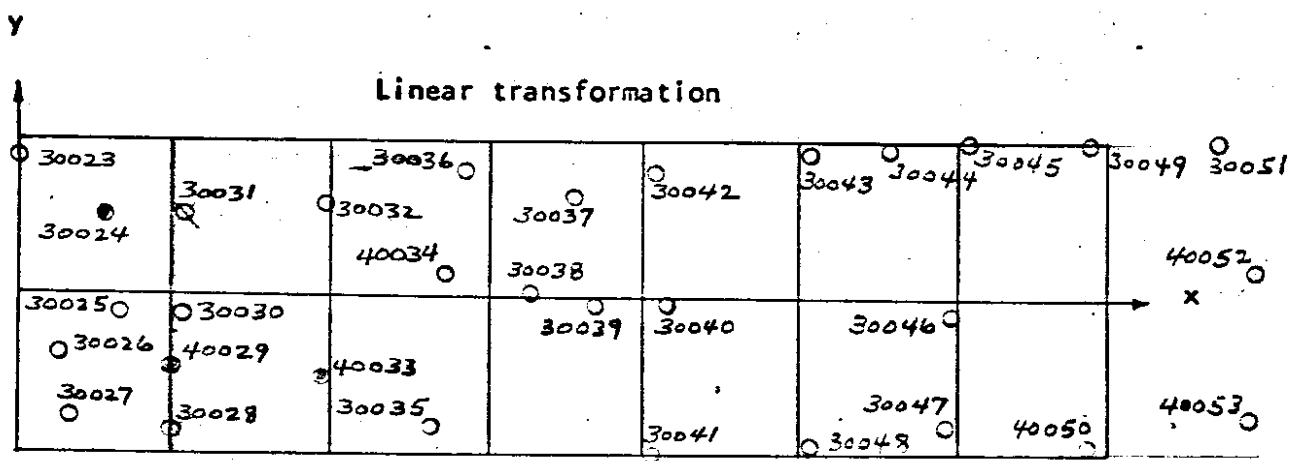
Horizontal control points: 6

Vertical control points: 31

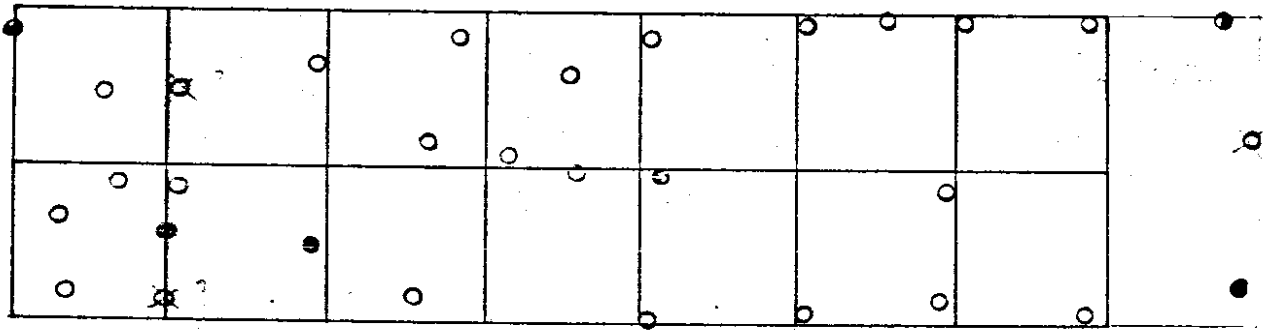
Location of all ground control points shown in Figure: 64

Residuals of all check points shown in Figure: 65

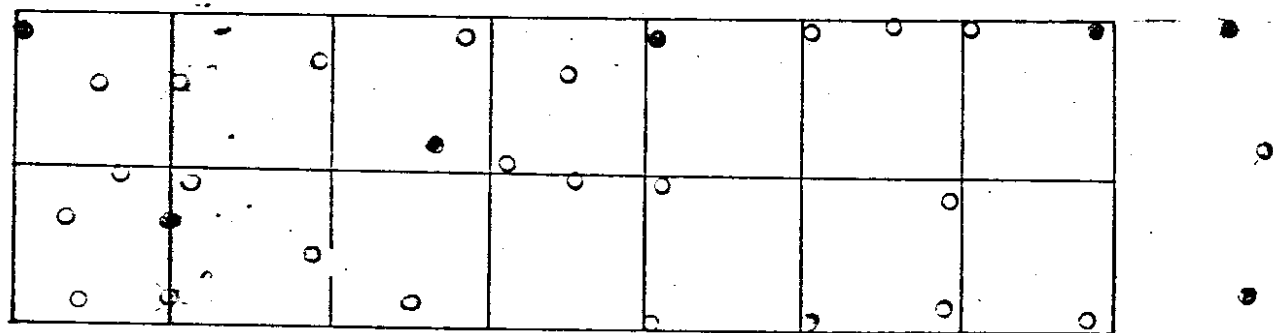
Stand errors of three different adjustment procedures of this strip  
shown in Table: 19



**Beginning, middle and end (2nd)**



**Traverse method (2nd)**



⊗ Detected ground control point in error

- Control points
- Check points

"2" Horizontal point; "3" Vertical point; "4" Horizontal & vertical point

Fig. 64 Layout of ground control points of test strip 16

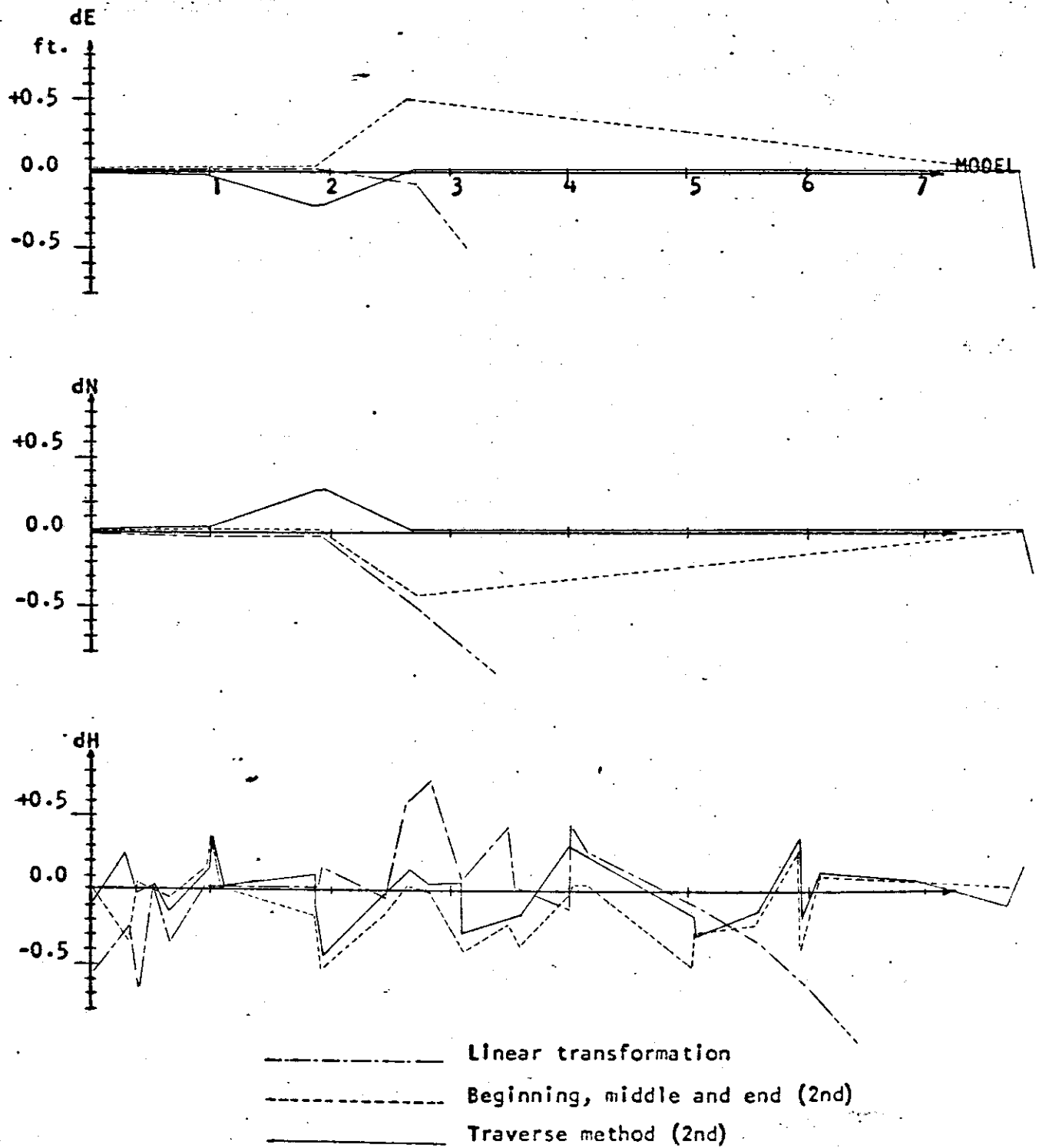


Fig. 65 Comparison of Discrepancies Resulting from Different Adjustment Procedures of Test Strip 16 at Flight Height of 3000 Feet

TABLE 19 RESULTS OF DIFFERENT ADJUSTMENT  
 PROCEDURES OF TEST STRIP 16 AT FLIGHT  
 HEIGHT OF 3000 FEET

Method	Linear Transformation	Beginning, Middle and End (2nd)	Traverse Method(2nd)
<b>Control points only</b>			
RMSE of dE in ft.	0.00	0.00	0.00
RMSE of dN	0.00	0.00	0.00
RMSE of dP	0.00	0.00	0.00
RMSE of dH	0.00	0.10	0.15
MAX, dE	0.00	0.00	0.00
MAX, dN	0.00	0.00	0.00
MAX, dH	0.00	0.18	0.30
<b>Check points</b>			
RMSE of dE in ft.	1.58	0.46	0.38
RMSE of dN	1.68	0.98	0.60
RMSE of dP	1.63	0.76	0.50
RMSE of dH	1.10	0.29	0.22
MAX, dE	2.71	0.48	0.61
MAX, dN	7.21	1.33	0.98
MAX, dH	3.35	0.55	0.45

5-5-7.

TEST STRIP NO. 17

Test area: N. Ft. Lewis to King Co. Line. 70-3-10.

Flight height  $\cong$  3000 feet. Mean elevation  $\cong$  280 feet.

Models: 9

Horizontal control points: 7

Vertical control points: 19

Location of all ground control points shown in Figure: 66

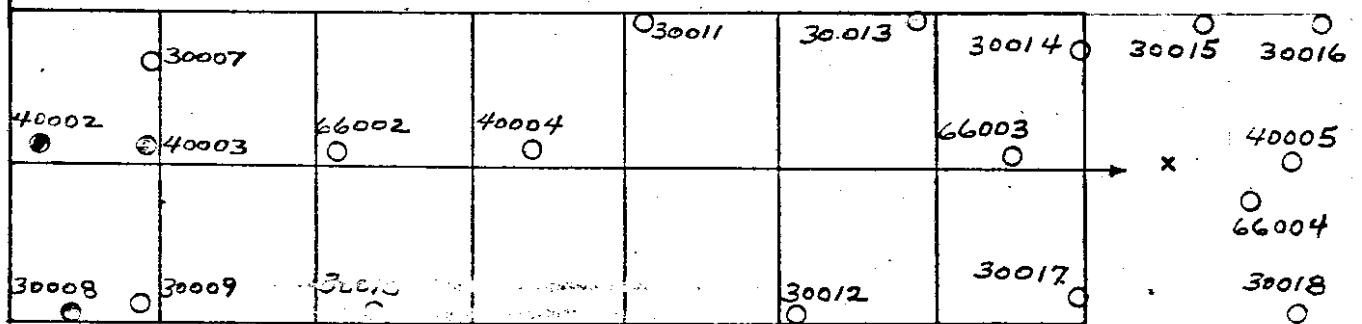
Residuals of all check points shown in Figure: 67

Stand errors of three different adjustment procedures of this strip  
shown in Table: 20

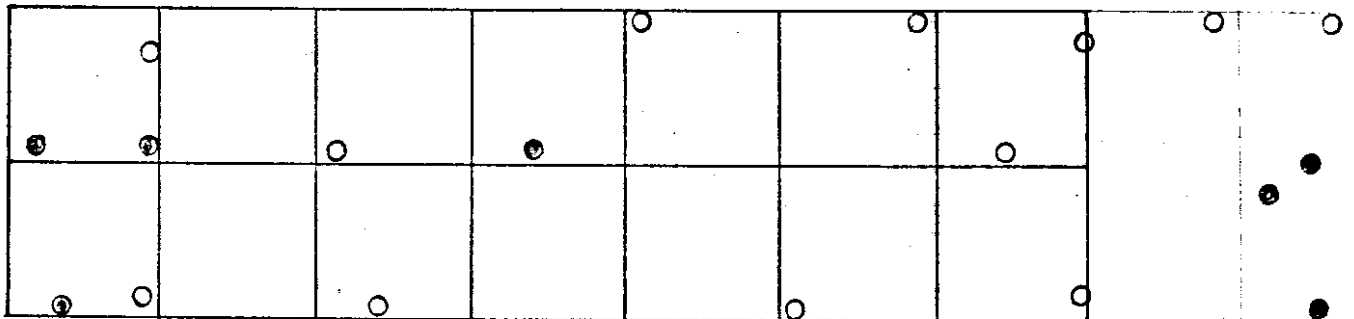


Y

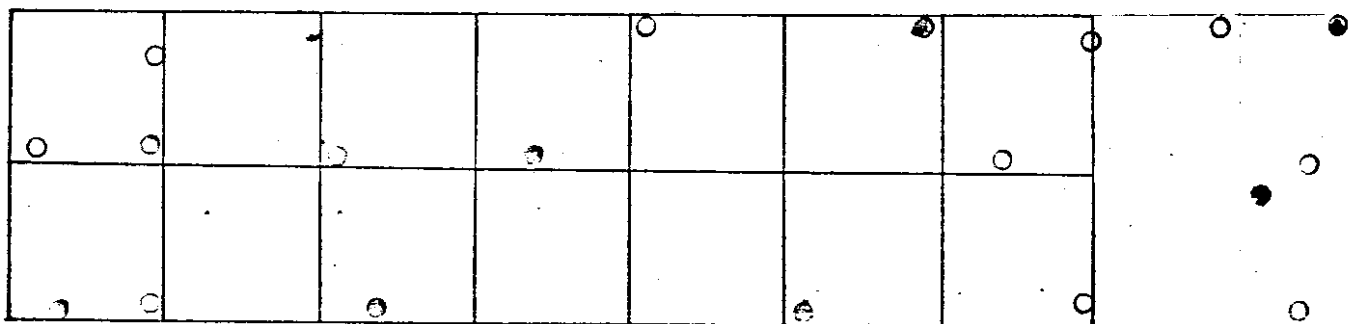
Linear transformation



Beginning, middle and end (2nd)



Traverse method (2nd)



● Control points

○ Check points

"2" Horizontal point; "3" Vertical point; "4" Horizontal & vertical point

Fig-66 Layout of ground control points of test strip 17

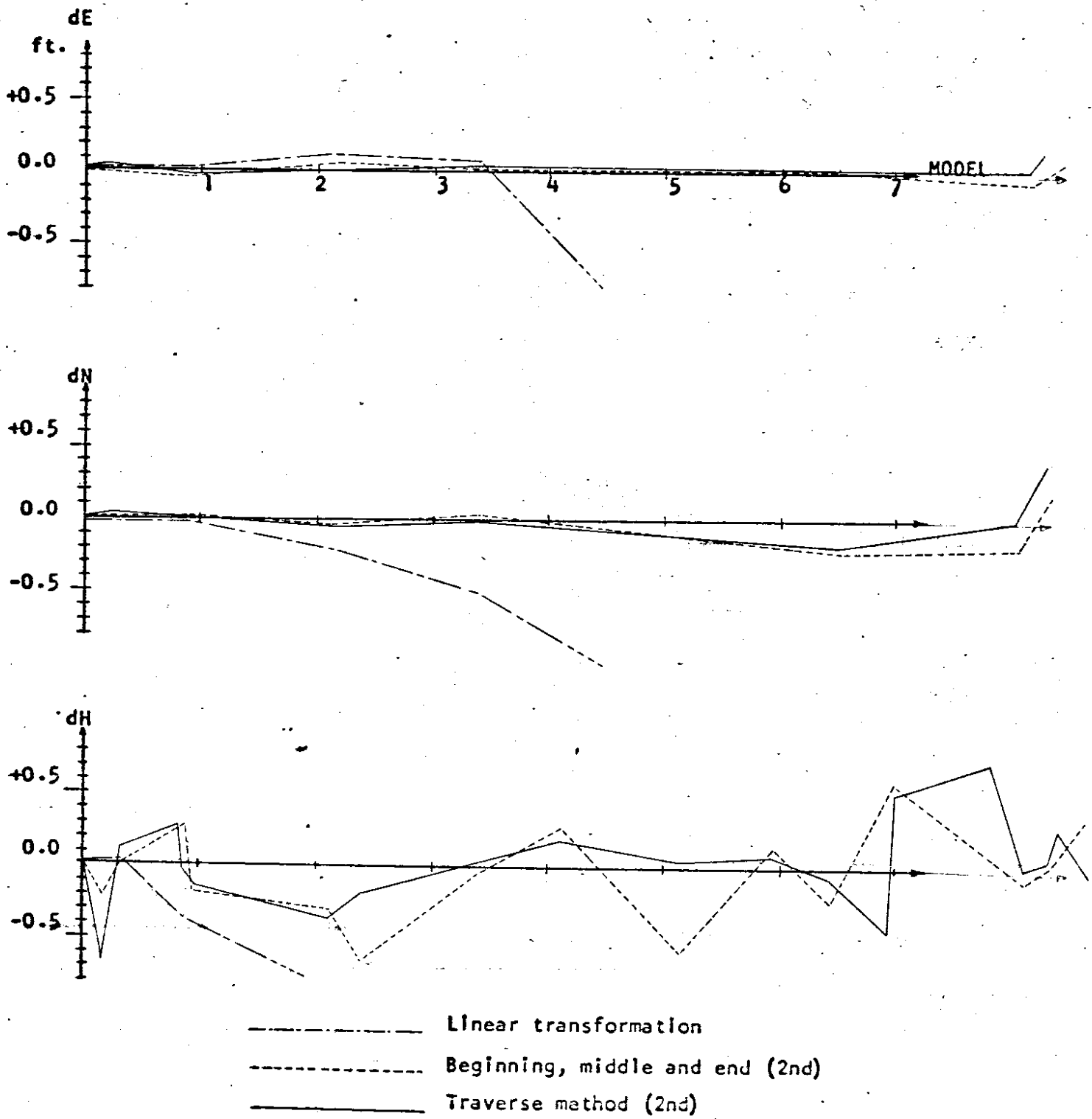


Fig. 67 Comparison of Discrepancies Resulting from Different Adjustment Procedures of Test Strip 17 at Flight Height of 3000 Feet

TABLE 20 RESULTS OF DIFFERENT ADJUSTMENT  
PROCEDURES OF TEST STRIP 17 AT FLIGHT  
HEIGHT OF 3000 FEET

Method	Linear Transformation	Beginning, Middle and End (2nd)	Traverse Method(2nd)
<b>Control points only</b>			
RMSE of dE in ft.	0.00	0.05	0.00
RMSE of dN	0.00	0.12	0.00
RMSE of dP	0.00	0.09	0.00
RMSE of dH	0.00	0.15	0.09
MAX, dE	0.00	0.07	0.00
MAX, dN	0.00	0.19	0.00
MAX, dH	0.00	0.29	0.20
<b>Check points</b>			
RMSE of dE in ft.	0.73	0.02	0.07
RMSE of dN	2.79	0.15	0.22
RMSE of dP	2.04	0.11	0.16
RMSE of dH	3.67	0.53	0.40
MAX, dE	1.36	0.03	0.11
MAX, dN	4.47	0.21	0.41
MAX, dH	5.81	0.96	0.69

5-5-8.

TEST STRIP NO. 18

Test area: Pullman Bypass Bridge Sites, 70-10-28.

Flight height  $\approx$  3000 feet. Mean elevation  $\approx$  2500 feet.

Models: 8

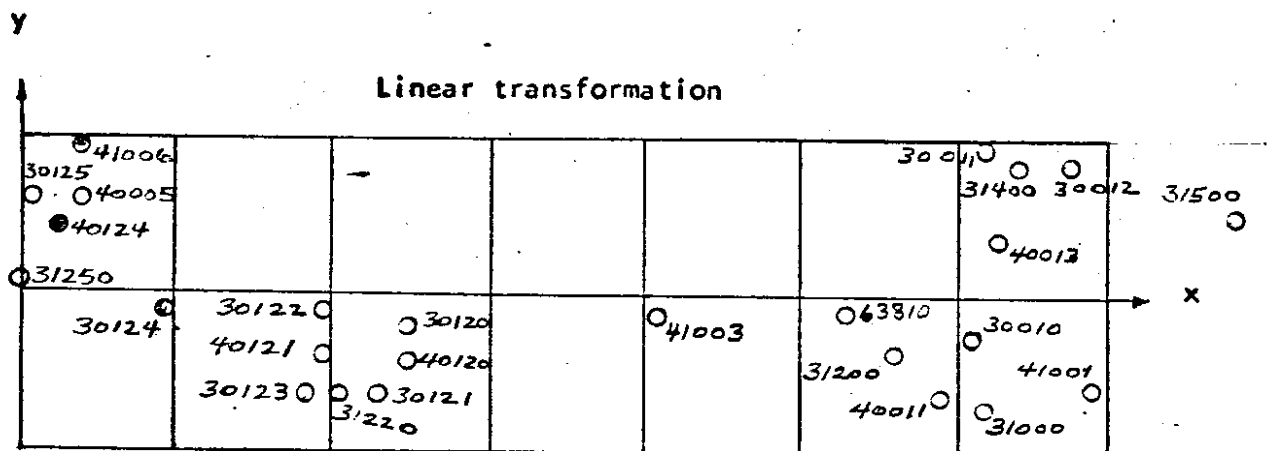
Horizontal control points: 9

Vertical control points: 25

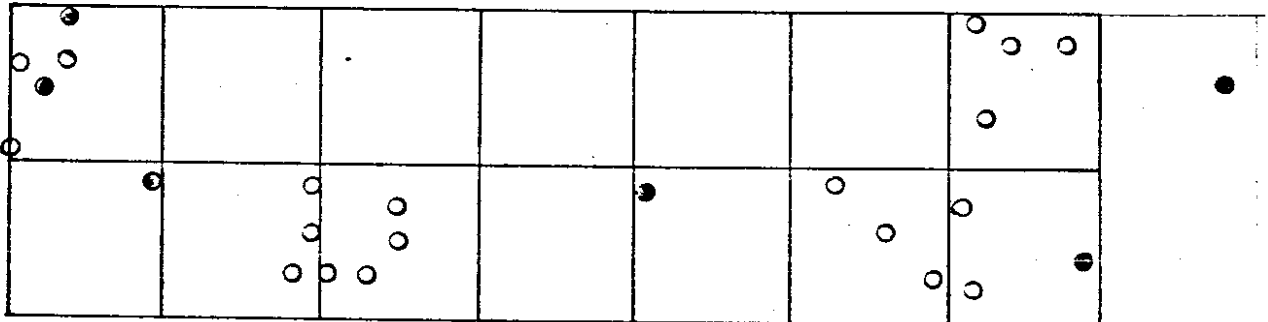
Location of all ground control points shown in Figure: 68

Residuals of all check points shown in Figure: 69

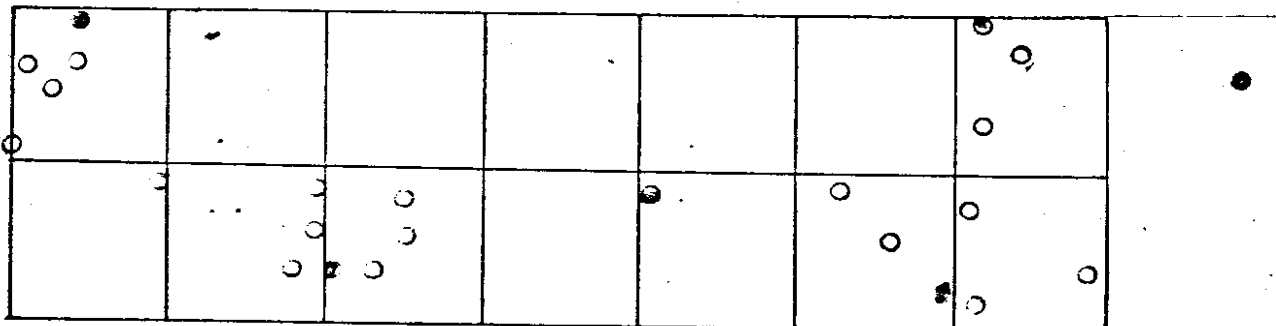
Stand errors of three different adjustment procedures of this strip  
shown in Table: 21



**Beginning, middle and end (2nd)**



**Traverse method (2nd)**



● Control points

○ Check points

"2" Horizontal point; "3" Vertical point; "4" Horizontal & vertical point

**Fig-68 Layout of ground control points of test strip 18**

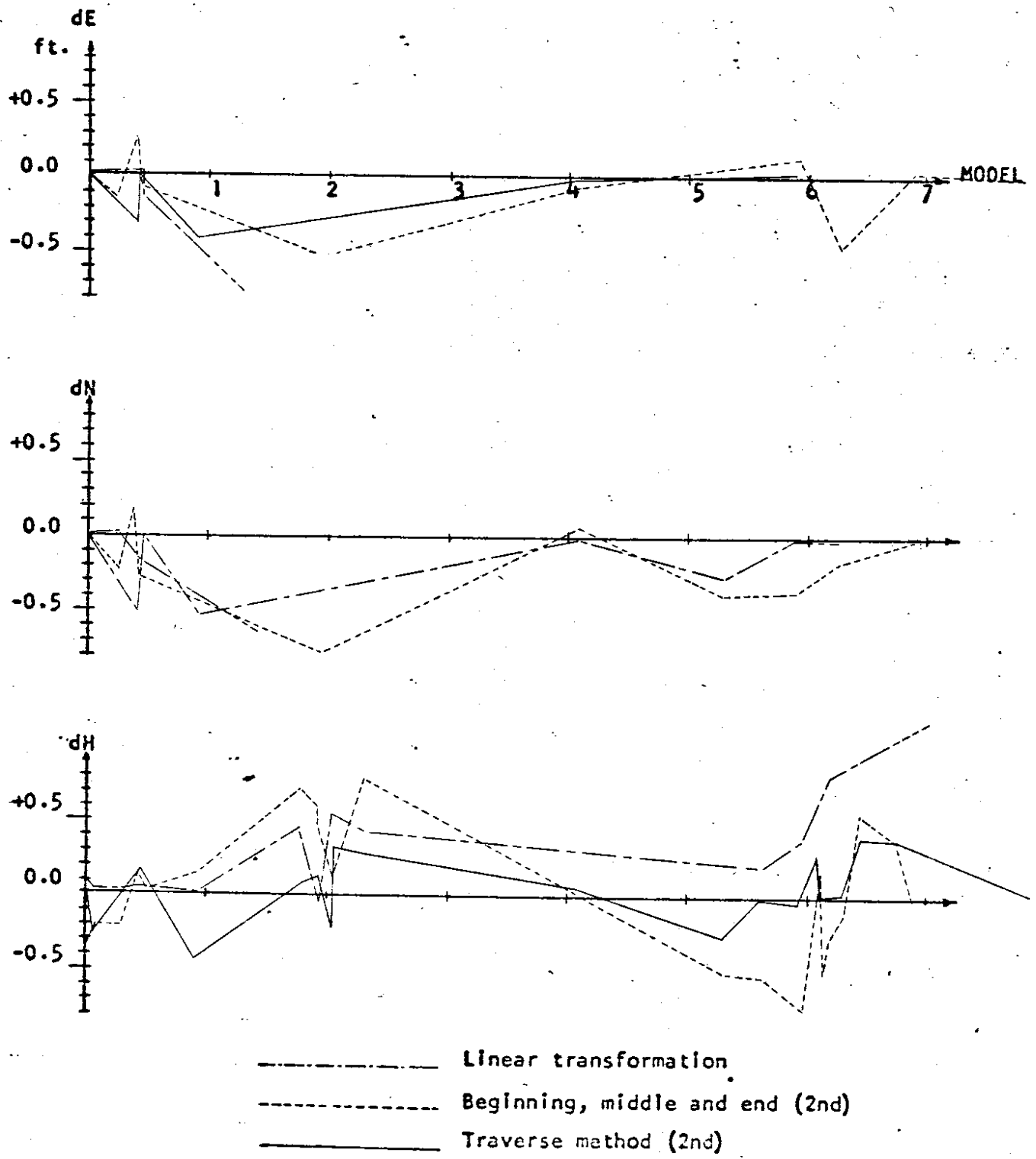


Fig. 69 Comparison of Discrepancies Resulting from Different Adjustment Procedures of Test Strip 18 at Flight Height of 3000 Feet

TABLE 21 RESULTS OF DIFFERENT ADJUSTMENT  
 PROCEDURES OF TEST STRIP 18 AT FLIGHT  
 HEIGHT OF 3000 FEET

Method	Linear Transformation	Beginning, Middle and End (2nd)	Traverse Method(2nd)
<b>Control points only</b>			
RMSE of dE in ft.	0.00	0.15	0.00
RMSE of dN	0.00	0.14	0.00
RMSE of dP	0.00	0.15	0.00
RMSE of dH	0.00	0.11	0.20
MAX, dE	0.00	0.23	0.00
MAX, dN	0.00	0.18	0.00
MAX, dH	0.00	0.20	0.38
<b>Check points</b>			
RMSE of dE in ft.	1.13	0.33	0.46
RMSE of dN	2.79	0.56	0.71
RMSE of dP	2.13	0.46	0.60
RMSE of dH	0.96	0.46	0.40
MAX, dE	1.86	0.54	0.86
MAX, dN	6.03	1.02	1.30
MAX, dH	2.77	0.88	0.94

\*

\*

\*More control points needed.

5-8-9.

TEST STRIP NO. 19

Test area: Pullman Bypass #13, 70-10-28.

Flight height  $\approx$  3000 feet. Mean elevation  $\approx$  2600 feet.

Models: 7

Horizontal control points: 9

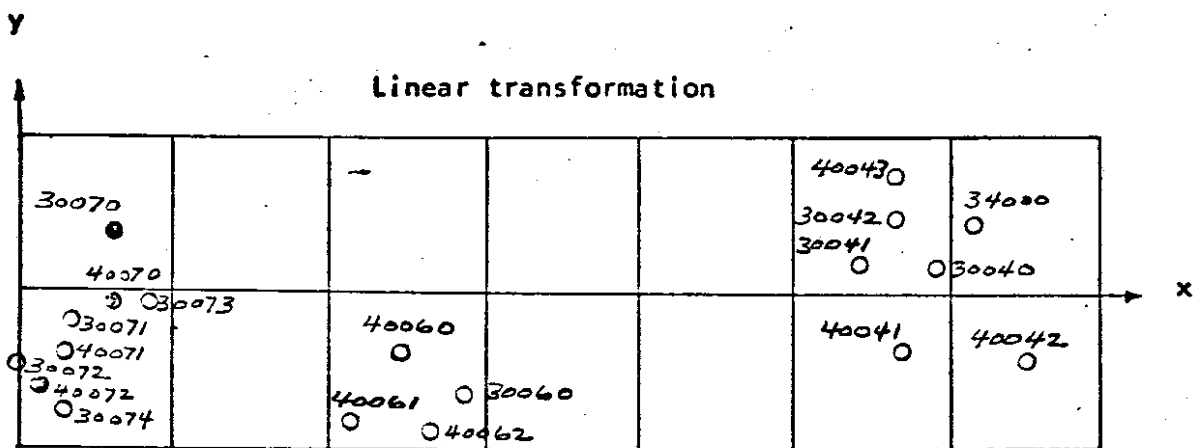
Vertical control points: 19

Location of all ground control points shown in Figure: 70

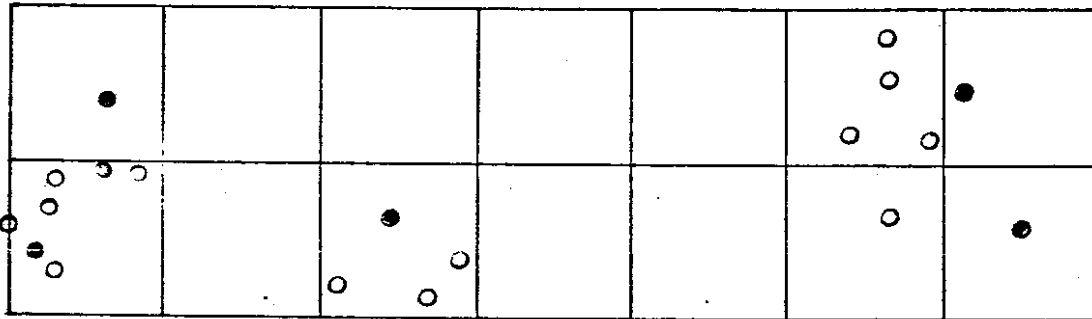
Residuals of all check points shown in Figure: 71

Stand errors of three different adjustment procedures of this strip  
shown in Table: 22

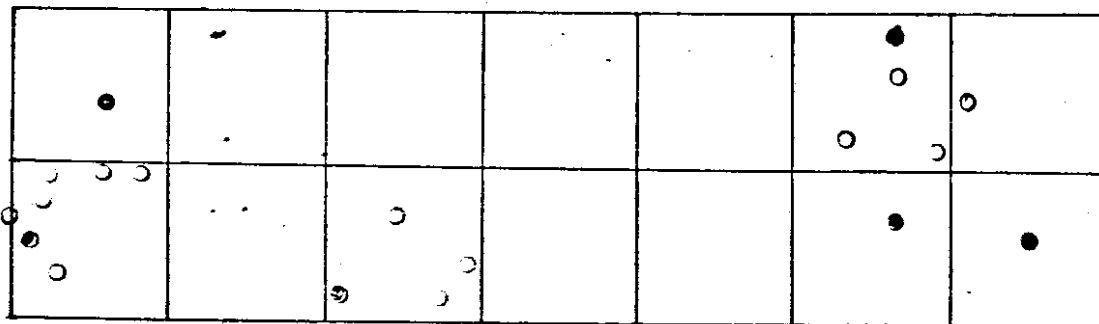




**Beginning, middle and end (2nd)**



**Traverse method (2nd)**

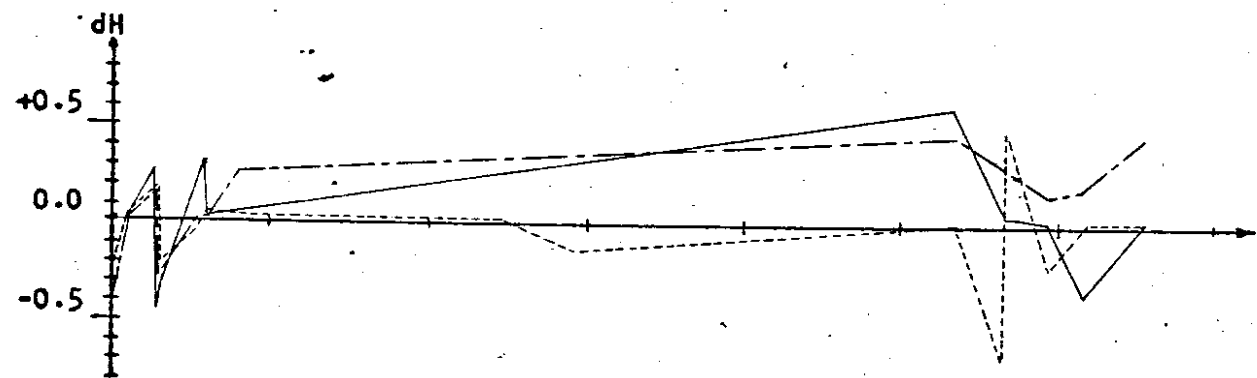
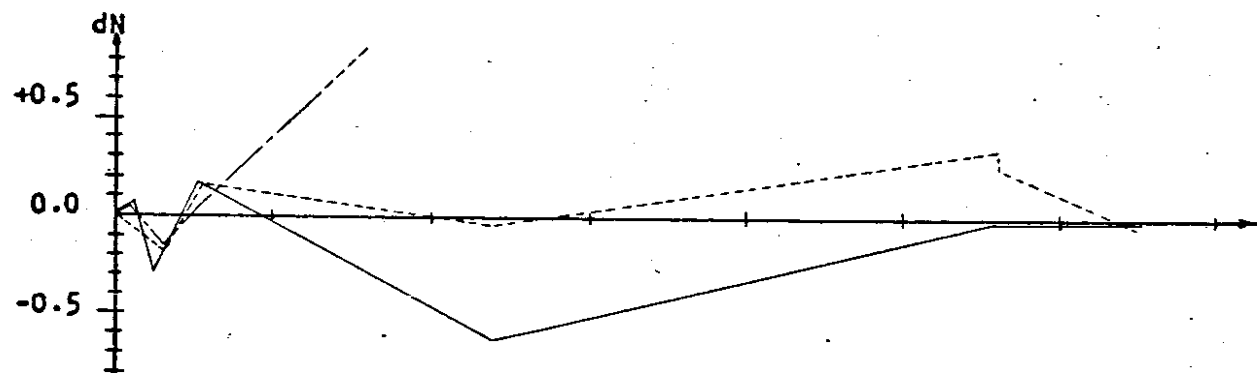
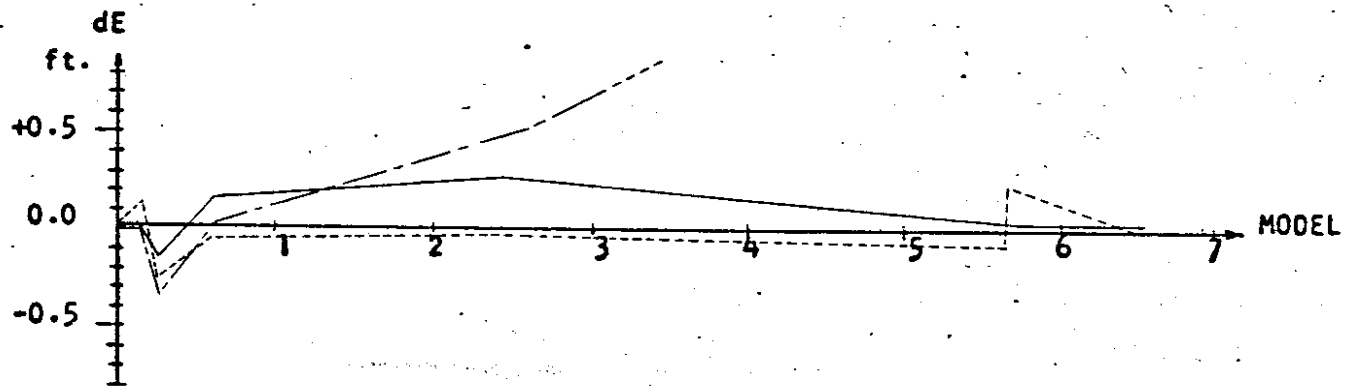


● Control points

○ Check points

"2" Horizontal point; "3" Vertical point; "4" Horizontal & vertical point

**Fig-70 Layout of ground control points of test strip 19**



- Linear transformation
- - - - - Beginning, middle and end (2nd)
- · - · - Traverse method (2nd)

Fig. 71 Comparison of Discrepancies Resulting from Different Adjustment Procedures of Test Strip 19 at Flight Height of 3000 Feet

TABLE 22 RESULTS OF DIFFERENT ADJUSTMENT  
 PROCEDURES OF TEST STRIP 19 AT FLIGHT  
 HEIGHT OF 3000 FEET

Method	Linear Transformation	Beginning, Middle and End (2nd)	Traverse Method(2nd)
<b>Control points only</b>			
RMSE of dE in ft.	0.00	0.07	0.04
RMSE of dN	0.00	0.11	0.04
RMSE of dP	0.00	0.09	0.04
RMSE of dH	0.00	0.04	0.00
MAX, dE	0.00	0.11	0.06
MAX, dN	0.00	0.17	0.06
MAX, dH	0.00	0.09	0.00
<b>Check points</b>			
RMSE of dE in ft.	3.62	0.22	0.25
RMSE of dN	0.93	0.29	0.37
RMSE of dP	2.64	0.26	0.35
RMSE of dH	0.48	0.29	1.42
MAX, dE	5.98	0.29	0.30
MAX, dN	2.00	0.33	0.61
MAX, dH	1.12	0.69	3.39

\*

\*Large residuals, more control points needed.

5-8-10.

TEST STRIP NO. 20

Test area: Pullman Bypass #16.

Flight height  $\approx$  3000 feet. Mean elevation  $\approx$  2500 feet.

Models: 6

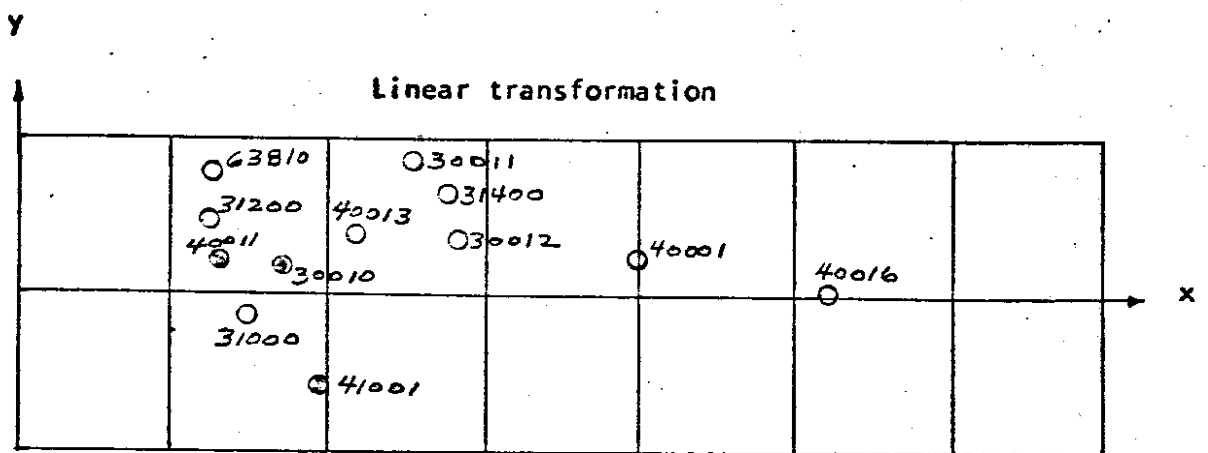
Horizontal control points: 6

Vertical control points: 12

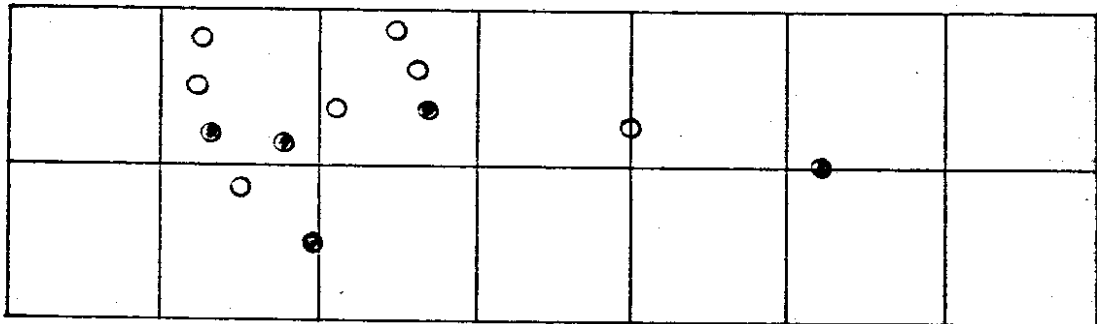
Location of all ground control points shown in Figure: 72

Residuals of all check points shown in Figure: 73

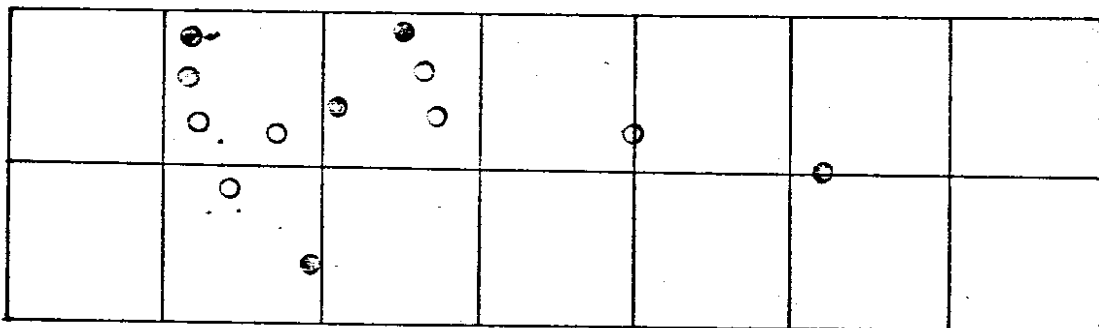
Stand errors of three different adjustment procedures of this strip  
shown in Table: 23



**Beginning, middle and end (2nd)**



**Traverse method (2nd)**

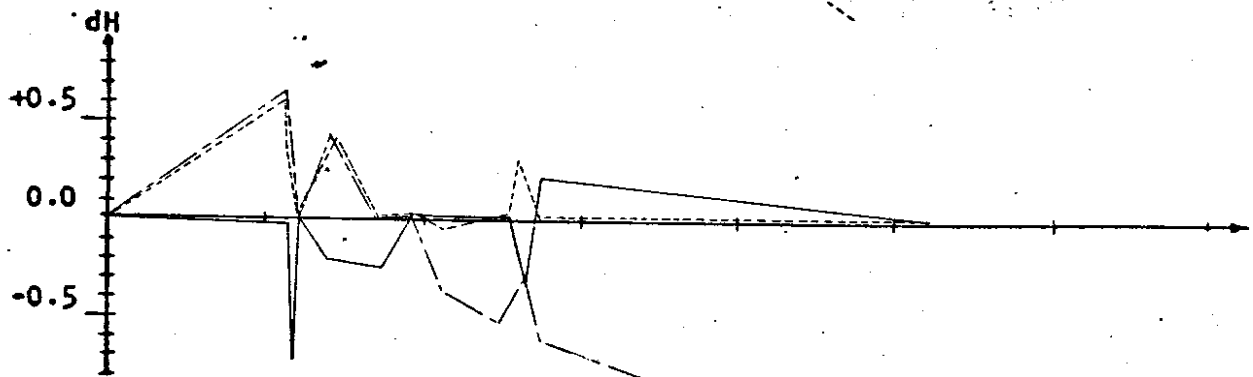
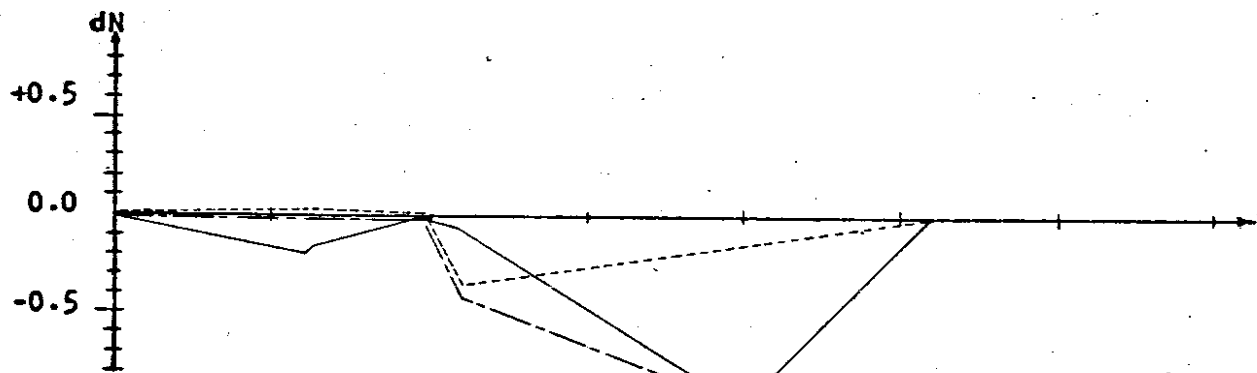
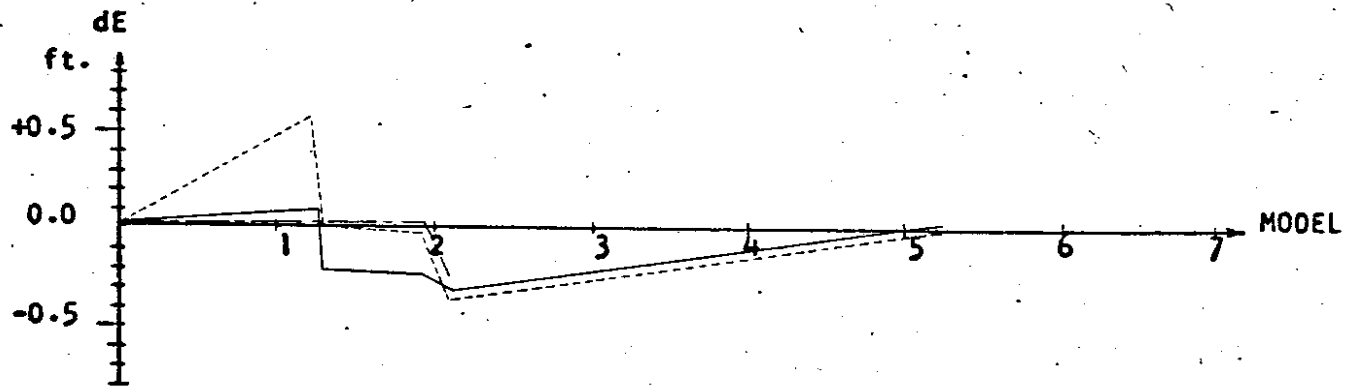


● Control points

○ Check points

"2" Horizontal point; "3" Vertical point; "4" Horizontal & vertical point

Fig-72 Layout of ground control points of test strip 20



- Linear transformation
- Beginning, middle and end (2nd)
- .-.-.-.- Traverse method (2nd)

Fig. 73 Comparison of Discrepancies Resulting from Different Adjustment Procedures of Test Strip 20 at Flight Height of 3000 Feet

TABLE 23 RESULTS OF DIFFERENT ADJUSTMENT  
PROCEDURES OF TEST STRIP 20 AT FLIGHT  
HEIGHT OF 3000 FEET

Method	Linear Transformation	Beginning, Middle and End (2nd)	Traverse Method(2nd)
<b>Control points only</b>			
RMSE of dE in ft.	0.00	0.00	0.21
RMSE of dN	0.00	0.00	0.08
RMSE of dP	0.00	0.00	0.16
RMSE of dH	0.00	0.00	0.00
MAX. dE	0.00	0.00	0.34
MAX. dN	0.00	0.00	0.14
MAX. dH	0.00	0.00	0.00
<b>Check points</b>			
RMSE of dE in ft.	0.41	0.52	0.33
RMSE of dN	0.82	0.41	0.41
RMSE of dP	0.65	0.47	0.37
RMSE of dH	1.72	0.55	0.48
MAX. dE	0.74	0.60	0.41
MAX. dN	1.40	0.63	0.55
MAX. dH	3.46	1.11	0.92

5-6. Testing of Two Strips of the Flight at 6000 Feet.

5-6-1. TEST STRIP NO. 21

Test area: Sunset Interchange, 69-1-5.

Flight height  $\cong$  6000 feet, Mean elevation  $\cong$  2300 feet.

Models: 4

Horizontal control points: 13

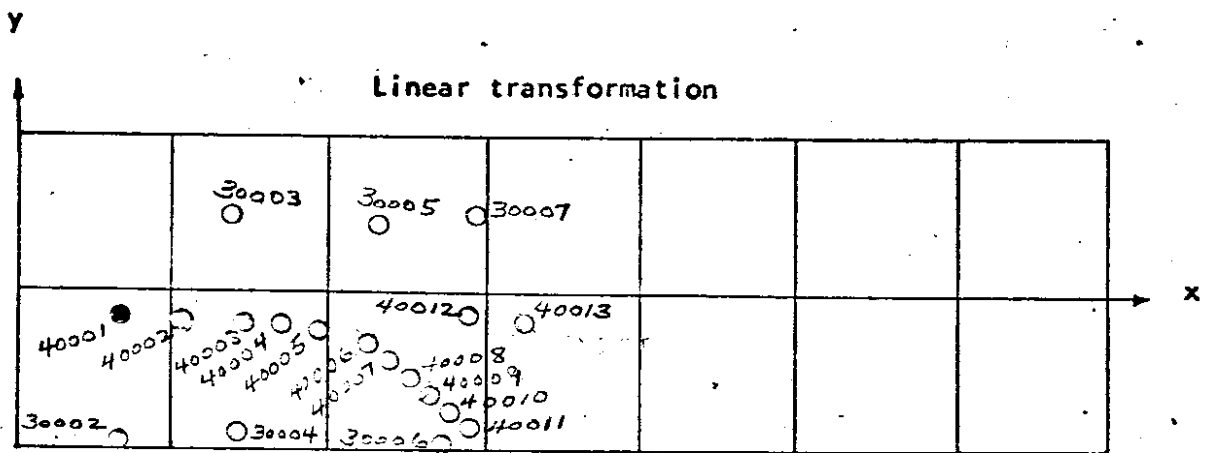
Vertical control points: 19

Location of all ground control points shown in Figure: 74

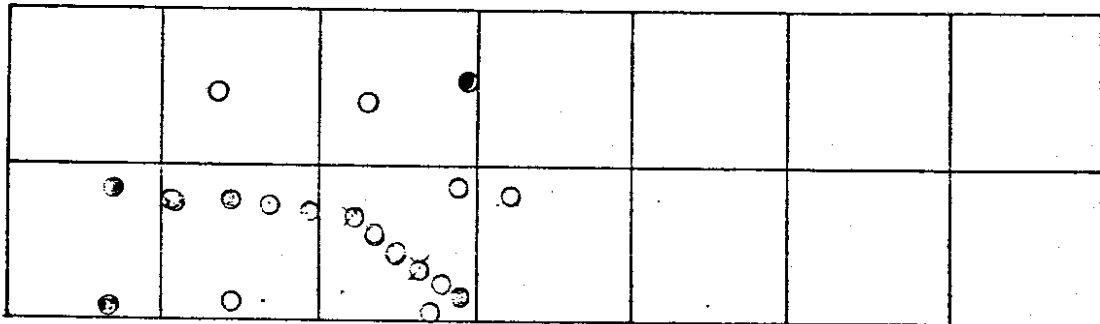
Residuals of all check points shown in Figure: 75

Stand errors of three different adjustment procedures of this strip  
shown in Table: 24

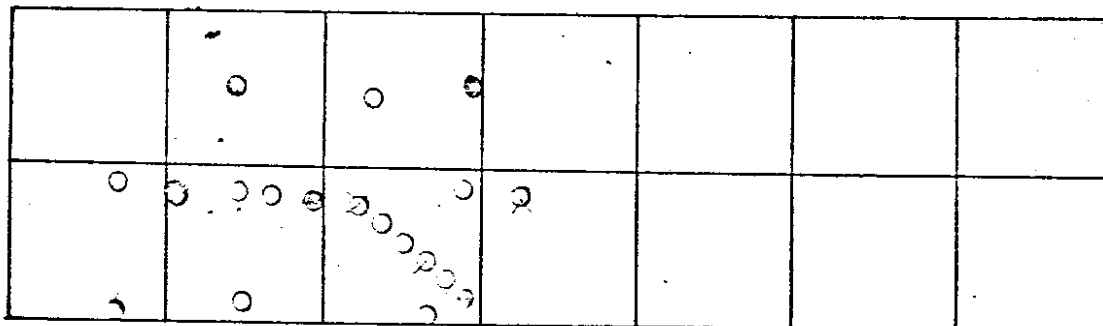




**Beginning, middle and end (2nd)**



**Traverse method (2nd)**



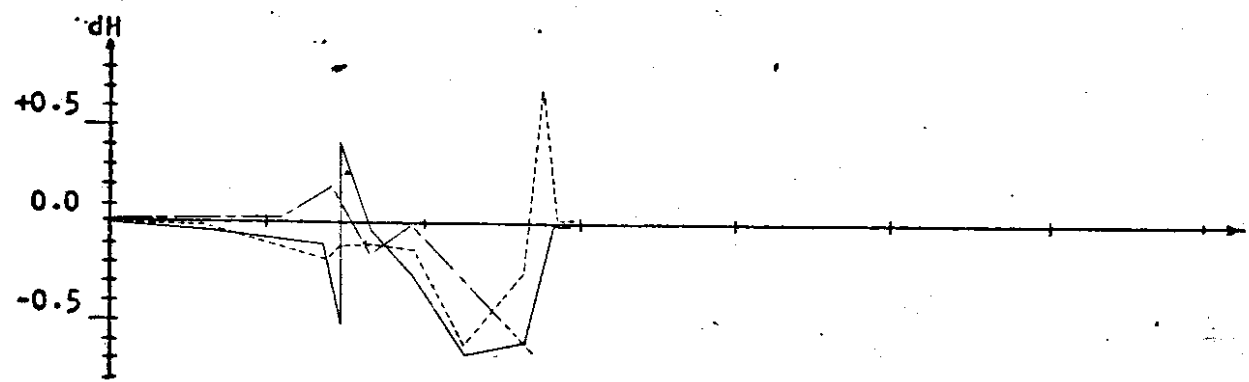
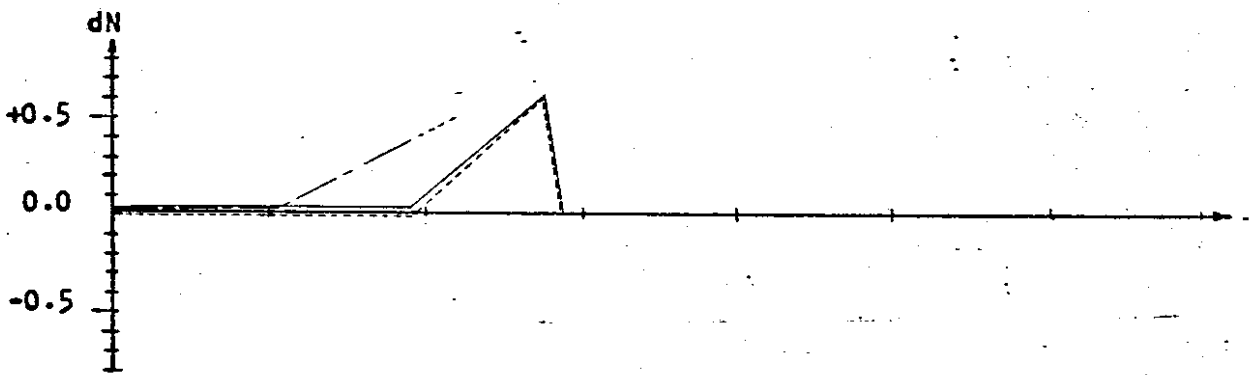
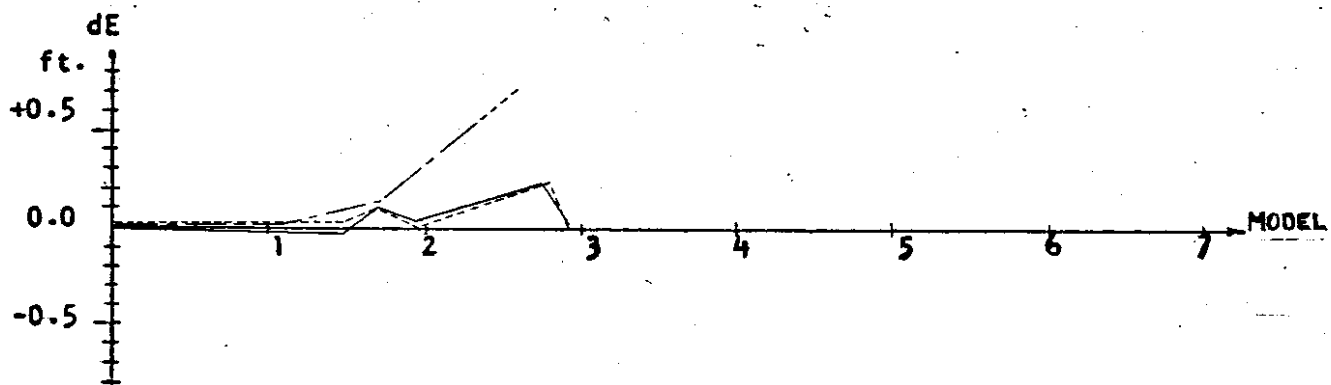
✕ Detected ground control point in error

● Control points

○ Check points

"2" Horizontal point; "3" Vertical point; "4" Horizontal & vertical point

Fig-74 Layout of ground control points of test strip 21



- Linear transformation
- Beginning, middle and end (2nd)
- Traverse method (2nd)

Fig. Comparison of Discrepancies Resulting from Different Adjustment Procedures of Test Strip 21 at Flight Height of 3000 Feet

TABLE 24 RESULTS OF DIFFERENT ADJUSTMENT  
 PROCEDURES OF TEST STRIP 21 AT FLIGHT  
 HEIGHT OF 6000 FEET

Method	Linear Transformation	Beginning, Middle and End (2nd)	Traverse Method(2nd)
<b>Control points only</b>			
RMSE of dE in ft.	0.00	0.00	0.00
RMSE of dN	0.00	0.00	0.00
RMSE of dP	0.00	0.00	0.00
RMSE of dH	0.04	0.08	0.21
MAX. dE	0.00	0.00	0.00
MAX. dN	0.00	0.00	0.00
MAX. dH	0.07	0.14	0.27
<b>Check points</b>			
RMSE of dE in ft.	1.32	1.21	0.92
RMSE of dN	3.17	0.83	0.90
RMSE of dP	2.43	1.03	0.91
RMSE of dH	0.89	0.67	0.74
MAX. dE	2.41	0.58	2.03
MAX. dN	4.49	1.38	1.38
MAX. dH	1.75	1.61	1.51

\*More control points needed.

5-6-2.

TEST STRIP NO. 22

Test area: Jct. SR 104 to JCT SR 113, 69-6-6.

Flight height  $\cong$  6000 feet. Mean elevation  $\cong$  300 feet.

Models: 8

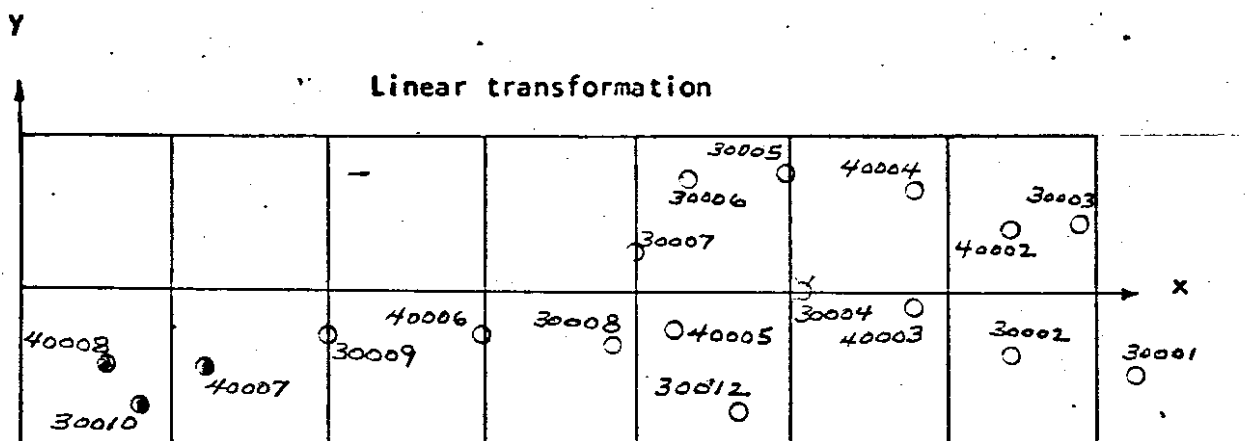
Horizontal control points: 7

Vertical control points: 19

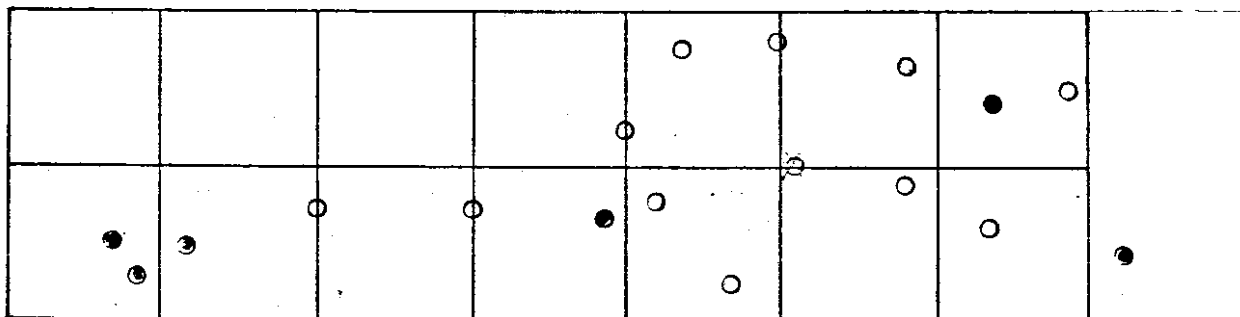
Location of all ground control points shown in Figure: 76

Residuals of all check points shown in Figure: 77

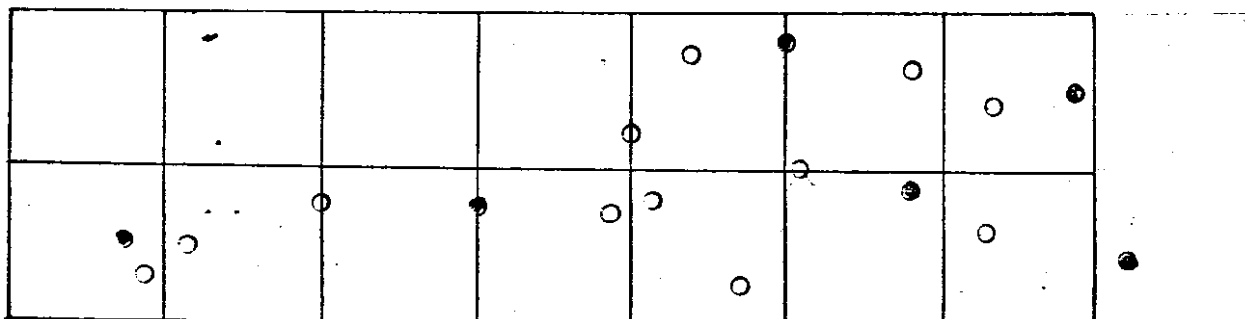
Stand errors of three different adjustment procedures of this strip  
shown in Table: 25



**Beginning, middle and end (2nd)**



**Traverse method (2nd)**



⊗ Detected ground control point in error

● Control points

○ Check points

"2" Horizontal point; "3" Vertical point; "4" Horizontal & vertical point

Fig-76 Layout of ground control points of test strip 22

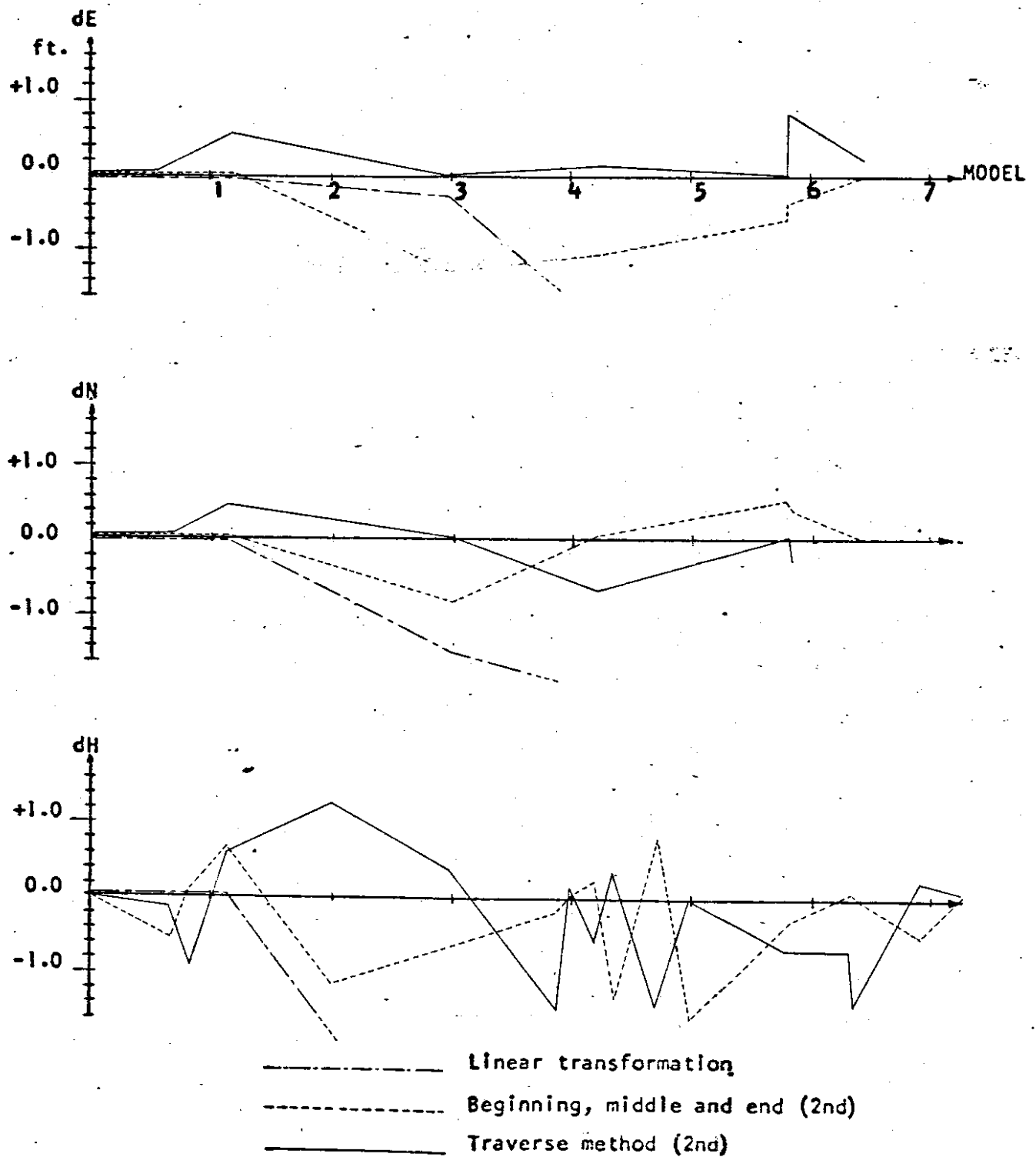


Fig. 77 Comparison of Discrepancies Resulting from Different Adjustment Procedures of Test Strip 22 at Flight Height of 6000 Feet

TABLE 25 RESULTS OF DIFFERENT ADJUSTMENT  
 PROCEDURES OF TEST STRIP 22 AT FLIGHT  
 HEIGHT OF 6000 FEET

Method	Linear Transformation	Beginning, Middle and End (2nd)	Traverse Method(2nd)
<b>Control points only</b>			
RMSE of dE in ft.	0.00	0.00	0.00
RMSE of dN	0.00	0.00	0.00
RMSE of dP	0.00	0.00	0.00
RMSE of dH	0.00	0.35	0.37
MAX. dE	0.00	0.00	0.00
MAX. dN	0.00	0.00	0.00
MAX. dH	0.00	0.63	0.70
<b>Check points</b>			
RMSE of dE in ft.	5.63	0.78	0.46
RMSE of dN	1.66	0.48	0.87
RMSE of dP	4.15	0.64	0.70
RMSE of dH	9.62	1.01	0.85
MAX. dE	10.30	1.23	0.85
MAX. dN	2.64	0.82	1.37
MAX. dH	19.19	1.56	1.48

5-7. Testing of three strips of the flight at 12,000 feet.

5-7-1.

TEST STRIP NO. 23

Test area: SR 16 to Pt. Southworth, 71-3-1.

Flight height  $\approx$  12,000 feet, mean elevation  $\approx$  200 feet.

Models: 6

Horizontal control points: 20

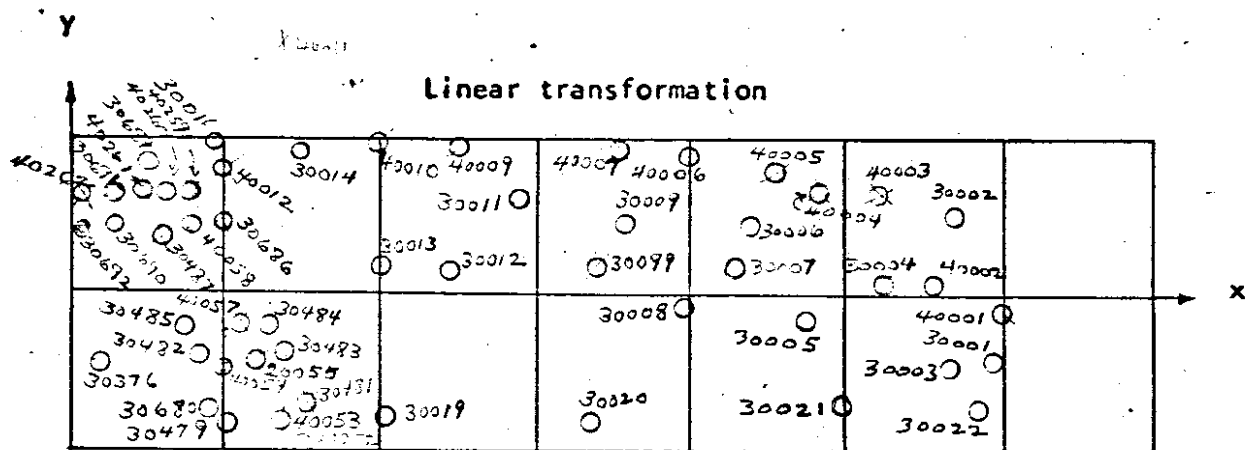
Vertical control points: 52

Location of all ground control points shown in Figure: 78

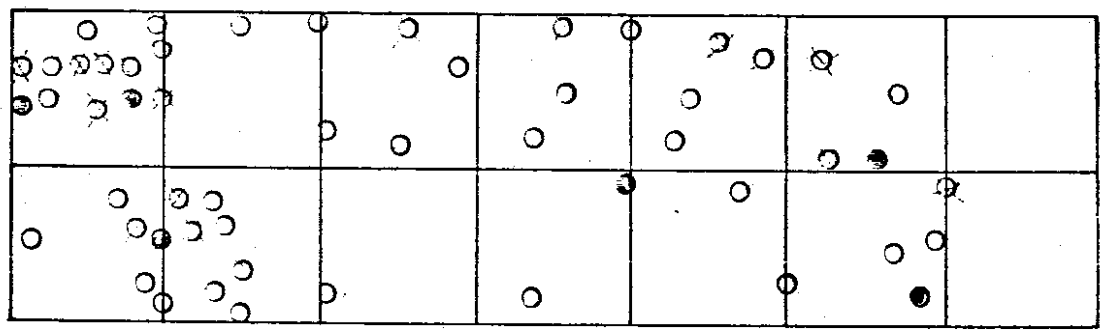
Residuals of all check points shown in Figure: 79

Stand errors of three different adjustment procedures of this strip  
shown in Table: 26

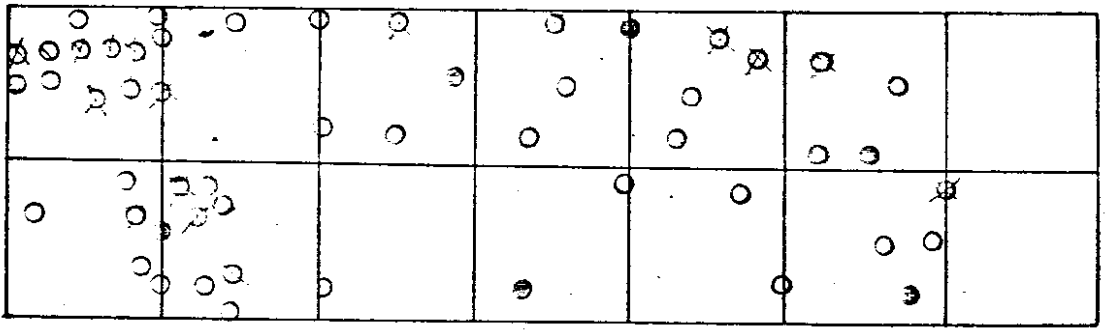




**Beginning, middle and end (2nd)**



**Traverse method (2nd)**



- ⊗ Detected ground control point in error
- Control points
- Check points

"2" Horizontal point; "3" Vertical point; "4" Horizontal & vertical point

**Fig.78** Layout of ground control points of test strip 23

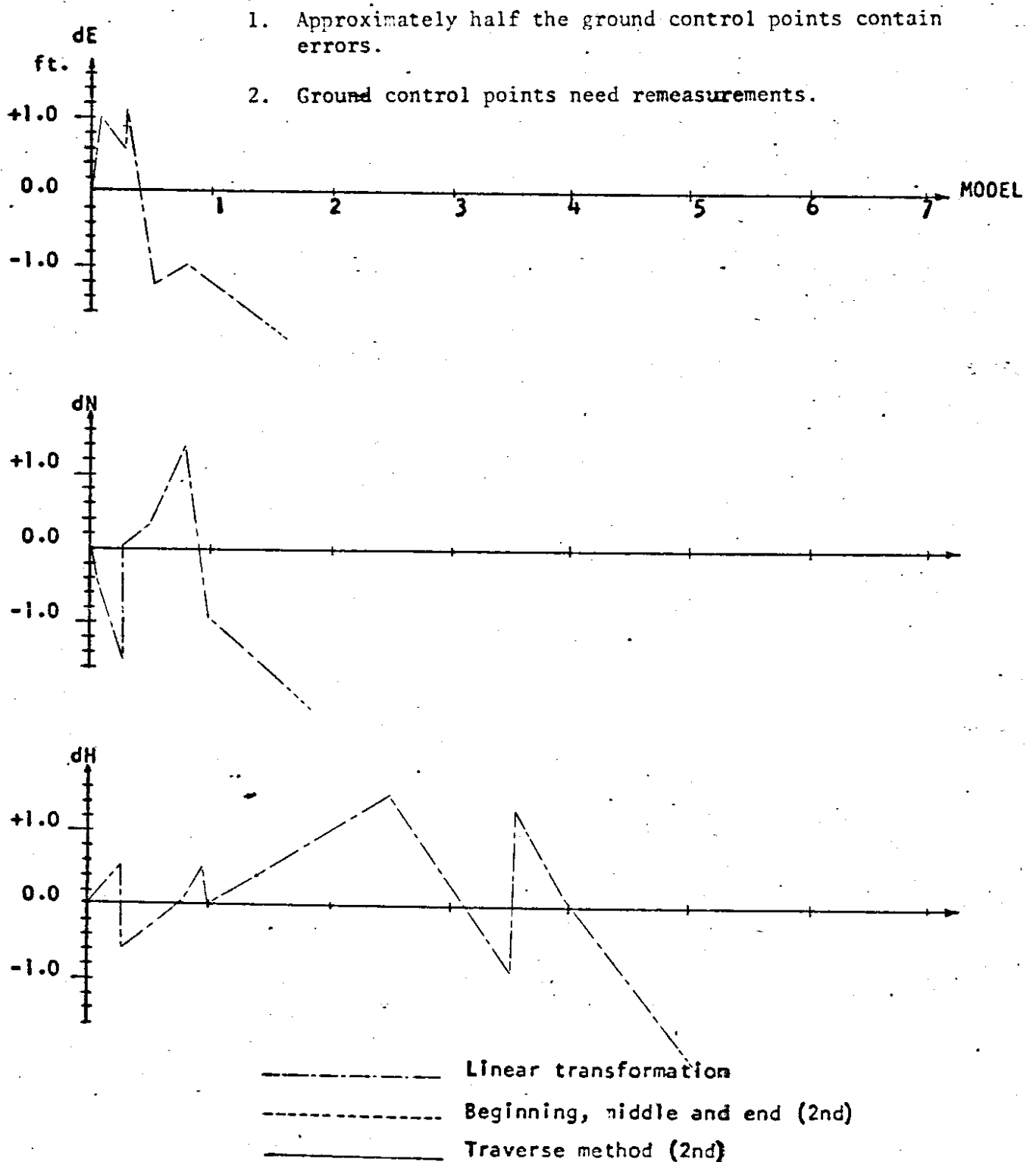


Fig. 79 Comparison of Discrepancies Resulting from Different Adjustment Procedures of Test Strip 23 at Flight Height of 6000 Feet

TABLE 26 RESULTS OF DIFFERENT ADJUSTMENT  
 PROCEDURES OF TEST STRIP 23 AT FLIGHT  
 HEIGHT OF 12000 FEET

Method	Linear Transformation	Beginning, Middle and End (2nd)	Traverse Method(2nd)
<b>Control points only</b>			
RMSE of dE in ft.	0.81	0.95	1.97
RMSE of dN	1.01	0.91	1.55
RMSE of dP	0.92	0.93	1.78
RMSE of dH	0.00	0.00	0.00
MAX, dE	1.00	1.49	2.72
MAX, dN	1.40	1.39	1.58
MAX, dH	0.00	0.00	0.00
<b>Check points</b>			
RMSE of dE in ft.	1.	Approximately half the amounts of ground control points contain errors.	
RMSE of dN	2.	Ground control points need remeasurements.	
RMSE of dP			
RMSE of dH			
MAX, dE	22.21	21.82	25.59
MAX, dN	94.31	94.12	94.90
MAX, dH	17.96	43.07	12.23

5-7-2.

TEST STRIP NO. 24

Test area: Jct. SR 410 to ECL Naches, 70-4-22.

Flight height  $\approx$  12,000 feet; mean elevation  $\approx$  2000 feet.

Models: 6

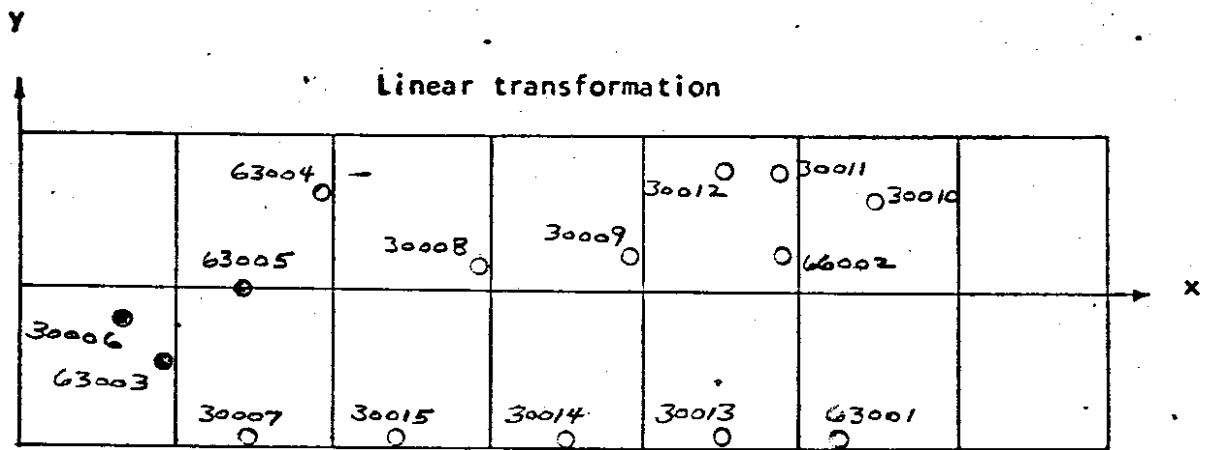
Horizontal control points: 5

Vertical control points: 15

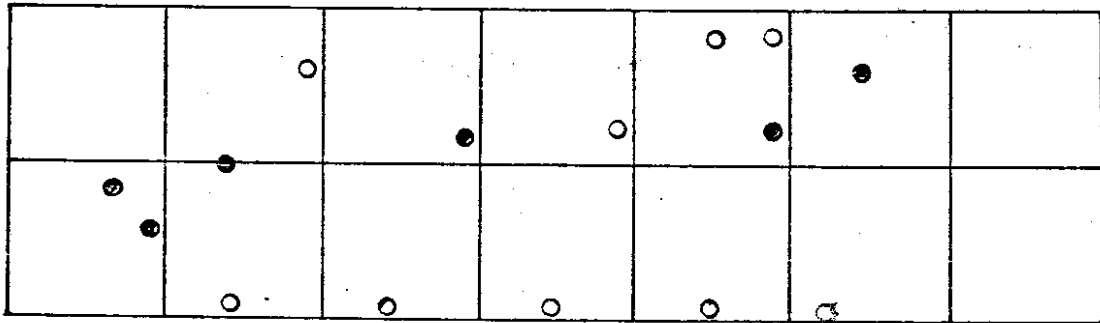
Location of all ground control points shown in Figure: 80

Residuals of all check points shown in Figure: 81

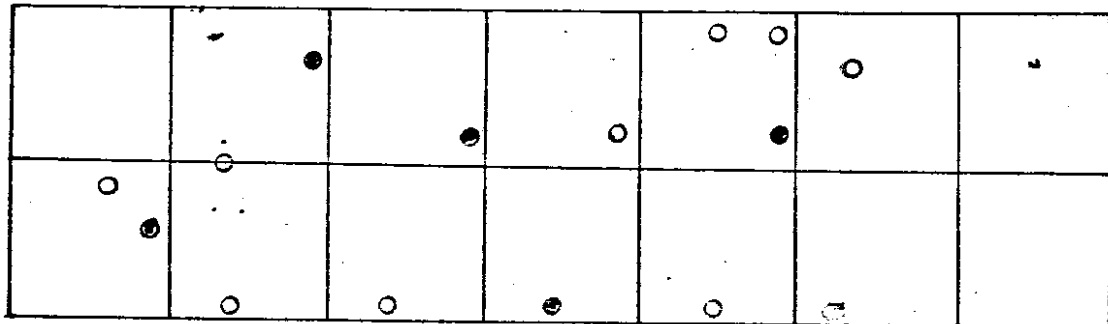
Stand errors of three different adjustment procedures of this strip  
shown in Table: 27



**Beginning, middle and end (2nd)**



**Traverse method (2nd)**



⊗ Detected ground control point in error

● Control points

○ Check points

"2" Horizontal point; "3" Vertical point; "4" Horizontal & vertical point

**Fig. 80** Layout of ground control points of test strip 24

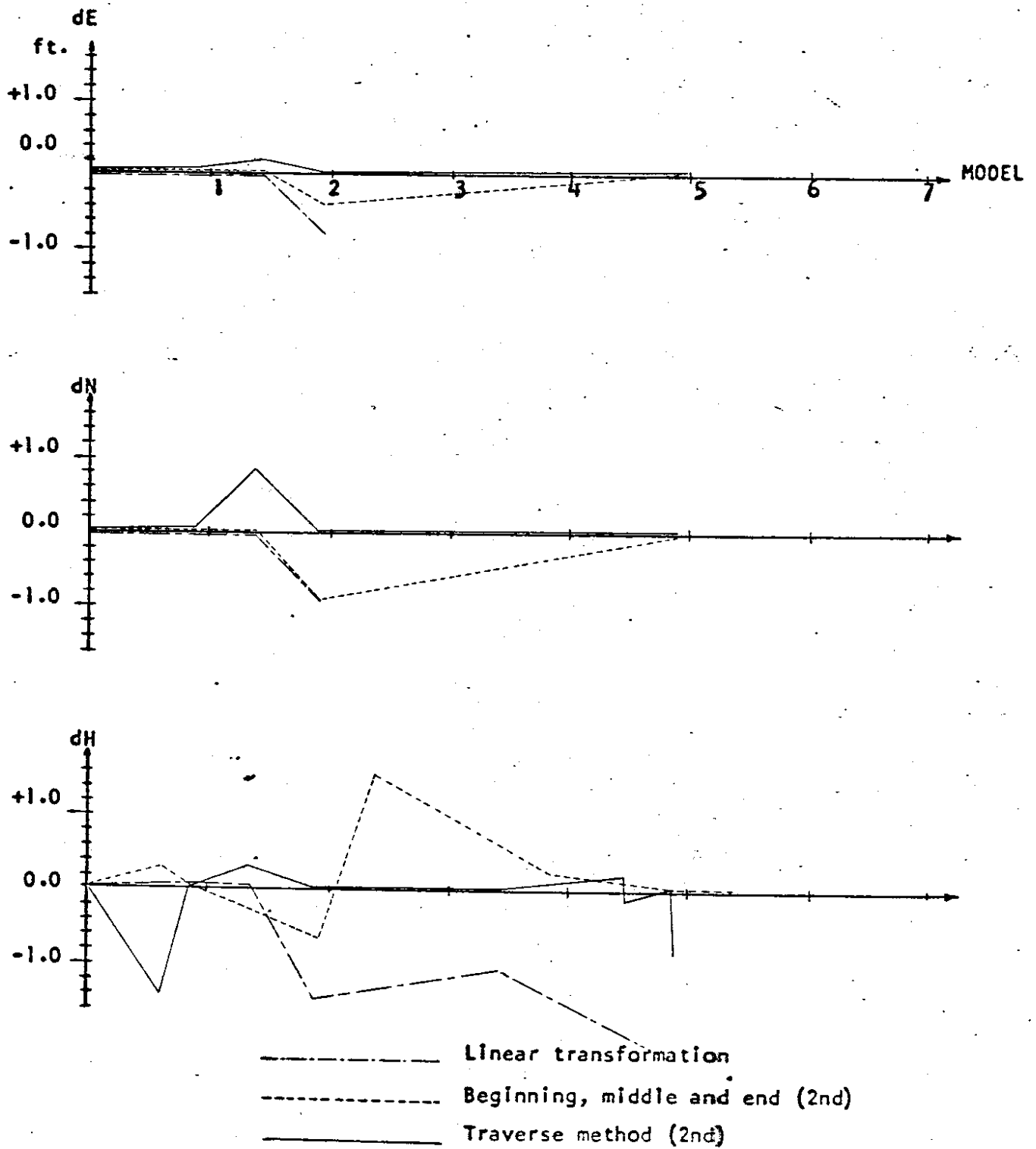


Fig. 81 Comparison of Discrepancies Resulting from Different Adjustment Procedures of Test Strip 24 at Flight Height of 12,000 Feet

TABLE 27 RESULTS OF DIFFERENT ADJUSTMENT  
PROCEDURES OF TEST STRIP 24 AT FLIGHT  
HEIGHT OF 12000 FEET

Method	Linear Transformation	Beginning, Middle and End (2nd)	Traverse Method(2nd)
<b>Control points only</b>			
RMSE of dE in ft.	0.00	0.00	0.00
RMSE of dN	0.00	0.00	0.00
RMSE of dP	0.00	0.00	0.00
RMSE of dH	0.00	0.25	0.00
MAX, dE	0.00	0.00	0.00
MAX, dN	0.00	0.00	0.00
MAX, dH	0.00	0.46	0.00
<b>Check points</b>			
RMSE of dE in ft.	3.25	0.39	0.21
RMSE of dN	2.49	0.91	0.80
RMSE of dP	2.90	0.70	0.58
RMSE of dH	13.10	3.76	1.98
MAX, dE	5.58	0.39	0.21
MAX, dN	4.21	0.91	0.80
MAX, dH	29.27	7.81	3.26

\*More control points needed.

5-7-3.

TEST STRIP NO. 25

Test area: Fawn Lake Fire Map (DNR) 71-7-21.

Flight height  $\cong$  12,000 feet; mean elevation  $\cong$  3,500 feet.

Models: 5

Horizontal control points: 8

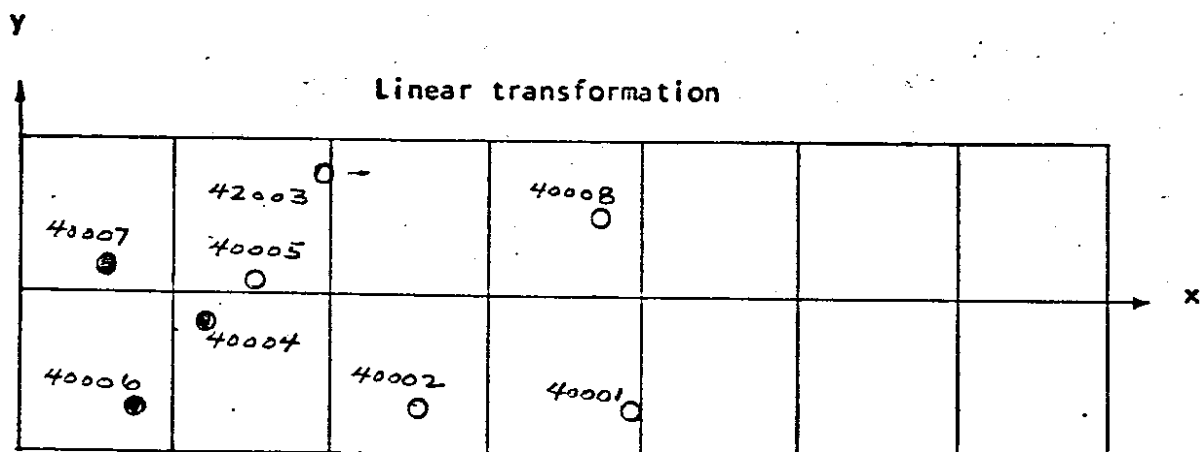
Vertical control points: 7

Location of all ground control points shown in Figure: 82

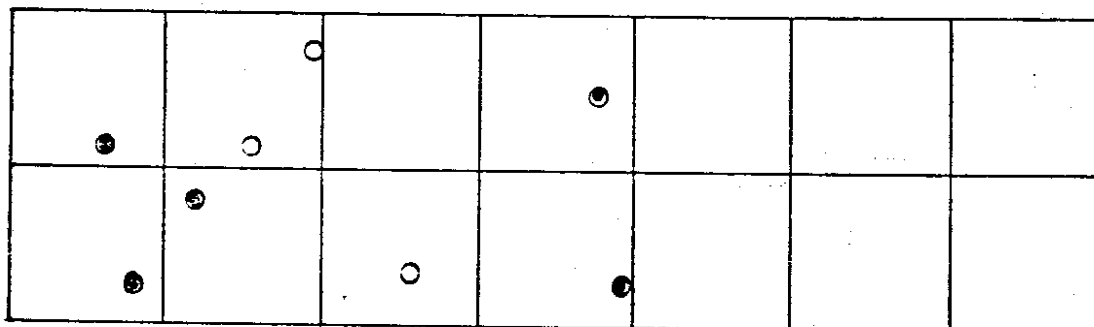
Residuals of all check points shown in Figure: 83

Stand errors of three different adjustment procedures of this strip  
shown in Table: 28

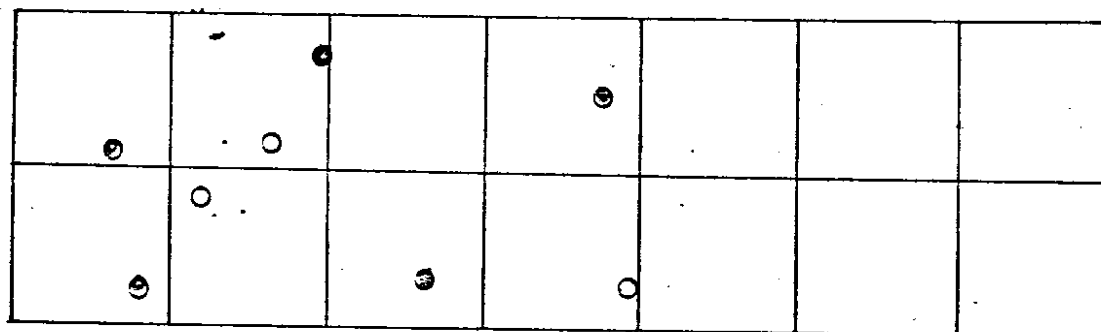




**Beginning, middle and end (2nd)**



**Traverse method (2nd)**

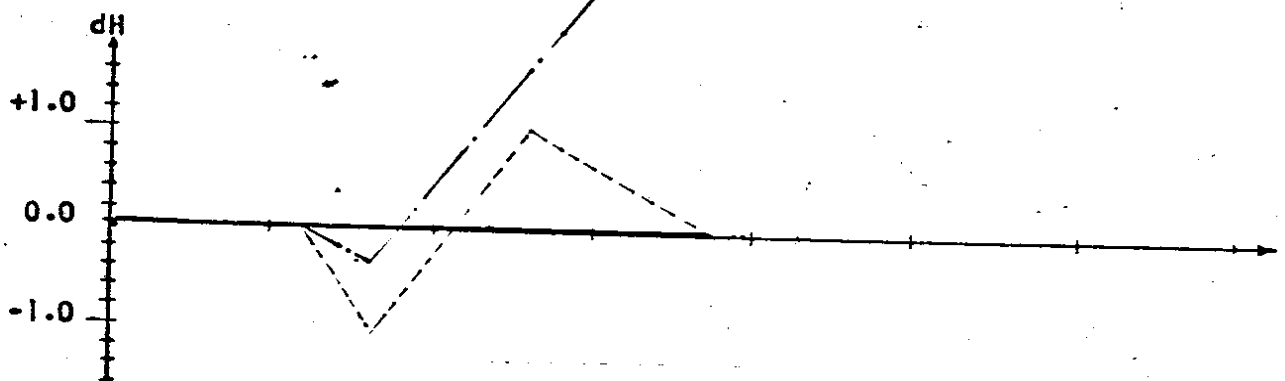
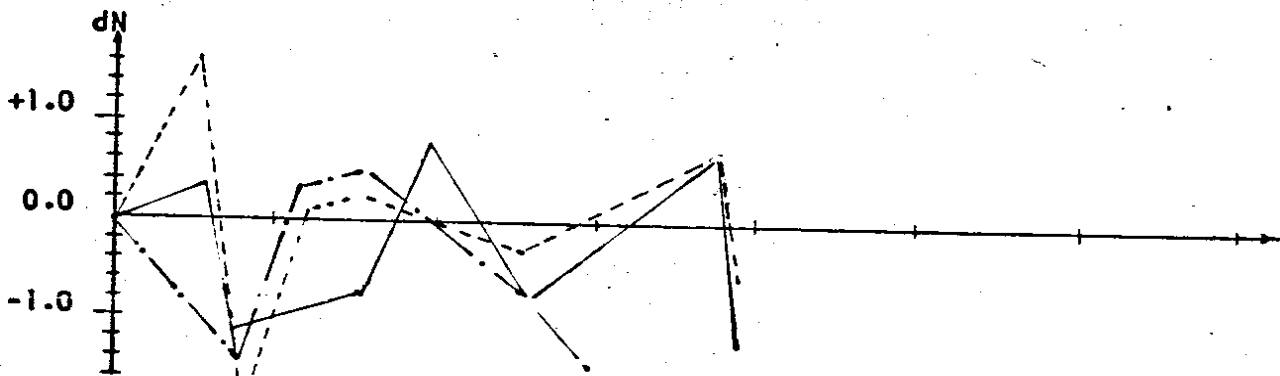
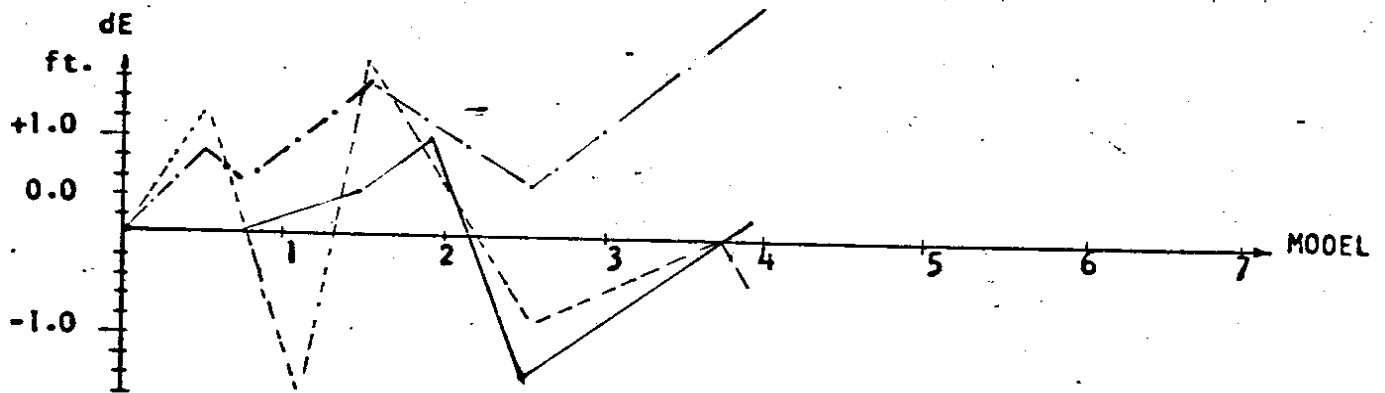


● Control points

○ Check points

"2" Horizontal point; "3" Vertical point; "4" Horizontal & vertical point

Fig. 82 Layout of ground control points of test strip 25



- ..... Linear transformation
- Beginning, middle and end (2nd)
- Traverse method (2nd)

Fig. 83 Comparison of Discrepancies Resulting from Different Adjustment Procedures of Test Strip 25 at Flight Height of 12,000 Feet.

TABLE 28 RESULTS OF DIFFERENT ADJUSTMENT  
PROCEDURES OF TEST STRIP 25 AT FLIGHT  
HEIGHT OF 12000 FEET

Method	Linear Transformation	Beginning, Middle and End (2nd)	Traverse Method(2nd)
Control points only			
RMSE of dE in ft.	1.14	0.93	0.88
RMSE of dN	1.10	1.23	0.82
RMSE of dP	1.12	1.09	0.85
RMSE of dH	0.00	0.00	0.00
MAX. dE	1.60	1.47	1.40
MAX. dN	1.42	1.97	1.15
MAX. dH	0.00	0.00	0.00
Check points			
RMSE of dE in ft.	3.13	2.73	1.60
RMSE of dN	2.10	1.29	0.72
RMSE of dP	2.67	2.13	1.13
RMSE of dH	13.80	1.01	5.76
MAX. dE	4.18	4.29	2.50
MAX. dN	3.13	2.22	0.84
MAX. dH	19.18	1.02	6.93

\*More control points needed.

5-8. Precision Determination of the Aerotriangulation Requirements of Highway Engineering.

After testing twenty-five strips, it should be possible to determine the practical accuracies that can be expected from flight strips of given heights, lengths, and with various distributions and densities of control points.

Given the standard errors at different flight heights, it is possible to express them in polynomial form as a function of flight height to be used to determine if the precision of the aerotriangulation will meet the requirements of Highway Engineering.

In Fig. 84, it is shown that the accuracy changes in form with increasing flight height. If the accuracy, as a function of flight height, is plotted, the mathematical function of precision can be found. Assuming the polynomial of first, second, and third degree, the most probable value for the coefficient in the polynomial can be found by using least squares. This is to fit a polynomial function to the observations so that minimum deviation will result.

The equation of an empirical formula is:

$$e_i = K_0 + K_1 H_i + K_2 H_i^2 + K_3 H_i^3 \quad (80)$$

where

$e_i$  = standard error of aerotriangulation

$H_i$  = various flight height

$K_0, K_1, K_2, K_3$  = coefficients of the flight height.

These coefficients are the unknowns. ( $K_0 = 0.00$ )

Equation (80) can also be assumed as observation equation and in matrix form as:

$$\bar{V} = \bar{A}\bar{X} - \bar{L} \quad (81)$$

Where

$$\bar{V} = \begin{bmatrix} V_{e1} \\ \vdots \\ V_{e25} \end{bmatrix} \quad \bar{A} = \begin{bmatrix} H_1 & H_1^2 & H_1^3 \\ \vdots & \vdots & \vdots \\ 1 & H_{25}^2 & H_{25}^3 \end{bmatrix} \quad \bar{X} = \begin{bmatrix} K_0 \\ K_1 \\ K_2 \\ K_3 \end{bmatrix} \quad \bar{L} = \begin{bmatrix} e_1 \\ \vdots \\ e_{25} \end{bmatrix}$$

By applying the least squares condition,

$\bar{X}$  (unknown) is chosen such that for equal weight the sum of the squares of the residuals is a minimum, thus:

$$\begin{aligned} \bar{V}^T \bar{V} &= (\bar{X}^T \bar{A}^T - \bar{L}^T) \cdot (\bar{A}\bar{X} - \bar{L}) \\ &= \bar{X}^T \bar{A}^T \bar{A} \bar{X} - 2\bar{X}^T \bar{A}^T \bar{L} + \bar{L}^T \bar{L} \end{aligned} \quad (82)$$

For minimization, the partial differentials of this function with respect to each independent variable must be zero. The partial derivative matrix is:

$$\begin{aligned} \frac{\partial}{\partial \bar{X}} \bar{V}^T \bar{V} &= 2\bar{A}^T \bar{A} \bar{X} - 2\bar{A}^T \bar{L} = 0 \\ \text{Realizing that the } \bar{L}^T \bar{L} &\text{ is constant, or} \\ \bar{A}^T \bar{A} \bar{X} - \bar{A}^T \bar{L} &= 0 \end{aligned} \quad (83)$$



NO.	FLIGHT HEIGHT IN FEET	HORIZONTAL IN FEET	VERTICAL IN FEET	REMARKS
1	1500	0.13	0.15	
2	"	0.13	0.15	
3	"	0.12	0.13	
4	"	0.11	0.14	
5	"	0.12	0.16	
6	"	0.07	0.09	
7	"	0.13	0.23	
8	"	0.30	0.15	
9	"	0.07	0.17	
10	"	0.02	0.23	
11	3000	0.33	0.34	
12	"	0.25	0.32	
13	"	—	—	*More control points needed.
14	"	0.27	0.38	
15	"	0.47	0.46	
16	"	0.50	0.22	
17	"	0.11	0.44	
18	"	0.46	0.40	
19	"	0.26	0.29	
20	"	0.37	0.48	
21	6000	—	—	*
22	"	0.64	0.85	
23	12000	—	—	**Ground control points need remeasurements.
24	"	0.58	1.98	
25	"	1.13	1.01	
1st polynomial $[VV]_H = 0.46$ ft. $[VV]_V = 0.75$ ft.				
2nd polynomial $[VV]_H = 1.95$ ft. $[VV]_V = 4.76$ ft.				
3rd polynomial $[VV]_H = 1.19$ ft. $[VV]_V = 1.26$ ft.				

Table 29. The standard errors in various flight height.

Using the following new notation:

$$\overline{A}^T \overline{A} = \overline{N} \quad \text{and} \quad \overline{A}^T \overline{L} = \overline{U} \quad (84)$$

Then the normal equation is:

$$\overline{N} \overline{X} = \overline{U} \quad (85)$$

The most probable values can be found by computing the inverse of  $\overline{N}$ , thus:

$$\overline{X} = \overline{N}^{-1} \overline{U} \quad (86)$$

And the variance:

$$\overline{\sigma} = \sqrt{\frac{\overline{U}^T \overline{U}}{\overline{V} \overline{V} (n-u)}} \quad (87)$$

Where  $n$  = number of the testing strips = 25

$u$  = number of unknowns

= 2 for first degree polynomial

= 3 for second degree polynomial

= 4 for third degree polynomial

$\overline{U}^T \overline{U}$  = sum of squares of the residuals

The numerical computation of the empirical equation (80) with various degree of polynomial has been calculated, and the results are shown in Table 29.

From Table 29, the best agreement of the relationships between standard errors and flight heights is in equation (89), with first degree of polynomial equation and traverse method of distributions of control points.



$$e_h = 0.000 + 8.2386E^{-5} \times H \text{ for Horizontal points.}$$

$$e_v = 0.000 + 1.1460 E^{-4} \times H \text{ for vertical points.} \quad (89)$$

Or simply assumed as:

$$e = 0.01\% \times H$$

#### 5-9. Conclusion

Theoretical studies of error propagation for aerotriangulation have been executed in Chapter (V) showing that the errors in aerotriangulation are essentially a double summation of errors.

After testing twenty-five strips, the practical experiments show the effects on the coordinates and elevations in aerotriangulation, without adjustment are similar double summation errors. Sources of those errors are naturally in observation errors that act on the individual model and make it deformed.

The number and the distribution of the ground control points indicates the quality of the aerotriangulation adjustment. The quality to be expected, depends of course upon the flight height as shown in equation (84) and Table (29). Thus, the traverse method of ground control points distribution is recommended. The control points should be about equally distributed throughout the strip.

In many strips, as shown in this testing, blunders of the ground control points are difficult to detect. These mathematical detections of ground control points will be given in next Chapter (VI).

## CHAPTER VI

### DATA REJECTION

#### 6-1. Introduction.

A major problem in refining and certifying aerotriangulation adjustments for control points is the detection and isolation of erroneous or misidentified ground control points.

It is sometimes very difficult to detect the blunders of ground control points in the aerotriangulation adjustment. For example, in testing strip No. 23, 20 horizontal control points and 52 vertical control points have been established and targeted; however, 14 horizontal control points and 17 vertical control points contained errors from 2 to 100 feet. In this manner aerotriangulation accomplishes a type of consistency check of ground control surveys.

Therefore, one possible solution to this problem is the development of an automated editing program with statistical and mathematical conceptions to check the consistency of input data prior to strip and block adjustment.

#### 6-2. General Working Equation.

The basic consideration for detection of ground control points is that the residuals of adjusted points should be smaller than three times the standard errors for various flight heights, which were determined in Chapter V. However, as the number of erroneous points increases the

residuals of all control points increase and it is difficult to indicate which points are in error and should be rejected. Therefore, it is required to have a mathematical conception to detect ground control points in error.

Assuming the residuals of all ground control points after linear transformation (79) are the direct observations.

as

$dE_1, dN_1, dH_1, \dots, dE_n, dN_n, dH_n$  from first point to nth point.

Then the mean value of the residuals can be computed by using absolute values:

$$MdE = \frac{|dE_1 + \dots + dE_n|}{n}$$

$$MdN = \frac{|dN_1 + \dots + dN_n|}{n} \quad (91)$$

$$MdH = \frac{|dH_1 + \dots + dH_n|}{n}$$

The deviations between the mean value and individual  $dE$ ,  $dN$ ,  $dH$  are:

$$VdE = MdE - |dE|$$

$$VdN = MdN - |dN| \quad (92)$$

$$VdH = MdH - |dH|$$

Where  $MdE, MdN, MdH$  = mean value of  $dE, dN, dH$

$|dE|, |dN|, |dH|$  = individual residuals after linear transformation

$VdE, VdN, VdH$  = deviations of  $dE, dN, dH$  (absolute values)

The standard errors are:

$$\begin{aligned} \sigma_{|dE|} &= \sqrt{\frac{[VdEi \cdot VdEi]}{n-1}} \\ \sigma_{|dN|} &= \sqrt{\frac{[VdNi \cdot VdNi]}{n-1}} \\ \sigma_{|dH|} &= \sqrt{\frac{[VdHi \cdot VdHi]}{n-1}} \end{aligned} \quad (7')$$

If  $VdE_i > 2 \sigma_{|dE|}$  ;  $VdN_i > 2 \sigma_{|dN|}$  ; and  $VdH_i > 2 \sigma_{|dH|}$  , then a blunder error exists in the strip which should be rejected. After the rejection of one or more points, the test for blunder errors should be repeated until no blunder is indicated.

### 6-3. Computer program.

The data rejection computer program and aerotriangulation adjustment are performed in two steps. These steps are performed one after the other without operator intervention.

As a first stage, the strip with all ground control points is a linear transformation to the ground coordinate system for detection and rejection of the blunders.

Having rejected all data errors, the strip adjustment is performed in the second stage.

The generalized flow chart for data rejection and adjustment is shown in Fig. 85.

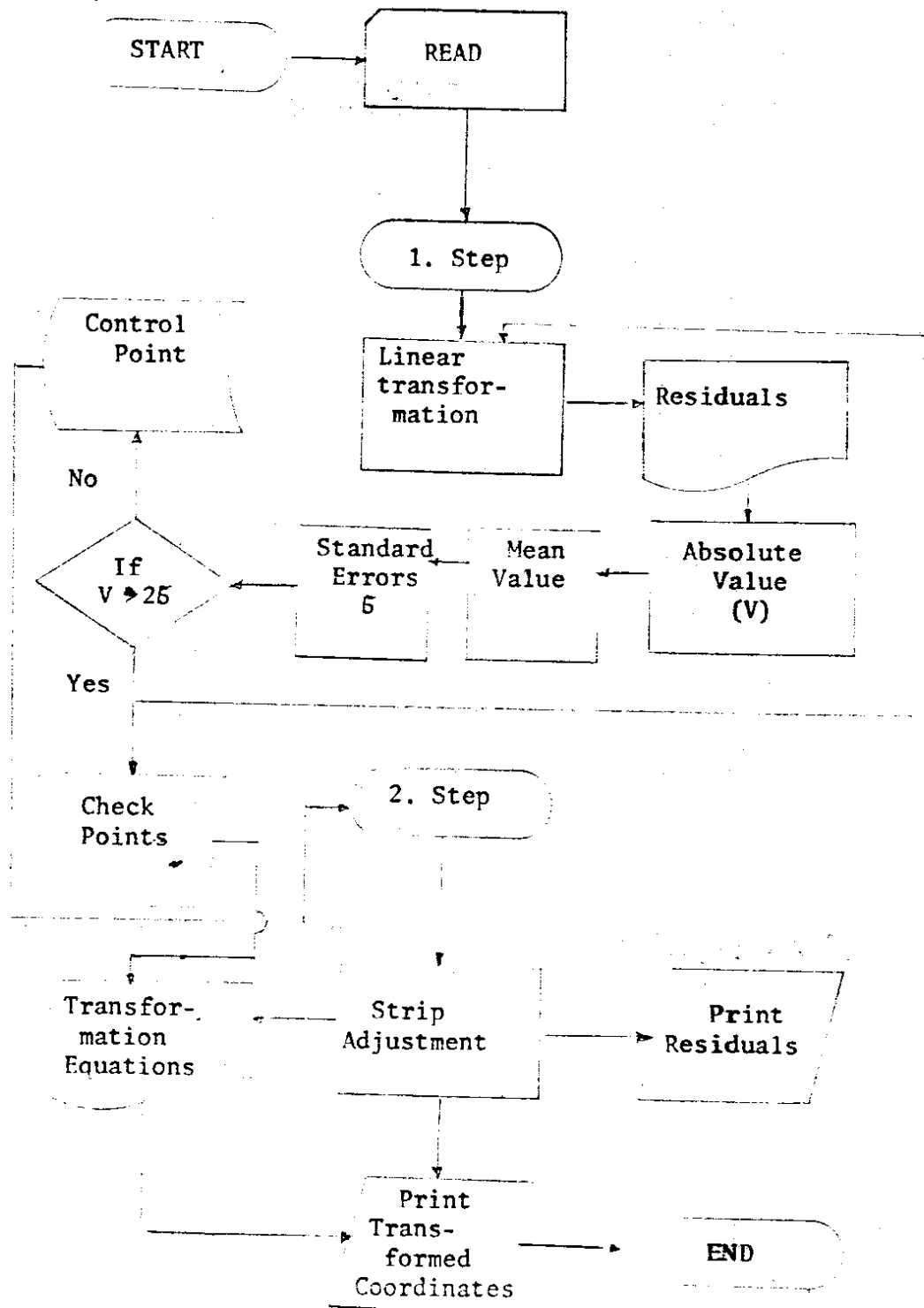


Fig. 85. Generalized flow for data rejection and adjustment.

6-4. Testing.

This test strip was taken from the job of "Tanner to Lower X-ing" which consists of seven models. The flight height is 1800 feet above the mean ground elevation of 1000 feet.

In this strip 12 horizontal control points and 38 vertical control points have been established and targeted as shown in Fig. 86.

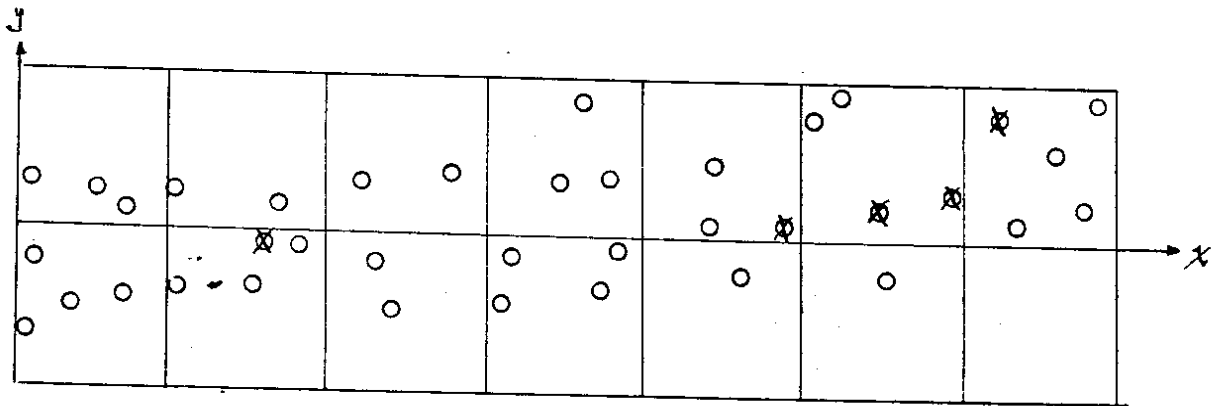


Fig. 86. Test strip for data rejection.

In order to detect the blunders and systematic errors for ground control survey and photographs this strip area has been flown and photographed three times. Strip adjustments were passed through the computer thirty-two times before attaining acceptable results.

However, by using the new developed computer program for "Data Rejection", this strip adjustment is performed in one pass through the computer, and five ground control point errors have been detected and rejected. The numerical sample, listing and instructions for this program can be found in appendices.

#### 6-5. Conclusion:

According to numerous tests, this program is found to be most accurate for detection of blunders in the strip adjustment. This program results in hand analysis and computer time savings.

## CHAPTER VII

### CONCLUSIONS AND RECOMMENDATIONS

In this investigation, several findings can be noted as follows:

1. The accuracy of the aerotriangulation is dependent upon the ground control surveying, photographic quality, and photogrammetric process. The blunders and systematic errors of ground control surveying and photographic quality must be avoided before photogrammetric processing.
2. The equation of the standard error for photogrammetric measurements of large scale photographs should equal  $\sqrt{\frac{[VV]}{n-1}}$  instead of the common equation of  $\sqrt{\frac{[VV]}{n}}$ .
3. The astronomic azimuths are not quite the same as those determined by a geodetic survey because of the deflection of vertical. It should be pointed out that reference [10] gives the questionable theory of azimuth closure.
4. The second term corrections in the traverse computation should be applied when the courses are longer than three miles. The angle correction of the second term is computed by the subtraction corrections to backsight with clockwise measurement. The demonstration traverse shows that application of the second term correction affects the azimuth up to five



seconds in a 22-mile course, on this course, with azimuth of  $75^\circ$ , the northing changed +2.76 feet, and easting changed -0.65 feet.

5. Most textbooks of surveying have given the questionable theory of systematic refraction in precise levels. The correction of systematic refraction is as much as the correction of the earth curvature with same sign.

6. The flight height should be determined as a function of the acceptable error tolerance with an empirical constant as shown in Chapter III, and V.

7. In order to avoid the hot spot and long shadows on the photograph, photography should not be taken at the time when the computed solar altitude is less than  $20^\circ$  or more than  $45^\circ$  (for RE8-6 inch camera).

8. The image blur depends on the aircraft velocity, rotation, and the image distance from the center of the format, the photo scale and camera shutter speed. It should be pointed out that the shutter speed should be chosen by using Fig. 16.

9. The systematic displacement of the film or diapositives should be corrected by changing the principal distance of the projectors for analogue plotters, or by affine restritution. The film distortion may be caused by the change in the temperature, relative humidity, tension of the film during the processing in the machine, and overly long retention of the film on the light table during editing.

10. According to the testings, RMSE in elevations were in the order of 0.14 to 0.23 feet for a flight height of 1500 feet using the following plotters: stereoplanigraph C8, Zeiss stereo-comparator PSK, Wild Autograph A7, A8, B8, Santoni IIC, and Kelsh plotters.

11. The theoretical studies of error propagation for aerotriangulation shows that the errors in aerotriangulation are essentially a double summation of errors which can be corrected by using polynomial equations. These polynomials are nonlinear because of the systematic accumulation of errors throughout the strip.

12. Practical experiments using 25 testing strips show that the effects on the coordinates and elevations in aerotriangulation without adjustment are similar to double summation errors. Sources of those errors are naturally in observation errors that act on an individual model and make it deformed. Table 27 shows the standard errors in various flight strips.

13. The flight height and the number and the distribution of the ground control points restricts the quality of the aerotriangulation adjustment.

14. The control points should be about equally distributed in Zig-Zag pattern throughout the strip.

15. Ground control point errors may be detected by using a linear transformation equations.

16. The data rejection computer program can be performed in one pass through the computer, with determined acceptable results.

17. In order to avoid the identification error of the ground control points, the listing of all ground control points should be printed and punched in card form and submitted to the Photogrammetry Branch.

18. The vertical control points for large scale photographs should be determined by precise levels.

19. The systematic errors of earth curvature, systematic refraction, and small instrument error in precise levels must be eliminated by the balanced sights.

20. When the vertical control points are to be determined by using the vertical angle measurements, it is recommended that the vertical angles should be measured simultaneously from both points in order to cancel the effects of earth curvature and refraction.

21. Distance measuring instruments, theodolite, camera, plotters, should be periodically calibrated in order to avoid the constant errors.

22. When all the residuals of the adjusted points in a flight are three times larger than the standard error, the photographs may contain nonsystematic film distortion which causes the model deformation.

23. It should be noted that the target to be used for large scale photographs should have the white bars with a dark background.

24. The empirical equation of relationship between the standard errors and flight heights are computed by choosing only the minimum number of ground control points in the strip adjustment. In practice, however, all check points are used as control, and the resulting equations meet the accuracies of production work.

The standard errors of vertical points are noticeably larger than horizontal point errors, however, the empirical equation:  $0.01\%$  times flight height, may be used for both horizontal and vertical in determination of acceptable errors.

CHAPTER VIII  
FUTURE RESEARCH

This investigation has given a range for different flight heights of the standard errors of the photogrammetric points in the strip. The investigation has included the mathematical formulation of the ground control point errors; photogrammetric errors; and errors of aerotriangulation. However, the following subjects may be needed for further research:

1. Semi-analytical and full-analytical aerotriangulation:

This research is expected to produce recommendations for methods suitable for proper and efficient use of semi-analytical and full-analytical aerotriangulation for low altitude, large scale engineering photogrammetry meeting highway requirements.

2. Sources of the film deformation:

According to the testings show the film enlarged, therefore, the sources of the film deformation must be continuously tested for mathematical corrections and the standard procedures for photographic processing should be established.

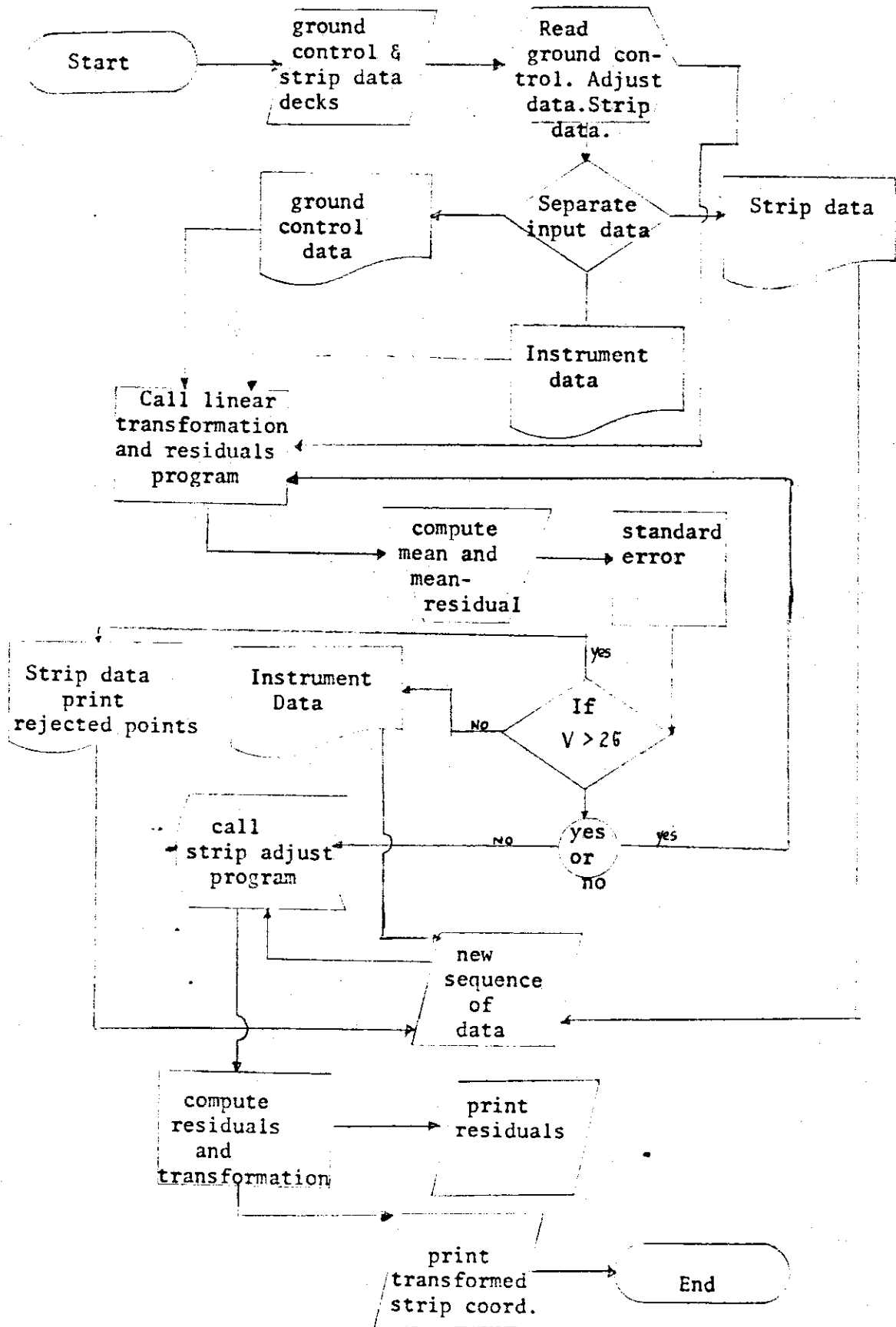
3. Triangulation and trilateration methods and computer programs for highway surveying:

It is known that the traverse method for establishing the ground control points within a large area is not accurate when traversed using a large number of course, distances, and angle measurements and computed only by three condition-equations. It is, therefore, suggested that triangulation and trilateration nets be established from and closed to National Geodetic Survey points, utilizing the Washington State Coordinate System.

It shows that the new procedures and computer programs for triangulation and trilateration are needed in the Department of Highways. The photogrammetry section has the facilities to accomplish this project.

APPENDICES

A. Strip and Block Adjustment and Data Rejection Flow Chart





## B. Instruction of Data Rejection and Strip Adjustment Program

### I. Preparation:

The data deck for each strip is made up of punched cards as follows:

1. Job card: columns 1-6; Job No., Columns 10-14; Flight height; Columns 19-20; number of adjusted control points; columns 40-64; Job Title.
2. Ground control cards: columns 5 to 9; point. no., 10-18; East, 19-27; North, 28-36; Elevation.
3. Equation Card: This instruction card contains the degree of polynomial of the strip adjustment. Column 1, a minus sign, column 2; the degree of the scale and azimuth corrections column 3; the degree of the longitudinal bend correction, column 4; the degree of the transversal bend correction.
4. First principal point card. Columns 1-4 Strip No. Columns 5-9; point No. 10-18; instrument coordinated x, 19-27; y, 28-36; z.
5. Last principal point card: same field as in step 4.
6. Instrument cards with the strip coordinates of all points which are used as control points; same field as step 4.
7. Divider card: column 3; a minus sign; column 4: punch 8.
8. Instrument cards of points to be transformed; same field as in step 4.
9. Last card ( end of strip or last strip of the group): zero card.

### II. Input data in computer:

Put the cards in sequence in card reader as shown in I. Then call the program "Adjust".

III. Output: (printed)

1. Rejected ground control points.
2. Residuals of all adjusted points.
3. Transformed ground coordinates of the strip.

C<sub>1</sub> Sample Data Sheets - Input data

71-207	01800	39	222	TANNER TO LOWER X-ING
30039				81963
30041				84886
30043				94445
30045				100503
30145				97375
30046				69294
30047				106559
30048				70509
30049				103340
30050				81660
30051				108690
30052				84002
30053				114323
30054				87016
30055				122489
30056				90181
30057				137013
30058				94323
30060				96849
30061				108970
30062				99028
30063				115611
30064				101334
30066				105158
30068				111136
33052				70284
40016178536592	16754861			84677
40017178544221	16700842			87380
40018178561494	16641048			90366
40019178582830	16595443			94982
42020178592866	16565612			
43020				99380
40021178619708	16512487			107620
40022178638370	16483715			106070
40023178680599	16433350			102480
40024178730801	16393353			104158
42025178779394	16361274			
43025				109064
40026178906782	16307387			110175
73137				132560
43015178536511	16820897			80310
-222				
15011212	136872	087836		081230
15011272	233850	083482		086052
15030039	137533	096347		082968
15030041	144407	091770		083407
15030043	149576	090993		084944
15030045	159267	087494		085858
15030145	154165	082102		085339
15030046	131381	090405		080997
15030047	165414	092014		086719
15030048	137876	086408		081160
15030049	164394	085482		086277
15030050	144677	085836		082940

15030051	173059	083002	087070
15030052	151659	082290	083271
15030053	179516	082442	087918
15030054	161253	078729	083670
15030055	184843	083389	089198
15030056	170934	074441	084102
15030057	189452	085783	091534
15030058	183007	067424	084692
15030060	193764	069566	084912
15030061	205334	078045	086648
15030062	201190	070761	085140
15030063	210760	081015	087642
15030064	210131	072910	085352
15030066	222980	077755	085726
15030068	241614	087620	086302
15033052	139646	072621	081269
15040016	144359	088613	083415
15040017	152310	084035	083808
15040018	162026	080134	084201
15040019	170289	078251	084867
15042020	175286	076471	085582
15043020	175286	076471	085582
15040021	185145	074325	086797
15040022	191023	073811	086374
15040023	201910	074418	085662
15040024	212408	076923	085748
15042025	222608	080336	086357
15043025	222608	080336	086357
15040026	242052	091322	086082

8

15011212	136872	087836	081230
15011213	134443	070744	080274
15011214	147039	087432	083519
15011216	135272	097095	082822
15011222	156581	087871	085479
15011223	155710	063626	079432
15011224	164025	085575	086257
15011226	157243	094578	086270
15011231	173824	096570	088740
15011232	174727	081689	086940
15011233	167837	061657	079408
15011234	183417	082250	088613
15011242	189343	080926	090126
15011243	190986	068691	084869
15011244	199437	080566	088533
15011246	192307	091079	093102
15011252	205761	078614	086793
15011253	204598	069724	085373
15011254	213044	076236	085728



C<sub>2</sub> Sample Data Sheets - Output Data Sheets

WASHINGTON STATE HIGHWAYS DEPARTMENT-PHOTOGRAMMETRY BRANCH  
AREOTRIANGULATION ADJUSTMENT

INVOICE NO :71-207

JOB TITLE :TANNER TO LOWER X-ING

DEGREE OF CORRECTION FOR SCALE, LONGITUDINAL-TRANSVERSAL-TILE 222

DATA REJECTION -

THE FOLLOWING POINTS HAVE BEEN REJECTED\*

42025  
40021  
40022  
42020  
43020

RESIDUALS	E	N	H
150 30039			0.13
150 30041			-0.12
150 30043			-0.10
150 30045			0.11
150 30145			-0.01
150 30046			-0.14
150 30047			-0.04
150 30048			-0.11
150 30049			-0.02
150 30050			0.11
150 30051			-0.01
150 30052			0.21
150 30053			-0.17
150 30054			0.16
150 30055			0.09
150 30056			0.18
150 30057			-0.05
150 30058			0.19
150 30060			0.04
150 30061			-0.39
150 30062			-0.06
150 30063			-0.21
150 30064			-0.16
150 30066			0.07
150 30063			0.24
150 33052			-0.27
150 40016	-0.09	0.11	-0.00
150 40017	0.02	-0.02	0.29
150 40018	-0.01	-0.21	0.02
150 40019	0.15	0.05	-0.11
150 40023	-0.14	0.17	-0.14
150 40024	0.09	-0.05	0.33
150 43025			0.04
150 40026	-0.02	-0.03	-0.11
150 43015	0.39	0.33	-0.23

D. List of References

- (1) Arthur, D.W.G. "Three-Dimensional Transformations of Higher Degree", Photogrammetric Engineering, January 1965
- (2) Baetsle, P.L. "Conformal Transformations in Three Dimension", Photogrammetric Engineering, September 1966
- (3) Barrell, H./ Sears, J.E. "The Refraction and Dispersion of Air for the Visible Spectrum" Phi. Trans. Royal Soc. London. Series A/1939, P.238
- (4) Brown, Earle B. "V/H Image Motion in Aerial Cameras", Photogrammetric Engineering. Vol. XXXI, No. 2, 1965
- (5) Calhoun, J.M., Keller, L.E., and Newell, R.F., Jr. "A Method for Studying Possible Local Distortions in Aerial Films" Photogrammetric Engineering. Vol. XXVI, No. 4. 1960
- (6) "Classification and Standard of Accuracy of Geodetic Control Surveys". Approved by the Bureau of the Budget and referred to in Bureau of the Budget Circular A-16, Exhibit C, dated October 10, 1958.
- (7) Colcord, J.E. "Aerial Triangulation Strip Adjustment With Independent Geodetic Control", Photogrammetric Engineering, Vol. 27, No. 1, 1961

- (8) Colcord, J.E., Lund, K., and Hussain, M. "A Study of the Accuracy of Visual Planimetric Pointings to Photographic Edges With Different Characteristics". Final Report U.S. Army Engineer Topographic Laboratories. No.ETL-CR-71-19, 1971
- (9) Davis and Foote "Surveying Theory and Practice" 1940
- (10) Dracup, Joseph F. "Suggested Specifications for Local Horizontal Control Surveys." American Congress on Surveying and Mapping, Control Surveys Division, Technical Monograph No. CS-1, First Edition, March 1969.
- (11) Faulds, A.H. "An Investigation of Errors in Aerial Triangulation" Photogrammetric Engineering Vol. XXV, No. 3, 1959
- (12) Ghosh, S.K. "Some Adjusted Thoughts on Errors in Aerial Triangulation" Photogrammetric Engineering. Vol. XXVI, No. 3, 1960
- (13) Gryzulin, S.I. "Atmospheric Refraction During Observation of a High Target", Geodesy and Aerophotography No.4, 1969 P.239-240
- (14) Hoepcke, W. "Ueber die Bahnkrümmung elektromagnetischer Wellen and ihren Einfluss auf die Streckenmessungen" Zeitschrift fuer Vermessungswesen, June, 1964.



- (15) Holsen, F. and Talhang, F. "A Program for Horizontal and Vertical Block Adjustment By Interpolation" XI International Congress for Photogrammetry. Lansanne 1968
- (16) Hosmer, G.L. "Geodesy". New York, 1949
- (17) Hou, C.Y. "Aerotriangulation". Dipl.-Arbeit, University of Stuttgart, Germany. 1965.
- (18) Hou, C.Y. "Dissertation" University of Washington, Seattle In Preparation.
- (19) Hou, C.Y., Veress, S.A., and Prothero, J.W. "A Quantitative Study of Biological Form". IEEE Transactions on Bio-Medical Engineering, Vol. BME-17, No. 2. 1970
- (20) Hou, C.Y. "Deflection of the Vertical in Traverse Computation" Washington State Highway Department, Photogrammetry Branch, 1971.
- (21) Hou, C.Y. "Block Adjustment by Employing a Time-Sharing Computer System". Paper Presented at the 1971 ASP Puget Sound Annual Meeting in Seattle. 1971

- (22) Hou, C.Y. and Veress, S.A. "Determination of Surface Area and Volume of a Specimen by Photogrammetry" Symposium on Close-Range Photogrammetry, American Society of Photogrammetry. P.195-209. 1971
- (23) Hou, C.Y. "Space Resection of Oblique Photography for Automatic Drawing of Perspective Views to Assist Highway Design". Photogrammetric Engineering, Vol. XXXVII, No. 5, 1971
- (24) Hou, C.Y. "Image Blur and Film Shrinkage of Aerial Photographs in the Photogrammetric Process". Published in ACSM & ASP 1972 Convention, Washington D.C. 1972.
- (25) Hou, C.Y., Veress, S.A., and Colcord, J.E. "Consideration of the Refraction in the Precise Leveling" in press.
- (26) Jensen, Niels "Optical and Photogrammetric Reconnaissance System" John Willey and Sons, Inc. New York 1968.
- (27) Jordan, Eggert, Kneissl "Handbuch der Vermessungswesen" Band VI Stuttgart 1956
- (28) Jordan, Eggert, Kneissl "Handbuch der Vermessungswesen". Band III, Stuttgart 1956

- (29) Jordan, Eggert, Kneissl "Handbuch der Vermessungswesen". Band V, Stuttgart, 1969. -
- (30) Juksie, Z. "The Chi-square Test Applied to a Photogrammetric Sample" The Canadian Surveyor. Vol. XVII, No. 5. 1963
- (31) Katibah, G..P. "Construction Control by Photogrammetric Method". ASCE National Meeting on Transportation Engineering. San Diego, California, February 1968.
- (32) Karara, H.M. & Marks, G.W. "Analytical Aerotriangulation for Highway Location and Design". Research Report No. 22, University of Illinois. July 1969.
- (33) Keller, M., Tewinkel, G.C. "Aerotriangulation Strip Adjustment" U.S.C.G.S. Technical Bulletin No. 23 August 1964
- (34) Kissam, P. "Surveying for Civil Engineers". New York, 1956
- (35) Kukkamaki, T.J. "Formelm und Tabellen zur Berechnung der Nivellitischen Refraktion" Veroeffentl. des Finnischen Geod. Instituts Nr. 27. Helsinki 1939.
- (36) Kushtin, I.F. "Effect of the Earth's Curvature on the Position of Points on Aerial Photographs" Geodesy and Aerophotography No. 4. 1969 P. 264 -267

- (37) Lampton, B.F. and Umbach, M.J. "Film Distortion Compensation Effectiveness" Photogrammetric Engineering, Vol. XXXII, No. 6 1966
- (38) Loescher, W. "Optimum Field Angle for Aerial Cameras" Photogrammetric Engineering. July 1964
- (39) Markuze, Yu. I. "Evaluation of the Residual Error In Solving Linear Systems" Geodesy and Aerophotography No. 4, 1969 P. 237- 239
- (40) Manual of Photogrammetry, third edition. American Society of Photogrammetry. 1965
- (41) Merritt, Everett L. "Image Aberration" Photogrammetric Engineering Vol. XXIX, No. 1, 1963
- (42) Mikhail, G.M. "Simultaneous Three-Dimensional Transformation of Higher Degrees", Photogrammetric Engineering. July, 1964
- (43) Moffit, F.H. "Surveying" 1965
- (44) Morgan, Peter "Rigorous Adjustment of Strips" Photogrammetric Engineering. Vol. XXXVII. No. 12, 1971

- (45) Perks, M. "A Numerical Adjustment Procedure for Aerotriangulation Programmed for IBM 650 Computer" The Canadian Surveyor. Vol. XVI, 1962. No. 3
- (46) Plane Coordinate Projection Tables - Washington U.S.C. and G.S. Special Publication No. 271
- (47) Pryor, W.T. "Accuracy of Highway Surveys" Photogrammetria, 25, 1969
- (48) Ramsayer, K. "Erdmessung" (class note) University Stuttgart, Germany. 1964
- (49) Rosenfield, G.H. "Automatic Data Verification" Symposium on Computational Photogrammetry ASP 1967
- (50) Rusinov, M.M. "Investigation of the Angular Aberration of a Single Spherical Refracting Surface", Geodesy and Aerophotography, No. 4, 1969 P. 291 - 295
- (51) Sakaton, P.S. "Lehrbuch der Hoeheren Geodaesie", VEB Verlag Technils Berlin, 1957
- (52) Schut, G.H. "Experiences with Analytical Methods in Photogrammetry" Photogrammetric Engineering. September 1960

- (53) Schut, G.H. "The Use of Polynomials In the Three-Dimensional Adjustment of Triangulated Strips" The Canadian Surveyor Vol. XVI, 1962. No. 3 .
- (54) Schut, G.H. "A Fortran Program For the Strip Adjustment and Blocks by Polynomial Transformation" National Research Council, 1966
- (55) Schut, G.H. "Conformal Transformations and Polynomials" Photogrammetric Engineering. September 1966
- (56) Schut, G.H. "Block Adjustment by Polynomial Transformations" Photogrammetric Engineering, September 1967
- (57) Schut, G.H. "Photogrammetric Refraction" Photogrammetric Engineering, Vol. XXXV. No. 1, January, 1969, P.76
- (58) Shcherbakov, Ya.Ye. "Determination of the Transfer Constant of and Aerial Camera - Camera Mount System". Geodesy and Aerophotography. No. 4. 1969 P.289=290
- (59) Soliman, A.H. "Standard Error in Strip Adjustment" Photogrammetric Engineering. January, 1969
- (60) Soliman, A.H. "Accuracy and Application" Photogrammetric Engineering Vol. XXXVII, No. 8, 1971

- (61) Schwidefsky, K. "New Aids for Numerical Photogrammetry"  
Photogrammetria No. 1. 1957/1958
- (62) USCOMM-C & GS-DC "Classification and Standards of Accuracy  
of Geodetic Control Surveys" 1958
- (63) Veress, S.A. "The Effect of the Fixation Disparity of Photo-  
grammetric Processes" Photogrammetric Engineering. Jan. 1964
- (64) Veress, S.A. "Model Deformation and Its Effect on Attainable  
Accuracy". Journal of the Japan Society of Photogrammetry.  
Vol. 6, No. 7, 1967 and also "Class Note - Aerotriangulation"  
University of Washington 1967
- (65) Veress, S.A. "The Use and Adoption of Conventional Stereo-  
plotting Instruments for Bridging and Plotting of Super Wide  
Angle Photography". Canadian Surveyor. Vol. XXIII. No.4, 1969
- (66) Veress, S.A. "Cooperative Photogrammetric Studies" Research  
Project, University of Washington, State Highways Department, and  
United States Department of Transportation. 1971-1972
- (67) Vinogradov, B.V. "Review of the Optimum Times for Making Aerial  
Surveys of the Principal Types of Landscapes." Geodesy and Aero-  
photography No. 4, 1969 P. 256 - 258

- (68) Yost, G.F. "Resolution and Sinewave Response as Measures of Photo-optical Quality". Photogrammetric Engineering. Vol. XXVI, No. 3. 1960